Exploring the immunology of small molecule inhibitors in chronic lymphocytic leukaemia

Chia Sharpe

Submitted in total fulfilment of the requirements
of the degree of Doctor of Philosophy

August 2019

Faculty of Medicine, Dentistry and Health Sciences

The University of Melbourne

ABSTRACT

Chronic lymphocytic leukaemia (CLL) is the most common adult leukaemia in the western world. CLL is associated with profound immunodeficiency which leaves patients with insufficient anti-tumour immunity and is often compounded by immunosuppressive treatments. Recent advances in the development of targeted small molecule inhibitors, including Bruton's tyrosine kinase (BTK) and B-cell lymphoma 2 (Bcl-2) inhibitors, has provided new, highly effective and less immunosuppressive treatment options. However, targeted therapies have not yet provided a cure for CLL, and there is still a need to improve the depth and durability of patient responses. Immunotherapies harness the patient's own immune system to target cancer cells and are an attractive modality for combination with targeted therapies. However, by both on- or off-target mechanisms targeted therapies also been shown to have the potential to disrupt normal immune populations. This study aimed to understand the effects of targeted therapies on the immune system, thereby providing insight into the potential opportunities and pitfalls for the combination of immunotherapy with targeted therapies in CLL.

This thesis explored the immunological impacts of the first-generation BTK inhibitor ibrutinib, as well as two more selective second-generation inhibitors zanubrutinib and acalabrutinib. The Bcl-2 inhibitor venetoclax was also investigated both as monotherapy and in combination with BTK inhibition. In Chapter 3, gene expression analysis was used to faithfully replicate a comprehensive immune profile comparable to more time consuming and costly flow cytometry analysis. Chapter 4 demonstrated that BTK and Bcl-2 inhibitors had distinct effects on the immune profile of patients after long-term treatment with targeted therapies. Chapter 5 utilised *in vitro* functional assays to demonstrate how effector functions of T cells and natural killer (NK) cells, including cytotoxicity, cytokine production, and proliferation, are impaired by BTK inhibitors whereas NK cells, but not T cells were sensitive to venetoclax treatment. Subsequently, Chapter 6 explored the effect of the immunomodulatory drugs lenalidomide and a PD-1 inhibitor BGB-A317 in combination with ibrutinib, showing that T cell activation is modulated by both ibrutinib and the immunotherapies.

These finding presented in this thesis demonstrate that targeted therapies have clear and distinct immunological effects. Ibrutinib broadly impair the function of multiple immune populations and in particular cellular cytotoxicity, suggesting that more selective BTK inhibitors are better candidates for combination with immunotherapies. Venetoclax affected the survival of specific T cell and NK cell populations, suggesting that long-term venetoclax treatment may result in alterations in the immune profile that may be exploited by combination therapy. These findings highlight the importance of understanding the immunological impacts of targeted therapies when incorporating immunotherapies into treatment combinations.

DECLARATION

This is to certify that:

- this thesis comprises only my original work towards the PhD except where indicated in the preface.
- due acknowledgement has been made in the text to all other materials used.
- this thesis is less than 100,000 words in length, exclusive of tables, maps, bibliographies and appendices.

PREFACE

This thesis contains experiments that were performed in collaboration with Dr Rachel Koldej and have been published in peer-reviewed journals:

1. Sharpe C, Davis J, Mason K, Tam C, Ritchie D, Koldej R. Comparison of gene expression and flow cytometry for immune profiling in chronic lymphocytic leukaemia. J Immunol Methods 2018;463:97–104. doi:10.1016/j.jim.2018.09.013.

ACKNOWLEDGMENTS

First and foremost, I have to thank my supervisors. Joanne Davis, PhD, I quite literally could not have done this without you as my teacher. Thank you for your time and patience, for being present for every failure and triumph, and for always taking time to listen. Thank you also to Dr Kylie Mason, for your guidance and wisdom and for being a bridge to the clinic and the patients that made this research possible. Dr David Ritchie, thank you for believing it was possible and for encouraging optimism. Thank you for making me better than I would have been without your perspective and clarity. To all of my supervisors, your time and expertise was everything that I could have asked for, I appreciate it more than I can put into words.

I also have to thank Rachel Koldej, PhD, without whom this research would not have been possible. Thank you for going above and beyond and for facilitating everything that we were able to do, I cannot thank you enough.

Dr Constantine Tam, thank you for seeing the value in correlative research and for being the consummate collaborator. Thank you also to Dr Sasanka Handunetti, for slogging through the patient records for me. I can only hope that I was some small help in return.

Dale Godfrey, Adam Aldrich and Nick Gerharden, thank you for opening the world of unconventional T cells to me, for supplying samples and reagents, time and expertise, I very much appreciate it.

I also very much appreciate the mentorship, advice, and career guidance of Misty Jenkins, PhD, every conversation with you made me think differently and made me a better researcher.

I also need to thank all the past and present members of the ACRF translational research laboratory I could not have asked for a more supportive team. Especially Matt Landsdown, for being a constant companion, thanks for sticking around. Dr Rachel Cooke, thank you for being a sympathetic ear when I really needed it, can you believe that it is really over? Mandy Ludford-Menting, thank you for knowing when I needed to talk thorough a problem and for the birthday cakes.

To all my friends and family, thank you for putting up with me, for believing in me and for all the material and emotional support that helped me to survive. I profoundly appreciate everyone who made this journey with me, I would not have made it on my own.

LIST OF TABLES

LIST OF FIGURES

ABBREVIATIONS

7AAD	7-aminoactinomucin D
ADCC	antibody dependent cellular cytotoxicity
AF	Alexa Fluor®
AICD	activation induced cell death
alloHSCT	Allogeneic haematopoietic stem cell transplant
AML	Acute myeloid leukaemia
ANOVA	analysis of variance
ATP	Adenosine triphosphate
Bad	Bcl-2-associated death promoter
BAFF	B-cell activating factor
Bak	Bcl-2 homologous antagonist/killer
Bax	Bcl-2-associated X protein
Bcl-2	B-cell lymphoma-2
Bcl-XL	B-cell lymphoma-extra large
BCR	B cell receptor
BH	Bcl-2 Homology
Bid	BH3 interacting-domain death agonist
Bim	bcl-2 interacting mediator of cell death
BLK	B Lymphoid Tyrosine Kinase
BMX	bone-marrow tyrosine kinase gene on chromosome X
BTK	Bruton's tyrosine kinase
BUV	BD Horizon Brilliant™ Ultraviolet
BV	Brilliant violet™
CCL	C-C Motif Chemokine Ligand
CCR	C-C Motif Chemokine Receptor
CD	Cluster of differentiation
CD40L	CD40 ligand
CFSE	carboxyfluorescein succinimidyl ester
CLL	Chronic lymphocytic leukaemia
CR	complete response
CRi	complete response with incomplete blood count recovery
CTV	CellTrace Violet
CXCL	C-X-C motif chemokine ligand
CXCR	C-X-C motif chemokine receptor
DC	Dendritic cells
FACS	Fluorescence activated cell sorting
FCR	Fludarabine, cyclophosphamide, and rituximab
FCS	Foetal calf serum
FCγR	Fc gamma receptor
FL	Follicular lymphoma

GVHD	Graft versus host disease
HLA	Human Leukocyte Antigen
IFN	Interferon
IGHV	Immunoglobulin heavy chain variable region
IgM	Immunoglobulin M
IL	Interleukin
ILC	Innate lymphoid cells
iNKT	invariant natural killer T cells
ITK	Interluken-2- inducible protein
LYN	Lck/Yes novel tyrosine kinase
M-CSF	macrophage cell stimulating factor
M-CSF	Macrophage colony-stimulating factor
mAb	monoclonal antibody
MCL	Mantle cell lymphoma
Mcl-1	Myeloid cell leukaemia 1
mDC	myeloid dendritic cells
MDSC	Myeloid derived suppressor cells
mg	Milligrams
MHC	Major histocompatibility complex
mL	Millilitres
mM	Millimolar
MZL	Marginal cell lymphoma
NCR	Natural cytotoxicity receptor
NFAT	Nuclear factor of activated T-cells
NFκB	Nuclear factor kappa-light-chain-enhancer of activated B cells
NK	Natural killer
NKG2D	Natural Killer Group 2D
Noxa	Phorbol-12-myristate-13-acetate-induced protein 1
ORR	Overall response rate
PBMC	Peripheral blood mononuclear cells
PD-1	Programmed death 1
PD-L1	Programmed death ligand 1
pDC	plasmacytoid dendritic cells
PFS	progression free survival
PI3K	Phosphatidylinositol-3 kinase
PLCγ	Phospholipase C gamma
PR	partial response
PUMA	p53 upregulated modulator of apoptosis
R/R	Relapsed or refractory
RPM	Rotations per minute
RPMI	Roswell Park Memorial Institute
RT	Room Temperature

SLL	Small lymphocytic leukaemia
SYK	Spleen tyrosine kinase
TCM	T cell media
TCR	T cell receptor
TGA	Therapeutic goods administration
TLR	Toll like receptor
TNFα	Tumour necrosis factor alpha
US FDA	United States food and drug administration
WM	Waldenstrom macroglobulinemia
xg	Times gravity force
Zap-70	Zeta-chain-associated protein kinase 70
µg	Micrograms
µL	Microliter
µM	Micromolar

1 TABLE OF CONTENTS

1 LITERATURE REVIEW AND INTRODUCTION

1.1 CHRONIC LYMPHOCYTIC LEUKAEMIA

Chronic lymphocytic leukaemia (CLL) is a lymphoproliferative disorder characterised by the accumulation of clonally derived malignant B cells in the peripheral blood, bone marrow and other lymphoid organs. CLL may be distinguished from other B cell neoplasms by its characteristic immunophenotype, CLL cells are light chain restricted and co-express CD20, CD19, CD5, and CD23[1]. CLL is predominantly a disease of the elderly, with a median age at diagnosis in Australia of 71 years[2]. It is the most common adult leukaemia in the western world, accounting for approximately one percent of all cancer diagnoses in Australia[3].

The diagnosis of CLL requires a peripheral blood leukaemia count of greater than 5000/μL and clinical staging is based on the Rai[4] and Binet[5] staging algorithms, which take into account lymphocytosis, lymphadenopathy and cytopenias to stratify patients into low, moderate and high risk categories. In addition to clinical staging, other prognostic indicators include advanced age and high B2-microglobulin concentration, as well as molecular variations, including complex karyotype[6–8], the loss of p53 either by deletion of gene locus on chromosome 17p (del17p) or mutation of the gene[9,10], and the mutation status of the immunoglobulin heavy chain variable region (IGVH)[11]. Together these markers provide for improved discrimination of prognostic groups both in terms of survival, disease progression and response to therapy[12–15].

While the majority of CLL patients are asymptomatic at diagnosis, the clinical presentation of CLL can be highly heterogeneous. Many patients experience a protracted indolent phase of disease that may not necessitate treatment but are rather managed using a 'watchful waiting' strategy. Current treatment guidelines are for treatment initiation only in patients with symptomatic or progressive disease[1]. In Australia the standard front line therapy for young, fit patients is combination chemo-immunotherapy, typically fludarabine, cyclophosphamide and rituximab (FCR)[16]. The addition of

immunotherapy, in the form of anti-CD20 monoclonal antibodies such as rituximab, to chemotherapy was found to increase both the progression free survival and the overall survival as compared to chemotherapy alone[15,17]. However, chemotherapy remains profoundly immunosuppressive; fludarabine in particular results in significant and prolonged T cell depletion [18–20].

While FCR has been shown to produce sustained remissions of more than ten years in a small number of low risk patients[15], for the vast majority of CLL patients chemo-immunotherapy does not provide a cure. The median progression free survival after frontline FCR is variably reported as between 4.7 years[21] and 6.4 years[15]. Importantly, the depth of the response to FCR is correlated with the time to disease progression. Patients who attain undetectable disease status having the longest progression free survival (PFS)[22]. Furthermore, FCR is best tolerated by young fit patients and many CLL patients are too frail or have comorbidities that preclude such aggressive chemotherapy. Finally, there are well characterised high-risk groups, in particular those with p53 dysregulation, for whom chemo-immunotherapy is particularly insufficient[14,23].

1.2 THE NEW ERA OF TARGETED THERAPIES

Advances in understanding of the molecular underpinnings of CLL pathogenesis have led to the discovery of a number of small molecule inhibitors. These targeted therapies inhibit specific molecular interactions in the malignant cells and perturb key pathways involved in the growth, survival and proliferation of the CLL cells. The two most clinically relevant classes of small molecule inhibitors in CLL are the B cell receptor (BCR) signalling inhibitors, of which the Bruton's tyrosine kinase (BTK) inhibitors have been the most successful and B cell llymphoma-2 (Bcl-2) inhibitors. Figure 1.1 outlines the timeline of approvals of these targeted therapies by the United States Food and Drug Administration and the Australian Therapeutic Goods Association (TGA) (outlined boxes).

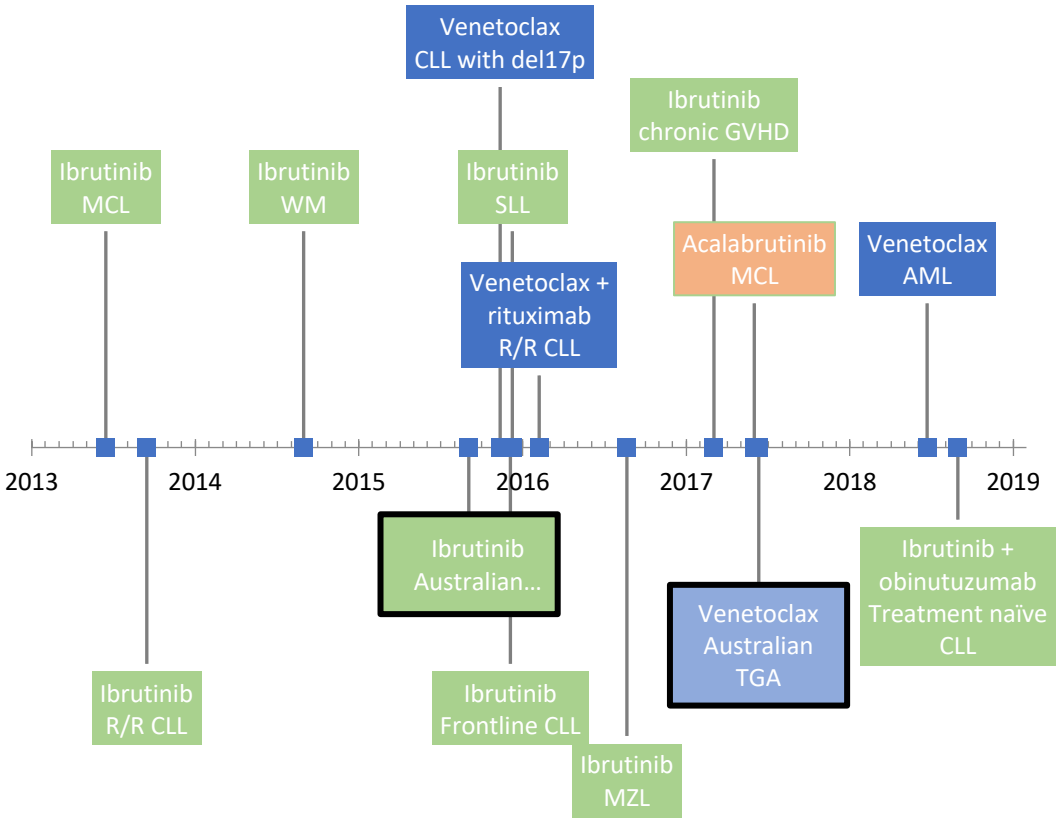

Figure 1.1 Timeline of approvals for targeted therapies

Timeline of United States Food and Drug Administration and the Australian Therapeutic Goods Association approvals. Mantle cell lymphoma (MCL); Relapse or refractory CLL (R/R CLL); Waldenstrom macroglobulinemia (WM); Small lymphocytic leukaemia (SLL); Graft versus host disease (GVHD); Marginal cell lymphoma (MZL); Acute myeloid leukaemia (AML).

1.2.1 BRUTON'S TYROSINE KINASE INHIBITORS

The strongest evidence for the importance of the BCR signalling in the pathogenesis of CLL comes from the prognostic consequences conferred by the IGHV mutation status of the malignant clone. The presence of mutations in the IGHV expressed by leukaemia cells was found to divide two subtypes of CLL with different aetiologies[24]. Unmutated IGHV denotes a more aggressive form of CLL[25,26] that responds poorly to conventional therapy[15].

Additional lines of evidence point to the importance of BCR signalling, not only to the development of the leukemic clone, but also in the maintenance and progression of CLL[27,28]. These includes observations of intrinsic leukaemia cell properties such as the recurring BCR sequences across multiple patients[29], antigen independent cell-autonomous BCR signalling by leukemic cells[30], as well as the continued *in vivo* interactions of CLL cells with antigen[31]. Finally, the observation that CLL cells cultured *in vitro* have poor viability compared to other lymphocytes[32] also supports the importance of extrinsic signalling to the survival of CLL cells.

The essential role of BTK was first indicated when it identified as the genetic aberration in X-linked agammaglobulinemia, a primary immunodeficiency characterised by the absence of mature B cells and the resultant immunoglobulin deficiency[33,34]. BTK is a member of the Tec family of tyrosine kinases, which is primarily expressed in haematopoietic cells and are involved in signalling downstream of a number of receptors including cytokine and chemokine receptors, TLR receptors, Fc receptors, and antigen recognition receptors and their co-stimulatory receptors [reviewed in 35,36]. BTK is a critical component of the BCR signalling cascade, without which B cell development and function is arrested. Upon BCR crosslinking, BTK phosphorylation results in the activation of the NFAT and NFκB pathways[37,38] which regulate B cell proliferation and survival[39].

In addition to its involvement in BCR signalling, BTK is also downstream of the costimulatory domains CD19, CD40, and CD38, as well as a number of other cell surface receptors including cytokine, chemokine, growth factor, and integrin receptors[40]. As such the rationale of BTK inhibition extends beyond simply BCR inhibition[41]. However, BTK

expression is not restricted to B cells and it is also expressed in cells of the myelomonocytic lineage. While BTK is dispensable for some myeloid cell functions, BTK deficient myeloid cells are functionally impaired and have reduced production of reactive oxygen species and inferior responses to inflammatory stimuli[42–45]. Furthermore, BTK is involved in macrophage survival through regulation of M-CSF and TLR mediated signalling pathways[46,47].

1.2.1.1 Ibrutinib

Ibrutinib is a first-in-class selective and irreversible inhibitor that covalently binds to cysteine 481 in the ATP binding site, thus inactivating BTK[48]. Early experiments showed ibrutinib effectively prevented leukaemia cell activation in response to BCR stimulation and produced objective responses in spontaneous canine B cell lymphoma[49]. Further *in vitro* data showed that ibrutinib effectively induced apoptosis in CLL cells whilst sparing normal leukocytes[50]. The induction of apoptosis is primarily attributed to the inhibition of BCR signalling and subsequent decrease in NFκB activation [51,52].

Early clinical trials found that ibrutinib had an acceptable safety profile and produced objective responses in a number of low-grade B cell malignancies including CLL[53]. A phase 2 clinical trial of ibrutinib in relapsed or refractory CLL reported an overall response rate (ORR) of 71%, with an additional 20% having a partial response (PR) with persistent lymphocytosis, and the estimated PFS at 26 months was 75% [54]. A three year follow up study found that patients responses were improved by continuous dosing [55] indicating that prolonged administration of the drug may be required to maintain responses. A subsequent trial of treatment naïve CLL demonstrated the superiority of ibrutinib over single agent chlorambucil, a therapy often used in patients unable to tolerate FCR, leading to the approval of ibrutinib for this indication in 2015[56].

During these clinical trials, patients who were otherwise responding to ibrutinib had a persistent increase in lymphocytosis. Prior response guidelines had precluded patients with elevated peripheral blood white cell counts from being classified as responders. The lymphocytosis, which is commonly associated with reduction in lymph node size, was

attributed to the redistribution of leukemic cells from protective niches. Specifically, on target inhibition of BTK downstream of the C-X-C motif chemokine receptor 4 (CXCR4) receptor[57] and therefore inhibition of C-X-C motif chemokine ligand 12 (CXCL12) mediated homing to lymph nodes[58]. Furthermore, an analysis of patients who experience prolonged lymphocytosis whilst being treated with ibrutinib concluded that progression free survival was not adversely affected[59]. As such new response criteria were proposed to include these patients as 'intermediate responses' or 'partial responses with lymphocytosis'[60].

Multiple studies have demonstrated that ibrutinib also inhibits a large number of other kinases at clinically achievable doses, nine of which have the same cysteine binding site resulting in similar irreversible binding as BTK. These alternate targets of ibrutinib include all members of the Tec family, namely IL-2–inducible T cell kinase (ITK), TXK*, TEC and bone-marrow tyrosine kinase gene on chromosome X (BMX), as well as ErbB family kinases, BLK and JAK3[49,61]. The off-target inhibition of these kinases is clinically relevant. Inhibition of ErbB family kinases by ibrutinib has been shown inhibit breast cancer cell growth[62,63] and inhibition of B Lymphoid Tyrosine Kinase (BLK) contributes to the efficacy of ibrutinib in B-acute lymphocytic leukaemia[64]. Furthermore, it has been hypothesised that the bleeding events associated with ibrutinib treatment may be due to the simultaneous inhibition of BTK and TEC impairing platelet function[65]. The impact of off-target TEC kinase inhibition on immune cells is further discussed in section 1.3.3.

1.1.1.2 Second generation BTK inhibitors

Bolstered by the success of ibrutinib, along with the recognition of its broader kinase inhibition profile, more selective BTK inhibitors were developed for the treatment of CLL. Spebrutinib (CC-292) is a highly BTK specific second generation BTK inhibitor[66]. Despite being well tolerated and accomplishing high BTK occupancy the clinical outcomes achieved with Spebrutinib were inferior to that of ibrutinib[67]. Subsequently, acalabrutinib (ACP-196), another highly selective BTK inhibitor, was shown in a phase 1 trial to have

* also known as Resting Lymphocyte Kinase (RLK)

more favourable overall response rate of 95% at 14.3 months[68]. Likewise, early clinical data from a phase 1 trial of CLL patients showed that another seconder generation BTK selective inhibitor zanubrutinib was also well tolerated, achieved high BTK occupancy, and with a median follow up of just 7.5 months produced an overall response rate of 90%[69]. However, the clinical data on second-generation BTK inhibitors is still in the early stages and it remains unclear what, if any clinical advantage these more targeted therapies will have over ibrutinib.

1.2.2 BCL-2 INHIBITORS

Bcl-2 was first identified as candidate oncogene in follicular lymphoma, in which Bcl-2 was found to promote the survival of neoplastic cells without concomitant proliferation[70]. Subsequently a family of proteins that contain shared structural homology with Bcl-2 homology (BH) domains (BH-1–4) have been discovered.

The Bcl-2 family is divided into pro-apoptotic and anti-apoptotic members. The pro-apoptotic members can be further divided into two groups, the BH3 only proteins BIM, BAD, PUMA, and NOXA, and the effector proteins BAK and BAX. BH3 only proteins are either transcriptionally induced or post- transcriptionally activated by cellular stressors such as cytokine deprivation or DNA damage. The BH3 only proteins then act by either binding the anti-apoptotic family members, preventing them from sequestering the pro-apoptotic effectors BAK and BAX or by directly activating BAK and BAX. When activated BAK and BAX form oligomers that permeabilize the mitochondrial membrane, releasing cytochrome C and thus initiating apoptosis. The anti-apoptotic family members include Bcl-2, Bcl-W, Bcl-X_L, Mcl-1, and A1. The anti-apoptotic members inhibit apoptosis by the sequestration of pro-apoptotic family members including both the BH3 only proteins as well as binding the BH3 domain of activated BAX and BAK preventing oligermisation[71,72]. Therefore it is the relative expression of the Bcl-2 family members determines a cells commitment to apoptosis[73].

Since its discovery Bcl-2 has been identified as a potential drug target leading to the development of BH3 mimetics, which compete with BH3 only proteins for binding to the anti-apoptotic proteins. As such, BH3 mimetics prevent Bcl-2 from sequestering

endogenous BH3 only pro-apoptotic proteins, tipping the balance toward increased cell death[74]. While the Bcl-2 family is ubiquitously expressed the over expression of Bcl-2 has been identified as a key contributor to CLL cell survival [75–77]. However, it has also been reported that there is significant heterogeneity in Bcl-2 family expression in CLL cells, which significantly overlaps with both Bcl-2 expression in t(14;18) lymphoma cell lines and the levels of expression observed in normal B cells [78,79]. Rather than the absolute expression of Bcl-2 determining CLL survival, it is the relative weighting of the Bcl-2 family expression toward cell survival that determines the survival of leukemic cells [80,81], a model depicted in Figure 1.2. These findings are commensurate with experimental evidence that mitochondrial priming, that is the balance of Bcl-2 family expression, determines the sensitivity of leukemic cells to cytotoxic therapies [81,82].

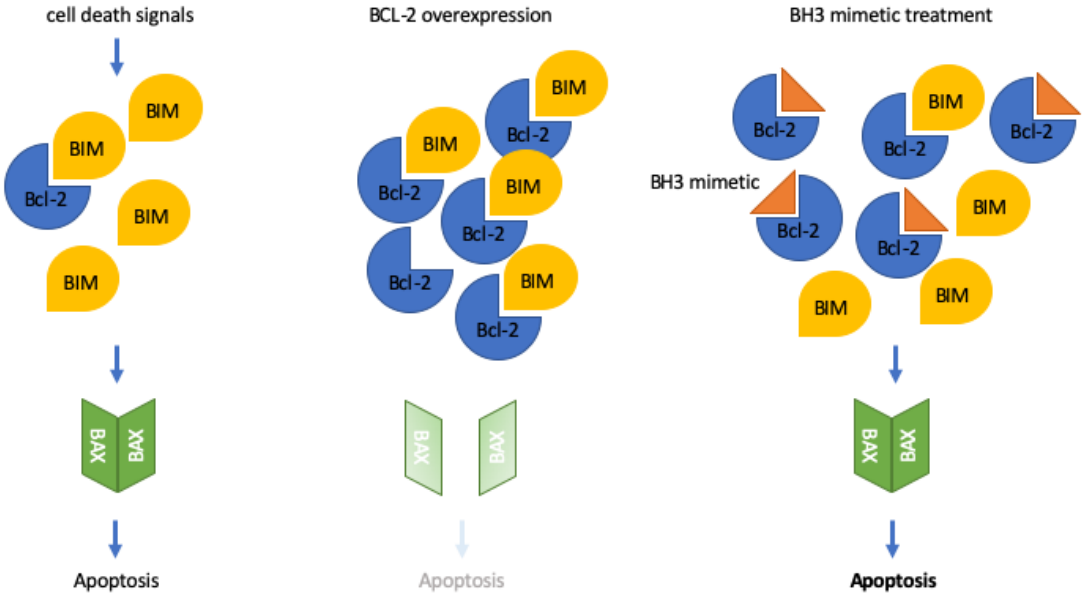

Figure 1.2 Diagram of effect of Bcl-2 inhibition

In normal cells, stress signals result in increased BIM expression, resulting in BAX oligomerisation and subsequent apoptosis. In cells which over express Bcl-2, cell death signals are insufficient to overcome the pro-survival proteins and apoptosis is not initiated. Venetoclax outcompetes BIM-Bcl-2 binding, preventing Bcl-2 from sequestering BIM and therefore cell death occurs.

1.2.2.1 Venetoclax

Venetoclax (ABT-199) is an orally bioavailable and Bcl-2 specific BH3 mimetic. It was developed in response to the dose limiting thrombocytopenia observed with the BH3 mimetic navitoclax (ABT-232) an inhibitor of both Bcl-2 and Bcl-X_L[83]. Venetoclax covalently binds Bcl-2, and was shown to effectively induce apoptosis in *in vitro* and xenograft mouse models of haematological malignancy independently of TP53[84,85]. A phase 1 study of 56 CLL patents found that 79% of patients responded to venetoclax monotherapy including 20% that achieved either a complete response (CR) or complete response with incomplete count recovery (CRi)[86]. However, despite deep responses at 15 months, 27% of patients had disease progression. In particular this was associated with patients who were fludarabine refractory, had a complex karyotype and with the depth of the response[87]. A phase 2 study of 107 R/R CLL patients with del17p also found that venetoclax had a response rate of 80%, with only 8% of patients achieving a complete response at 12 months[88].

In vivo studies also showed that venetoclax rapidly induced apoptosis of CLL cells independently of chromosome 17p deletions or mutations of in the TP53 gene and that TP53 status was not predicative of clinical response to venetoclax[85]. This study also found that sensitivity to venetoclax was determined by leukaemia cell mitochondrial priming[85]. Alternative mechanisms of venetoclax sensitivity have been proposed including that the phosphorylation status of Bcl-2 determines sensitivity to venetoclax[89]. Additionally, the upregulation of the other anti-apoptotic Bcl-2 family members, in particular Bcl-X_L, has been identified as a mechanism by which cells have decreased sensitivity to venetoclax[90]. Furthermore, mutations in Bcl-2 or BAX that conferred venetoclax resistance were found in mouse models[91] and acquired mutations in Bcl-2 (Gly101Val) in CLL patients confers resistance to venetoclax by decreasing the ability of venetoclax to disrupt BAX and BAX binding to Bcl-2[92–94].

1.3 THE IMMUNE MICROENVIRONMENT IN CLL

A key clinical feature of CLL is the profound immunosuppression, which leaves patients susceptible to recurrent infections and contributes to leukaemia related morbidity and mortality. Often exacerbated by therapy, the immune dysfunction is characterised by cytopenia and the dysregulation of immune cell function, preventing effective anti-tumour immunity and contributing to a leukaemia supportive microenvironment.

Historically the indolent but progressive nature of CLL was attributed to slow proliferation of the leukemic clone, accompanied by accumulation due to an intrinsic defect in apoptosis caused by the aberrant expression of pro-survival molecules, in particular Bcl-2 [76,95]. This theory of CLL was supported by the slow clinical evolution of CLL and by the observation that CLL cells in the peripheral blood display features of anergy and cell cycle arrest [96]. Later, using heavy water experiments to track newly born CLL-B cells, it was demonstrated that leukaemia cell populations are highly dynamic and there is substantial leukemic cell turnover and trafficking between the peripheral blood and other lymphoid organs[97].

There is now an increased appreciation of the differences between the *in vitro* behaviour of isolated CLL cells as compared to CLL cells interacting with the tumour microenvironment. This is most explicitly demonstrated by the low viability of purified CLL cells in *ex vivo* culture[32] which may be rescued by high density PBMC culture or co-culture with stromal cells[98–101]. Furthermore, stromal cell culture has been shown to regulate the expression of the Bcl-2 family and CLL-B cell survival[82,102,103]. Finally, lymph node resident CLL-B cells have higher expression of proliferation markers than either peripheral blood or bone marrow derived cells [104] and access to IL-21 and CD40 ligand (CD40L) interaction with follicular helper T cells[105] and follicular dendritic cells[106] induces CLL cell proliferation. Together these finding cement the critical role of the microenvironment in the pathogenesis of CLL which is critically dependent on these extrinsic signals for their survival and proliferation.

This section will briefly outline the immune populations that have been described as playing an important role in the CLL microenvironment, either providing support for CLL cells or as cells with the potential for anti-leukaemia immunity.

1.3.1 INNATE IMMUNE CELLS

The cells of the innate immune system can be divided into two lineages, myeloid and lymphoid. Myeloid cells are the most abundant haematopoietic cells in the human body and are an essential part of the innate immune system and are required for proper adaptive immunity. Terminally differentiated myeloid cells can be divided into two main groups, polymorphonuclear phagocytes (granulocytes) which includes neutrophils, eosinophils, mast cells and basophils and mononuclear cells which includes macrophages and dendritic cells (DC). Both macrophages and dendritic cells of can be derived from either myeloid progenitor cells in the bone marrow or from peripheral blood monocytes. Innate lymphoid cells (ILC) are derived from the common lymphoid progenitor and include NK cells and type 1 ILC (ILC1s), ILC2s, and ILC3s.

1.3.1.1 Monocytes

Monocytes constitute about 10% of PBMC and can be further classified into classical ($CD14^{high}$ CD16-), intermediate (CD14+ CD16+) and non-classical ($CD14^{low}$ CD16+) subsets[107]. Untreated CLL patients with elevated absolute monocyte counts have shorter time to disease progression[108,109] and shorter overall survival after first line therapy[110]. In particular, higher proportions of classical ($CD14^{++}CD16^{-}$) monocytes was found to be associated with shorter time to first treatment[111]. Furthermore, the monocyte profile of CLL patients is skewed toward non-classical ($CD14^{low}CD16^{+}$) monocytes which display a more immunosuppressive profile[112].

Indeed, *in vitro* experiments show that contact with CLL cells drives the derivation of immunosuppressive monocytes with the ability to inhibit T cell proliferation[113,114]. Additionally, in both the Eμ-TCL1 and xenograft mouse models of CLL, depletion of monocyte populations resulted in reduced expansion of CLL cells and prolonged survival[115,116]. However, *ex vivo* activated macrophages were capable of killing antibody labelled CLL cells[117] and macrophages stimulated by CD40L and a TLR agonist had anti-

tumour activity and were capable of killing spontaneously arising CLL cells in Eμ-TCL1 mice [118,119].

1.3.1.2 Myeloid derived suppressor cells

Myeloid derived suppressor cells (MDSC) are a heterogeneous population of immature myeloid cells that are expanded in pathogenic conditions including cancer[120]. They are defied by their ability to supress T cell function however they may be phenotypically identified as cells which co-express the common myeloid marker CD11b and CD33 with low or absent human leukocyte antigen -DR isotype (HLA-DR) expression[121]. MDSCs can be further classified into CD14+ myeloid MDSCs and CD15+ or CD66b+ granulocytic MDSCs. However, there is considerable variation in the markers used to define MDSCs in the literature. In CLL, CD14+HLADR$^{low/-}$ cells have been identified as being elevated in CLL, have the capacity to supress T cell function and are associated with poor prognosis[114,122,123].

1.3.1.3 Dendritic cells

DCs can be divided into two subsets, myeloid DCs (mDC) are characterised by the expression of CD11c and plasmacytoid DC (pDC) which express CD123 (IL-3 receptor)[124]. Plasmacytoid DCs specialise in the production of type I interferons and play a critical role in antiviral immunity. The frequency of pDCs is significantly elevated in indolent CLL but significantly decreased with progressive disease and in both circumstances have significantly decreased IFNα production[125]. Some have suggested the DCs are phenotypically altered in CLL and T cell cultures with CLL patients DCs showing significantly reduced proliferation and cytokine production[126,127]. However others have shown that DCs are phenotypically and functionally similar to healthy donor DCs[128–130]

1.3.1.4 Innate lymphoid cells

Innate lymphoid cells (ILC) are a family of lymphocytes that are defined by the lack of an acquired antigen receptor, but which mirror the functions of T cells. ILCs can be divided into 'cytotoxic' (NK cells) and 'helper' (ILC1, ILC2 and ILC3) subsets which correspond to CD8, T_H1, T_H2, and T_H17 T cells respectively. While NK cells constitute about 10 percent of PBMC in healthy adults[131,132], ILCs are mostly tissue resident cells[133]. NK cells play a

pivotal role in anti-tumour immunity[134,135]. NK cytotoxicity is regulated by the balance of recognition of ligands of the activating receptors such as Natural Killer Group 2D (NKG2D) receptor, and Natural Killer Receptors (NCR) and inhibitory receptors including NKG2A and killer-cell immunoglobulin-like receptors (KIR)[136]. NK cells are directly cytotoxic to tumour cells and also regulate anti-tumour immune response, promoting T_H1 immune responses and recruiting DCs. Peripheral blood NK subsets can be defined by the expression of CD56 and CD16. $CD56^{bright}$ CD16- NK cells are precursors of $CD56^{dim}$CD16+ NK cells which are more mature, abundant, and cytotoxic, though less proliferative than $CD56^{bright}$ NK cells.

Increased number of NK cells has been identified in CLL patients, but no change in total NK frequency was observed with disease progression or treatment[137]. However the selective loss of mature, cytotoxic NK cells was observed over time in CLL[138]. Low CLL to NK cell ratio is associated with poor prognosis [139]. Importantly CLL cells express multiple inhibitory ligands including CD200[140], HLA-G[141,142] and NK cells from CLL patients also have significantly lower expression of NKG2D than healthy donors resulting in impaired immune surveillance[143]. Similarly, ILCs are also expanded in CLL patients, but have an altered function, in particular decreased TNFα production[144]

1.3.2 T CELLS

T cells are recruited to the CLL microenvironment by CLL cells which express the C-C Motif Chemokine Receptor-4 (CCR4) specific chemokines C-C motif chemokine ligand-17 (CCL17) and CCL22[145]. From the earliest stages of CLL there is apparent T cell dysregulation including decreased T cell receptor signalling and cytokine production[146]. T cells from CLL patients have impaired immunological synapse formation[147] and display features of T cell exhaustion in particular elevated expression of the immune checkpoint programmed death 1 (PD-1)[148]. Perhaps the most overt T cell dysfunction observed in CLL is the inversion of the CD4 to CD8 ratio which is associated with disease progression[149]. Low CD4:CD8 ratio ($\leq$ 2.5) was also found to be associated with higher expression of exhaustion markers[150]. Interestingly, lower CD4 T cell counts at the end of chemotherapy

correlated with better disease control, which the authors attribute to the helper T cell derived CD40L survival signals[20].

The co-culture of leukemic cells with autologous T cells contributes to *in vitro* longevity and interactions with helper T cells were shown to result in CLL cell activation and the induction of proliferation[151]. These findings are supported by experiments showing interactions with activated T cells regulates CLL cell CD38 expression which has been shown to be associated with higher CLL cell proliferation[152], specifically in response to T_H1 derived cytokines[153]. This has been largely attributed to T cell derived cytokines such as CD40L, IL-15 and IL-21 which have been shown to induce CLL cell proliferation[105,154]. Furthermore, CD40/CD40L and IL-4 from CD4 T cells has been demonstrated to induce CD38 expression and increase the immunosuppressive capacity of CLL-B cells[155,156]. These studies highlighted the particular importance CD4 T cells in the CLL microenvironment.

1.3.2.1 Unconventional and innate-like T cells

Unconventional T cells are a diverse group of T cells with the capacity for activation independently of peptide-Major histocompatibility complex (MHC) interactions. These T cells have restricted TCR diversity and recognise lipids, small-molecule metabolites and phosphoproteins. Unlike unconventional T cells which are defined by the lack of canonical peptide-MHC interactions, innate-like T cells express a conventional TCR, but express the receptors and responses more akin to innate lymphocytes. Both unconventional T cells and innate-like T cells are rapidly activated and produce large amounts of cytokines in response to stimulation.

1.3.2.2 Invariant NKT cells

Invariant NKT cells (iNKT cells) are the most studied subset of NKT cells. They are defined by their recognition lipid antigens in the context of the MHC-like molecule CD1d. Upon antigen recognition, iNKT cells are rapidly activated and producing both T_H1 and T_H2 cytokines[157]. Uniquely, as all iNKT cells recognise the lipid antigen alpha-galactosylceramide (αGalCer)[158,159]. Uniquely, as all iNKT cells recognise the lipid antigen alpha-galactosylceramide (αGalCer)[158,159], which allowed for the generation of αGalCer-CD1d tetramers which can be used to define iNKT cells by flow cytometry. In this thesis

the term NKT cells will be used in reference to invariant NKT cells. In humans, iNKT cells comprise approximately 0.1% of T cells, however in some individuals they constitute up to 1% of T cells [160–162]. However, aging is associated with a rapid decrease in NKT cell prevalence in the peripheral blood[163]. Interestingly NKT cells are implicated in the age related decline of T cell immunity in mice[164].

In the TCL-1 mouse model of CLL, a lack of NKT cells accelerated disease progression and NKT cells are both directly cytotoxic to CLL cells and control pro-tumorigenic myeloid cells[165]. It has been demonstrated that iNKT cells are capable of killing human CLL cells presenting αGalCer[166]. However, while CLL cells have been shown to express CD1d, reports of the degree of CD1d expression in CLL cells varies significantly. Some reports suggesting that more than 75% of CLL cells express CD1d[167], albeit at a lower density than healthy B cells, a finding supported by independent studies[168]. Others have found that a wider diversity of CD1d expression on CD19+ cells with a mean of 40% expressing CD1d[169]. CLL patients have lower number of NKT cells than healthy donors, with a further reduction in fludarabine refractory CLL patients [168] and progressive CLL patients. However NKT cells from CLL patients retain their functional capacity[167].

1.3.2.3 γδT cells

γδT cells are a heterogeneous population T cells which express a TCR consisting of γ and δ chains as opposed to the more common α and β chains. Like αβT cells, γδT cells are derived from the common lymphoid progenitor and mature in the thymus. However, unlike αβT cells, γδT cells are able to respond to multiple antigens independently of presentation in the context of MHC. γδT cells comprise between 0.2-14% of peripheral blood lymphocytes[170]. The major subsets of γδT cells are defined by the Vδ chain used in the TCR. Vδ2 are the most abundant, and well characterised γδT cells subset. In CLL patients, Vδ2 γδT cells are numerically preserved but functionally impaired[171]. Vδ1 γδT cells are preferentially expanded in Concanavalin A stimulated *in vitro* cultures and are cytotoxic against CLL cells[172]. While there is evidence that γδT cells recognise CLL cells via TCR specific interactions[173] γδT cells also express a number of innate receptors including natural cytotoxicity receptors (NCR) which mediate γδT cell cytotoxicity. *Ex vivo* activated

Vδ1 γδT cells have enhanced antileukemia cytotoxicity due to the upregulation of NCRs[174] and NKG2D[175]. Similarly Vδ2 γδT cell cytotoxicity is also enhance by engagement of innate receptors, including CD16 (FcγRIII) engagement by rituximab opsonised cells[176].

1.3.2.4 Virtual memory T cells

Virtual memory T cells (T_{VM}) are a relatively newly defined subset of CD8 T cells. First identified in mice, this population represents peripherally derived, foreign antigen-inexperienced CD8+ T cells that express memory markers. This population is IL-4 dependent[177] and like innate lymphocytes are IL-12, IL-18 and IL-15 responsive[178,179]. In humans this subset can be defined as CD45RA+Eomes+KIR+ NKG2A+ CD8 T[178,179]. The role of T_{VM} cells in cancer is not yet well understood but may be a particularly important immune subset in CLL. T_{VM} cells are preferentially expanded in lymphodeplete settings[177,180,181] and as such may be more abundant in patients who have had prior chemotherapy treatment. Additionally, T_{VM} cells are more prevalent in older adults, a relevant demographic in CLL, and have a higher expression of Bcl-2 than naïve or memory CD8 T cells[182].

1.3.3 Effects of targeted therapy on the immune microenvironment

Both BTK and Bcl-2 are expressed in immune cells other than B cells. As such, BTK and Bcl-2 inhibitors are expected to have some on target effects in these populations. Furthermore, ibrutinib is known to inhibit multiple other kinases including all members of the TEC family and therefore also has a number of off target effects on both NK and T cell populations.

1.3.3.1 BTK inhibition in immune populations by ibrutinib

BTK is not only expressed in B cells but is also expressed in myeloid populations including monocytes, macrophages, myeloid DCs and MDSCs. Ibrutinib has been shown to impair macrophage chemokine production[183] and macrophage phagocytosis of rituximab-coated leukaemia cells[184,185]. Ibrutinib was also shown to impair macrophage responses to Mycobacterium tuberculosis[186]. Furthermore in a mouse model of CLL, ibrutinib was found to deplete MDSCs in a BTK dependent manner, potentially disrupting the CLL induced suppression of the immune system[187]. Ibrutinib altered the cytokine production

of DCs, reducing the expression of MHC-II, and ibrutinib treated DCs, when co-cultured with T cells, increased the proliferation and production of IL-17 by T cells[188]. These findings are in line with the phenotype of BTK deficient DCs which are also more mature and induce greater T cell proliferation [189].

1.3.3.1.1 Off target inhibition of immune populations by ibrutinib

Ibrutinib inhibits all the members of the Tec family at very low concentrations[49,61]. Three members of the Tec family are expressed in NK and T cells: ITK, TXK, and Tec. ITK is involved in signalling downstream of multiple immune receptors including CD2[190], chemokine receptors (particularly CXCR4)[191] and Fc receptors[192]. Crucially, ITK is also downstream of the T cell receptor (TCR). Upon TCR crosslinking Lck phosphorylates ITK which leads to ITK autophosphorylation and subsequent activation of PLCγ1[193,194]. T cells from ITK deficient mice have significant functional defects including defective activation[193,195], proliferation[196], adhesion[197] and migration[191]. While TXK deficient mice have a more mild T cell defect than ITK deficient T cells [198], the simultaneous loss of ITK and TXK results in a more severe phenotype than loss of either kinase alone[191].

The most prominent role of Tec kinases, in particular ITK is in helper T cell (T_H) development. Upon stimulation naïve CD4 T cells differentiate into distinct helper phenotypes including T_H1, T_H2, and T_H17 and inducible regulatory T cells (T_{regs})[reviewed in 199]. ITK deficient mice have diminished T_H2 immune responses [200–202] however the exact role that ITK and TXK play in the regulation of T_H differentiation is complex. Upon differentiation T_H2 cells upregulate ITK and down regulate TXK[203] while T_H1 cells maintain expression of both ITK and TXK[204]. As such it has been suggested that T_H1 skewing occurs as these cells have the capacity for compensatory signalling in the event of ITK deficiency. This is supported by experiments in which TXK overexpression rescued the function of ITK deficient T cells[205], however while TXK overexpression lead to increased cytokine production, it had no effect on T_H1/T_H2 balance [205,206].

Interestingly, TXK has been shown to traffic to the nucleus where it acts as direct transcriptional regulator of IFNγ [198,207,208] suggesting it has a positive role in T_H1 differentiation. However, it has been suggested that ITK is not necessary for T_H2 lineage

commitment but instead is only required for T_H2 functional responses[209]. Another mechanism for T_H1 skewing in ITK deficient settings may be due to the direct interaction of ITK with T-bet, which is required for T_H1 development and has been shown to negatively regulate GATA3 function in T_H2 cells [203,210].

ITK deficient mouse CD4 T cells also have diminished IL-17A production, a key cytokine for T_H17 cells and exhibit increased Foxp3 expression and have a higher propensity to differentiate into iT_{regs} [211]. Similar results were found using RNA knockdown in primary human CD4 T cells which also had increased FoxP3 expression, increased T_{reg} differentiation and decreased IL-17A expression[212]. However, while ITK is required for the production of IL17A, this may be due to a general requirement for strong TCR signalling rather than a specific role for ITK as these cells have competent T_H17 differentiation and production of other T_H17 cytokines including IL-17F[213].

In the setting of deficiency of both ITK and TXK T_H2 responses remained intact due to the simultaneously defective NFATc1 activation and failure to repress GATA3 expression. However, defective T_H1 responses remained[214]. Furthermore, when ITK deficient human T cells were treated with an inhibitor of both ITK and TXK the propensity for T_{reg} differentiation was reversed[212]. Tec deficient mice do not have an overt T cell defect[215], however Tec plays a role in linking TCR signalling to IL-2 production [216] and the upregulation of Tec multiple days after stimulation suggests that Tec may play a larger role in activated and effector T cell populations [217].

Figure 1.3 summarises the polarizing cytokines, master transcription factors, effector cytokines and effect of ITK deficiency for each subset. The roles that these CD4 T cell subsets play in CLL specifically is discussed in subsequent sections.

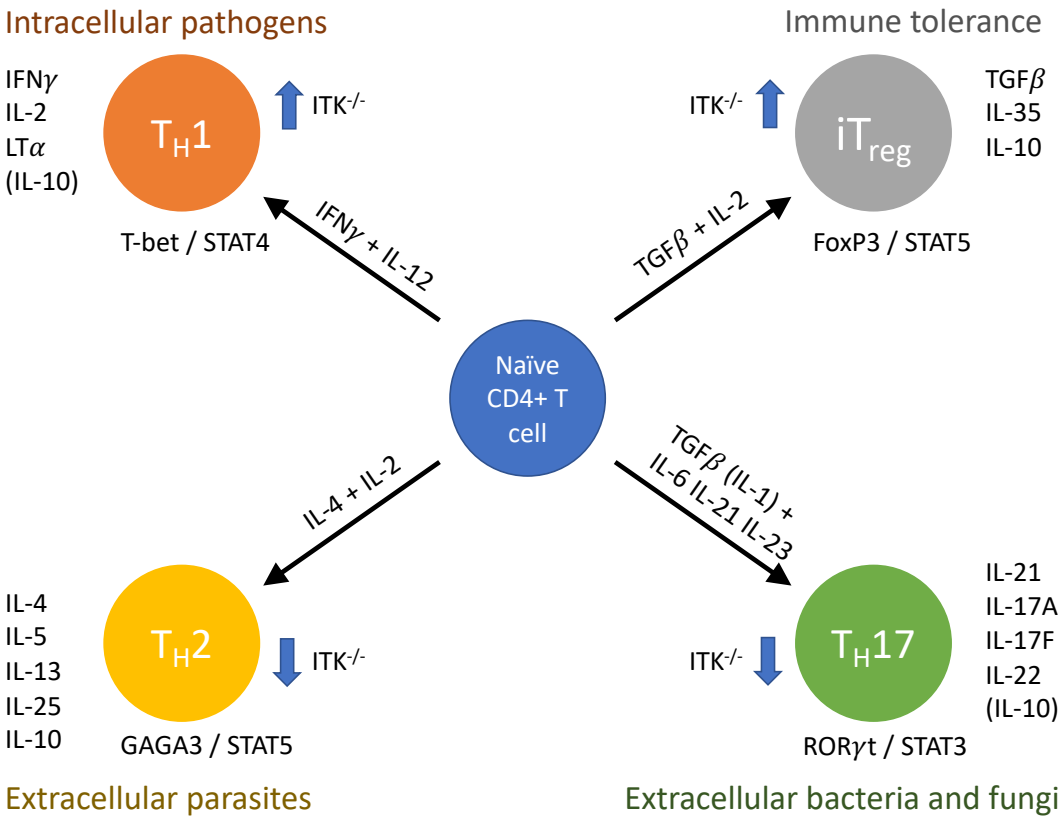

Figure 1.3 Summary of CD4 T cell subsets

In their seminal paper, Dubovsky et al. suggested that the inhibition of ITK by ibrutinib resulted in inhibition of pro-tumour Th2 cells while sparing the function of Th1 or CD8 T cells that are more capable of an anti-tumour response [218]. However, this effect relies on inhibition of ITK whilst maintaining the competent signalling of TXK, which in kinase inhibition assays is inhibited at lower concentrations than ITK[61,219].

Unlike the observed T_H1 skewing in mice treated with ibrutinib, in T cell lymphoma patients treated with ibrutinib no change was observed the percentage of Th1 % of CD4+ [220]. Conversely, a study which used T-bet expression in CD4 T cells to measure the T_H1 phenotype found that in CLL patients there was an increase in the frequency of T_H1 cells after 1 month of ibrutinib treatment [221]. However an analysis of CLL patients treated for 6 months with ibrutinib showed no alterations in the T_H1 or T_H2 subsets[222].

Similarly, data from ITK deficient mice show increased T_{regs} and decreased IL17A production in CD4 T cells. There are conflicting effects of ibrutinib treatment on the frequency of IL17A producing CD4 T cells in CLL patients which warrants further investiagation[222,223].

In addition to their role in CD4 T cells both ITK and TXK are essential for proper CD8 T cell function. While ITK deficient mice were able to clear an initial LCMV infection, there was inferior CD8 T cell proliferation and the resultant memory population had an altered cytokine profile[224]. Furthermore, the diminished cytolytic activity and degranulation of ITK deficient T cells could be recovered by IL-2 stimulation[225]. In a mouse model of listeria infection, Dubovsky et al. also found that ibrutinib treated mice had preserved anti-viral CD8 T cell function[218]. However, in this study there was no comparison of the effect of ibrutinib in the absence of leukaemia. It is therefore possible that the improvement in CD8 T cell function in ibrutinib treated mice was due to the effects on the leukaemia rather than a direct improvement in CD8 T cell function.

ITK deficient mice were also found to have a skewing toward a more innate-like T cell phenotype in both CD4 cells [226] and CD8 T cells[227,228]. In both ITK deficient and ITK and TXK deficient mice there was a predominance of a $CD44^{high}$ CD122+ NK1.1+ IL15 dependent CD8 T cells[224,229]. Similarly, ITK deficient mice have increased numbers of $\gamma\delta$T cells with an innate phenotype common to NKT cells (CD4+ NK1.1+, express the transcription factor PLFZ, and are able to produce both IFNγ and Th2 cytokines)[230]. Interestingly ITK activity is not essential for iNKT maturation, but is required for αGalCer induced cytokine production[231]. Furthermore ITK may be required for maintenance of peripheral NKT cells as aging ITK deficient mice have a progressive loss of NKT cells[232].

In addition to the potential of ITK inhibition to result in T_H1 skewing, multiple studies have focused on T cell exhaustion in the setting of ibrutinib treatment. Ibrutinib treated patients have reduced checkpoint molecule expression on T cells [222,233]. T cells from ibrutinib treated patients had diminished cytokine production, including IL-6, IL-10 and TNF-α, all of which have been implicated in the propagation of CLL[50]. Prior ibrutinib treatment was also suggested to have improved *ex vivo* killing by CLL patients T cell, in contrast to prior chemo-immunotherapy which had no effect on T cell cytotoxicity[234].

Further evidence of the clinical impact due to off target inhibition of kinases was demonstrated when ibrutinib treated NK cells had diminished activity against rituximab coated tumour cells in vitro and in vivo [235,236]. Furthermore, unlike ibrutinib, neither acalabrutinib or zanubrutinib had an inhibitory effect on the antibody dependent cellular cytotoxicity (ADCC) of NK cells [237]. This may allow the combination of these inhibitors with antibody therapies such as the anti-CD20 antibodies that partially rely on NK cell ADCC.

Given that ibrutinib can inhibit ITK, it has been studied for broader clinical in several immune mediated pathogenic settings. It has been suggested that ibrutinib modulation of CD4 T cell populations after ASCT contributes to the improvement of the graft-vs-leukaemia effect[238]. Ibrutinib has also been suggested to be an effective treatment for graft-vs-host disease[239] and autoimmune arthritis[49,240].

1.3.3.2 Effect of venetoclax on immune populations

Within the immune system, different immune subsets, and different stages of maturation have variable expression of Bcl-2. Regulation of Bcl-2 plays a critical role in T cell thymic selection [241,242] and maintenance of T cell memory in the periphery [243]. Importantly, Bcl-2 expression is higher in healthy donor naive CD8 T cells compared to memory CD8 T cells expressing high levels of PD-1 [244]. Furthermore, expression of Bcl-2 and Bim increase in effector and memory T cells, the balance of which determines population contraction at the end of infection[245,246].

Little is known about the effect of Bcl-2 inhibition on immune populations other than B cells. In an *in vitro* cell death assay, the LC_{50} for venetoclax treated CD4 and CD8 T cells from healthy donors was 2.5±0.6 mM and 1.3±0.7 mM respectively, which was much

higher than the LC_{50} for B cells (3.0±0.9 nM)[247]. However, venetoclax treated mice (100mg/kg) were found to have significantly decreased numbers of multiple immune subsets in the spleen[248]. In particular Bcl-2 has been identified as indispensable for cell cycle progression in NK cells[249] and for the survival of plasmacytoid DCs[250].

1.4 IMMUNOTHERAPY IN CLL

Recently a number of different immunotherapies have tested in CLL patients to improve long-term outcomes. Currently, only allogeneic stem cell transplant (ASCT) has the potential to cure CLL[251,252]. However, despite advances in the conditioning regimens, the age and comorbidities of most CLL patients precludes the use of transplant. The efficacy of ASCT relates in part to the graft-versus-leukaemia effect and emphasizes the potential of the immune system to cure CLL. Attempts to capture the benefits of ASCT without the attendant safety concerns have incorporated CAR-T cells, checkpoint blockade, monoclonal antibody therapies and immunomodulatory agents.

1.4.1 MONOCLONAL ANTIBODIES

1.4.1.1 Anti-CD20 antibodies

The most commonly used immunotherapy in CLL are CD20 antibodies, of which rituximab was the first in class and is now a mainstay of CLL treatment. The combination of rituximab and chemotherapy increases both PFS and OS over chemotherapy alone [15,17]. Rituximab has been shown to guide NK cell and macrophage antibody dependent cellular cytotoxicity (ADCC) of CLL cells[117,253]. However, both direct cytotoxicity and complement dependent cellular cytotoxicity have also been implicated in the mechanism of rituximab[254]. Second generation anti-CD20 antibodies such as ofatumumab are fully humanised, thus reducing the potential for immune reactions. In addition, third generation anti-CD20 antibodies such as obinutuzumab have an F_C region engineered to increase interactions with $F_C\gamma R$.

1.4.1.2 Checkpoint inhibitors

Programmed death 1 (PD-1) and its ligands PD-L1 (CD154) and PD-L2 are important immune checkpoints in the homeostatic regulation of immune responses. However

aberrantly high expression of PD-1 ligands by many tumours leads to increased T cell exhaustion and prevents effective anti-tumour immunity. The interaction of PD-1 and PD-L1 leads to inhibition of T cell proliferation and a reduction in the cytotoxic capacity of T cells [255]. The success of anti-CTLA4 antibodies in the treatment of solid malignancies there has been a validated of the concept of reversing the negative regulation of immune effector functions and checkpoint blockade aimed at both PD-1 and PD-L1 were subsequently developed.

Anti-PD-L1 blocking antibody treatment was associated with improved *in vitro* cytokine production of NTK cells derived from the peripheral blood of non-small cell lung cancer patients[256]. Likewise anti-PD-L1 antibody therapy was found to contribute to tumour control in an Eμ-TCL1 adoptive transfer mouse model of CLL[257]. Furthermore in this model checkpoint blockade mitigated some of the immune dysfunction that is characteristic of this CLL model, including preventing myeloid skewing and T cell exhaustion[258].

1.4.2 LENALIDOMIDE

Lenalidomide is a member of the immunomodulatory drug (IMiD) family. Like other thalidomide analogues, lenalidomide has demonstrated clinical efficacy in a variety of haematological malignancies. While it is most often used in conjunction with Dexamethasone for the treatment of multiple myeloma, lenalidomide is also effective in the treatment of other B cell malignancies including CLL. Early trials of Lenalidomide in R/R CLL (25mg/day) showed promise, with 47% response rate but with few CRs (4 patients, 9%)[259]. Further trials in relapsed CLL raised questions about the risk of tumour flair syndrome and dose limiting toxicities that were associated with upregulation of activation markers (CD86 and CD40) on CLL cells[260]. Alternatively, reduced dose lenalidomide (10mg/day) in a R/R CLL cohort resulted in a similar clinical efficacy with an overall response rate of 32% but with only 3 patients (7%) achieving a CR[261]. However, this study demonstrated a more acceptable toxicity profile. A combination of Lenalidomide and the anti-CD20 antibody ofatumumab resulted in 24% complete response rate and an overall response rate of 47% in patients previously treated with a

purine analogue[262]. In a retrospective studies lenalidomide consolidation increased the PFS of patients treated with chemoimmunotherapy, and in patients receiving salvage therapy after relapse from FCR, lenalidomide resulted in similar survival outcomes to patients treated with repeat FCR[23]. A recent review resolved that a step wise dose escalation to a maximum tolerated dose of typically 10-15mg per day provided the best clinical outcomes[263]. However, the low response rates and rare complete remissions suggest that combination strategies would be required.

Lenalidomide exerts a plethora of effects on both the tumour and the microenvironment. Lenalidomide has been shown to inhibit the production of CXCL12 by stromal cells in the microenvironment which may reduce the migration of CLL cells to protective niches[264,265]. Lenalidomide also markedly increases the proliferation of NK and T cells in *in vitro* cultures of CLL PBMC[266]. *In vitro* lenalidomide treatment also appears to repair the CLL induced down-regulation of interferon response genes in NK cells from CLL patients[267]. T cells from CLL patients have impaired immunological synapse formation with CLL cells and it has been proposed that lenalidomide improves the formation of the synapse and therefore the effectiveness of T cell mediated killing[147]. Lenalidomide may also repair chemotherapy induced T cell dysregulation[268].

Leukaemia cell apoptosis induced by lenalidomide treatment correlated with the percentage of non-malignant immune cells and with the percentage of NKT-like cells in *in vitro* cultures, indicating that the CLL apoptosis is mediated by cytotoxic cells. Lenalidomide also enhanced the NKT cell activation response to αGalCer presented by DCs[269]. Lenalidomide was shown to contribute to the immune re-education of CLL associated macrophages leading to improved proliferation, phagocytic capability and T cell stimulatory capacity[270]. A phase 2 study involving CLL patients receiving 5mg per day found that Lenalidomide treatment resulted in reduced peripheral blood counts and increased T cell cytokine production[271].

For many years the mechanism by which lenalidomide exerted its effect in CLL was not well understood. However, recent breakthroughs identified the protein Cereblon, a subunit of the E3 ubiquitin ligase complex $CRL4^{CRBN}$, as the target of thalidomide binding

[272]. Further investigation determined that Lenalidomide binding to $CRL4^{CRBN}$ leads to the degradation of Ikaros and Aiolos[273] which are transcription factors essential for lymphoid development and differentiation[274]. While Lenalidomide does not have a direct cytotoxic effect in CLL cells it does suppresses CLL proliferation by inducing the upregulation of the cell cycle regulator $p21^{WAF1/Cip1}$ which has been shown to be important for the proliferative consequences of CD40L stimulation of CLL[275]. Lenalidomide treatment increases the costimulatory molecule expression of CLL cells[260,276] and decreases the inhibitory molecule expression, in particular the PD-L1, on T cells from CLL patients[255,277]. However, in CLL patients treated with either Lenalidomide alone, or lenalidomide in combination with a PD-1 antibody there was no effect on the proportion of CD4 or CD8 T cells which expressed PD-1[278]. Interestingly the combination of Lenalidomide with either PD-1 or PD-L1 blocking antibodies had an additive effect on the cytotoxic function of T cells in *in vitro* cultures of multiple myeloma patient's blood[279].

1.4.3 CAR T CELLS

Chimeric antigen receptor (CAR) T cells are genetically modified T cells, usually created using the patient's own T cells which are engineered to express a CAR with the internal signalling domains of a TCR coupled to a tumour specific antibody external recognition domain. In CLL patients, CD19 targeting CAR T cells have been highly successful, demonstrating that CAR-T therapy can establish long lived anti-tumour effector function[280] and CAR-T cell therapy have proved successful in patients who relapse after ibrutiib[281] and ASCT[282]. However, there remain a number of barriers to successful CAR-T cell therapy including technical challenges relating to determining the most effective CAR-T cells, the generation of sufficient time- and cost-effective infusion products and managing the significant toxicity profile of CAR-T therapy including a substantial risk of cytokine release syndrome. Despite the very good responses achieved in some patients, a meta-analysis of 134 CLL patients who received CAR-T cell therapy found the complete response rate to be only 20-30% of CLL patients and it remains unclear why many CLL patients fail to respond to CAR-T therapy. The fitness of the patients T cells used to make CAR-T cells[283,284] and the immunosuppressive environment that the CAR-T cells encounter in the patient have been implicated as potential barriers to CAR-T cell efficacy.

Interestingly, prior or concurrent ibrutinib treatment has been suggested to ameliorate both the risk of cytokine release syndrome[285] as well as contributing to improved CAR-T generation and engraftment[286]. These studies suggest that improved understanding of CLL patient T cell biology, especially after exposure to targeted therapies may help design future CAR-T manufacturing and potential combination treatment strategies.

1.5 COMBINATION THERAPIES FOR THE TREATMENT OF CLL

Despite demonstrating efficacy as monotherapies none of the targeted therapies in clinical development have yet demonstrated a cure for CLL. The initial clinical experiences with these therapies have suggested the need for continuous treatment to sustain remissions. This leads to increased risk of patients developing resistance, side effects and, given the high cost of these drugs, may be prohibitively expensive. As such there is significant interest in combination therapies with the goal of deepening responses and potentially leading to sustained remission after withdrawal of therapy. This has taken many avenues including combining different targeted therapies and combining targeted therapies with immunotherapy.

1.5.1 COMBINING MULTIPLE TARGETED THERAPIES

There is a substantial body of pre-clinical work supporting the combination of a BTK inhibitor and a Bcl-2 inhibitor[90,287–290]. While BTK inhibition results in CLL cell death due to inhibition of pro-survival signals from the microenvironment and the liberation of leukaemia cells from protective microenvironments, BTK inhibitors are not principally cytotoxic. Furthermore, BTK inhibition has been shown to upregulate pro-apoptotic Bcl-2 family members, importantly BIM[290]. Conversely, venetoclax is particularly effective at clearing tumour burden in the peripheral blood, however CLL cells in protective niches were more resistant to venetoclax[88]. Therefore, the combination of ibrutinib with venetoclax both liberates CLL cells from their protective niches and induces cell death, potentially to improving clinical responses over either drug as monotherapy.

Clinical evidence supporting the combination of ibrutinib and venetoclax is also emerging. In another indolent B cell malignancy Mantle cell lymphoma (MCL) a trial of ibrutinib plus

venetoclax resulted in significant clinical benefit, after only 16 weeks of therapy the ORR was 75% with 42% achieving a PET confirmed CR[291]. An early trial of ibrutinib, venetoclax and obinutuzumab in CLL showed 11 of the 12 patients responding after 1 year combination therapy, including 4 CR and 1 CRi[292].

1.5.2 Combining targeted therapy and immunotherapy

Multiple studies have investigated the combination of targeted therapies with anti-CD20 antibodies. However, despite the significant efficacy of both ibrutinib and rituximab as monotherapies, large phase 3 clinical studies of the combination of ibrutinib and rituximab have shown no clinical benefit over single agent ibrutinib in either in R/R or treatment naïve CLL[293,294]. Venetoclax on the other hand has been successfully combined with rituximab and obinutuzumab, achieving very high ORR[295,296]. Venetoclax plus lenalidomide treatment has not yet been reported in CLL, however current clinical trials include the combination of venetoclax, lenalidomide and rituximab in untreated MCL patients (NCT03523975) and obinutuzumab, venetoclax, and lenalidomide in treatment of patients with R/R B-cell Non-Hodgkin Lymphoma (NCT02992522).

The combination of ibrutinib and lenalidomide plus or minus rituximab is also being investigated in early phase clinical trials. A study of 11 CLL patients who received ibrutinib and lenalidomide suggested that the combination was tolerable, however 1 in 3 patients required lenalidomide dose reductions[297]. Early results from a phase 1 dose escalation trial of 12 CLL patients treated with ibrutinib, rituximab and lenalidomide had an ORR of 67%, and adverse effects were common, frequently leading to dose reduction or study withdrawal[298]. Notably, a trial of 48 follicular lymphoma patients treated with ibrutinib, lenalidomide and rituximab had an ORR of 97%, however 15% or patients had adverse events leading to drug withdrawal[299].

In BTK independent mouse models of cancer the therapeutic antitumor immunity induced by checkpoint blockade was enhanced by ibrutinib, presumably due to its effect on myeloid populations[300]. Multiple early phase clinical trials using ibrutinib in conjunction with PD-1 blockade have proven unsuccessful in CLL[301] but the combination remains promising as a treatment for Richter's transformation [302–304].

Finally, after promising results in mouse models[305] the combination of ibrutinib and CAR-T cells was found to increase response rates and decrease cytokine release syndrome[285]. Furthermore, in patients not achieving a response to ibrutinib at 6 months, the addition of CAR-T cells resulted in MRD negative CR in 8 of 9 patients[306].

1.6 AIMS

The importance and possible utility of the immune system to cancer treatment has become increasingly appreciated over the last decade. While the success of allogeneic haematopoietic stem cell transplants as a cure for CLL has long demonstrated the effectiveness of immune mediated control in CLL, the more recent success of adding immunotherapy to established chemotherapy regiments in the form of anti-CD20 antibodies has cemented immunotherapy as a viable treatment modality in CLL[307]. However, the use of immunotherapy for the treatment of CLL has been far from straightforward. The profound immune dysregulation that is caused by CLL, as well as the impact of established CLL treatments, limit the efficacy of immunotherapies that aim to reinvigorate existent immune cells.

The introduction of small molecule inhibitors into the treatment landscape of CLL has opened new avenues for the combination of immunotherapy. However, the rational combination of immunotherapies with targeted therapies requires understanding the immunological effects of the drugs with which immunotherapies are preceded by and combined with. To this end, this dissertation aims to answer the following questions.

1. Can gene expression analysis be used to understand the immune profile in CLL? (Chapter 3)
2. How does long-term continuous treatment with novel targeted therapies impact the immune profile of patients? (Chapter 4)
3. How do emerging targeted therapies for CLL impact the function of cytotoxic immune populations? (Chapter 5)
4. How does combination with targeted therapy augment the *in vitro* effects of immunotherapy? (Chapter 6)

2 MATERIALS AND METHODS

2.1 HUMAN SAMPLES

Peripheral blood and bone marrow aspirate samples were collected with informed consent from CLL patients at the Peter MacCallum Cancer Centre and Royal Melbourne Hospital under ethics approval of the respective institutions human research ethics committee and in accordance with the Declaration of Helsinki. Peripheral Blood Mononuclear Cells (PBMC) were isolated using Ficoll-Paque plus (GE Healthcare, Little Chalfont, UK) density gradient separation and cryopreserved in freeze mix containing 90% heat inactivated foetal calf serum (FCS) (Thermo Fisher Scientific, Massachusetts, USA), and 10% Dimethyl sulfoxide (DMSO) (Sigma Aldrich, Missouri, USA) and stored in liquid nitrogen. Peripheral blood samples from age matched healthy donors were obtained from the Australian Red Cross Blood Service with ethics approval from the Melbourne Health Human Research Ethics Committee.

2.2 CELL THAWING

Cryopreserved samples were incubated in a 37 °C water bath, until nearly thawed then added dropwise to 10 mL per 1 mL cells in pre-warmed T cell culture medium (TCM) consisting of Gibco RPMI media 1640 (Thermo Fisher Scientific), 10% v/v heat inactivated foetal calf serum (FCS) (Thermo Fisher Scientific), 1% v/v 4-(2-hydroxyethyl)-1-piperazineethanesulfonic acid (HEPES) (Thermo Fisher Scientific), 50 mM 2-Mercaptoethanol (2ME) (Sigma Aldrich, Missouri, USA), 1X Gibco GlutaMAX (Thermo Fisher Scientific), 1X Gibco MEM non-essential amino acids (Thermo Fisher Scientific), 1 mM Gibco sodium pyruvate (Thermo Fisher Scientific), 100 U/mL Penicillin/Streptomycin (Thermo Fisher Scientific). The cells were then washed twice by pelleting at 300 xg for 10 minutes, the aspirate discarded, and the cells resuspended in fresh warm TCM. Viable cell counts were obtained using a Countess II FL Automated Cell Counter (Thermo Fisher).

2.3 CELL CULTURE

Unless otherwise stated, cell cultures were performed in a humidified incubator at 37 °C with 5% CO_2 using TCM culture media

2.4 FLOW CYTOMETRY

Staining procedures were performed in round bottom 96 well plates or 5 mL FACS tubes, washing steps were performed by centrifugation of plates and tubes at 450 and 300 xg respectively and the supernatant vacuum aspirated and discarded. All incubation steps were performed in the dark at 4 °C. Prior to acquisition cells were filtered through a 70-micron cell strainer. Unless otherwise indicated flow cytometry was performed at the Flow Cytometry Facility (Doherty Institute, University of Melbourne) using a BD LSRFortessa and FACSDiva software.

Table 2.1 Reagents and buffers used in flow cytometry experiments

Reagents and buffers	Source or ingredients
Phosphate buffered saline (PBS)	Sigma Aldrich
FACS buffer	PBS containing 2% v/v FCS
Live/Dead™ aqua	Thermo Fisher Scientific
Fixable Viability Stain 700 (FVS700)	BD Biosciences
Human BD Fc Block™	BD Biosciences
FACS fix buffer	PBS containing 2% paraformaldehyde (Electron Microscopy Sciences)
Transcription Factor Buffer Set	BD Biosciences
Cytofix/Cytoperm™ kit	BD Biosciences

2.4.1 SURFACE MARKER STAINING PROTOCOL

Prior to staining with specific antibodies, cell preparations were stained with a fixable viability dye to facilitate dead cell exclusion in the analysis. Cells were washed in room temperature (RT) PBS, then stained with either 1/200 Live/Dead aqua or 1/1000 FVS700 depending on the flow panel used, concurrently treated with 1/100 F_C Block and were incubated for 20 minutes. Samples and appropriate single colour and fluorescent-minus-one (FMO) controls were washed once in ice-cold FACS buffer and resuspended in master mix containing the surface staining antibodies at pre-determined optimal dilutions and

incubated for 30 minutes. Stained cells were washed twice in FACS buffer before resuspension in FACS fix buffer.

2.4.2 *Intracellular cytokine staining*

Intracellular cytokine staining was performed using the Cytofix/Cytoperm kit according to manufacturer's instructions. Briefly, after staining for surface markers the cells were resuspended in 100 µL 1X Fix/Perm reagent and incubated for 20 minutes. Permeabilised cells were washed twice in 1X permwash buffer and stained with intracellular antibodies for 30 minutes, washed twice in 1X permwash buffer and resuspended in FACS buffer and immediately acquired.

2.4.3 *Intranuclear staining*

Intranuclear staining was performed using the Transcription Factor Buffer Set according to manufacturer's instructions. Briefly, after surface marker staining, the cells were fixed and permeabilised by incubation in 1X Transcription Factor Fix/Perm Buffer for 45 minutes. Permeabilised cells were then washed twice in 1X Transcription Factor Perm/Wash Buffer and stained with master mix containing the appropriate intracellular antibodies for 30 minutes. The cells were washed twice and resuspended in FACS buffer and immediately acquired.

2.5 Magnetic-activated cell sorting

2.5.1 *NK cell isolation*

NK cells were isolated from healthy donor PBMC using a negative selection magnetic-activated cell sorting (MACS) NK cell isolation kit (Miltenyi Biotec). Working on ice, PBMCs were washed once in cold MACS buffer (PBS, 0.5% FCS, 2 mM EDTA), resuspended in 40 µL of MACS buffer and 10 µL NK Cell Biotin-Antibody Cocktail per 1.0 x10^7 cells, mixed well and incubated at 4 °C for 5 minutes. 30 µL MACS buffer and 20 µL of NK Cell microbead cocktail per 1.0 x10^7 was added and incubated for 10 minutes at 4 °C. LS MACS columns were placed in the appropriate magnet and washed once with 3 mL MACS buffer prior to the application of cells. Cells were applied to the column through a 30 µm pre-

separation filter, the columns washed once with an additional 3 mL MACS buffer and flow through containing purified NK cells was collected.

2.5.2 CD19 DEPLETION

CLL cells were removed from CLL donor PBMC by positive selection using human CD19 microbeads (Miltenyi Biotec). Working on ice, the PBMCs were washed in cold MACS buffer then resuspended in 80 μL MACS buffer and 20 μL CD19 microbeads per 1.0 x10^7 cells and incubated at 4 °C for 15 minutes. LS MACS columns were placed in the appropriate magnet and washed once with 3 mL MACS buffer prior to the application of cells. Cells were washed in 1 mL MACS buffer per 1.0 x 10^7 cells and applied to LS column though a 30 μm pre-separation filter. The column was washed once with an additional 3 mL MACS buffer and the flow through containing depleted PBMC was collected.

2.6 IN VITRO FUNCTIONAL ASSAYS

Table 2.2 Targeted therapies used in in vitro experiments

Name	Target	Concentration	Vehicle	Source
Ibrutinib	BTK	1 μM	DMSO	Selleckchem
Acalabrutinib	BTK	1 μM	DMSO	Selleckchem
Zanubrutinib	BTK	1 μM	DMSO	BeiGene
Venetoclax	Bcl-2	1 nM	DMSO	Selleckchem

Table 2.3 Immunotherapies used in in vitro experiments

Name	Target	Concentration	Vehicle	Source
Lenalidomide	Cereblon	10 μM	DMSO	Cayman Chemical
BGB-A317	PD-1	10 μg/mL	PBS	BeiGene

Table 2.4 Reagents used in functional assays

Reagent	Role	Source
Human T Cell Activation/Expansion kit	CD2/CD3/CD28 T cell stimulation beads	Miltenyi Biotec
Human NK Activation/Expansion kit	CD2/NKp46 NK stimulation beads	Miltenyi Biotec
Golgistop™	Protein transport inhibitor	BD Biosciences
Golgiplug™	Protein transport inhibitor	BD Biosciences

2.6.1 *DEGRANULATION ASSAYS USING BEAD STIMULATION*

Cryopreserved samples from healthy donors or from CLL patients were thawed and plated at 1.0 x10^6 cells per mL in a 24 well plate either as whole PBMC for T cell degranulation assays or MACS purified NK cells for NK degranulation assays. Cultures were treated with the targeted therapies outlined in Table 2.2 or equivalent volume DMSO and were incubated for twelve hours prior to stimulation for four hours with CD2/CD3/CD28 T cell stimulation beads or CD2/NKp46 NK cell stimulation beads in the presence of a 1/1000 dilution protein transport inhibitors and a 1/20 dilution anti-human CD107a APC conjugated antibody (clone H4A3, BD). The cells were then stained according to the standard ICS protocol (section 2.4.2) using the antibodies detailed in Table 2.5 and analysed according to gating strategy in Figure 2.1.

Table 2.5 Antibodies used in degranulation assay

Specificity	Clone	Fluorochrome	Dilution	Source
CD8α	RPA-T8	Brilliant violet™ 650	1/400	BioLegend
IL-4	MP4-25D2	Brilliant violet™ 711	1/20	BD Biosciences
CD3	OKT3	Brilliant violet™ 785	1/200	BioLegend
CD107a	H4A3	APC	1/20	BD Biosciences
CD4	RPA-T4	APC Cy7	1/200	BD Biosciences
Granzyme B	GB11	FITC	1/20	BD Biosciences
CD56	B159	BB700	1/25	BD Biosciences
IFNγ	B27	PE	1/20	BD Biosciences
CD19	SJ25-C1	PE Cy7	1/200	BD Biosciences

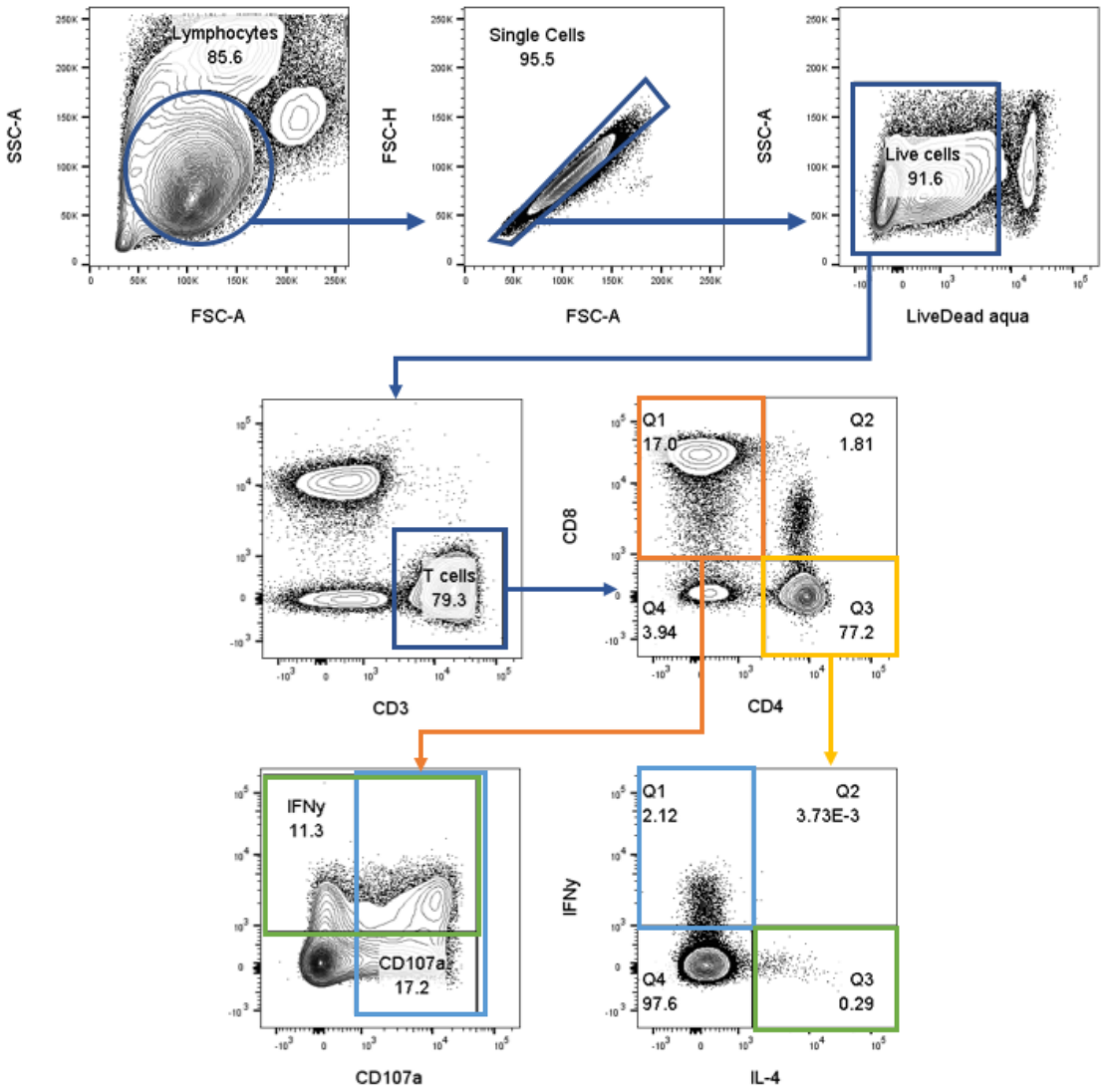

Figure 2.1 Gating strategy used in analysis of T cell degranulation and cytokine production

Lymphocytes were initially gated based on forward scatter (FSC) and side scatter (SSC), followed by sequential singlet gating. Dead cells were excluded by positive staining with the fixable viability dye LiveDead aqua. CD8 T cells were defined as CD3+CD19-CD4-CD8+ (orange), of this population the percent positive for IFNγ (green) and CD107a (blue) were gated. CD4 T cells were defined as CD3+CD19-CD8-CD4+ (yellow) and the percent positive for IFNγ (blue) and IL-4 gated (green).

2.6.2 *NKT DEGRANULATION ASSAY USING CLL AS ANTIGEN PRESENTING CELLS*

Cryopreserved healthy donor derived *ex vivo* expanded purified NKT cells and alpha-galactosylceramide (αGalCer) (KRN7000 in tween/sucrose buffer) were kindly provided by the Godfrey laboratory (Doherty Institute, University of Melbourne). CLL cells from a single donor with a CD19+CD5+ cell purity of >95% were thawed and co-cultured with irradiated (30 gray) adherent HS-5 bone marrow stromal cells (provided by Giles Best, University of Sydney). Co-cultures were either treated with αGalCer or left untreated and incubated for 18 hours. At the same time, NKT cells were thawed and aliquoted at 1.0 x10^5 cells per well in 100 μL TCM and treated with targeted therapies (Table 2.2) or equivalent volume DMSO and incubated for 18 hours with 100 IU/mL recombinant human IL-2 (rhIL-2) (Teceleukin) supplemented TCM. Experimental procedure is outlined in Figure 2.2.

CLL cells were removed from co-culture and resuspended in fresh TCM. NKT cells were washed in TCM to remove free drug and treated with protein transport inhibitors and 1/20 dilution anti-CD107a antibody immediately prior to stimulation with CD2/CD3/CD28 T cell stimulation beads or co-culture with activated CLL target cells at a 1:3 effector to target ratio and cultured for 4 hours. The cells were then stained using standard staining procedures and panel detailed in Table 2.6 and analysed by flow cytometry (gating strategy outlined in Figure 2.3.

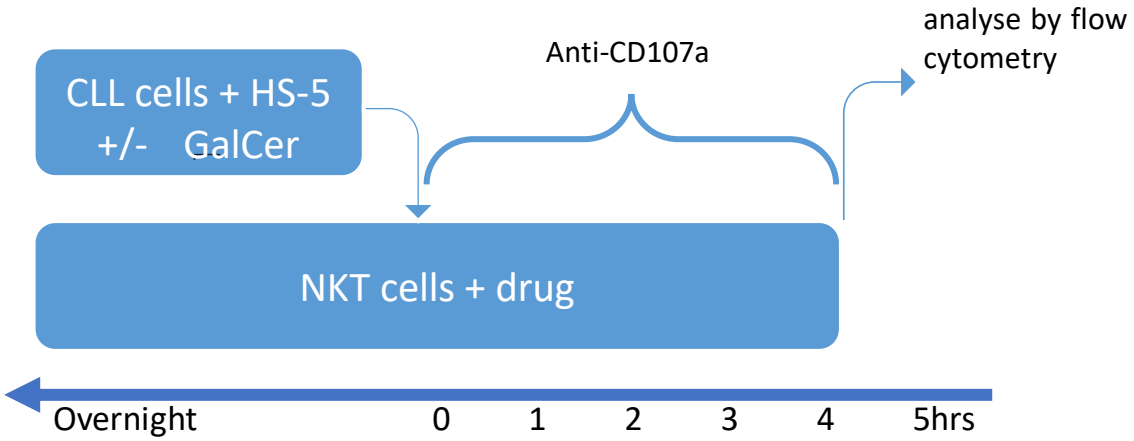

Figure 2.2 Diagram of degranulation assay using CLL as APC

Table 2.6 Antibodies used in the NKT degranulation assay

Specificity	Clone	Fluorochrome	Dilution	Source
NKT tetramer	hCD1d-PBS44	Brilliant violet™ 421	1/1000	Godfrey
CD8	RPA-T8	BD Horizon Brilliant™ Ultraviolet (BUV) 395	1/200	BD Biosciences
CD3	OKT3	BUV805	1/100	BD Biosciences
CD107a	H4A3	APC	1/20	BD Biosciences
CD4	RPA-T4	APC Cy7	1/200	BD Biosciences
GrB	GB11	FITC	1/20	BD Biosciences
IFNγ	B27	PE	1/20	BD Biosciences
CD19	SJ25-C1	PE Cy7	1/200	BD Biosciences

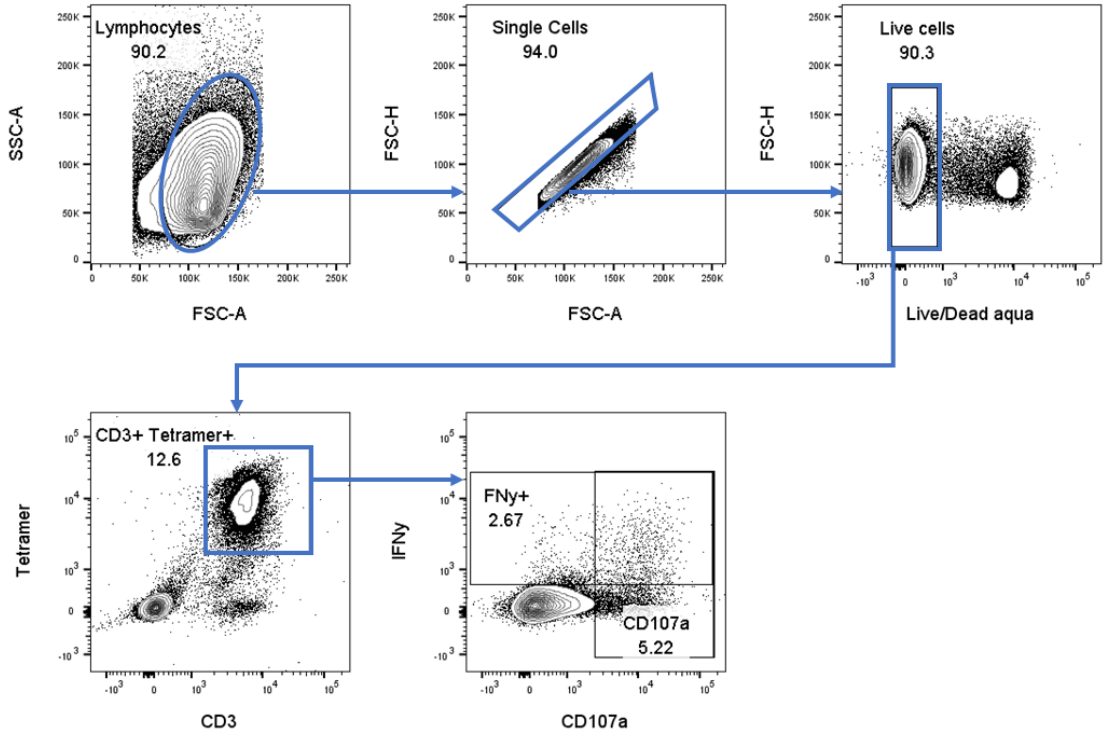

Figure 2.3 Gating strategy for the identification of NKT cell degranulation

Single cell lymphocytes were initially gated based on FSC and SSC. Dead cells were excluded by staining using the fixable viability dye LiveDead aqua. NKT cells were defined as CD3+Tetramer+ cells and the percent positive for IFNγ and CD107a gated.

2.6.3 *NKT CELL KILLING ASSAY*

As in the NKT cell degranulation assay, NKT cells from 5 donors were thawed, treated with targeted therapies outlined in Table 2.2 and cultured overnight in 100 IU/mL recombinant human IL-2 supplemented TCM. PBMC from a single donor CLL donor were co-cultured over night with irradiated HS-5 cells and 100 ng/mL αGalCer. NKT cells were washed in fresh media to remove free drug. CLL cells were removed from co-culture, stained with carboxyfluorescein succinimidyl ester (CFSE) (BD Biosciences) prior to co-culture at an effector target ratio of 1:3 for 6 hours with NKT cells. Cells were collected, stained with surface markers according to standard protocol using antibodies in Table 2.7 and then resuspended in annexin binding buffer and incubated at RT for 15 minutes with 1/20 7-aminoactinomucin D (7AAD) and 1/20 annexin V APC (BioLegend) before the addition of 400 μL annexin binding buffer and acquisition.

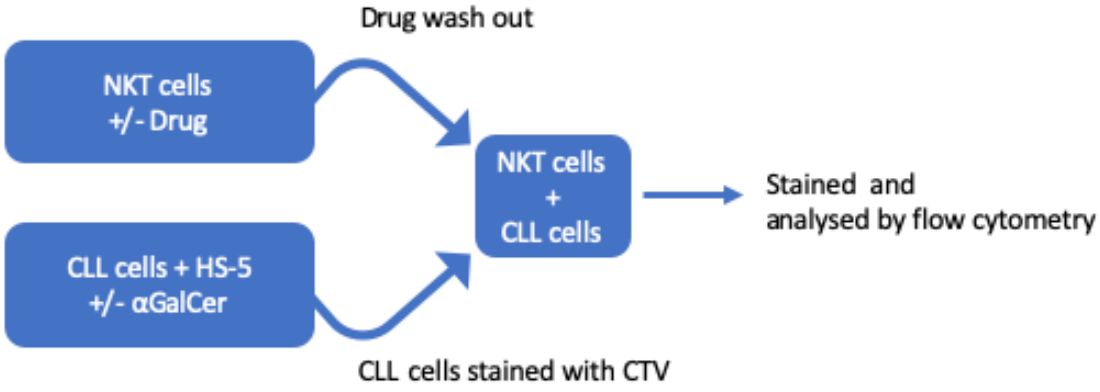

Figure 2.4 Diagram of NKT cell killing assay

Table 2.7 antibodies used in NKT cell killing assay

Specificity	Clone	Fluorochrome	Dilution	Source
NKT tetramer	hCD1d-PBS44	Brilliant violet™ 421	1/1000	Godfrey
CD8α	RPA-T8	Brilliant violet™ 650	1/400	BioLegend
CD3	OKT3	Brilliant Violet™ 785	1/200	BD Biosciences
CD4	RPA-T4	APC Cy7	1/200	BD Biosciences

2.6.4 *PROLIFERATION CULTURES*

Whole PBMC from healthy donors or CLL patients, CD19 depleted CLL patient PBMC and MACS isolated NK cells were stained with 5 μM CellTrace violet (CTV) (Thermo Fisher Scientific) according to manufacturer's instructions and plated at 1.0 x 10^6 /mL TCM in a 24 well plate with 5 μL/mL T cell or CD2/NKp46 NK cell stimulation beads. Cultures were treated with the targeted therapies in Table 2.2 alone or in combination with immunotherapies listed in Table 2.3 or equivalent volume DMSO as a vehicle control. Cultures were maintained for seven days. For T cell proliferation experiments half the cells were removed from culture for analysis, the media refreshed and 20 IU/mL rhIL-2 was added on days 3, 5 and 7. For NK proliferation experiments 500 IU/mL rhIL-2 was included from day 0 and the media refreshed on days 3, 5 and 7. Drug concentrations were maintained throughout the expansion. The cells were stained according to the standard surface staining protocol using the antibodies outlined in Table 2.8 or Table 2.9.

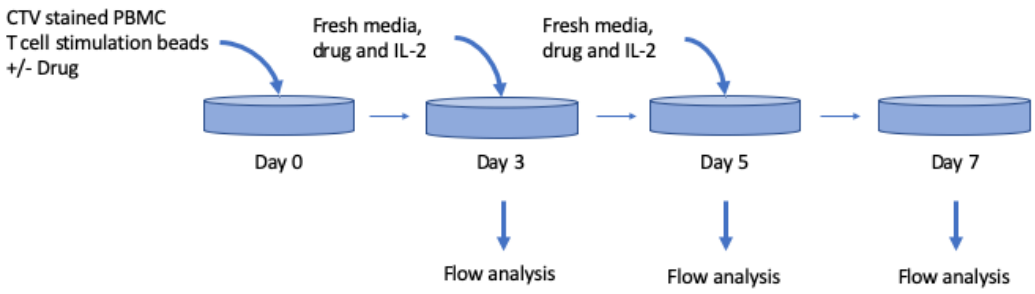

Figure 2.5 Diagram of T cell proliferation assay experimental procedure

Table 2.8 Antibodies used in T cell proliferation assays

Specificity	Clone	Fluorochrome	Dilution	Supplier
LAG-3	T47-530	APC	1/100	BD Biosciences
HLA DR	G46-6	APC-H7	1/200	BD Biosciences
CD27	O323	Brilliant Violet™ 711	1/100	BioLegend
PD-1	EH12.1	Brilliant Violet™ 786	1/50	BD Biosciences
TIM-3	7D3	PE	1/50	BD Biosciences
CD19	SJ25-C1	PE-Cy7	1/200	BD Biosciences
γδ TCR	TCRγ/δ-1	FITC	1/50	BD Biosciences
CD45RA	HI100	PerCP-Cy5.5	1/100	Thermo Fisher Scientific
CD4	SK3	BUV395	1/200	BD Biosciences
CD3	UCHT1	BUV496	1/100	BD Biosciences
CD8	SK1	BUV805	1/100	BD Biosciences

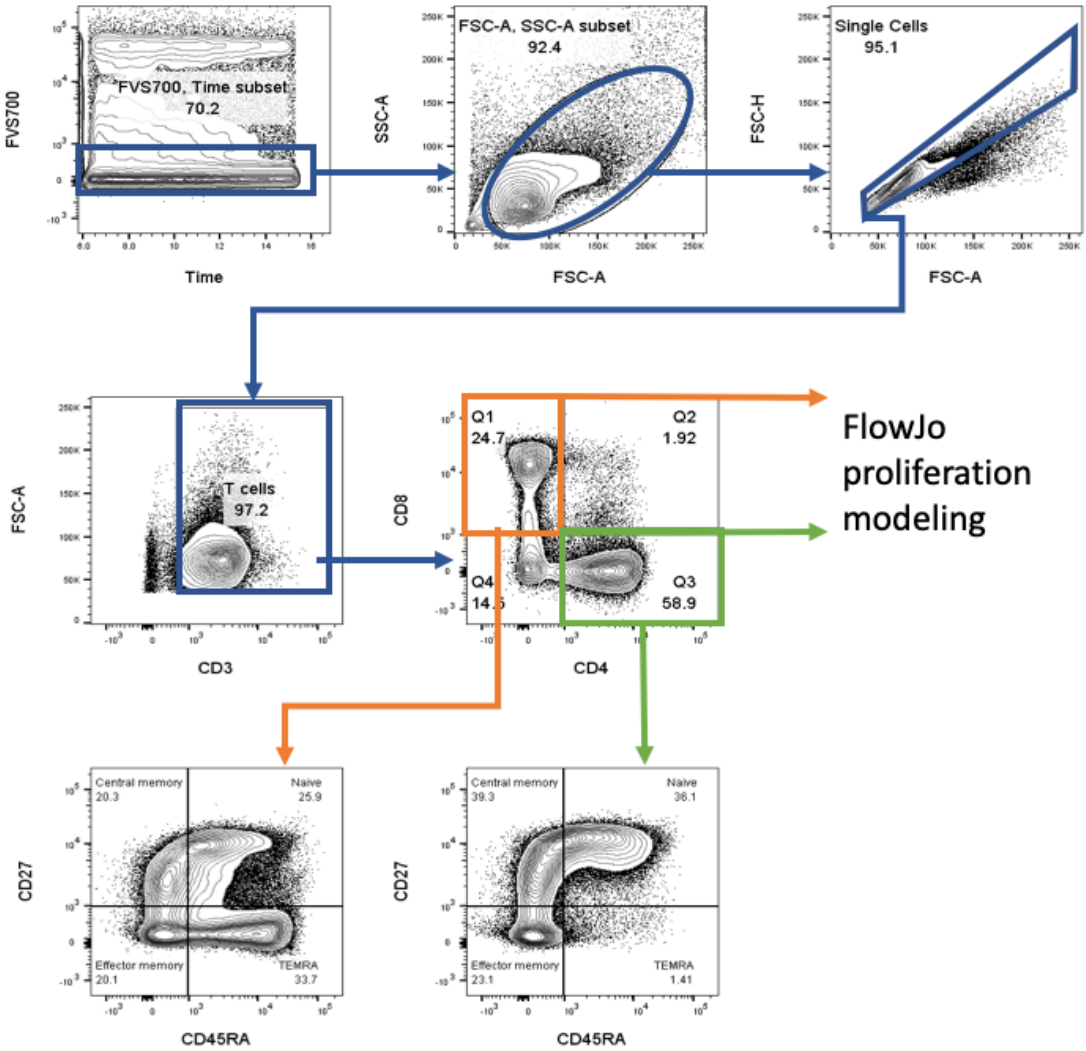

Figure 2.6 Gating strategy for the analysis of T cell proliferation

Dead cells were excluded by staining for the fixable viability dye FVS700. Single cells were gated based on FSC and SSC. CD8 T cells were defined as CD3+CD19-CD4-CD8+ (orange) and CD4 T cells were defined as CD3+CD19-CD8-CD4+ (green). Of the CD4 and CD8 populations Naïve (CD45RA+CD27+), central memory (CD45RA-CD27+), effector memory (CD45RA-CD27-) and T_{EMRA} (CD45RA+CD27-) were gated.

Table 2.9 Antibodies used in NK cell proliferation assays

Specificity	Clone	Fluorochrome	Dilution	Supplier
NKG2A	REA110	APC	1/100	Miltenyi Biotec
HLA-DR	G46-6	APC-H7	1/200	BD Biosciences
CD16	3G8	Brilliant Violet™ 650	1/100	BioLegend
CD11b	M1/70	Brilliant Violet™ 711	1/400	BioLegend
CD27	CD27	Brilliant Violet™ 786	1/25	BD Biosciences
KIR2D	NKVFS1	PE	1/400	Miltenyi Biotec
KIR3DL1	DX9	PE	1/100	Miltenyi Biotec
NKG2D	1D11	PE-CF594	1/50	BD Biosciences
CD19	SJ25-C1	PE-Cy7	1/200	BD Biosciences
CD57	HCD57	FITC	1/50	BioLegend
CD56	B159	Brilliant™ Blue 700	1/25	BD Biosciences
CD14	MϕP9	BUV395	1/100	BD Biosciences
CD3	UCHT1	BUV496	1/25	BD Biosciences
CD8	SK1	BUV805	1/100	BD Biosciences

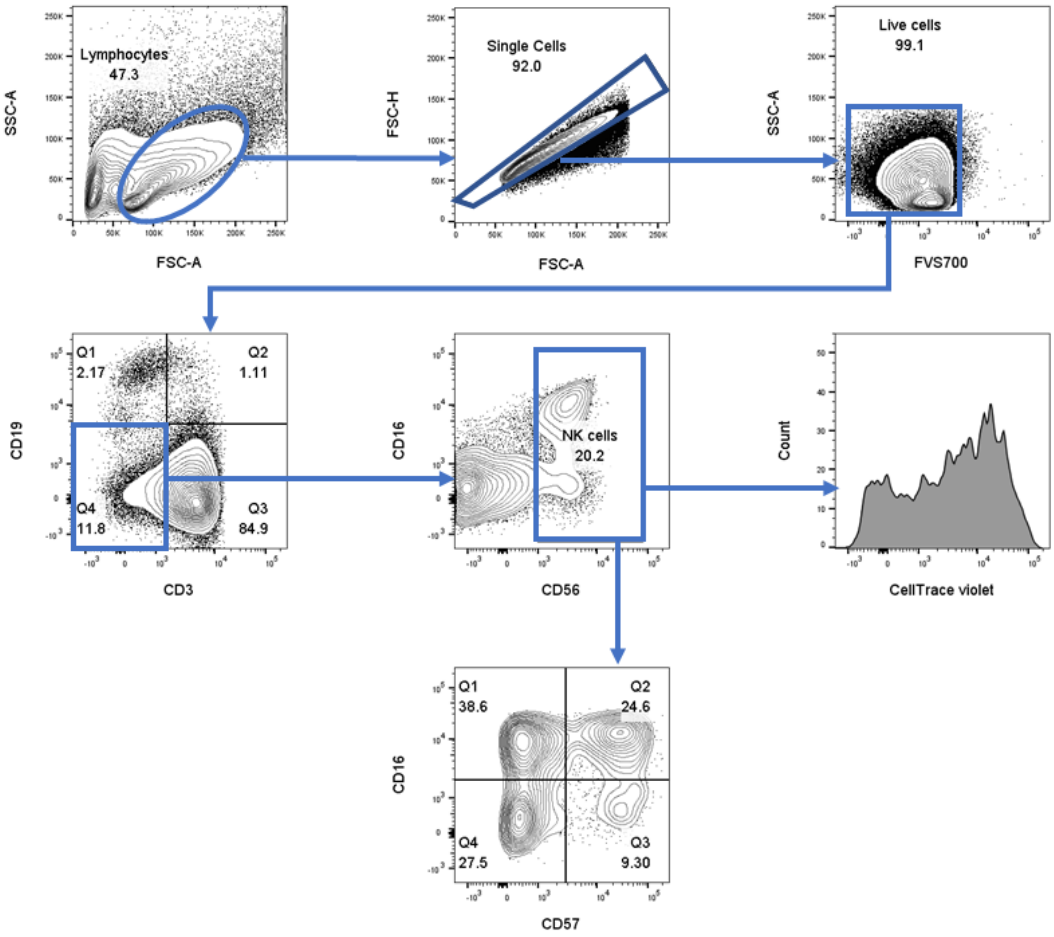

Figure 2.7 Gating strategy used in the analysis of NK cell proliferation

Single lymphocytes were initially gated based on FSC and SSC. Dead cells were excluded by staining using the fixable viability dye LiveDead aqua. NK cells were defined as CD3-CD19-CD56+ cells. Proliferation modelling was performed based in CTV dilution.

2.6.5 *CYTOMETRIC BEAD ARRAY*

Whole PBMC was cultured in TCM at 1.0 x10^6 /mL in a flat bottom 24 well plate. 5 μL CD2/CD3/CD28 T cell stimulation beads were added per 1.0x10^6 PBMC for 24 hours. Cell culture plates were centrifuged at 450g for 5 minutes and 100 μL of the supernatant collected and stored at -20 °C prior to analysis. The Human Th1/Th2/Th17 cytokine cytometric bead array kit (BD Biosciences) was used to quantify the concentration of IL-2, IL-4, IL-6, IL-10, IL17A, IFNγ and TNFα. Experiments were performed according to the manufacturer's instructions. 10 μL of each thawed supernatant or standard in triplicate, 10 μL of the bead master mix and 10 μL PE detection reagent was added to a 96 well plate and incubated for 3 hours at room temperature. The beads were washed in 200 μL wash buffer, centrifuged at 200 g for 5 minutes and the supernatant discarded. The beads were resuspended in 300 μL wash buffer before acquisition on a BD FACSCanto using the appropriate FACS Diva template. Analysis was performed using the FCAP Array program (BD).

2.7 IMMUNE PROFILING

2.7.1 FLOW CYTOMETRY

Cryopreserved PBMC samples acquired from CLL patients treated with either ibrutinib, zanubrutinib or venetoclax were thawed and stained according to the standard protocols detailed in Section 2.2 and Section 2.4.1 using the flow panels indicated below.

Table 2.10 Antibodies used in innate cell immune profiling

Specificity	Clone	Fluorochrome	Dilution	Supplier
CD123	9F5	Brilliant Violet™ 421	1/100	BD Biosciences
CD5	UCHT2	Brilliant Violet™ 605	1/200	BD Biosciences
CD163	GHI/61	Brilliant Violet™ 711	1/25	BD Biosciences
CD3	OKT3	Brilliant Violet™ 786	1/200	BioLegend
CD56	B159	APC	1/50	BD Biosciences
PD-L1	130021	Alexa Fluor®700	1/50	R&D systems
HLA-DR	G46-6	APC-H7	1/200	BD Biosciences
CD11b	M1/70	FITC	1/200	BioLegend
CD16	3G8	PerCP Cy5.5	1/100	BioLegend
CD19	SJ25-C1	PE	1/50	BD Biosciences
CD14	MϕP9	PE-CF594	1/400	BD Biosciences
CD11c	B-ly6	PE-Cy5	1/200	BD Biosciences
CD33	P67.6	PE-Cy7	1/200	BD Biosciences

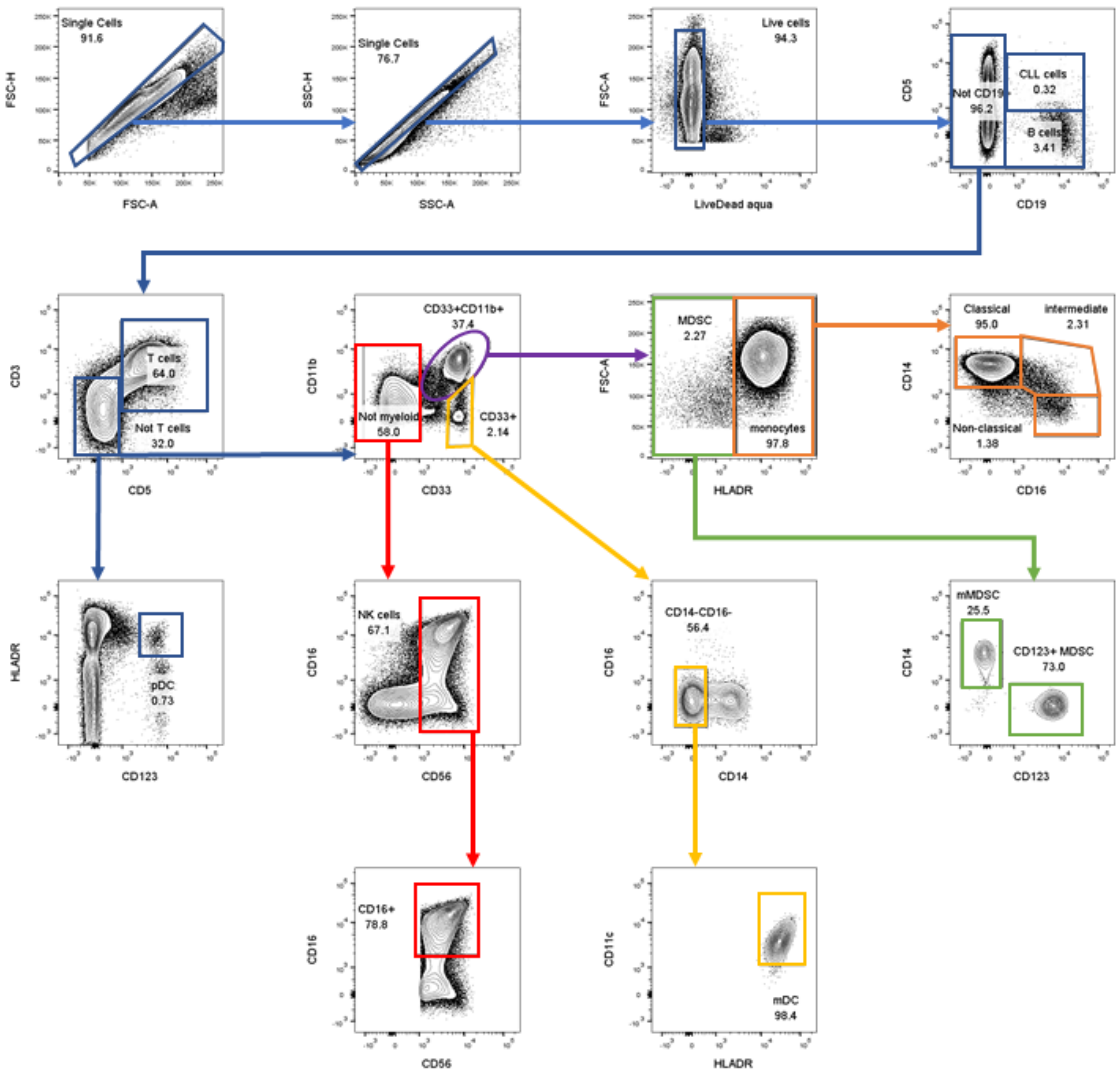

Figure 2.8 Gating strategy used in the analysis of innate immune cells

Single cell lymphocytes were initially gated based on FSC and SSC. Dead cells were excluded by staining using the fixable viability dye LiveDead aqua. T cells were gated as CD19-CD3+. pDCs were gated as CD19-CD3-CD123+HLADR+. mDC (yellow) were gated as CD19-CD3-CD33+CD11c+HLADR+. Monocytes (orange) were gated as CD19-CD3-CD11b+CD33+HLADR+, and further classified into classical (CD14++CD16-), intermediate (CD14+CD16+), and classical (CD14low CD16+) subsets. MDSC (green) were gated as CD19-CD3-CD11b+CD33+HLADR^{low} and further subsetted based on CD14 and CD123 staining. NK cells (red) were gated as CD19-CD3-CD33-CD56+ cells and further subsetted by CD16 expression.

Table 2.11 Antibodies used in T cell immune profiling

Specificity	Clone	Fluorochrome	Dilution	Supplier
NKT tetramer	hCD1d-PBS44	Brilliant Violet™ 421	1/1000	Godfrey Lab
CD5	UCHT2	Brilliant Violet™ 605	1/200	BD Biosciences
CD8a	RPA-T8	Brilliant Violet™ 650	1/400	BioLegend
CD27	O323	Brilliant Violet™ 711	1/200	BioLegend
CD3	OKT3	Brilliant Violet™ 786	1/200	BioLegend
CD19	SJ25-C1	APC	1/100	BD Biosciences
CD45RO	UchL1	Alexa Fluor®700	1/200	BioLegend
CD4	RPA-T4	ACP-Cy7	1/200	BD Biosciences
γδ TCR	TCRγ/δ-1	FITC	1/50	BD Biosciences
CD45RA	PerCP Cy5.5	PerCP-Cy5.5	1/100	Thermo Fisher Scientific
CD1d	CD1d42	PE	1/20	BD Biosciences
CD62L	DREG-56	PE-CF594	1/400	BD Biosciences
CCR7	3D12	PE-Cy7	1/100	Thermo Fisher Scientific

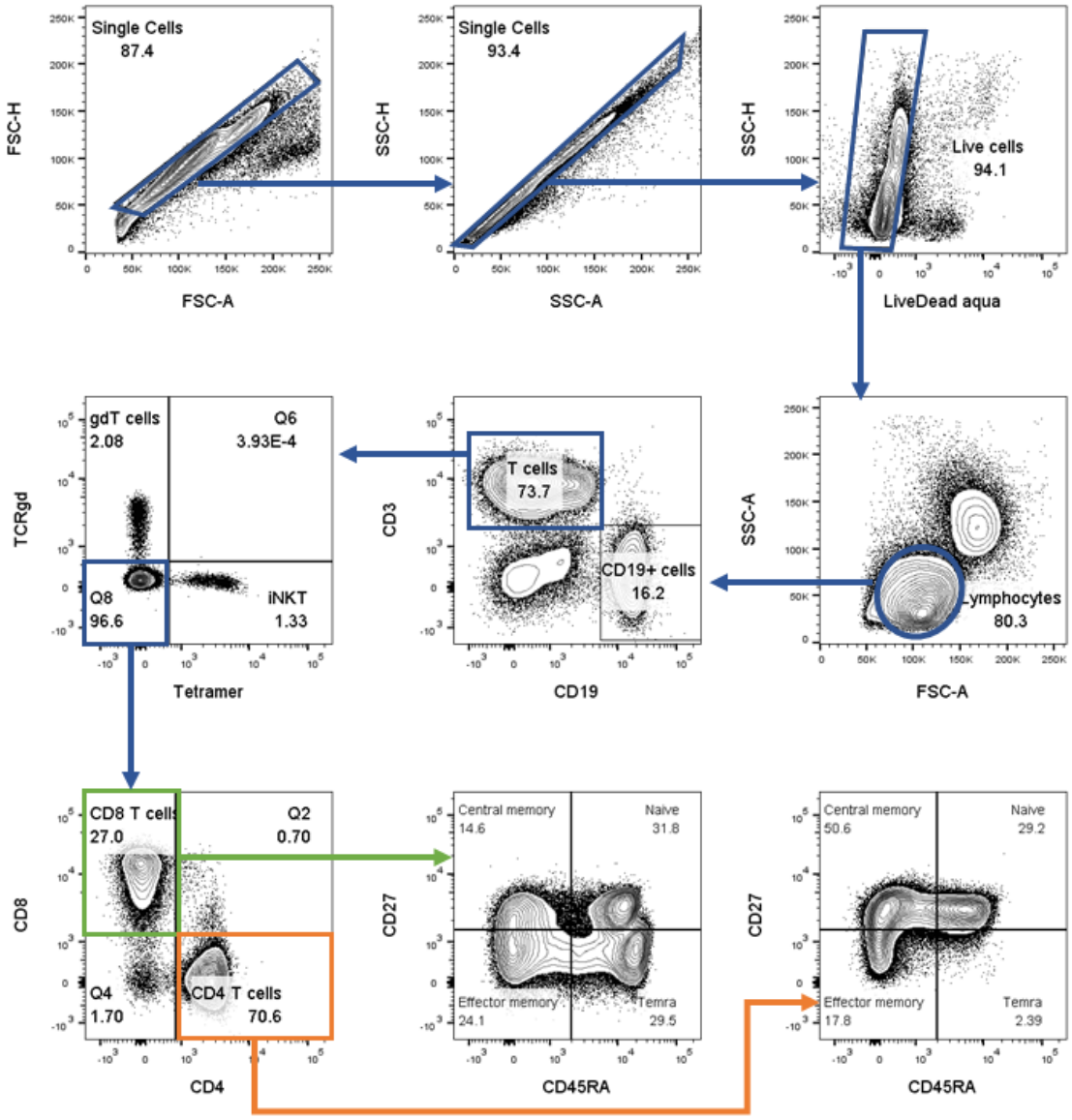

Figure 2.9 Gating strategy for the identification of T cell populations

Single lymphocytes were initially gated based on FSC and SSC. Dead cells were excluded by staining using the fixable viability dye LiveDead aqua. γδT cells were gated as CD3+γδTCR+. NKT cells were CD3+Tetramer+. CD4 cells (green) were CD3+γδTCR-Tetramer-CD8-CD4+ and CD8 T cells (orange) were gated as CD3+γδTCR-Tetramer-CD8+CD4-. The CD4 and CD8 populations were distinguished as naïve (CD45RA+CD27+), central memory (CD45RA-CD27+), effector memory (CD45RA-CD27-) and T_{EMRA} (CD45RA+CD27-).

Table 2.12 Antibodies used in CD4 T cell subpopulation analysis

Target	Clone	Fluorochromes	Dilution	Supplier
CD127	HIL-7R-M21	Alexa Fluor®647	1/25	BD Biosciences
HLA-DR	G46-6	APC-H7	1/50	BD Biosciences
CCR7(CD197)	150503	Brilliant Violet™ 421	1/50	BD Biosciences
CD38	HB7	Brilliant Violet™ 605	1/200	BD Biosciences
CD27	CD27	Brilliant Violet™ 786	1/25	BD Biosciences
CCR6(CD196)	11A9	PE	1/50	BD Biosciences
FOXP3	259D/C7	PE-CF594	1/20	BD Biosciences
CD45RO	UCHL1	PE-Cy7	1/100	BD Biosciences
CD25	M-A251	BB515	1/25	BD Biosciences
CXCR3(CD182)	1C6/CXCR3	BB700	1/50	BD Biosciences
CD4	SK3	BUV395	1/200	BD Biosciences
CD3	UCHT1	BUV496	1/200	BD Biosciences
CD8	SK1	BUV805	1/100	BD Biosciences

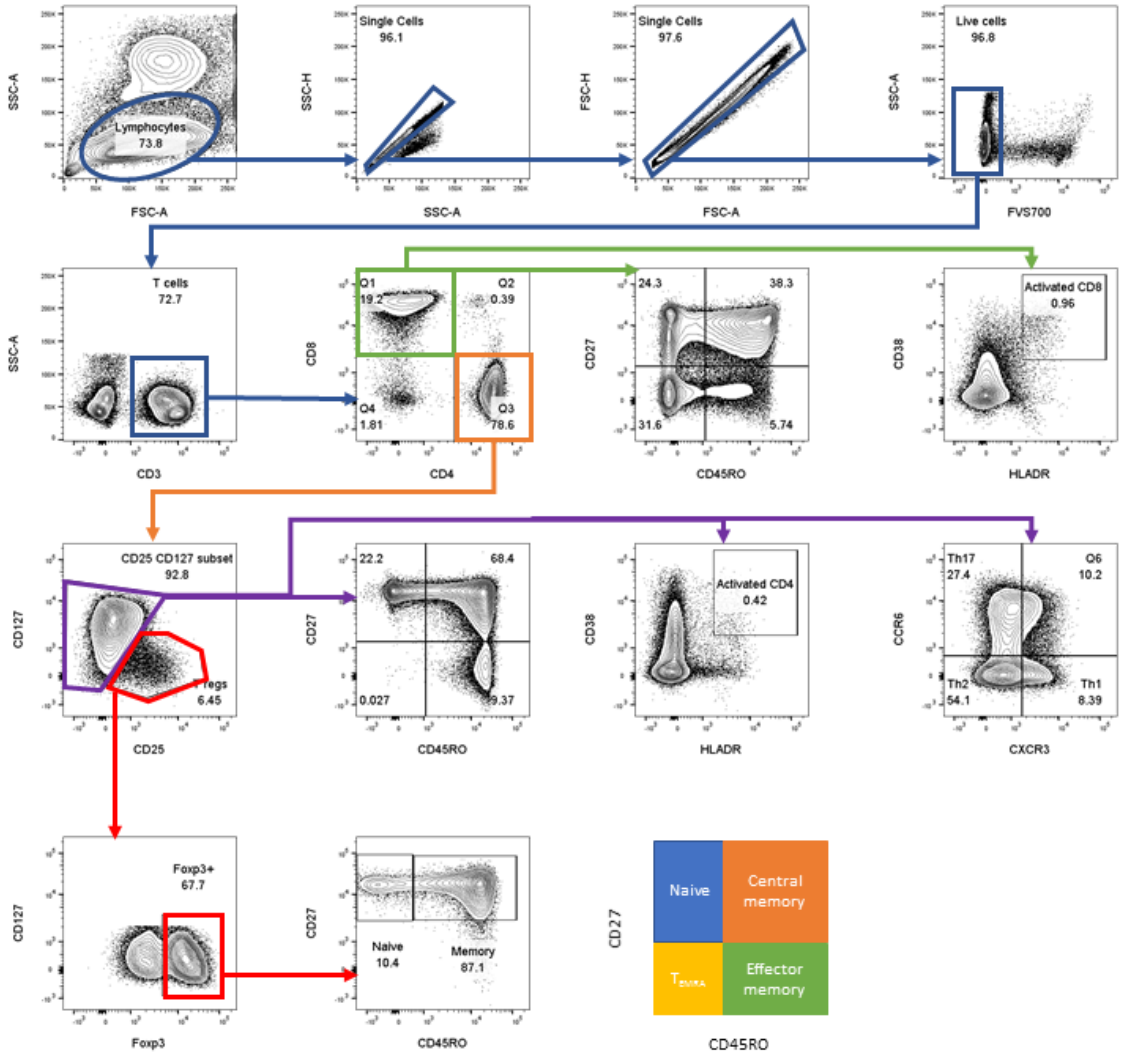

Figure 2.10 Gating strategy for the identification of CD4 T cell populations

Single lymphocytes were initially gated based on FSC and SSC. Dead cells were excluded by staining using the fixable viability dye FVS700. CD8 T cells were gated as CD3+CD8+ and further subsetted into memory phenotype by CD45RO and CD27 expression. Activated CD8 T cells were defined as CD3+CD8+CD38+HLADR+. CD4 T cells were gated as CD3+CD4+ and further subsetted into CD3+CD4+CD25+CD127-FoxP3+ T_{regs} (red). The CD127+CD25- CD4 T cells were further subsetted into memory phenotype by CD45RO and CD27 expression. Activated CD8 T cells were defined as CD3+CD4+CD38+HLADR+. T_H1 cells were gated as CD3+CD4+CXCR3+CCR6-, T_H2 cells were gated as CD3+CD4+CXCR3-CCR6- and T_H17 cells were gated as CD3+CD4+CXCR3-CCR6+.

Table 2.13 Antibodies used in unconventional T cell analysis

Target	Clone	Fluorochrome	Dilution	Supplier
NKG2A	REA110	APC	1/100	Miltenyi Biotec
CD45RA	HI100	APC-H7	1/25	BD Biosciences
NKT Tetramer	hCD1d-PBS44	Brilliant Violet™ 421	1/1000	Godfrey
CD27	L128	Brilliant Violet™ 480	1/100	BD Biosciences
CD56	B159	Brilliant Violet™ 650	1/100	BD Biosciences
Vδ2	B6	Brilliant Violet™ 711	1/50	BioLegend
KIR2D	NKVFS1	PE	1/400	Miltenyi Biotec
KIR3DL1	DX9	PE	1/100	Miltenyi Biotec
NKG2D	1D11	PE-CF594	1/50	BD Biosciences
γδ TCR	11F2	PE-Cy7	1/50	BD Biosciences
Vδ1	TS8.2	FITC	1/50	Thermo Fisher Scientific
CD8	RPA-T8	BUV395	1/25	BD Biosciences
CD3	UCHT1	BUV496	1/25	BD Biosciences
CD4	SK3	BUV805	1/100	BD Biosciences

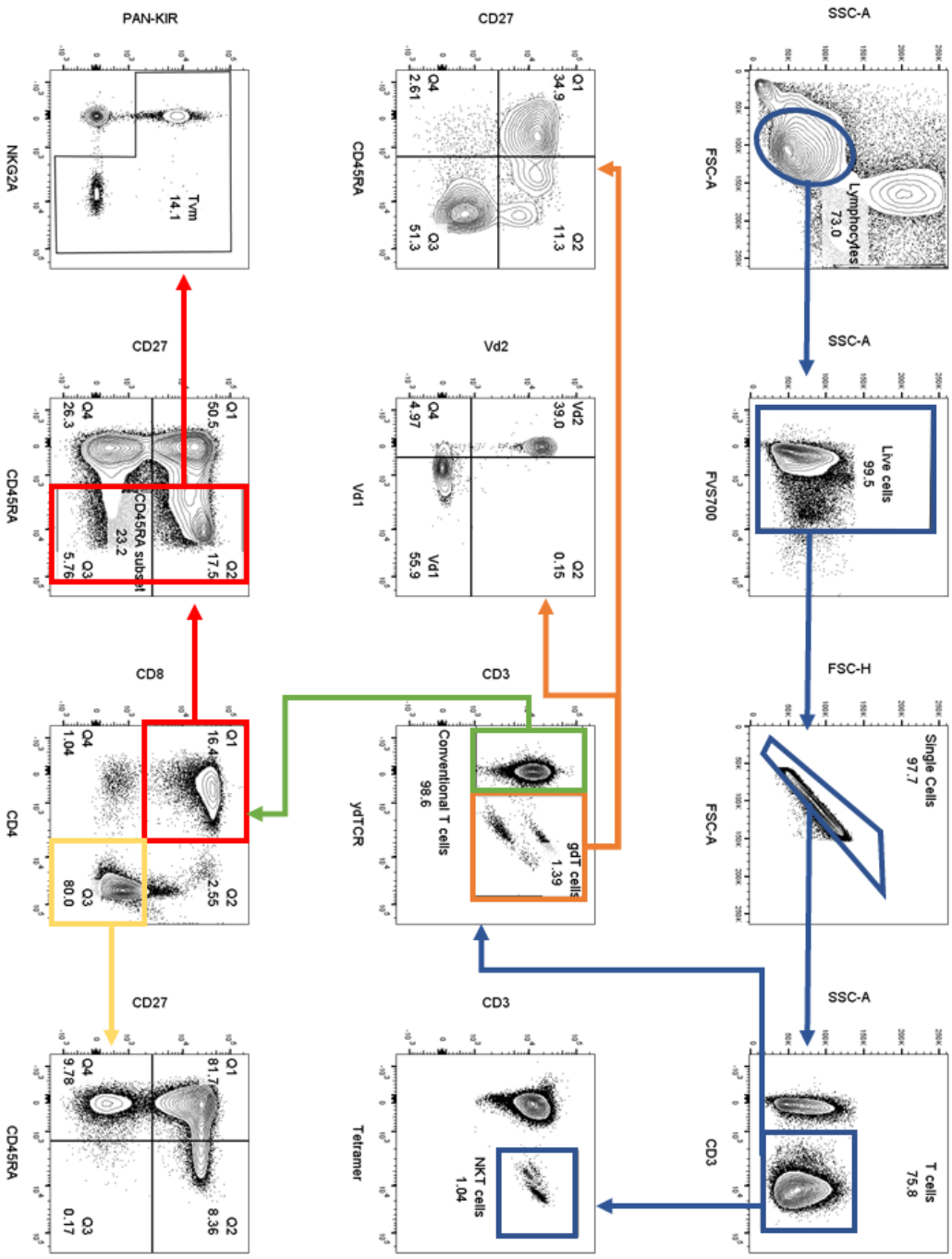

Figure 2.11 Gating strategy for the identification of unconventional T cell subsets
Single lymphocytes were initially gated based on FSC and SSC. Dead cells were excluded by staining using the fixable viability dye FVS700. NKT cells were defined as CD3+Tetramer+. γδT cells were defined as CD3+γδTCR+ and further stratified into Vδ1 and Vδ2 subsets. CD4 T cells were defined as CD3+γδTCR-CD8-CD4+. CD8 T cells were defined as CD3+γδTCR-CD8+CD4-. T_{VM} cells were defined as CD3+γδTCR-CD8+CD45RA+NKG2A+/panKIR+

2.7.2 GENE EXPRESSION ANALYSIS

Gene expression analysis was performed using the NanoString planform and the nCounter PanCancer immune profiling panel. Comprehensive methods are detailed in Chapter 3.

2.8 DATA VISUALISATION AND STATISTICAL ANALYSIS

Analysis of flow data analysis was performed using FlowJo Version 10 (FlowJo LLC, Oregon, USA). CBA data was analysed using FCAP array software (BD Biosciences). All statistical analysis and graphical representations in Chapters 3-6 was performed using GraphPad Prism V8 (GraphPad software, California, USA) except Figure 4.2 which was generated in Microsoft PowerPoint (Microsoft, Washington, USA) each circle represents an immune population with the diameter denoting to the average proportion of live cells as determined by flow cytometry analysis. NanoString gene expression data analysis is detailed in Chapter 3.

3 COMPARISON OF GENE EXPRESSION AND FLOW CYTOMETRY FOR IMMUNE PROFILING IN CHRONIC LYMPHOCYTIC LEUKAEMIA

3.1 SUMMARY

A particular focus of this study was on the long-term changes to the immune system that occur while patients are treated with targeted therapies. While flow cytometry is a powerful tool to understand the immune system, longitudinal analysis requires investigator forethought and expensive processing and storage of viably cryopreserved samples. Most commonly only molecular samples are stored and therefore the ability to use gene expression to understand the immune profile would expand the possibilities for analysis of retrospective cohorts. Using the NanoString PanCancer immune profiling panel, this analysis examined PBMC samples from CLL patients treated with either targeted therapy for 12 months. This data demonstrates that gene expression provides an immune abundance score that was highly correlated to the quantification of the same subsets by flow cytometry.

Journal of Immunological Methods 463 (2018) 97–104

Contents lists available at ScienceDirect

Journal of Immunological Methods

journal homepage: www.elsevier.com/locate/jim

Comparison of gene expression and flow cytometry for immune profiling in chronic lymphocytic leukaemia

Chia Sharpe[a,b,*], Joanne Davis[a,b], Kylie Mason[a,b,c], Constantine Tam[d,e], David Ritchie[a,b,c], Rachel Koldej[a,b]

[a] ACRF Translational Research Laboratory, Royal Melbourne Hospital, Melbourne, Victoria, Australia
[b] Faculty of Medicine, Dentistry and Health Sciences, University of Melbourne, Melbourne, Victoria, Australia
[c] Clinical Haematology and Bone Marrow Transplantation Service, The Royal Melbourne Hospital, Melbourne, Victoria, Australia
[d] Peter MacCallum Cancer Centre, Melbourne, Victoria, Australia
[e] Department of Haematology, St Vincent's Hospital, Melbourne, Victoria, Australia

ABSTRACT

Understanding how cancer and cancer therapies affect the immune system is integral to the rational application of immunotherapies. Flow cytometry is the gold standard method of peripheral blood immune cell profiling. However, the requirement for viable cells can limit its applicability, especially in studies of retrospective clinical cohorts. We aimed to determine if gene expression, analysed using the NanoString platform, could be used to quantify the immune populations present in cryopreserved peripheral blood mononuclear cell (PBMC) samples from patients with chronic lymphocytic leukaemia. Cell abundance scores derived from gene expression analysis were significantly correlated with the population frequency quantified by flow cytometry for all subsets analysed, including T cells, NK cells and Monocytes. This study demonstrates that gene expression analysis can be applied to cryopreserved PBMC and provides a concordant and complementary understanding of the immune profile to flow cytometry.

1. Introduction

Chronic lymphocytic leukaemia (CLL) is characterised by the accumulation of clonally derived malignant B cells in the peripheral blood, bone marrow and lymphoid organs. Understanding the immune microenvironment has become essential to understanding the pathogenesis, treatment and prognosis of CLL. CLL is associated with significant immune dysfunction, which prevents proper anti-tumour immunity and leaves patients susceptible to recurrent infections (Forconi & Moss, 2015; Christopoulos et al., 2011). Immune dysfunction is further exacerbated by the therapies used to treat CLL, which traditionally utilise chemotherapies but increasingly includes novel small molecule inhibitors such as BTK inhibitors and BH3 mimetics (Gordon et al., 2016; Lazzarino et al., 1999; Bergmann et al., 1993). Despite these recent advances, CLL remains incurable and combining new therapies with immunotherapy provides a promising avenue of research (Riches & Gribben, 2014). However, rational application of immunotherapies requires understanding the specific immunological impacts of the therapies with which they will be combined.

While the dysfunction of specific immune populations is best illuminated using functional assays, immune profiling provides information about the frequency, activation and distribution of immune populations. Furthermore, immune profiling of longitudinal samples allows analysis of the in vivo changes to immune populations over time. The objective of this analysis was to evaluate two methods of quantifying peripheral blood immune populations, flow cytometry and gene expression analysis, in the context of CLL.

Flow cytometry is the gold standard method of immune profiling, particularly as it applies to peripheral blood immune populations (Maecker et al., 2012). The increasing number of parameters that can be simultaneously measured, either on flow cytometry or mass cytometry (CyTOF) platforms, allows for the parallel quantification of a number of immune populations, as well as subset specific expression of markers that illuminate immune cell functional states. Unfortunately, there are a number of feasibility considerations for robust cytometry analysis. Cytometry requires viable cells, and thus more costly and time-consuming processing and storage. Furthermore longitudinal sample collection and analysis, such as in conjunction with clinical trials, requires cryopreservation, which has been shown to alter the surface expression of some important markers of immune subsets such as CD62L and CD57 and PD-1 (Costantini et al., 2003; Weinberg et al., 2009; Campbell et al., 2009).

Whilst most major immune populations can be easily distinguished using relatively few surface markers, more detailed analysis of immune

* Corresponding author at: ACRF Translational Research Laboratory, Royal Melbourne Hospital, Lab Cluster 3, Level 10, Victorian Comprehensive Cancer Centre, 305 Grattan St, Melbourne, VIC 3000, Australia
E-mail address: cesharpe@student.unimelb.edu.au (C. Sharpe).

https://doi.org/10.1016/j.jim.2018.09.013
Received 23 April 2018; Received in revised form 8 August 2018; Accepted 25 September 2018
Available online 26 September 2018
0022-1759/

Table 1
Markers used in flow cytometric identification of T cell subsets.

Marker	Fluorochrome	Clone	Manufacturer	Dilution	Immune cell
CD19	APC	SJ25-C1	BD	1/100	CLL/B cells
CD5	BV605	UCHT2	BD Horizon	1/200	CLL cells
CD3	BV785	OKT3	BioLegend	1/800	T cells
CD4	APC Cy7	RPA-T4	BD Pharmingen	1/200	CD4 T cells
CD8a	BV650	RPA-T8	BioLegend	1/400	CD8 T cells
TCRγδ	FITC	TCRγ/δ-1	BD	1/50	γδ T cells
CD1d-αGalCer tetramer	BV421	PBS44	Godfrey*	1/1000	NKT cells
CD45RA	PerCP Cy5.5	HI100	eBioscience	1/100	T cell memory
CD45RO	AF700	UchL1	BioLegend	1/200	T cell memory
CD62L	PE CF594	DREG-56	BD Horizon	1/400	T cell memory
CCR7	PE Cy7	3D12	eBioscience	1/100	T cell memory
CD1d	PE	CD1d42	BD Pharmingen	1/20	Antigen presentation
CD27	BV711	O323	BioLegend	1/200	Activation
Viability	Live/Dead Aqua		Invitrogen	1/200	Dead cell exclusion

* Provided as a kind gift from Prof. Dale Godfrey, The University of Melbourne.

subpopulations often necessitates more complex and time consuming intracellular staining for master transcription factors such as FoxP3 in regulatory T cells (Fontenot et al., 2005). Analysis of immune subpopulations is further complicated when subsets occur in low frequency. Reliable detection of rare cell subsets requires either depletion of bulk populations or a very large number of cells to be analysed. Samples from patients pose an additional challenge as leukaemia cells often exceed 90% of the peripheral blood mononuclear cells, further diluting rare populations.

An alternate method of immune profiling utilises immune cell type characteristic gene sets to algorithmically infer the composition of the immune populations from bulk gene expression data sets either from tumour (Newman et al., 2015; Bindea et al., 2013) or whole peripheral blood (Shannon et al., 2014). NanoString Technologies developed the nCounter® PanCancer Immune Profiling Panel and associated analysis software with the intent of providing an off-the-shelf panel which, in addition to a large gene expression data set, can be used to determine a broad immune profile from bulk samples.

NanoString immune profiling results have been shown to correlate with flow quantification of B, T and NK cell populations in healthy donor peripheral blood (Danaher et al., 2017). While this method of immune population quantification has been successfully applied to biopsy samples in a number of solid malignancies (Bresler et al., 2017; Ghidini et al., 2017; Gray et al., 2016; Lizotte et al., 2016), the application of the nCounter® PanCancer Immune Profiling Panel to peripheral blood samples from patients with haematological malignancies has only recently been explored (Crassini et al., 2017; Kolhe et al., 2017; Vadakekolathu et al., 2017) and has not been correlated with flow cytometry analysis.

In this study we compared immune population quantification in samples from patients with CLL patients by two methodologies, flow cytometry and NanoString gene expression profiling. Herein we show that these two methods provide highly concordant and complementary understanding of the immune populations in the peripheral blood of leukaemia patients.

2. Materials and methods

2.1. Patients and sample preparation

After obtaining informed consent according to ethics approved by the Peter MacCallum Cancer Centre and the Royal Melbourne Hospital, peripheral blood samples were obtained from 30 CLL patients (median age 67) who were treated with Ibrutinib (n = 12), BGB-3111 (n = 11), or Venetoclax (n = 6). Samples were obtained at a median of 16.5 days (range 0–45 days) prior to commencement of therapy and after a median of 357.5 days (range 147–387 days) on therapy. Peripheral blood mononuclear cells (PBMCs) were isolated by Ficoll-Paque (GE Healthcare, Little Chalfont, UK) density gradient centrifugation and cryopreserved. Mononuclear cells were similarly isolated from the peripheral blood of ten age-matched healthy donors obtained from the Australian Red Cross blood service.

At the time of analysis PBMC were thawed in a 37 °C water bath, then washed twice in pre-warmed T cell Media (Gibco RPMI media 1640 (Thermo Fisher, Massachusetts, USA), 10% heat inactivated foetal calf serum (FCS) (Thermo Fisher, Massachusetts, USA), 1% 4-(2-hydroxyethyl)-1-piperazineethanesulfonic acid (HEPES) (Thermo Fisher, Massachusetts, USA), 50 mM 2-Mercaptoethanol (2ME) (Sigma Aldrich, Missouri, USA), 1× Gibco GlutaMAX (Thermo Fisher, Massachusetts, USA), 1× Gibco MEM non-essential amino acids (Thermo Fisher, Massachusetts, USA), 1 mM Gibco sodium pyruvate (Thermo Fisher, Massachusetts, USA), 100 U/mL Penicillin/Streptomycin (Thermo Fisher, Massachusetts, USA). Viable cell counts were then obtained using Countess II FL Automated Cell Counter (Thermo Fisher, Massachusetts, USA), and two aliquots of 2.0×10^6 viable cells per sample dispensed into a 96 well plate, the cells pelleted by centrifugation at 450 xg for 5 min at room temperature. The cells were then washed twice with FACS buffer (phospho buffered saline (PBS) (Sigma Aldrich, Missouri, USA), 2% FCS) in preparation for staining. A further two aliquots of 2.0×10^6 viable cells per sample were washed in PBS, snap frozen in dry ice and stored at −80 °C. Insufficient numbers of cells were recovered from one time point of one ibrutinib patients and two venetoclax patients for both flow cytometry and gene expression analysis to be performed and were therefore not included in the analysis. Total RNA was isolated from the cell pellets using the AllPrep RNA/DNA mini kit (Quiagen, Hilden, Germany) according to manufacturer's instructions. RNA concentration and quality were analysed using the Agilent 2200 TapeStation System (Agilent Technologies, Waldbronn, Germany). RNA was stored for 1 month at −80 °C before gene expression analysis.

2.2. Flow cytometry

For each of the flow panels detailed in Tables 1 and 2, antibody dilutions were determined by staining healthy donor PBMC with serial dilutions of antibodies and whole panel staining of CLL samples. Dilutions were chosen to optimise population resolution and brightness. Master mixes were prepared including each of the fluorochrome conjugated antibodies at the predetermined optimal dilution in FACS buffer. After preparation, PBMC were incubated with the appropriate master mix at 4 °C in the dark for 30 min. The samples were then washed twice in FACS buffer and fixed with PBS, 2% paraformaldehyde (Electron Microscopy Sciences, Pennsylvania, USA). Samples were stored at 4 °C in the dark before filtering through 70 μm cell strainer

Table 2
Markers used in flow cytometric identification of innate immune subsets.

Marker	Fluorochrome	Clone	Manufacturer	Dilution	Immune cell
CD19	PE SJ25-C1	SJ25-C1	BD	1/50	CLL /B cells
CD5	BV605	UCHT2	BD Horizon	1/200	CLL cells
CD3	BV786	OKT3	BioLegend	1/800	T cells
CD56	APC	B159	BD Pharmingen	1/50	NK cells
CD16	PerCP Cy5.5	3G8	BioLegend	1/100	NK cells/ monocytes
CD11b	FITC	ICRF44	BD Pharmingen	1/200	Myeloid cells
CD33	PE-Cy7	P67.6	BD	1/200	Myeloid cells
HLA-DR	APC-H7	G46–6	BD Pharmingen	1/200	Monocytes/ DCs
CD14	PE-CF594	MφP9	BD Horizon	1/400	Monocytes
CD163	BV711	GHI/61	BD Horizon	1/25	Monocytes
PD-L1	AF700	130,021	R&D systems	1/50	Immune suppression
CD11c	PE-Cy5	B-ly6	BD Pharmingen	1/200	Monocytic DC
CD123	BV421	9F5	BD Horizon	1/100	Plasmacytoid DC
Viability	Live/Dead Aqua		Invitrogen	1/200	Dead cell exclusion

and at least 1.0×10^6 viable cells were acquired using a BD LSRFortessa using FACSDiva software (BD Biosciences, San Jose, CA). Appropriate single colour and fluorescence-minus-one controls were simultaneously acquired. Analysis was performed using FlowJo Version 10 (FlowJo LLC, Oregon, USA). After time and debris filtering for quality, the live singlets were designated as the total population of leukocytes. A representative gating strategy is described in **Supplementary Fig. 1**. The frequency of each immune population was calculated as a percentage of the live cell gate unless another parent population is specified.

2.3. NanoString

The NanoString nCounter® Human PanCancer Immune Profiling Panel (Cesano, 2015) (NanoString Technologies, Washington, US) was used to enumerate the mRNA of 730 immune related genes and 40 internal reference genes in 50 ng total RNA run according to manufacturers protocol. RNA count data was normalised and analysed using the nSolver Analysis Software Version 3.0 and the nSolver Advanced Analysis Module Version 1.1.5 (NanoString Technologies, Washington, US). NanoString analysis software reports cell abundance scores for 14 immune subsets according to the expression of genes determined to be characteristic of their respective immune populations (Table 3).

The nCounter Advanced Analysis module also calculates an abundance score named “Total TILs” which is calculated by taking the average of the cell type abundance scores that correlate ($r \geq 0.6$) with the PTRPC (CD45) expression (Shannon et al., 2014). The nomenclature reflects the expectation that this platform will be used most frequently in the context of solid tumours where this is a measure of tumour infiltrating leukocytes. However, in the context of PBMC samples if taken as a measure of the total leukocyte population then cell scores relative to “Total TIL's” can be more easily interpreted as a total leukocyte abundance in the sample. Cell scores are also reported relative to total leukocyte abundance (total TILs), or to another cell abundance score (i.e. T cells) to provide information about the relative composition of the total immune profile.

Table 3
Gene sets used in NanoString cell type abundance calculations.

Cell Type	P =	Selected genes	Discarded genes
B cells	0.00	BLK, CD19, MS4A1 (CD20), TNFRSF17	
T cells	0.00	CD3D, CD3E, CD3G, CD6, SH2D1A	
CD8 T cells	0.00	CD8A, CD8B	
NK cells	0.07	NCR1, XCL2	
CD56 dim NK cells	0.05	KIR_inhibiting_Subgroup 2, KIR3DL1, KIR3DL2	IL21R
Macrophages	0.05	CD163, CD68	CD84

3. Statistics

The nCounter cell type abundance scores were calculated as the average of the log2 normalised counts of the gene set specified in Table 3. For each cell type score the degree to which this data set supported the gene set expression was calculated by the nCounter Advanced Analysis software using a permutation *t*-test. Candidate genes from the set were discarded if the correlation between the genes in the set deviated substantially from a slope of 1 **(Supplementary fig. 2).** Cell type scores were reported if $p < .1$. Relative abundance scores represent the log ratios of two cell types' abundance scores.

The correlation between the nCounter cell type abundance scores and the immune population quantification by flow cytometry was determined using a two tailed Pearson's correlation, calculated using GraphPad Prism v7.0c (GraphPad software, California USA). Statistical significance was accepted for p values $< .05$.

4. Results

4.1. NanoString cell type scores are highly correlated with flow cytometric quantification of immune population abundance

The first objective of this study was to determine if, in samples from patients with CLL, immune profiling using gene expression analysis could provide comparable peripheral blood immune profiling to flow cytometry. We therefore simultaneously analysed PBMC samples using flow cytometry and the NanoString nCounter® PanCancer Immune Profiling panel.

Of the possible 14 immune populations reportable by the nCounter Advanced Analysis software 12 immune populations were determined to be significantly supported by the expression data, $p < .1$. Of these, the two flow cytometry panels identified seven populations: B cells, total T cells, CD8 T cells, CD4 T cells, total NK cells, CD56dim NK cells and Monocytes. We observed strong positive correlation between the abundance score and the immune population frequency calculated using flow cytometry for all immune populations analysed (Fig. 1 A-F).

Samples were collected from patients with CLL before and after treatment and compared to age-matched healthy donors. The inclusion of both pre-treatment and post-treatment samples provided the opportunity to observe the correlation of the two measures of abundance in samples with varying tumour burden and a wide range of cell frequencies far outside the ‘normal’ range that is observed in healthy donors. As CLL is a B cell malignancy, the leukaemia cells have an expression profile highly similar to B cells and therefore constitute a subset of the ‘B cell’ population. Due to the high leukaemia burden in some pre-treatment samples and the effective elimination of leukaemia

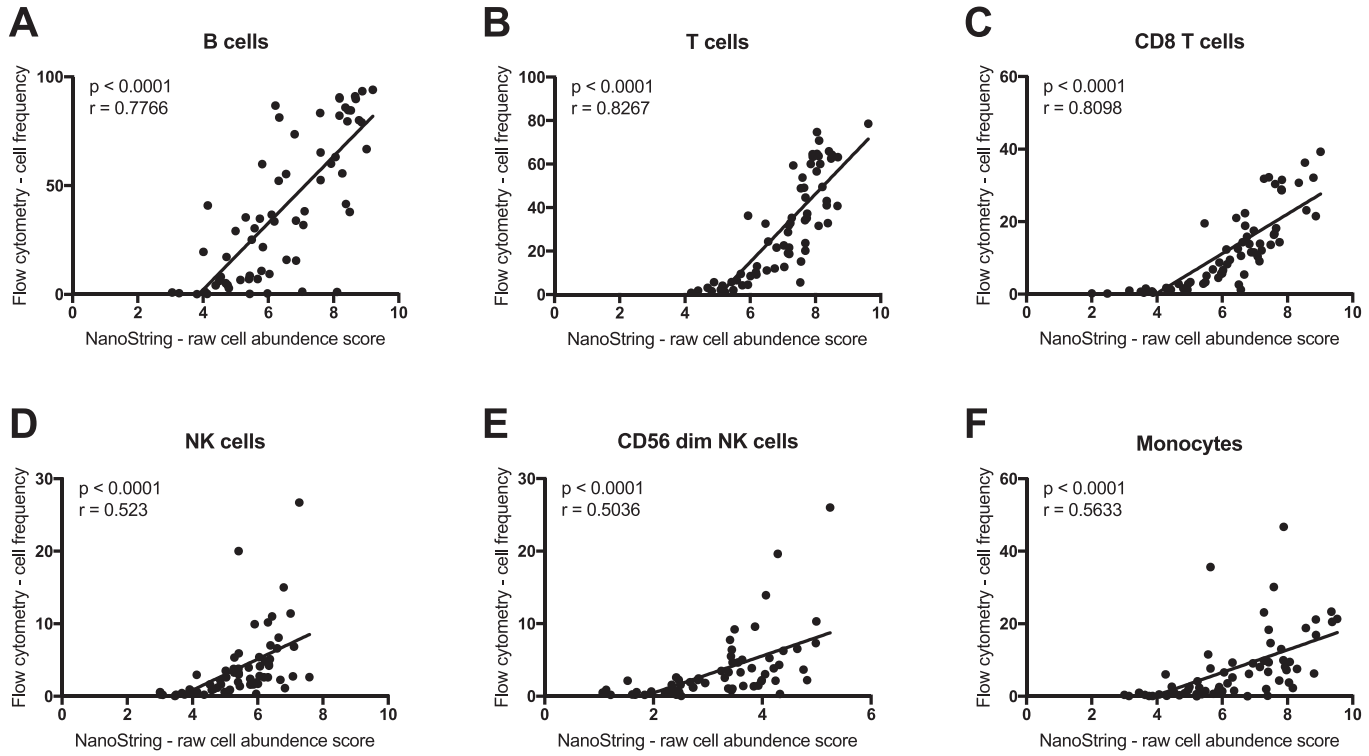

Fig. 1. Immune cell type abundance scores calculated using gene expression strongly correlate with cell frequencies determined by flow cytometry quantification for all cell types assessed. Correlation of immune cell population frequency calculated as a percentage of total live cells by flow cytometry and the nCounter raw cell type abundance scores. Linear regression is plotted, and Pearson correlation coefficient and p value are reported, $n = 65$.

cells after treatment, the 'B cell' frequency ranged from 0.19% to 94% of the PBMC in the flow cytometry analysis (Fig. 1A). The nCounter B cell abundance score correlated strongly with the flow cytometric quantification ($p < .0001$, $r = 0.7766$), demonstrating the large dynamic range of the NanoString platform. Similarly, the correlation of the flow and nCounter T cell abundance score was highly significant for the T cell population that ranged from 0.8% to 78.5% of the total PBMC by flow cytometry (Fig. 1B) ($p < .0001$, $r = 0.8098$).

Analysis performed herein used PBMC, and the flow panel was designed to quantify monocytes as the major myeloid cell population. Conversely, the gene expression panel was designed to identify macrophages. As peripheral blood monocytes and macrophages share expression of genes in the 'macrophage' gene set, CD68 and CD163(Moniuszko et al., 2006; Buechler et al., 2000), this cell score significantly correlated with the proportion of monocytes (Fig. 1F) ($p < .0001$, $r = 0.5633$).

In the low abundance populations, namely NK and monocytes, significant outliers were observed. The samples with unusually high NK frequency were from different patients than those with unusually high monocyte frequency. However, these populations appeared to be true populations in the flow analysis and in order to not bias the correlation these outliers were not excluded. This study was not sufficiently powered to determine an upper or lower limit for which the flow cytometry and NanoString abundance scores correlated.

4.2. Cell type scores are not significantly influenced by gene expression intensity

The nCounter cell type abundance scores assume that higher expression of the gene set in Sample A than Sample B implies greater abundance of the cell type in sample A and not merely the upregulation of the genes by a population the same size. NanoString quantification of gene expression has been previously shown to correlate with flow cytometric quantification of protein expression in acute leukaemia cells (Fernandez et al., 2012). Four genes used to calculate abundance scores were also measured by flow cytometry, CD19, CD163, CD3ε and CD8α. In order to determine if the expression of these genes, as inferred from median fluorescence intensity (MFI), influenced the cell type abundance scores we compared the MFI of each marker to the population abundance score for which it was a constituent gene. There was no correlation between the expression intensity of the MFI of CD19 on B cells and the B cell abundance score, similarly there was no correlation between the CD3 MFI and T cells, CD8 and CD8 T cells or CD168 and monocytes (Fig. 2A-D). This data set strongly suggests that cell type abundance scores calculated using gene expression are correlated with the frequency of the cell population and not with the expression intensity of the candidate genes in the set.

4.3. Relative cell type scores provide insight into the comparative composition of the immune profile

In addition to the raw cell scores, the nCounter Advanced Analysis software reports relative cell abundance scores. Relative scores represent the log ratios of the two cell type abundance scores and therefore can provide information about the abundance relative to the "total TILs" or other immune population. Cell type scores relative to 'total TILs' were reported for six populations with corresponding flow analysis (Fig. 3A-F). The relative abundance scores were significantly correlated with the respective immune population frequency calculated by flow cytometry. As with raw cell scores, the strongest correlation was observed in the most abundant cell types, B cells ($p < .0001$, $r = 0.8328$) and T cells ($p < .0001$, $r = 0.7871$) (Fig. 3 B&C). Relative abundance scores also allow for inferences about the relative composition of the T cell population. The CD4 T cell score, reported relative to the total T cells score significantly correlates with the CD4+ T cell population as proportion of total T cells by flow cytometry (Fig. 3G). This score is not calculated directly from a gene set but rather represents the portion of total T cells that are not accounted for by the

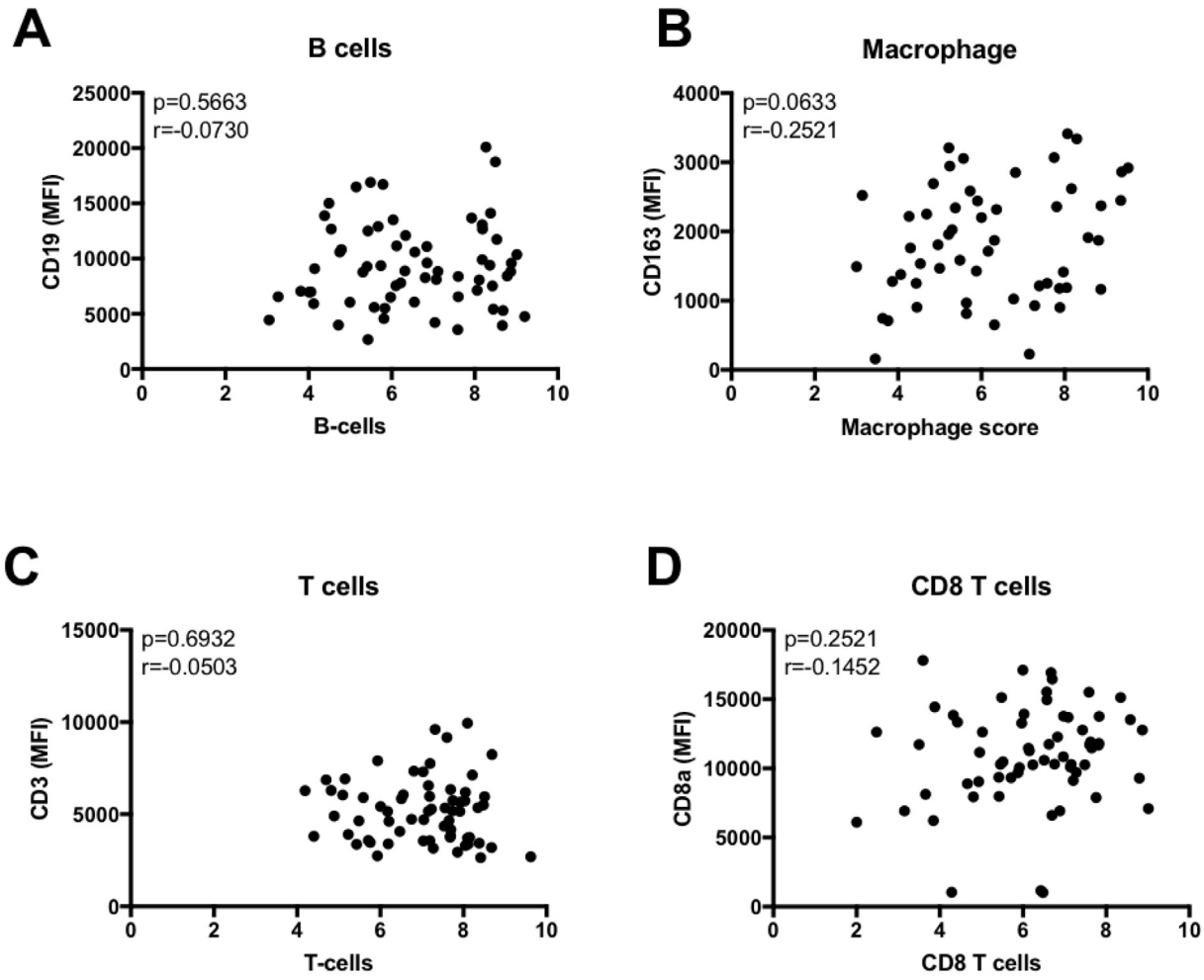

Fig. 2. Cell scores do not correlate with the expression intensity of candidate genes No correlation between the A) B cell populations CD19 expression quantified by flow cytometry and the B cell score B) Monocyte CD163 and the macrophage score C) T cell CD3 expression and the T cells score or D) the expression of CD8a by CD8 T cells and the CD8 T cell score. Pearson correlation coefficient and p values are indicated, $n = 57$.

CD8 T cell population.

5. Discussion

Herein we demonstrate that the NanoString nCounter® PanCancer immune profiling panel and the accompanying gene expression analysis software can provide immune cell abundance quantification comparable to flow cytometry in samples from patients with CLL with widely divergent immune profiles. Gene expression analysis and flow cytometry resulted in significantly correlated immune abundance measurements for all cell types assessed, including NK and T cell subpopulations.

The nCounter® PanCancer Immune Profiling panel has a number of advantages over flow cytometry. While the flow cytometry requires panel design and optimisation depending on the specific populations of interest, the nCounter® PanCancer Immune Profiling panel and the associated analysis software is an 'off the shelf' product which may be applied to a wide variety of samples in which there is an immune component. Furthermore, the nCounter platform only requires 25–100 ng of total RNA, which can be extracted from far fewer cells than were needed for the flow cytometric analysis. Therefore, this technology allows for retrospective analysis of immune populations in sample cohorts in which only molecular samples are available or the underlying disease makes the collection of enough sample for analysis difficult. In the clinical context there is an increasing demand on sample analysis, more testing is now required thus decreasing the amount of sample available for these tests. Immune profiling using the NanoString platform allows for a snapshot of immune population abundance using less sample than required for a comparable flow cytometry profile. In addition, the nCounter® PanCancer Immune Profiling Panel provides information about other immune markers such as chemokine/cytokine expression, activation status and cytotoxicity.

Conversely, flow cytometry provides greater flexibility in the immune populations that can be quantified. The nCounter cell type abundance analysis is restricted to 14 immune populations determined to have genes with expression characteristics sufficient for quantification (Danaher et al., 2017). This precludes quantification of innate like T cells, naive and memory phenotypes, or more specific subpopulations of monocytes and DCs. Flow cytometry has the advantage of more detailed, single cell analysis whilst the nCounter cell type abundance score provides only a measure of the bulk population. For example, the flow cytometry analysis in this study was able to distinguish between CD5+ and CD5- B cells, and as such, healthy B cells from CLL cells. However, despite the flow cytometry analysis in this study being performed on at least four times as many cells, it was not able to quantify regulatory T cells or helper T cell subpopulations due to the requirement for intracellular staining for robust quantification.

Gene expression analysis of whole PBMC from patients with CLL was complicated by the high degree of similarity between CLL cells and the counterpart non-malignant B cell population. As CLL is a B cell malignancy, leukemic cells in peripheral blood contribute to the total gene expression of a large number of genes in the panel. For example,

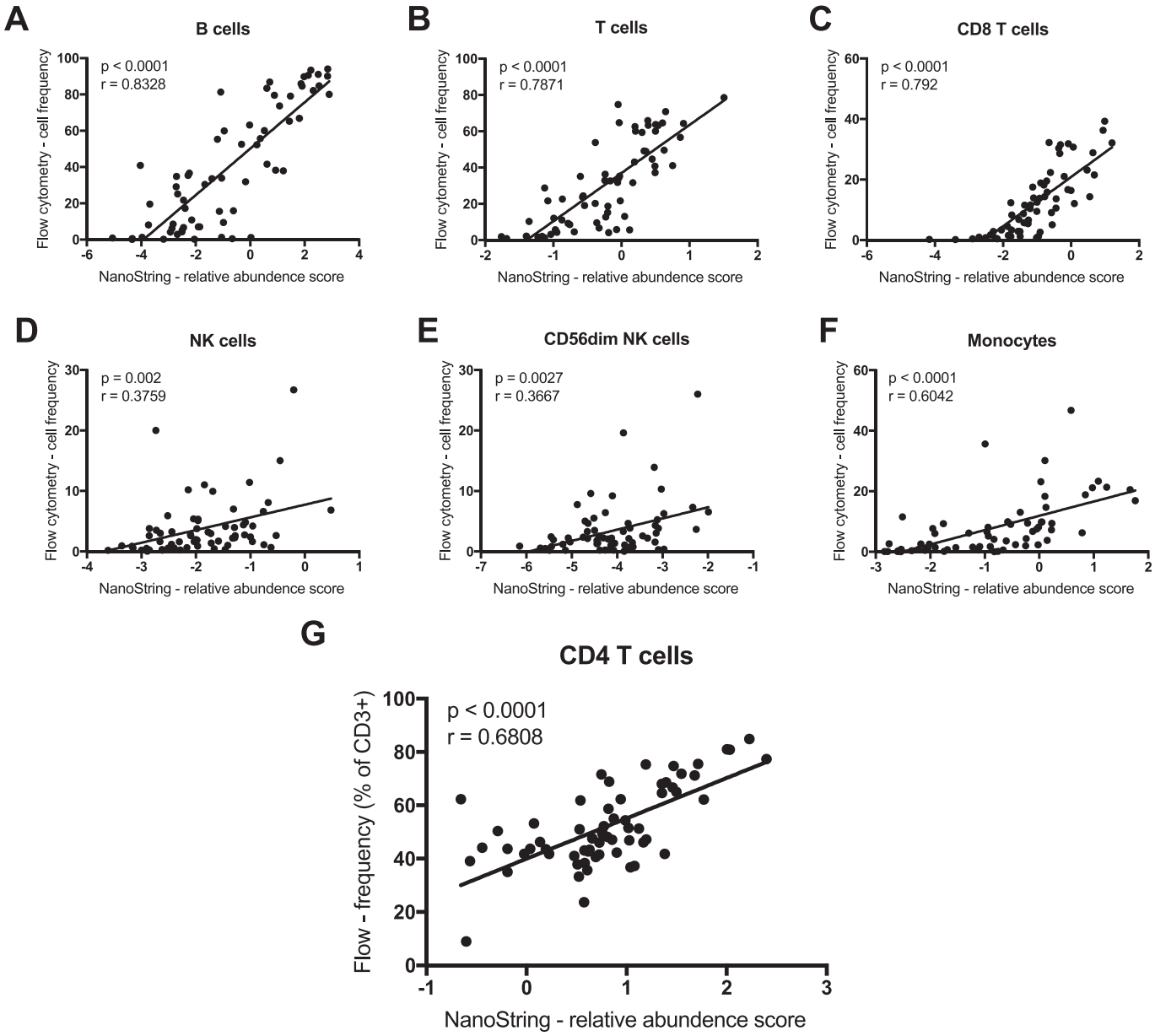

Fig. 3. Relative cell scores maintain significant correlation with population frequencies, including for T cell subpopulations. A-F) Correlation of immune cell population frequency calculated as a percentage of total live cells by flow cytometry and the nCounter cell type abundance scores relative to "total TILs", $n = 65$. G) Correlation of CD4 T cell quantification by Flow (CD3 + CD4+ cells as a percentage of total CD3+ cells) and nCounter relative cell type abundance score (CD4 T cells relative to total T cells). Linear regression is plotted, and R and *P* value are reported, $n = 63$.

IL21R is expressed by CLL cells (De Totero et al., 2006), which may explain the deviation of this genes expression from the other genes in the NK cell gene set and the subsequent exclusion of this gene from cell type calculations (Supplementary Fig. 2). Similarly, CLL cells express CD84 (Marom et al., 2017) which may also explain the exclusion of this gene from the monocyte score. These findings demonstrate both the importance of understanding the underlying disease biology of the malignant cells analysed, as well as the importance of the quality assurance analysis in selecting only genes that are substantially correlated with each other to determine abundance scores.

By default, the NanoString nCounter analysis software reports all cell types regardless of the degree to which the experiments gene expression pattern conforms to the expected cell-type specific expression. In this data set cell types with lower frequency had lower correlation of the gene set used to calculate abundance (Monocytes and NK cells, Table 3). These abundance scores also had weaker correlation to the flow data, (Fig. 1D-F). This represents an important limitation of the NanoString cell type abundance scores, especially those calculated relative to 'total TILs', which are less strongly correlated in lower abundance populations. Interestingly the lower correlation coefficients for NK and monocyte populations is consistent with data comparing cell type abundance scores and flow cytometry in healthy donors and may therefore be a function of the gene sets cell type specific expression characteristics rather than the population abundance (Danaher et al., 2017). The immune abundance scores calculated using the nCounter Advanced Analysis module should therefore be used with reference to the strength to which the expression data supports the cell type scores. Furthermore, for immune populations that are calculated using a single gene, such as regulatory T cells, which cannot have such quality assurance analysis should be assessed accordingly.

The expression intensity of candidate genes for B cell, Monocyte, T cell and CD8 T cells scores did not significantly correlate with the

abundance of the population. However, theoretically a strong enough uniform change in the expression of the genes used for quantification could influence the abundance measurement, otherwise the candidate gene would lack significant correlation with the other genes in the set, a possibility is mostly easily conceptualised in cytotoxic cells. Cytotoxic cell quantification relies on the expression of genes including granzymes and perforin, which are upregulated upon activation. As such a sample with fewer, more activated cells may have an equal abundance score with a sample with a larger population of inactive cytotoxic cells. While this study found that the expression intensity of candidate genes was not correlated with abundance measurements, it highlights the importance of the QA analysis to ensure that the abundance score is supported by the gene expression in the samples.

If the primary objective of a specific study is the simple quantification of immune populations from peripheral blood and sample is abundant then flow cytometry will give a more precise answer. The advantage of gene expression immune profiling using the NanoString platform is that understanding of the immune profile is possible where viable cells are limited (a common limitation in clinical trial sample collection) and the nCounter® PanCancer Immune Profiling Panel also provides a comprehensive 730 immune related gene expression data set allowing a broader understanding of immune fitness than the cell abundance quantifications.

6. Conclusion

A detailed profile of a patient's immune system provides valuable understanding of the immunological impacts of cancer and its treatment, potentially illuminating novel mechanisms of immunosuppression and opportunities for immunotherapies. Data presented herein demonstrates that gene expression analysis provided immune population quantification comparable to flow cytometry in samples with highly divergent immune profiles. Whilst this study was performed using blood collected from patients with CLL, we expect that gene expression immune profiling could be similarly applied to peripheral blood in other haematological malignancies or other diseases with an immune or inflammatory component. Furthermore, the nCounter® PanCancer Immune Profiling Panel allows for a broad insight into the immune microenvironment through exploration of a large gene expression data set. Gene expression analysis requires far fewer cells than traditional flow cytometry methods and thus expands the ability to analyse retrospective cohorts and clinical trial correlative samples where samples are limited.

Acknowledgements

We thank D Godfrey for the kind gift of the CD1d-αGalCer tetramer. We thank the Department of Immunology and Microbiology University of Melbourne flow cytometry facility for help with FACS experiments. This work was supported by NHMRC, Australia (GrantID GNT1090500) fellowship to KM and Fight Cancer Foundation, Australia.

Author contributions

CS, JD, KM, DR and RK designed the study. CS, JD, KM and RK designed the experiments. CS performed the flow cytometry experiments. CS and RK performed the NanoString experiments. KM, CT and DR facilitated access to patient samples. CS wrote the paper with input from all co-authors.

Appendix A. Supplementary data

Supplementary data to this article can be found online at https://doi.org/10.1016/j.jim.2018.09.013.

References

Bergmann, L., Fenchel, K., Jahn, B., Mitrou, P.S., Hoelzer, D., 1993. Immunosuppressive effects and clinical response of fludarabine in refractory chronic lymphocytic leukemia. Ann. Oncol. 4, 371–375. https://doi.org/10.1093/oxfordjournals.annonc.a058515.

Bindea, G., Mlecnik, B., Tosolini, M., Kirilovsky, A., Waldner, M., Obenauf, A.C., et al., 2013. Spatiotemporal dynamics of intratumoral immune cells reveal the immune landscape in human cancer. Immunity 39, 782–795. https://doi.org/10.1016/j.immuni.2013.10.003.

Bresler, S.C., Min, L., Rodig, S.J., Walls, A.C., Xu, S., Geng, S., et al., 2017. Gene expression profiling of anti-CTLA4-treated metastatic melanoma in patients with treatment-induced autoimmunity. Lab. Investig. 97, 207–216. https://doi.org/10.1038/labinvest.2016.126.

Buechler, C., Ritter, M., Orsó, E., Langmann, T., Klucken, J., Schmitz, G., 2000. Regulation of scavenger receptor CD163 expression in human monocytes and macrophages by pro- and antiinflammatory stimuli. J. Leukoc. Biol. 67, 97–103.

Campbell, D.E., Tustin, N.B., Riedel, E., Tustin, R., Taylor, J., Murray, J., et al., 2009. Cryopreservation decreases receptor PD-1 and ligand PD-L1 coinhibitory expression on peripheral blood mononuclear cell-derived T cells and monocytes. Clin. Vaccine Immunol. 16, 1648–1653. https://doi.org/10.1128/CVI.00259-09.

Cesano, A., 2015. nCounter® PanCancer Immune Profiling Panel (NanoString Technologies, Inc., Seattle, WA). J Immunother Cancer 3 (42). https://doi.org/10.1186/s40425-015-0088-7.

Christopoulos, P., Pfeifer, D., Bartholomé, K., Follo, M., Timmer, J., Fisch, P., et al., 2011. Definition and characterization of the systemic T-cell dysregulation in untreated indolent B-cell lymphoma and very early CLL. Blood 117, 3836–3846. https://doi.org/10.1182/blood-2010-07-299321.

Costantini, A., Mancini, S., Giuliodoro, S., Butini, L., Regnery, C.M., Silvestri, G., et al., 2003. Effects of cryopreservation on lymphocyte immunophenotype and function. J. Immunol. Methods 278, 145–155. https://doi.org/10.1016/S0022-1759(03)00202-3.

Crassini, K.R., Shen, Y., Christopherson, R., Stevenson, W.S., Mulligan, S., Best, O.G., 2017. Analysis of mRNA Expression in Peripheral, Bone Marrow and Lymph Node Derived CLL Cells Using the Nanostring Ncounter Platform. Blood 130, 4279.

Danaher, P., Warren, S., Dennis, L., D'Amico, L., White, A., Disis, M.L., et al., 2017. Gene expression markers of Tumor Infiltrating Leukocytes. J Immunother Cancer 5, 18. https://doi.org/10.1186/s40425-017-0215-8.

De Totero, D., Meazza, R., Zupo, S., Cutrona, G., Matis, S., Colombo, M., et al., 2006. Interleukin-21 receptor (IL-21R) is up-regulated by CD40 triggering and mediates proapoptotic signals in chronic lymphocytic leukemia B cells. Blood 107, 3708–3715. https://doi.org/10.1182/blood-2005-09-3535.

Fernandez, P., Solenthaler, M., Spertini, O., Quarroz, S., Rovo, A., Lovey, P.Y., et al., 2012. Using Digital RNA Counting and Flow Cytometry to Compare mRNA with Protein Expression in Acute Leukemias. PLoS One 7. https://doi.org/10.1371/journal.pone.0049010.

Fontenot, J.D., Rasmussen, J.P., Williams, L.M., Dooley, J.L., Farr, A.G., Rudensky, A.Y., 2005. Regulatory T cell lineage specification by the forkhead transcription factor Foxp3. Immunity 22, 329–341. https://doi.org/10.1016/j.immuni.2005.01.016.

Forconi, F., Moss, P., 2015. Perturbation of the normal immune system in patients with CLL. Blood 126, 573–581. https://doi.org/10.1182/blood-2015-03-567388.

Ghidini, M., Cascione, L., Carotenuto, P., Lampis, A., Trevisani, F., Previdi, M.C., et al., 2017. Characterisation of the immune-related transcriptome in resected biliary tract cancers. Eur. J. Cancer 86, 158–165. https://doi.org/10.1016/j.ejca.2017.09.005.

Gordon, P.M., Porter, C.C., Pikman, Y., Labelle, J.L., Ludwig, L.M., Nassin, M.L., et al., 2016. Killing Two Cells with One Stone: Pharmacologic BCL-2 Family Targeting for Cancer Cell Death and immune Modulation. Front Pediatr 4. https://doi.org/10.3389/fped.2016.00135.

Gray, M.J., Gong, J., Hatch, M.M.S., Nguyen, V., Hughes, C.C.W., Hutchins, J.T., et al., 2016. Phosphatidylserine-targeting antibodies augment the anti-tumorigenic activity of anti-PD-1 therapy by enhancing immune activation and downregulating pro-oncogenic factors induced by T-cell checkpoint inhibition in murine triple-negative breast cancers. Breast Cancer Res. 18, 50. https://doi.org/10.1186/s13058-016-0708-2.

Kolhe, R., Pundkar, C., Mondal, A., Pantin, J., Kota, V., Clemmons, A., et al., 2017. Molecular Characterization By Cancer Immune Profiling in Acute Promyelocytic Leukemia (APL) May Identify Patients at Risk of Early Death. Blood 130.

Lazzarino, M., Orlandi, E., Baldanti, F., Furione, M., Pagnucco, G., Astori, C., et al., 1999. The immunosuppression and potential for EBV reactivation of fludarabine combined with cyclophosphamide and dexamethasone in patients with lymphoproliferative disorders. Br. J. Haematol. 107, 877–882. https://doi.org/10.1046/j.1365-2141.1999.01765.x.

Lizotte, P.H., Ivanova, E.V., Awad, M.M., Jones, R.E., Keogh, L., Liu, H., et al., 2016. Multiparametric profiling of non–small-cell lung cancers reveals distinct immunophenotypes. JCI Insight 1, 1–18. https://doi.org/10.1172/jci.insight.89014.

Maecker, H.T., McCoy, J.P., Nussenblatt, R., 2012. Standardizing immunophenotyping for the Human Immunology Project. Nat. Rev. Immunol. 12, 191–200. https://doi.org/10.1038/nri3158.

Marom, A., Barak, A.F., Kramer, M.P., Lewinsky, H., Binsky-Ehrenreich, I., Cohen, S., et al., 2017. CD84 mediates CLL-microenvironment interactions. Oncogene 36, 628–638. https://doi.org/10.1038/onc.2016.238.

Moniuszko, M., Kowal, K., Rusak, M., Pietruczuk, M., Dabrowska, M., Bodzenta-lukaszyk, A., 2006. Monocyte CD163 and CD36 Expression in Human Whole Blood and Isolated Mononuclear Cell Samples : Influence of Different Anticoagulants Monocyte CD163 and CD36 Expression in Human Whole Blood and Isolated Mononuclear Cell

Samples : Influence of Different An. Society 13, 704–707. https://doi.org/10.1128/CDLI.00417-05.

Newman, A.M., Liu, C.L., Green, M.R., Gentles, A.J., Feng, W., Xu, Y., et al., 2015. Robust enumeration of cell subsets from tissue expression profiles. Nat. Methods 12, 453–457. https://doi.org/10.1038/nmeth.3337.

Riches, J.C., Gribben, J.G., 2014. Immunomodulation and Immune Reconstitution in Chronic Lymphocytic Leukemia. Semin. Hematol. 51, 228–234. https://doi.org/10.1053/j.seminhematol.2014.05.006.

Shannon, C.P., Balshaw, R., Ng, R.T., Wilson-McManus, J.E., Keown, P., McMaster, R., et al., 2014. Two-stage, in Silico deconvolution of the lymphocyte compartment of the peripheral whole blood transcriptome in the context of acute kidney allograft rejection. PLoS One 9. https://doi.org/10.1371/journal.pone.0095224.

Vadakekolathu, J., Patel, T., Reeder, S., Schaarschmidt, H., Schmitz, M., Bornhäuser, M., et al., 2017. Immune Gene Expression Profiling in Children and Adults with Acute Myeloid Leukemia Identifies Distinct Phenotypic Patterns. Blood 130.

Weinberg, A., Song, L.Y., Wilkening, C., Sevin, A., Blais, B., Louzao, R., et al., 2009. Optimization and limitations of use of cryopreserved peripheral blood mononuclear cells for functional and phenotypic T-cell characterization. Clin. Vaccine Immunol. 16, 1176–1186. https://doi.org/10.1128/CVI.00342-08.

4 LONG-TERM TREATMENT WITH TARGETED THERAPIES HAS IMMUNOLOGICAL CONSEQUENCES

4.1 SUMMARY

This chapter aims to understand how long-term treatment with targeted therapies altered the abundance of specific immune populations in order to inform the future combination of targeted therapies and immunotherapy. The effect of targeted therapies was explored using flow cytometric analysis to identify key peripheral blood immune populations. This analysis found that treatment with the different targeted therapies, venetoclax, ibrutinib, and zanubrutinib, resulted in distinctly different changes to the immune profile of patients. Venetoclax treated patients had a relative increase in the abundance of myeloid cells and unconventional T cells. Whereas, ibrutinib treated patients had no consistent changes in the T cell compartment. Finally, the more specific BTK inhibitor zanubrutinib did not significantly alter the immune profile supporting the hypothesis that more selective BTK inhibitors may be more amenable to combination with immunotherapies.

4.2 INTRODUCTION

Unlike the more established chemoimmunotherapy regimens used to treat CLL that have relatively short, defined treatment durations, targeted therapies are administered until contraindicated. For many patients this means mean years of continuous treatment for many years, even after a complete response is achieved. The impact of long-term drug exposure on the immune system of patients remains ill-defined. Therefore, the first objective of this study was to determine if targeted therapies altered the composition of the immune system. This analysis included multiple cohorts of CLL patients treated with targeted therapies including patients treated with ibrutinib, zanubrutinib, or venetoclax on phase 1-3 studies of these agents, or as best standard of care. Furthermore, a cohort of CLL patients receiving the combination of ibrutinib and venetoclax (ibrutinib monotherapy for three months followed by combination ibrutinib and venetoclax) as part of a phase 2 clinical trial (NCT02910583). The patient characteristics of these cohorts are summarised in Table 4.1.

Table 4.1 Characteristics of CLL patient cohorts

	Ibrutinib	Zanubrutinib	Venetoclax	Ibrutinib + venetoclax
Number	13	11	6	14
Median age	67 (48-74)	65 (47-79)	57 (45-81)	55 (28-68)
% Male sex	79%	57%	84%	64%
Rai I/II at baseline	7/13 (53%)	5/5 (100%)	4/6 (67%)	--
17p del or TP53 mutation	6/13 (47%)	3/5 (60%)	4/6 (67%)	--
Lines of previous therapy	2.5 (0-7)	5 (1-7)	2.5 (0-8)	0
Months from last therapy	5 (0-46)	14 (0-85)	11 (1-27)	--
Fludarabine refractory	9/10 (90%)	3/5 (60%)	4/4 (100%)	--

-- data not available

This unique sample set allowed for longitudinal analysis of the immunological impacts of targeted therapies. Flow cytometric analysis of PBMCs collected prior to the initiation of the targeted therapy and throughout treatment allowed for quantification of the changes in the abundance of multiple innate immune and T cell populations. The cohorts of treated patents were also compared to age matched healthy donors and a cohort of untreated CLL patients who were not enrolled on clinical trials.

Inclusion of patients in the single agent treatment cohorts were restricted to patients who remained on therapy for at least 12 months and therefore only represent patients for whom the respective treatment provided clinical benefit. However, the rate of complete remission at 1 year in all cohorts is low (Table 4.2). Similarly, the ibrutinib plus venetoclax treated cohort was restricted to patients for whom PBMC samples were available at baseline, and after 3 and 6 months. At the time of analysis not all patients had reached the 12-month timepoint, and as such the best responses, rather than the response at 12 months is outlined in Table 4.2. It is therefore notable that the CR rate was higher at 36% in the combination treatment cohort.

Table 4.2 Clinical responses of CLL patients treated with targeted therapies

Response at 12 months	Ibrutinib	Zanubrutinib	Venetoclax	Ibrutinib + venetoclax*
Stable Disease (SD)	0 (0%)	1 (20%)	0 (0%)	0 (0%)
Partial Response (PR)	9 (69%)	2 (40%)	5 (83%)	9 (64%%)
PR with lymphocytosis	3 (23%)	1 (20%)	--	0 (0%)
Complete response (CR)	1 (8%)	1 (20%)	1 (17%)	5 (36%)

* Best response assessment as not all patients had reached the 12-month timepoint at the time of data collection

Multiple previous studies have assessed the effect of ibrutinib treatment on specific immune populations. However, these studies were narrowly focussed and have explored early timepoints, usually extending to no later than 6 months into treatment. These studies have indicated that T cells have decreased expression of exhaustion markers[222,308] and an increase in T cell receptor repertoire diversity[309]. Studies of ibrutinib treated patients have focussed on mainly on CD4 T cell subpopulations with inconsistent findings and very little has been published on the effects of more specific BTK inhibitors or venetoclax on immune populations in CLL patients.

As discussed in section 1.3.3, in addition to its critical role in B cells, BTK is also expressed in myeloid populations. While the effect of BTK inhibition on both CLL cells and healthy B cells has been extensively characterised, the effect of BTK inhibition on myeloid subsets is less clear. *In vitro* ibrutinib treatment has been shown to inhibit peripheral blood monocyte FcγR-mediated cytokine production[310] and chemokine production[183], as well as macrophage phagocytosis [184,236]. In mouse models of CLL, ibrutinib treatment was shown to deplete myeloid derived suppressor cells (MDSC) populations in a BTK dependent manner[187]. However, to date there have not been any long-term studies of myeloid cell populations in CLL patients treated with either ibrutinib or more selective BTK inhibitors.

There has also been very little investigation of the impacts of treatment with venetoclax on the human immune system. While *in vitro* venetoclax treatment does not result in overt effects on normal immune populations other than B cells, previous studies have demonstrated that different immune subsets have varying Bcl-2 dependence. Data from mice have suggested that the loss of Bcl-2 may result in depletion of multiple lymphoid subsets[249]. However, it has been suggested that CLL patients treated with venetoclax and the anti-CD20 antibody obinutuzumab have no change in the absolute number of NK and T cells[311]. As such, this study aimed to understand how venetoclax treatment, both alone and in combination with ibrutinib affects the immune profile of CLL patients after long-term treatment.

4.3 RESULTS

Given the clinical success of all of the therapies under investigation in this analysis, it was expected that the peripheral blood leukaemia burden deceased with treatment. All three targeted therapies in the analysis resulted in a significant decrease in the proportion of CD19+ cells after 12 months on therapy (Figure 4.1 b-d). It is notable that in the venetoclax treated cohort the proportion of CD19+ cells were lower than in the healthy donor cohort, supporting findings from others that both malignant and non-malignant CD19+ populations are decreased by venetoclax treatment[247]. Conversely, even after 12 months of BTK inhibitor treatment leukaemia cells remained the majority population in the PBMC in some patients. Some of these patients has achieved a PR and the high peripheral blood burden may be attributed to the redistributive effect of BTKi on CLL cells, via inhibition of CXCR4 signalling and subsequent diminished homing to lymph nodes[57]. As such, the measurement of decrease in the peripheral blood may not be representative of the total reduction in tumour burden and the persistence of lymphocytosis is not an indicator of poor clinical response[59].

Given the high burden of disease in some patients, a clear distinction between CLL cells and untransformed B cells on the basis of CD5 expression was not sufficient to clearly define these populations and as such, untransformed B cells were not part of this analysis. Furthermore, as demonstrated in Figure 4.2 the large change in the leukaemia cell population obscures changes in the frequency of other immune populations if reported as a frequency of the total population. Therefore, the data presented in this chapter reports immune population abundance as a proportion of the CD19 negative population.

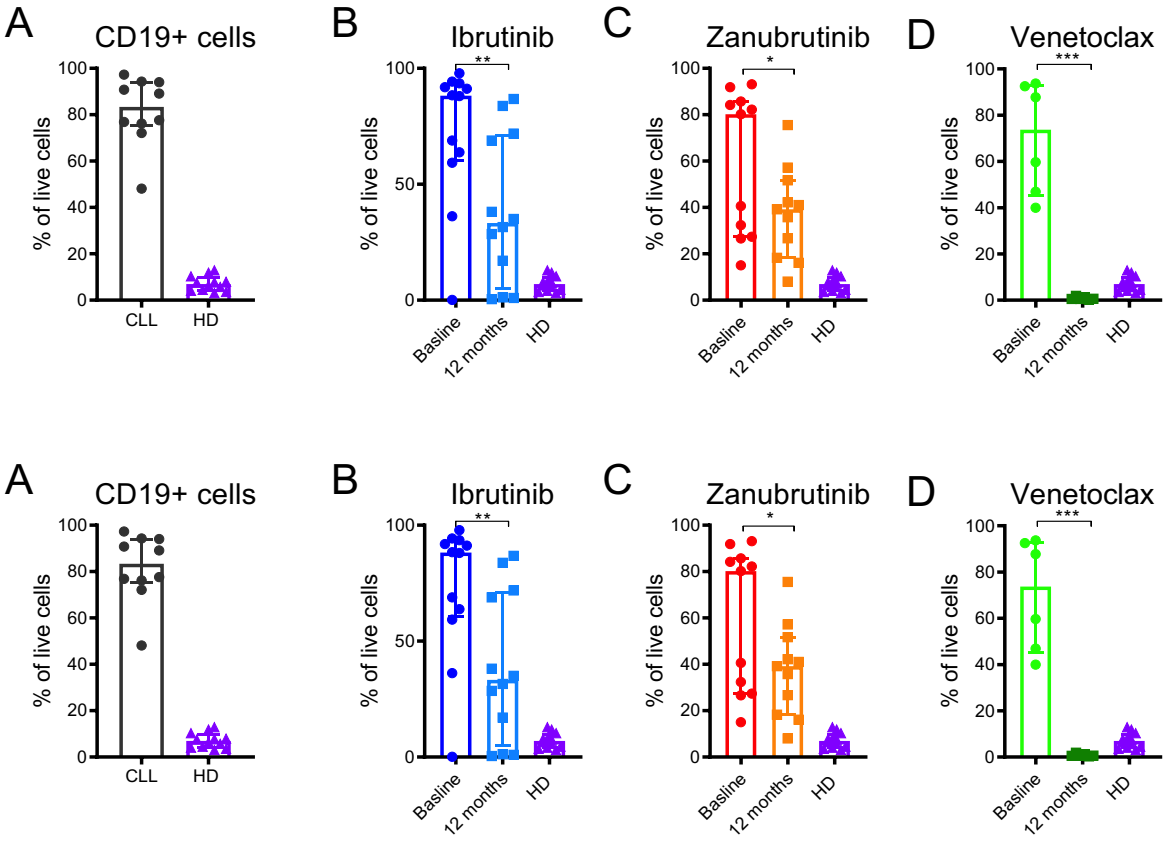

Figure 4.1 Targeted therapies reduce the frequency of CD19+ cells in the peripheral blood

CD19+ cells as a percentage of total live cells in PBMC from A) untreated CLL patients and healthy donors and from R/R CLL patients prior to treatment and after 12 months on either B) ibrutinib, C) zanubrutinib or D) venetoclax. Bars represent median with interquartile range. Differences between timepoints determined using a Wilcoxon matched-pairs signed rank test, * $p < 0.05$ ** $p < 0.01$, *** $p < 0.001$.

Ibrutinib treated patients

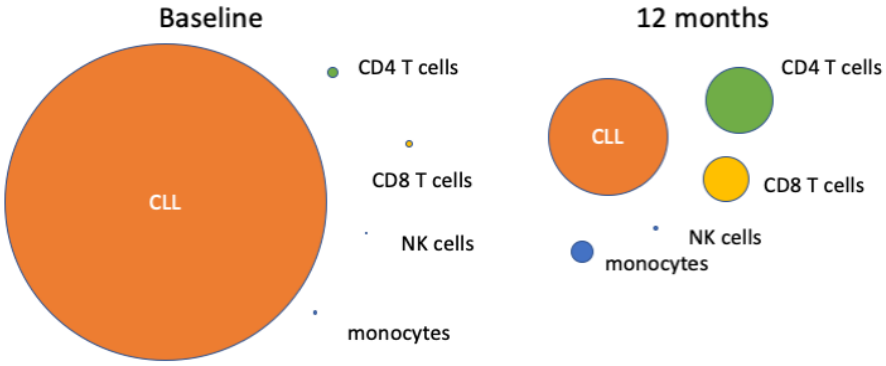

Zanubrutinib treated patients

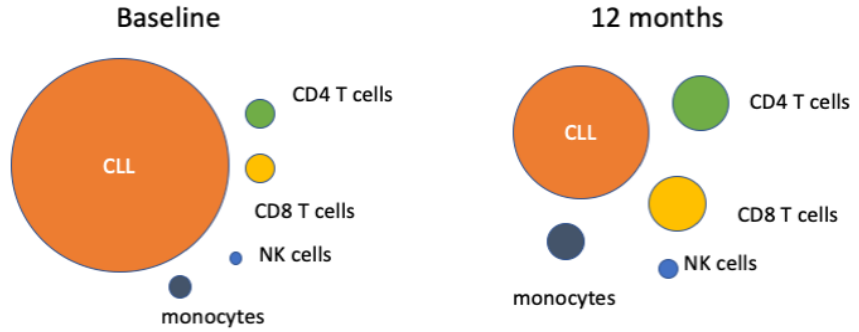

Venetoclax treated patients

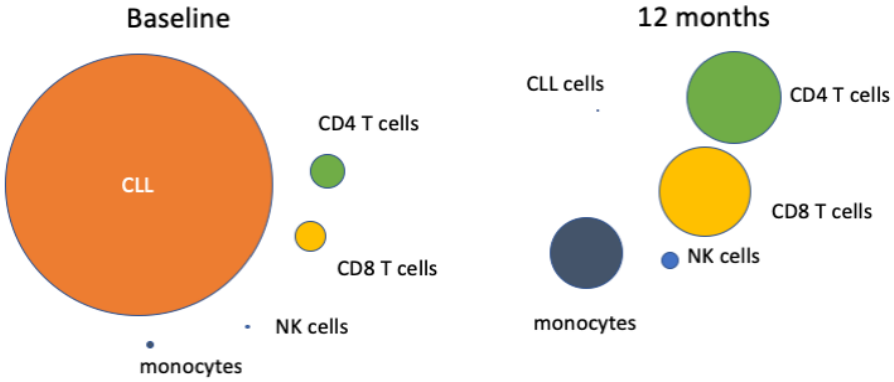

Healthy donors

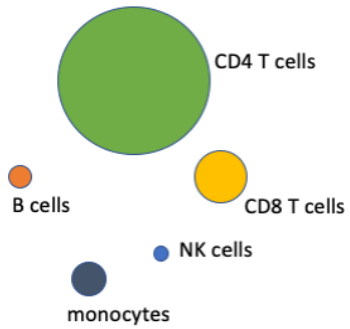

Figure 4.2 Summary of changes in the frequency of immune populations in the peripheral blood of CLL patients after 12 months treatment with targeted therapy treatment

Comparison of the frequency of immune population abundance in the peripheral blood of CLL patients treated with ibrutinib or venetoclax and age-matched healthy donors. Size represents relative frequency (percent of live cells). Only major immune populations represented.

4.3.1 *MYELOID CELL SUBSETS*

The first objective on this analysis was to measure the changes to myeloid immune populations in patients treated with either ibrutinib, zanubrutinib or venetoclax for 12 months. The frequency of monocytes (CD11b+ CD33+ HLADR+), MDSC (CD11b+ CD33+ $HLADR^{low/neg}$), myeloid DC (CD33+ CD11b– CD11c+ HLADR++), and plasmacytoid DC (CD123+ HLADR++) subsets was quantified as a proportion of the CD19 negative (non-leukaemia) population, as described in Figure 2.9.

Ibrutinib treated patients had a significant increase in the frequency of monocytes (Figure 4.3 b), which was associated with a significant increase of the proportion of monocytes that were of a classical (CD14++ CD16–) and intermediate (CD14++CD16+) phenotypes (Figure 4.3 e). No change in the overall proportion of monocytes nor in the composition of the monocyte subsets was seen in patients treated with the more selective BTK inhibitor zanubrutinib (Figure 4.3 c, f). However, there was a significant increase in the expression of PD-L1 on both intermediate and non-classical monocytes (CD14 low CD16+) (Figure 4.3 h-j). Similarly, ibrutinib treated patients, but not those treated with zanubrutinib, had a significant increase in the proportion of CD14+ MDSC (Figure 4.4 b-c). Furthermore, ibrutinib treated patients had an increased frequency of mDC (Figure 4.5 b). Notably, untreated CLL patients and the R/R CLL patients at baseline had significantly lower frequency of plasmacytoid DCs (Figure 4.5 e). However, treatment with targeted therapies did not result in a significant change in the frequency plasmacytoid DC frequency after treatment (Figure 4.5 f-h).

In the venetoclax treated cohort there was a significant increase in the proportion of total monocytes without an associated change in the subset composition (Figure 4.3 d, g). This increase resulted in venetoclax treated patients having a significantly greater proportion of monocytes that was observed in age matched healthy donors. Furthermore, venetoclax treated patients also had a significant increase in the proportion of CD14+ myeloid derived suppressor cells and myeloid dendritic cells (Figure 4.4 d and Figure 4.5 d).

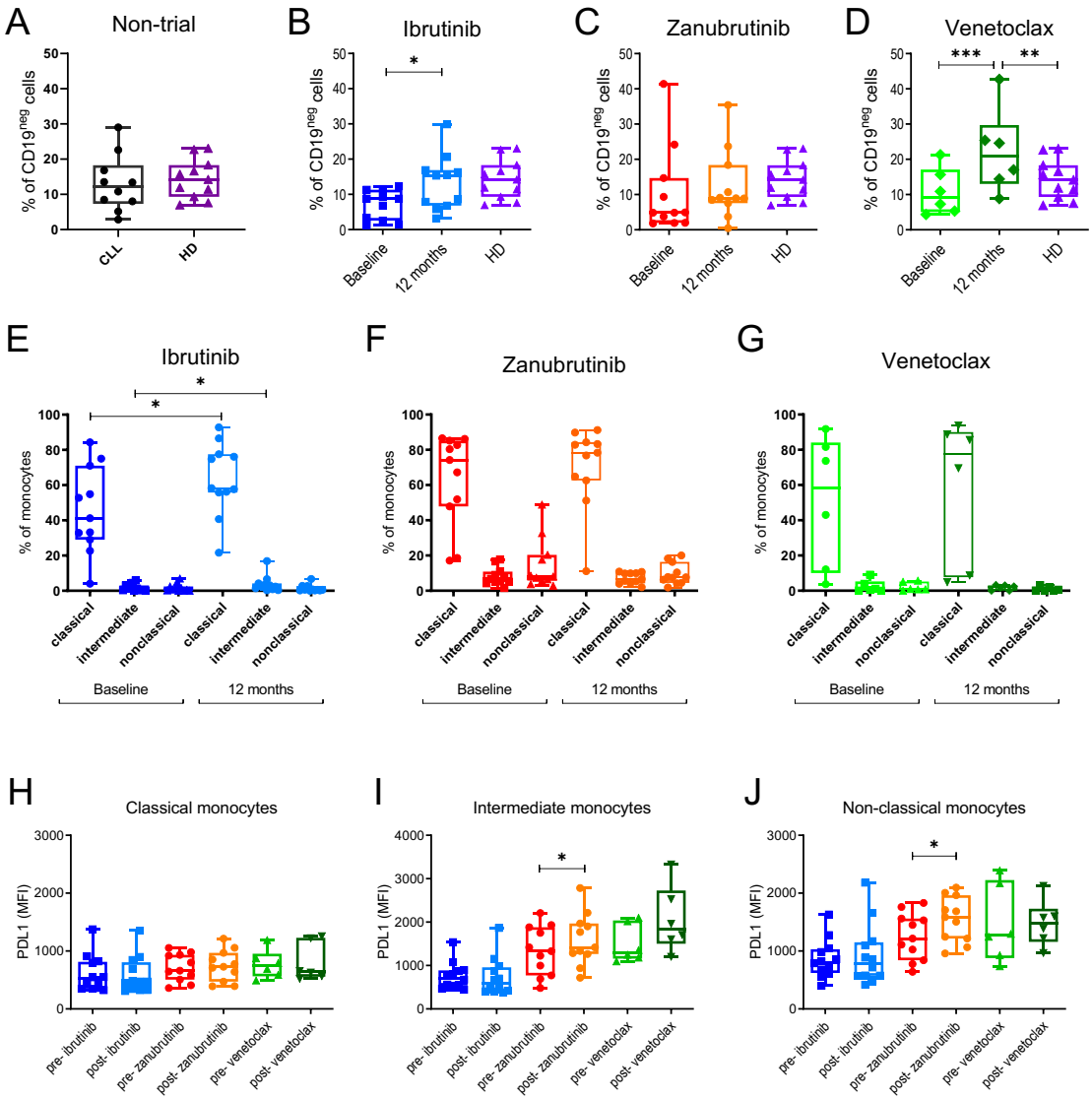

Figure 4.3 Monocytes and monocyte subsets are differentially affected by targeted therapies

PBMC was isolated from untreated CLL patients, age matched healthy donors and R/R CLL patients prior to initiation of novel therapy and after 12 months continuous daily therapy with either ibrutinib, zanubrutinib or venetoclax. A-D) Monocytes (CD11b+CD33+HLADR+) as a frequency of the total non-leukaemia cells. E-G) Classical (CD14++CD16–) intermediate (CD14++ CD16+) and nonclassical (CD14lowCD16+) monocyte subsets as a proportion of total monocytes. H-J) Expression (MFI) of PD-L1 on monocyte subsets in H) classical, I) intermediate and J) non-classical monocytes from treated patients. Differences between timepoints determined using a Wilcoxon matched-pairs signed rank test, * p <0.05 ** p <0.01, *** p <0.001.

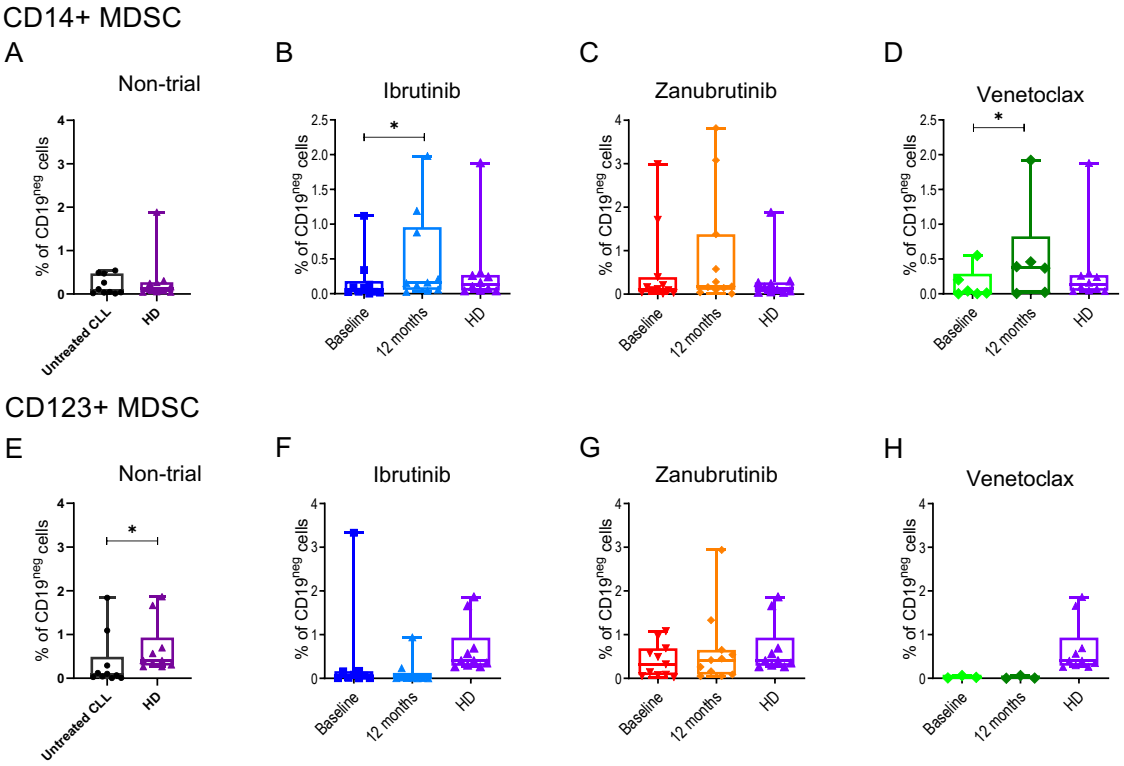

Figure 4.4 Myeloid derived suppressor cell frequency increased in venetoclax treated patients

PBMC from untreated CLL patients, age matched healthy donors and R/R CLL patients treated with either ibrutinib, zanubrutinib, or venetoclax for 12 months were analysed by flow cytometry. A-D) frequency of CD14+ MDSC (CD11b+CD33+HLADR$^{low/neg}$CD14+) as a proportion of non-leukaemia cells. E-H) CD123+ MDSC (CD11b+CD33+HLADR$^{low/neg}$ CD123+) as a proportion of non-leukaemia cells. Differences between timepoints determined using a Wilcoxon matched-pairs signed rank test, * $p < 0.05$.

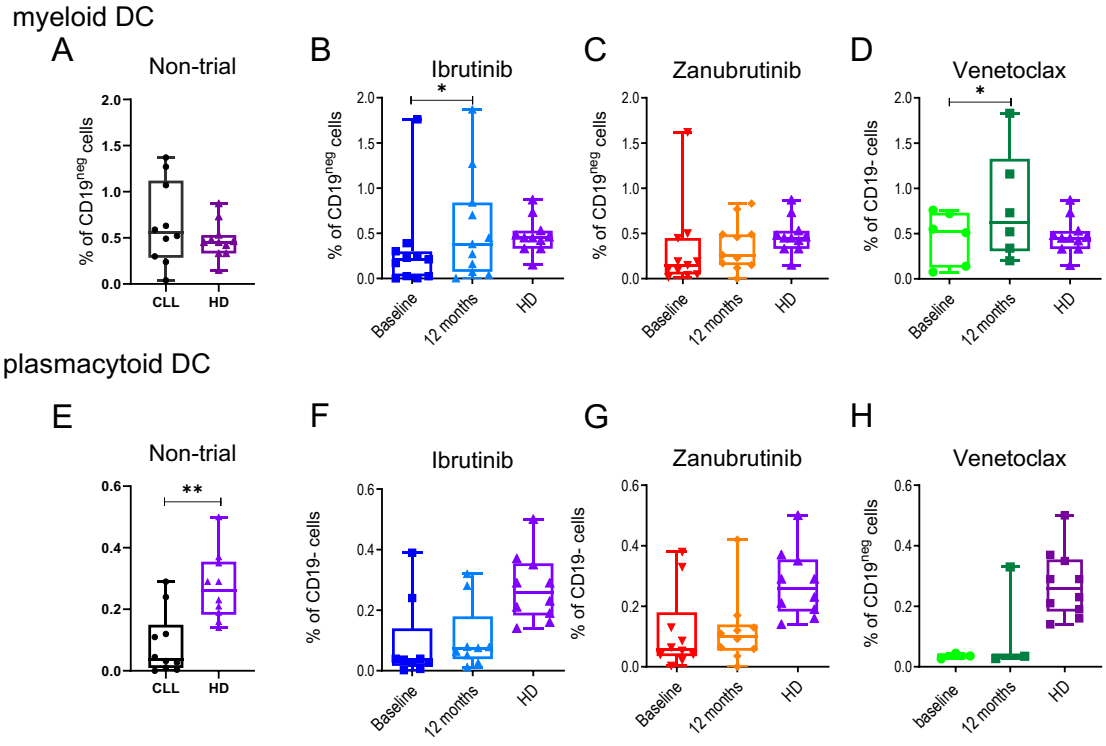

Figure 4.5 Frequency of dendritic cell subsets are not altered by treatment with targeted therapy

PBMC was isolated from untreated CLL patients, age matched healthy donors and R/R CLL patients prior to initiation of novel therapy and after 12 months continuous daily therapy with either ibrutinib, zanubrutinib or venetoclax. A-D) Boxplots summarising the frequency of myeloid dendritic cells (mDC) (lineage ^{neg} HLADR+CD11c+CD123–) as a proportion of total CD19- cells. E-H) Boxplots summarising the frequency of plasmacytoid dendritic cells (pDC) (lineage ^{neg} HLADR+ CD11c– CD123+) as a proportion of total CD19^{neg} cells. Differences between timepoints determined using a Wilcoxon matched-pairs signed rank test, * p <0.05.

Given the changes observed in patients treated with either ibrutinib or venetoclax, the changes to the immune profile in patients treated with the combination of ibrutinib and venetoclax was also investigated. As was observed in the monotherapy cohorts, patients treated with combination ibrutinib and venetoclax had a significant increase in the frequency of monocytes at 6 months (3 months on combination therapy) (Figure 4.6 a). However, in contrast to either the ibrutinib or venetoclax treated cohorts, there was a simultaneous significant decrease in the proportion of total MDSC (Figure 4.6 b). Furthermore, in the combination treatment cohort there was a significant increase in the proportion of mDC, which was significantly increased at 6 months as compared to both the baselines and pre-venetoclax timepoints (Figure 4.6 c). There was no significant change in the proportion of plasmacytoid DC at either 3 or 6 months (Figure 4.6 d). While ibrutinib monotherapy was associated with a change in the composition of monocyte subsets, venetoclax was not. In the combination treated cohort there was a significant increase in the proportion of classical monocytes at both 3 and 6 months as compared to baseline (Figure 4.6 e-g).

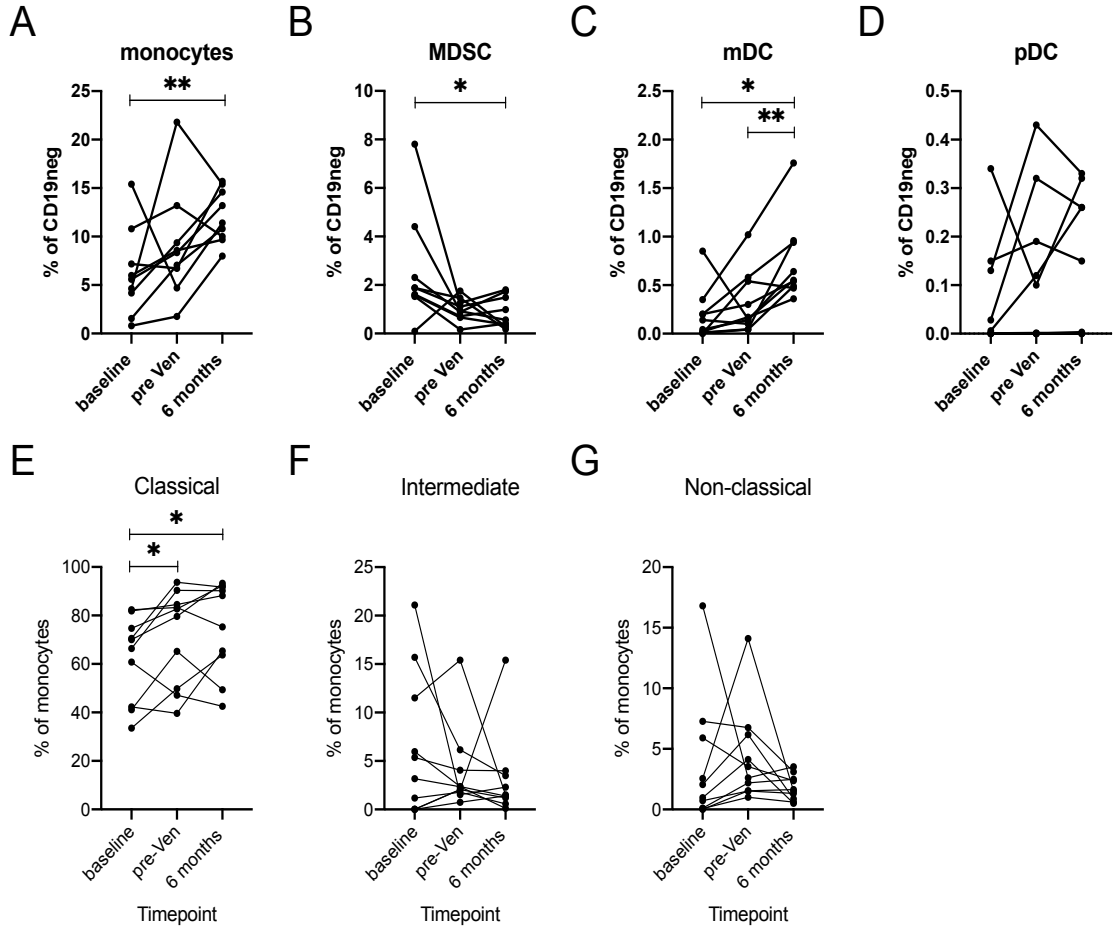

Figure 4.6 Myeloid subsets in patients treated with combination ibrutinib and venetoclax

Treatment naïve CLL patients were treated for 3 months with single agent ibrutinib prior to addition of venetoclax. PBMC were isolated from samples taken at baseline, prior to the introduction of venetoclax and after 3 months combination treatment. A) Frequency of monocytes B) Frequency of MDSC C) frequency of myeloid DC and E) frequency of plasmacytoid DC as a proportion of CD19 negative cells. E-F) frequency of monocyte subsets as a proportion of total monocytes. RM one-way AONVA with Fisher's LSD test, * $p < 0.05$ ** $p < 0.01$.

4.3.2 LYMPHOID SUBSETS

This analysis also investigated the effects of targeted therapies on multiple lymphoid subsets, including NK and T cell subsets. No significant change in the frequency of total NK cells was observed in any of the treatment groups (Figure 4.7 a-d). However, there was a trend to decreased total NK cells in the venetoclax treated patients ($p = 0.06$) and the proportion of $CD56^{dim}CD16+$ NK cells was significant decreased after venetoclax but not either of the BTK inhibitors (Figure 4.7 h).

While the frequency of total T cells in the peripheral blood of any cohort analysed did not change (Figure 4.8 a-d), there was a trend to a decreased CD4/CD8 ratio in the untreated CLL patient cohort as compared to healthy donors. At baseline all of the R/R cohorts had significantly lower CD4/CD8 ratios as compared to healthy donors, (ibrutinib $p=0.019$, zanubrutinib $p=0.014$, venetoclax $p=0.021$). However, there was no significant change in the CD4/CD8 ratio after treatment. Similarly, there were no significant changes in the memory phenotype of CD4 or CD8 T cells in any of the monotherapy treated cohorts examined at one year (Figure 4.9 and Figure 4.10).

Innate-like T cells have been demonstrated as having different expression of both ITK and Bcl-2 as compared to conventional T cells. Therefore, this analysis also investigated multiple innate like T cell subsets including NKT cells, γδT cells and virtual memory T cells (T_{VM}). There were no significant differences in the frequency of NKT cells in any cohort analysed (Figure 4.11 a-e). There was also no significant difference in the frequency of γδT cells between healthy donors and either the untreated CLL patients or the treated CLL cohorts at baseline and neither BTK inhibitor altered the γδT cell frequency (Figure 4.11 f-h). However, despite no significant change in the total T cell frequency, there was a significant increase in the frequency of γδT cells as a proportion of total T cells in venetoclax treated patients after one year on therapy (Figure 4.12 i), resulting in a greater proportion of gamma delta T cells than was observed in the healthy donor cohort. This effect was not observed in the ibrutinib and venetoclax combination treated patients which had a significant reduction in the γδT cell frequency at both 3 and 6 months (Figure 4.12 j).

To further investigate this finding an expanded cohort of venetoclax treated patients was identified. This cohort had samples collected over a median of 3 years of continuous venetoclax therapy. When compared to age matched healthy donors[†] there was no difference in the frequency of the total γδT cell population at baseline, however there was a trend toward a lower proportion of the Vδ2 subset in particular (Figure 4.12 a, b). In this cohort there was a significant increase in the proportion of γδT cells from one month, which remained consistently higher across the sample follow-up period (Figure 4.12 c). This was associated with an increase in the frequency of the Vδ2 subset of γδT cells. In order to assess if the increase in the γδT cell population in venetoclax treated patients was due to an expansion of the γδT cells or a preferential survival, the memory phenotype of these cells was also assessed (as described in Figure 2.11). There was a trend to decreased naïve and central memory γδT cells and an increase in the effector memory cells, indicating an expansion of the γδT cell population (Figure 4.12 e-h).

Another immune subset of interest was the virtual memory T cells, which have been identified as having a greater capacity for homeostatic proliferation in the context of lymphodepletion and higher Bcl-2 expression than naïve CD8 T cells[182]. To investigate if this difference in Bcl-2 expression altered the abundance of this subset the frequency of T_{VM} cells was tracked over several years of venetoclax treatment. When compared to age matched healthy donors the frequency of T_{VM} in the R/R CLL cohort, who had undergone prior lymphodepleting therapy, was not significantly altered. T_{VM} cells have also been shown to have higher expression of Bcl-2 than true naïve CD8 T cells[182]. Therefore, we examined this subset in the long term venetoclax treated patients. There was a significant increase in this subset after 1 month of venetoclax treatment, a trend that was maintained over the next 3 years (Figure 4.13).

[†] Independent cohort from the HDs in the previous analysis of γδT cells in Figure 5.7 due to availability of HD samples at the time of analysis

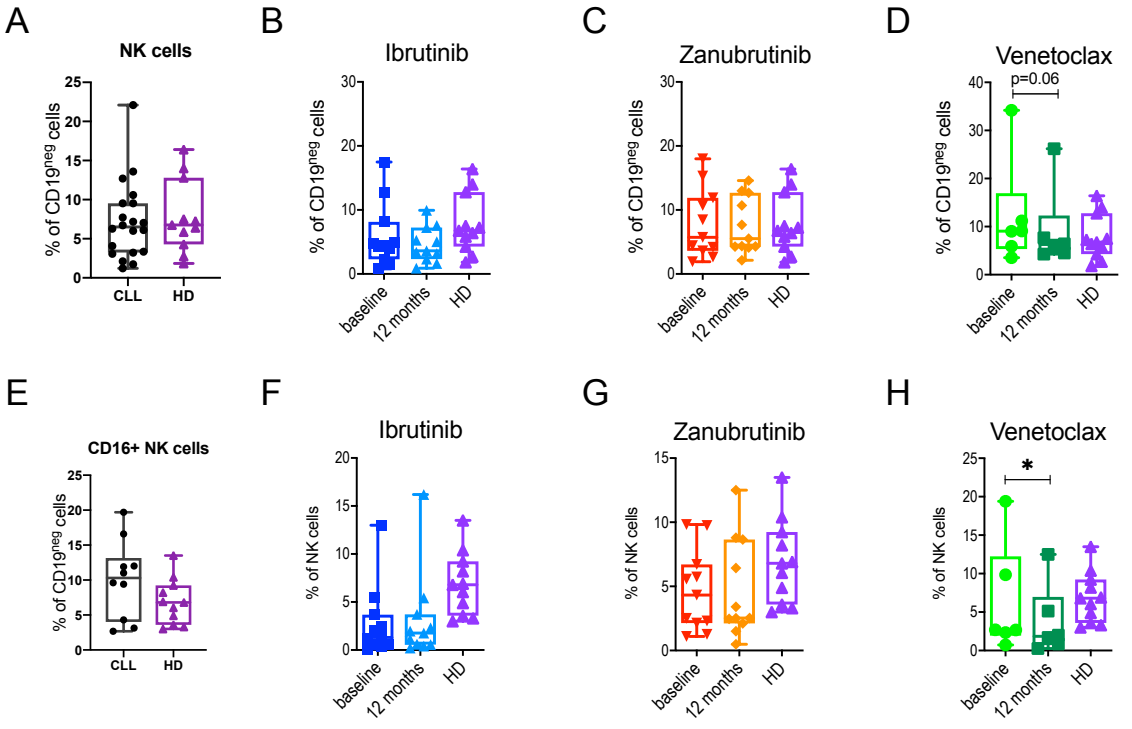

Figure 4.7 NK cell frequency in CLL patients treated with novel targeted therapies
PBMC isolated from CLL patients prior to initiation of novel therapy and after 12 months continuous daily therapy. A-C) boxplots summarising the frequency of total NK cells (Lin-CD56+) as a proportion of non-leukaemia cells. D-F) boxplots summarising the frequency of CD16+ NK cells as a proportion of total NK cells. Wilcoxon matched-pairs signed rank test *p<0.05.

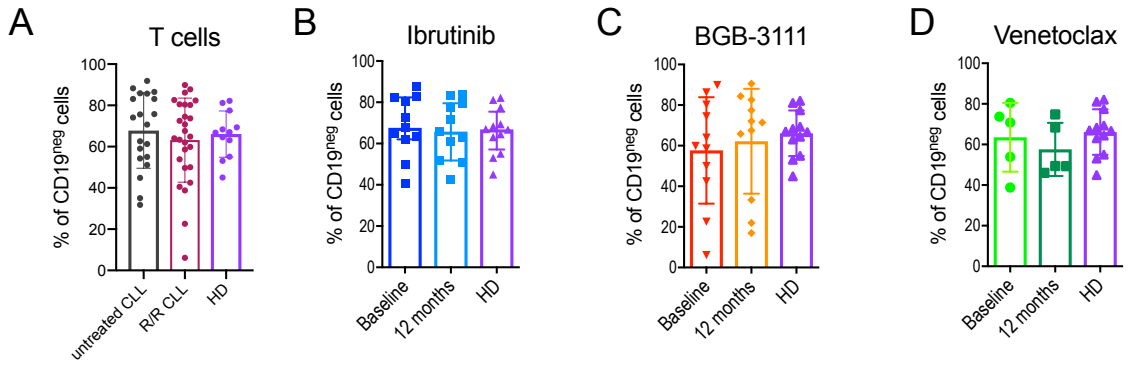

Figure 4.8 Frequency of T cells as a proportion of non-leukaemia cells in the peripheral blood of CLL patients

Frequency of T cells (CD3+) as a proportion of total CD19 negative cells in A) non-trial CLL patients and healthy donors B) ibrutinib treated C) zanubrutinib and D) venetoclax treated CLL patients. CD4 to CD8 ratio in E) non-trial CLL patients and healthy donors F) ibrutinib treated G) zanubrutinib and H) venetoclax treated CLL patients. Error bars represent median with interquartile range. Differences between CLL and healthy donors determined using Mann-Whitney test, * $p<0.05$

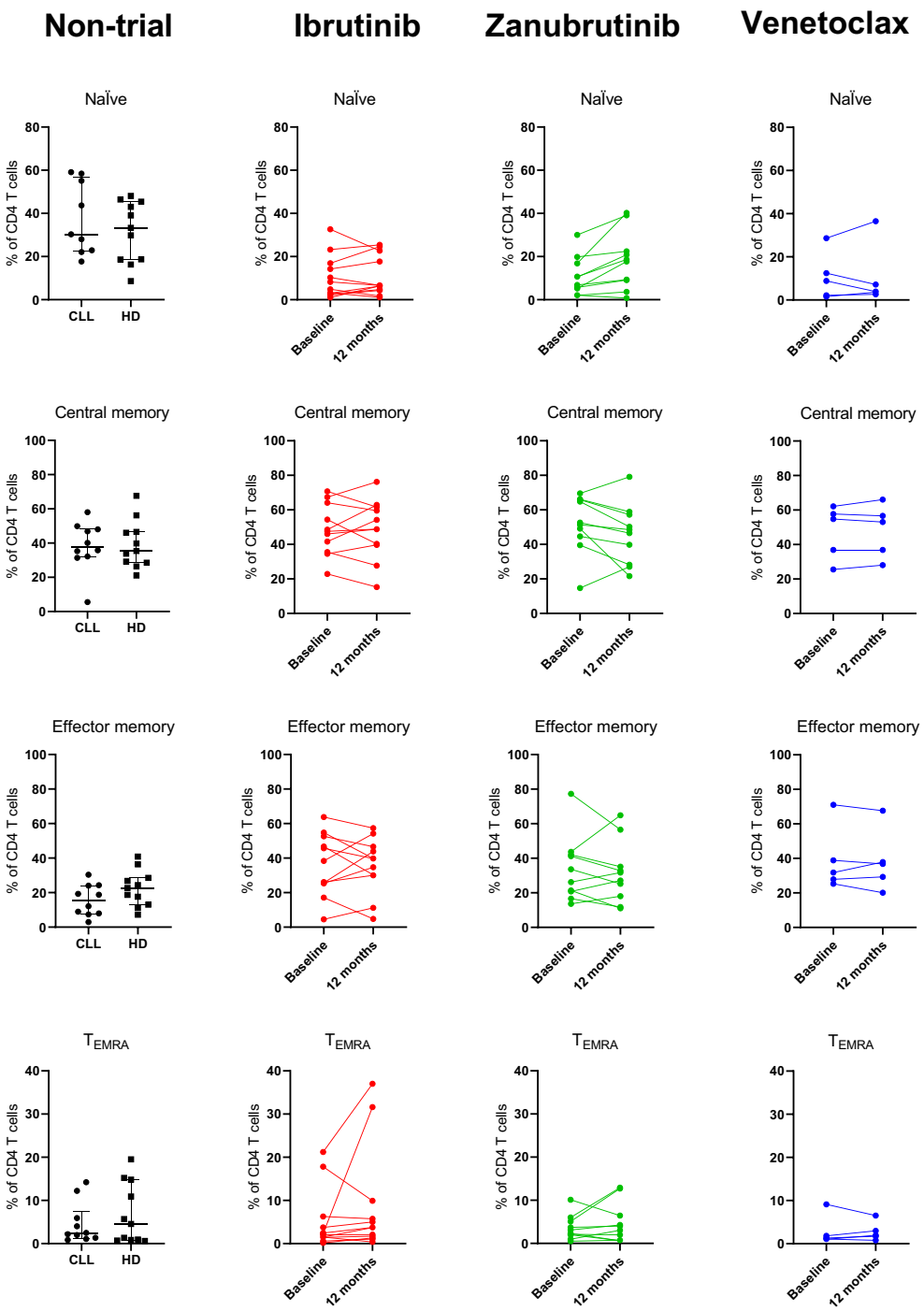

Figure 4.9 CD4 T cell memory phenotype is not significantly changed with treatment

Naïve (CD27+CD45RA+) central memory (CD27+ CD45RA-) effector memory (CD27-CD45RA-) and T_{EMRA} (CD27-CD45RA+) subsets as a percentage of total CD4+ T cells. T cells in untreated CLL patients, age matched healthy donors, ibrutinib treated patients, zanubrutinib treated patients and venetoclax treated patients after 12 months continuous therapy. Lines represent individuals.

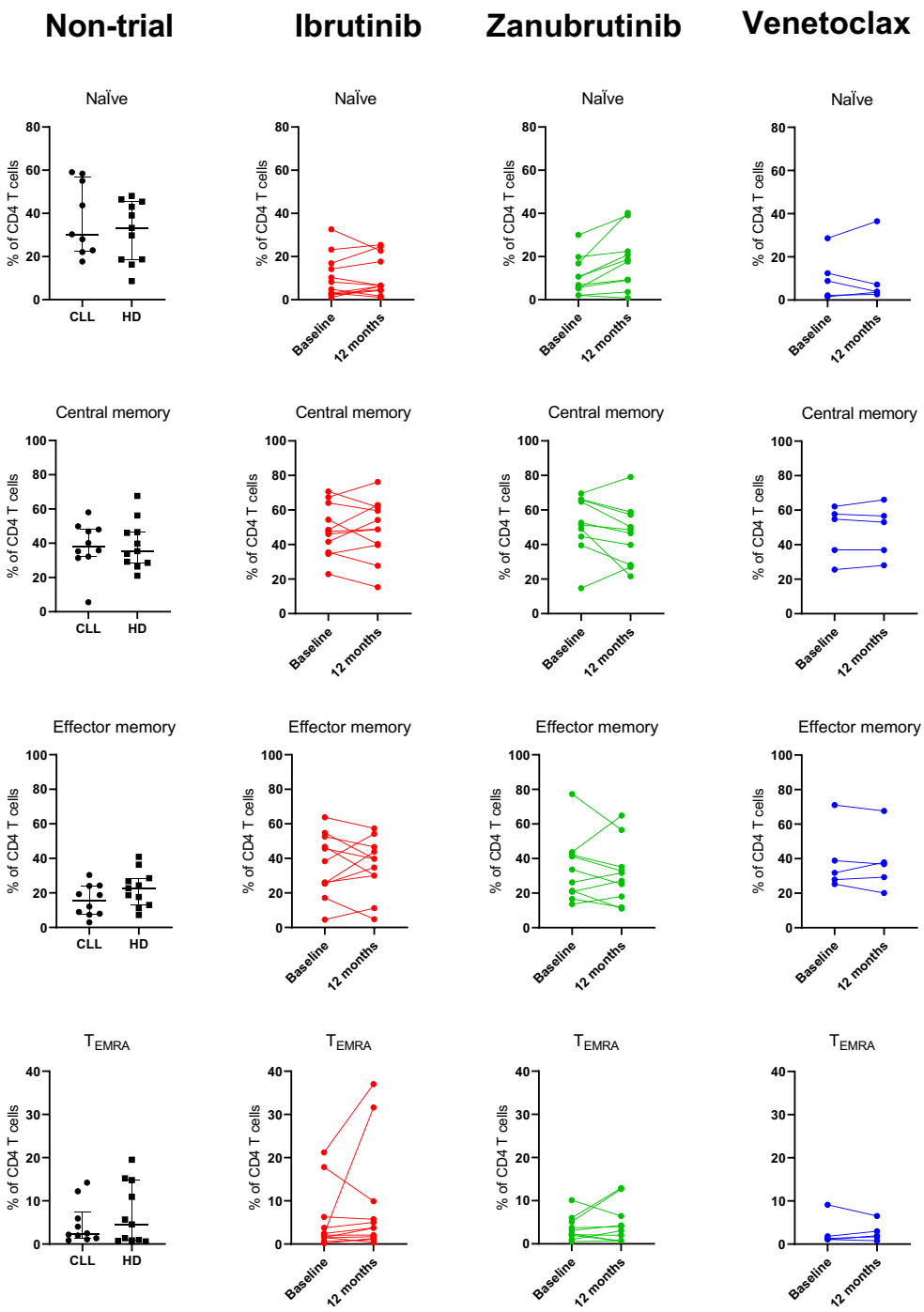

Figure 4.10 CD8 T cell memory phenotype is not significantly altered by targeted therapy

Memory subsets, Naïve (CD27+CD45RA+) central memory (CD27+ CD45RA-) effector memory (CD27-CD45RA-) and T_{EMRA} (CD27-CD45RA+) subsets as a percentage of total CD8+ T cells in untreated CLL patients, age matched healthy donors, ibrutinib treated patients, zanubrutinib treated patients and venetoclax treated patients after 12 months continuous therapy. Lines represent individuals.

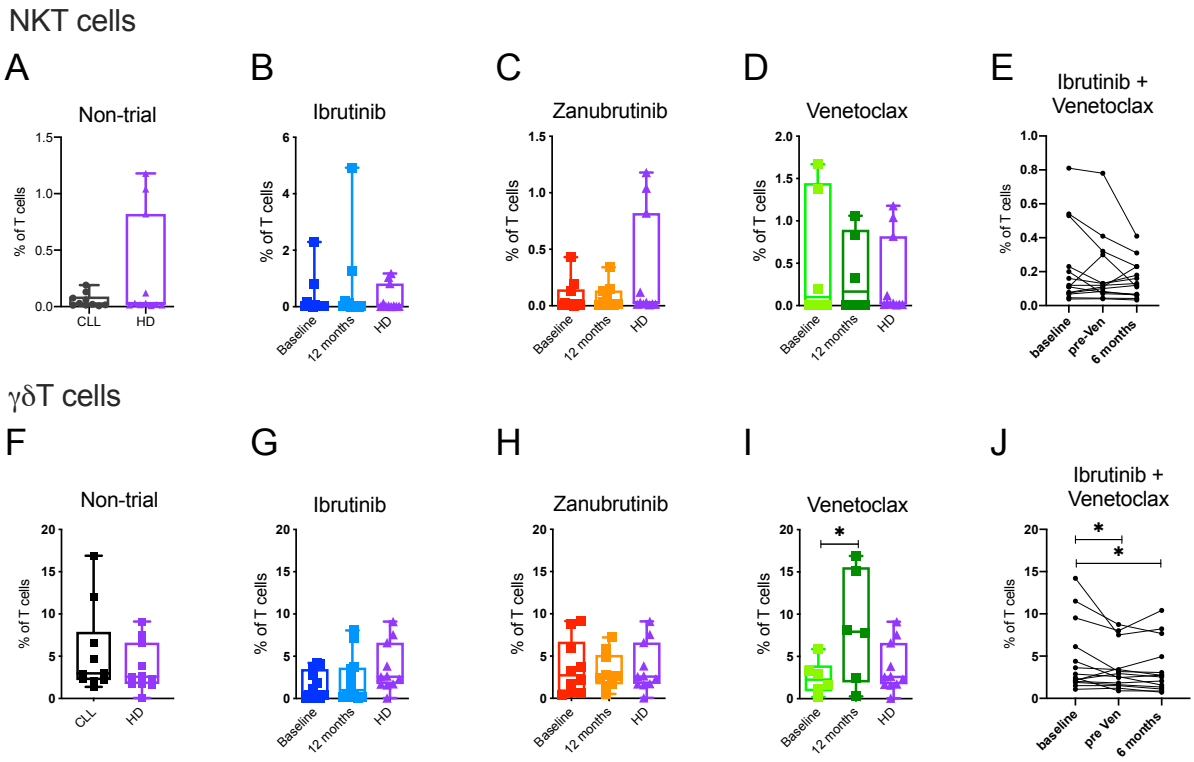

Figure 4.11 Frequency of unconventional T cells in CLL patients treated with targeted therapies

PBMC from untreated CLL patients, healthy donors, R/R CLL patients treated with either ibrutinib, zanubrutinib or venetoclax and previously untreated CLL patients treated with combination ibrutinib and venetoclax was analysed by flow cytometry. The frequency of A-E) NKT cells and F-j) γδT cells as a percentage of total T cells. Paired Wilcoxon test * $p < 0.05$.

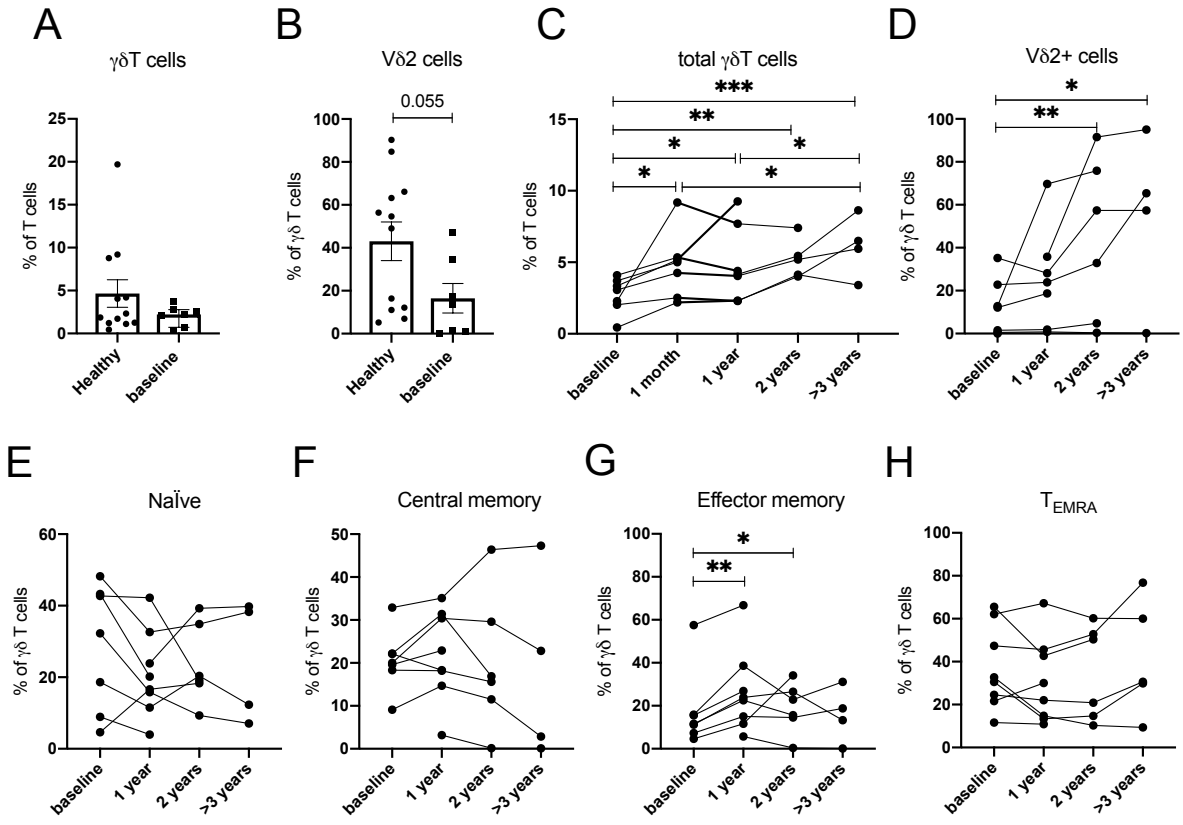

Figure 4.12 γδT cell subsets are increased in long term venetoclax treated patients

In an expanded cohort of long term venetoclax treated CLL patients, the frequency of γδT cells were quantified using flow cytometry according to Figure 2.11. A) frequency of γδT cells in R/R CLL patients prior to venetoclax treatment and age-matched healthy donors B) frequency of Vδ2 cells as a proportion of total γδT cells in R/R CLL and age matched healthy donors. C) frequency of γδT cells in CLL patients treated with venetoclax. D) frequency of Vδ2 γδT cells in CLL patients treated with venetoclax. E-H) memory phenotype of γδT cells in long-term venetoclax treated patients. Lines represent individual patients, significance determined using ANOVA with Fishers LSD multiple comparisons, * $p < 0.05$ ** $p < 0.01$ *** $p < 0.001$

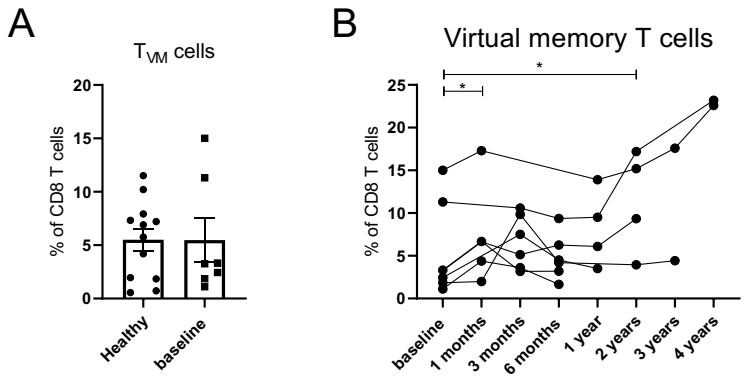

Figure 4.13 Virtual memory T cell increased in CLL patients treated with venetoclax

In an expanded cohort of long term venetoclax treated CLL patients, the frequency of T_{VM} cells was quantified using flow cytometry according to Figure 2.11. A) T_{VM} cells were defined as CD8+CD45RA+NKAG2+/Pan-KIR+ T cells as a proportion of total CD8 T cells in age-matched healthy donors and R/R cell patients. B) the change in T_{VM} frequency over venetoclax treatment in R/R CLL patients. ANOVA with Tukey-Kramer test for multiple comparisons, * $p < 0.05$ ** $p < 0.01$

Prior studies into the effect of ibrutinib on T cells has focused on CD4 T cell subpopulations. It has been suggested that ITK inhibition by ibrutinib results in T_H1 skewing[218]. Therefore, the frequency of T_H1 T_H2 and T_H17 cells after long term treatment with ibrutinib was of interest. This analysis found that there were dramatic changes in the T_H1 and T_H2 frequency over the time of ibrutinib treatment, but no consistent trend was observed (Figure 4.14). Other groups had shown that after short periods of ibrutinib treatment, of less than 6 months, there was a significant decrease in regulatory T cells[222,312]. In this analysis multiple timepoints were analysed over a median of 3.5 years. The frequency of regulatory T cells oscillated over the course of treatment with no consistent trend (Figure 4.15).

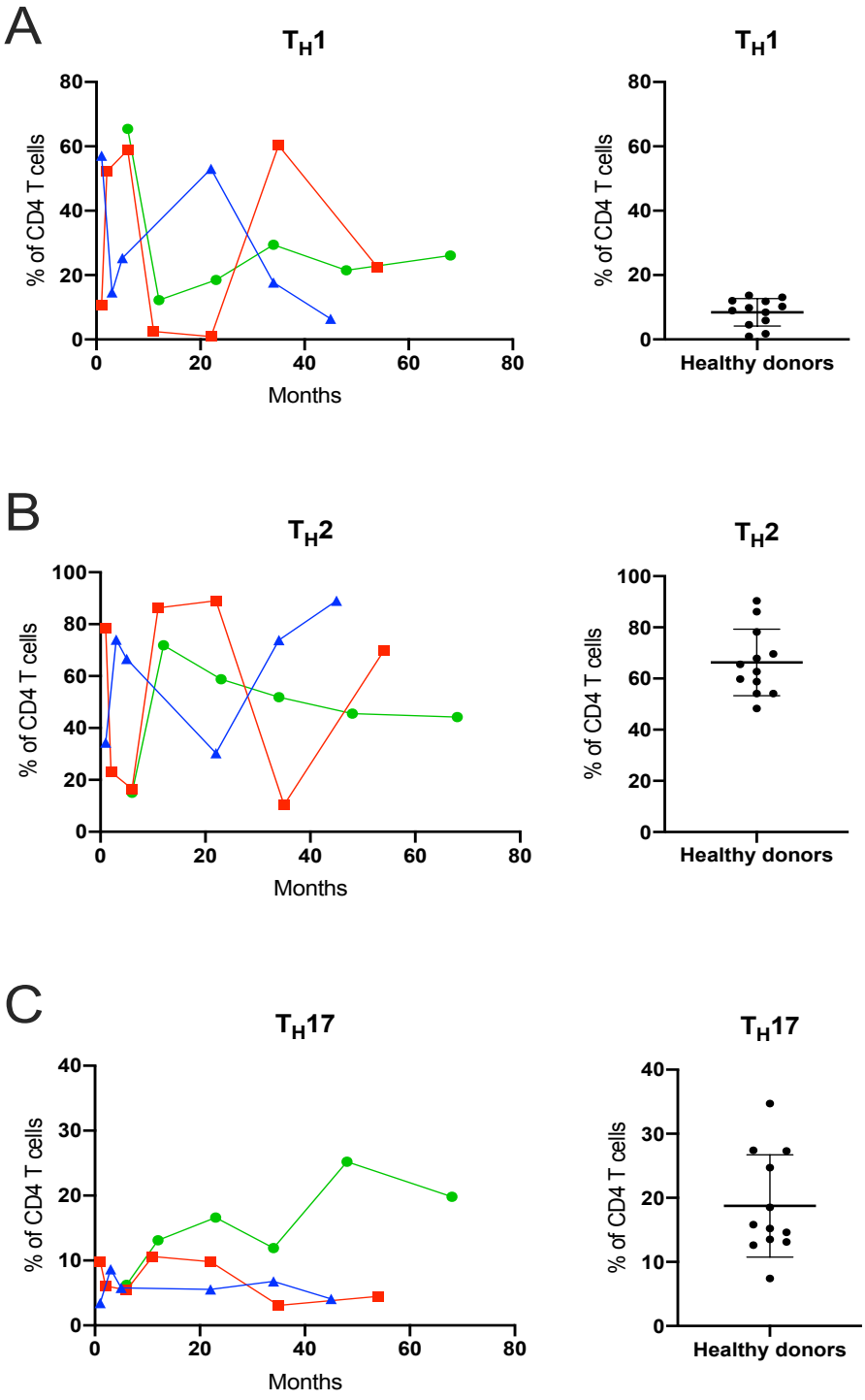

Figure 4.14 Helper T cell subsets in long term ibrutinib treated CLL patients and healthy donors

PBMC from CLL patients treated with ibrutinib for 4 years and age matched healthy donors were analysed by flow cytometry the frequency of CD4 T cell subpopulations according to Figure 2.10. of A) T_H1 cells (CD4+CXCR3+CCR6-) B) T_H2 cells (CD4+CXCR3-CCR6-) C) T_H17 cells CXCR3- CCR6+). Lines represent 3 different patients.

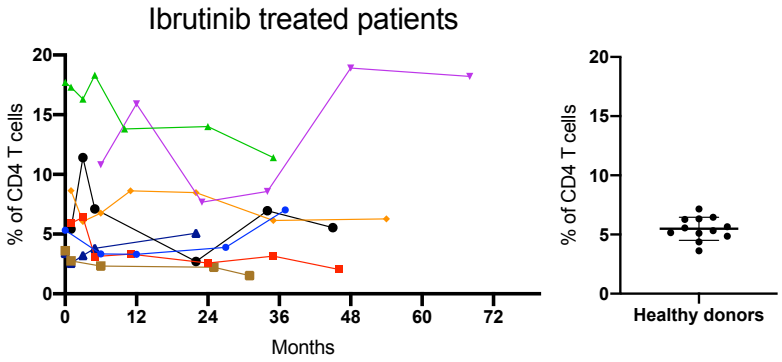

Figure 4.15 Regulatory T cell frequency in long term ibrutinib treated patients and healthy donors

Regulatory T cells (CD4+CD127-CD25+FoxP3+) were identified by flow cytometry according to Figure 2.10 in PBMC samples taken from ibrutinib treated patients at multiple timepoints over the course of treatment and from age matched healthy donors. Lines represent individuals.

4.3.3 Ex vivo T cell function

Based on the results presented in Chapter 3 which showed that *in vitro* treatment with ibrutinib significantly impaired CD8 T cell function, an *ex vivo* T cell function was analysed on matched samples taken for patients at baseline and after 6 months of either ibrutinib, zanubrutinib or venetoclax monotherapy. Only in the ibrutinib treated cohort was there a significant decrease in the CD8 T cell degranulation response between the baseline and post treatment timepoints (Figure 4.16). PBMC from the same venetoclax and ibrutinib treated patients were also analysed for the production of cytokines after *in vitro* stimulation with CD2/CD3/CD28 T cell stimulation beads for 24 hours. Supernatant cytokines levels were consistently decreased in the post-ibrutinib treatment samples while there was no pattern in the samples isolated from venetoclax treated patients Figure 4.17 and Figure 4.18.

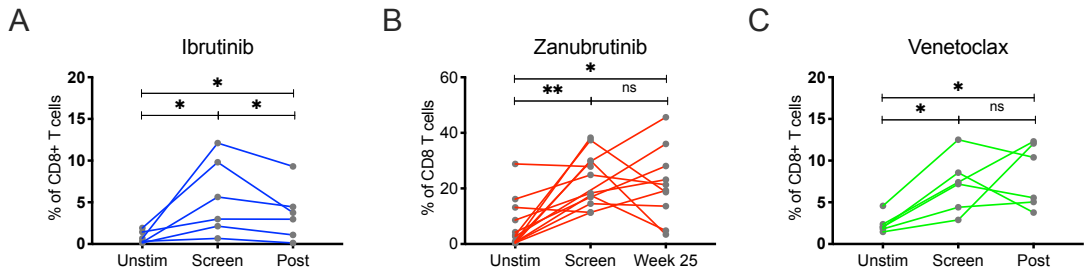

Figure 4.16 Ibrutinib significantly decreased ex vivo degranulation responses

PBMC samples from patients treated with A) venetoclax B) ibrutinib or C) zanubrutinib were stimulated with CD2/Cd3/CD28 T cell stimulation beads for 4 hours in the presence of anti-CD107a antibody. CD107a+ CD8 T cells from A) venetoclax B) ibrutinib and C) zanubrutinib treated patients. Bars represent median and interquartile range, Wilcoxon matched-pairs signed rank test *$p < 0.05$, ** $p<0.01$

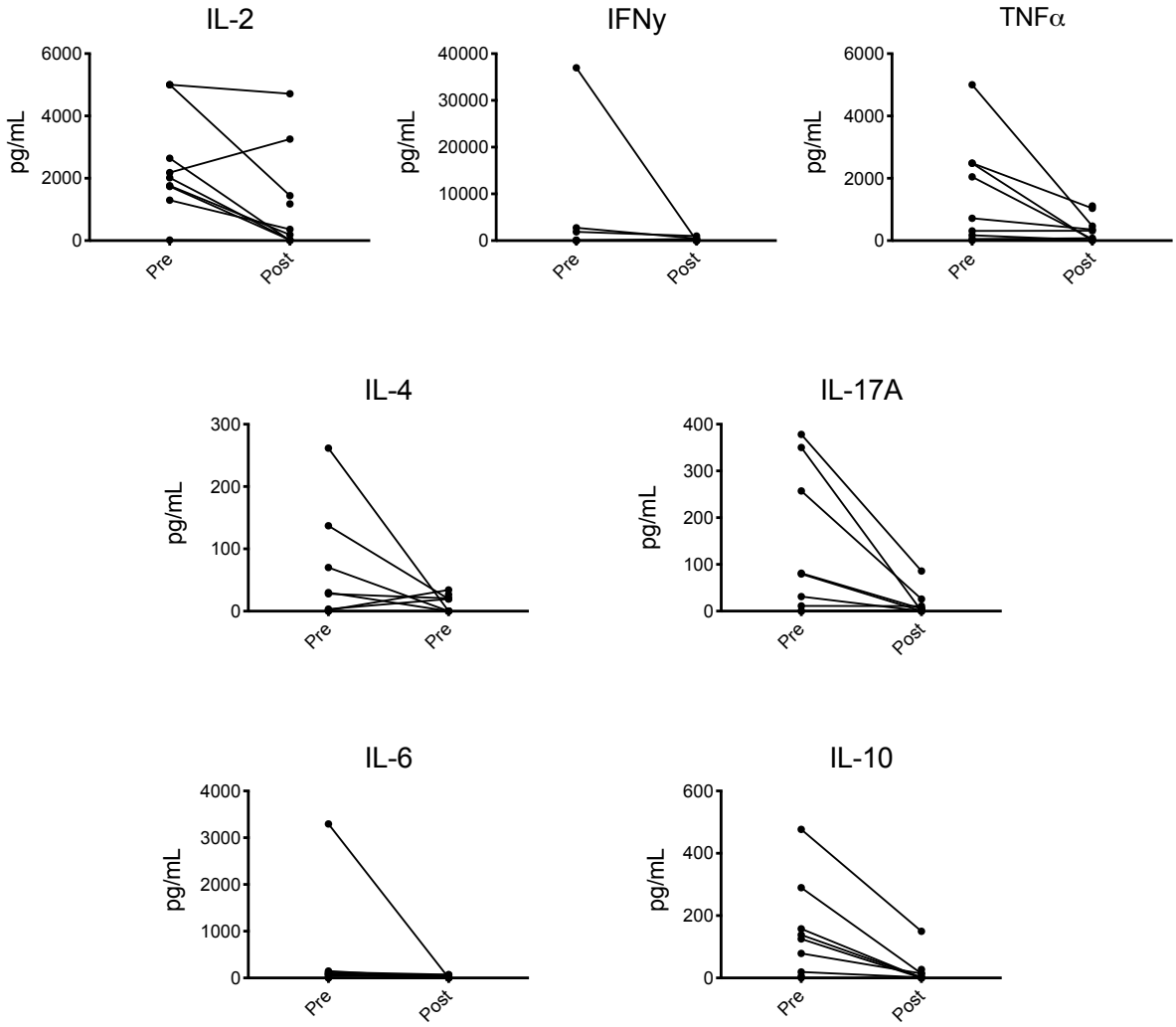

Figure 4.17 Ibrutinib treated patients have decreased in vitro cytokine production

PBMC from CLL patients at baseline and after 6 months treatment with ibrutinib were stimulated with CD2/CD3/CD28 T cell stimulation beads for 24 hours and supernatant cytokine concentrations measured by cytometric bead array.

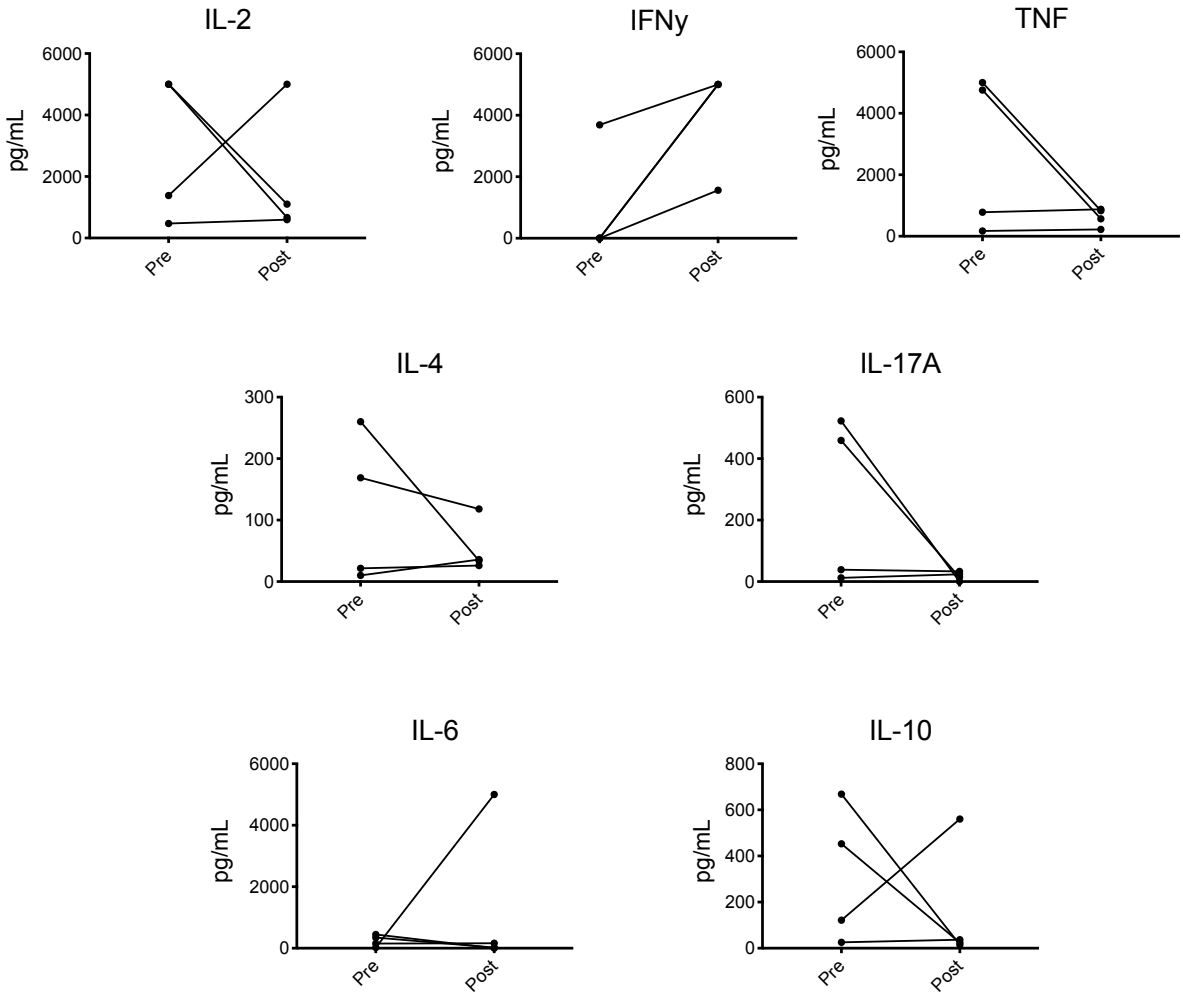

Figure 4.18 Venetoclax treated patients have no consistent change in cytokine production

PBMC from CLL patients at baseline and after 6 months treatment with venetoclax were stimulated with CD2/CD3/CD28 T cell stimulation beads for 24 hours and supernatant cytokine concentrations measured.

4.4 DISCUSSION

This analysis utilised a unique set of CLL patient cohorts to analyse the effect of long-term treatment with ibrutinib, zanubrutinib and venetoclax on the immune system. The study expands on previous studies which focused on early post-treatment timepoints, usually analysing samples taken in the first 6 months on therapy [222,308,312]. Furthermore, this analysis was intentionally broad in the immune populations it identified, with the intention to capture a general understanding of the immune profile. This study is the first to report the long-term effects of continuous treatment with targeted therapies on the immune system of CLL patients and the first exploration of the in vivo effects of combination ibrutinib and venetoclax on the immune system. Together these results suggest that small molecule inhibitors have distinct effects on the composition of the immune system.

Venetoclax treated patients were found to have a relative increase in the frequency of myeloid populations in the peripheral blood. These patients also had a significant decrease in mature NK cells and an increase in innate-like T cell populations, specifically γδT cells and virtual memory T cells. The two BTK inhibitors investigated, ibrutinib and zanubrutinib, induced distinctly different changes to the immune profile. Ibrutinib treatment (but not zanubrutinib) resulted in altered CD14+ monocyte and MDSC populations. While ibrutinib did not have a consistent effect on the frequency of CD4 T cell subpopulations, the *ex vivo* functional assays indicate that ibrutinib treated patients had suppressed T cell function. When used in combination, ibrutinib and venetoclax significantly altered the frequency of multiple myeloid populations, including increased frequencies of monocytes and myeloid DCs and a decreased frequency of MDSCs.

While a key strength of this analysis is that it represents the real-world effect of novel therapies on the immune system of CLL patients, there are a number of important limitations to this analysis. An important limitation in this analysis is that absolute cell counts could not be reported. This study relied on cryopreserved PBMC precluding the most accurate method of obtaining cell counts in which counting beads are added to fresh blood samples. Furthermore, in these patient cohorts the collection of

contemporaneous white cell counts was inconsistent. Finally, it was determined that as the method of PBMC isolation used excludes some immune populations, in particular granulocytes, from the final product, using contemporaneous white cell counts would be potentially misleading.

A further limitation of this study is that only peripheral blood was available for analysis. Therefore, this analysis cannot delineate immune population redistribution from changes in the abundance of the population. In particular it has been reported that lymph node and peripheral blood samples from CLL patients have important differences in the frequency of key populations, in particular a greater skewing of the CD4:CD8 ratio on the lymph nodes[311]. The differences observed between the peripheral blood and other CLL niches suggests that targeted therapies may have distinct effects on different immune populations, particularly after ibrutinib treatment. The transient lymphocytosis that is observed in patients treated with BTK inhibitors has been attributed to the inhibition of BTK downstream of the CXCR4 receptor[57]. However, other members of the Tec Family such as ITK that are also inhibited by ibrutinib, are key downstream mediators of CXCR4 signalling in NK and T cells[191,313]. While this would suggest that there should be increased mobilisation of these populations into the peripheral blood, the effect of ibrutinib or other Tec kinases on T cell homing has not been investigated.

This analysis measured changes to the frequency of immune populations over time. As such an important caveat to the analysis is the inability to delineate the changes that are occurring due to the effect of the microenvironment and the direct effects on the immune populations. Importantly, data was not available about incidences of infection in these cohorts. While the rates of infections in patients treated with targeted therapies are not significantly different to conventionally treated patients[314] infections are common in CLL patients and may cause significant changes in the immune profile. This may explain the oscillation of immune subset frequencies over time, in particular CD4 T cell populations (Figure 4.14 and Figure 4.15).

Targeted therapies also directly impact the microenvironment. Specifically, ibrutinib disrupts macrophage-CLL interactions[223] and has been shown to reduce the

immunosuppressive capacity of CLL cells resulting in reduced T cell dysfunction [233]. Therefore, changes in the immune microenvironment may account for some of the alterations in the immune profile of treated patients. This is highly relevant to understanding the different effects of BTK inhibitors on monocyte populations. In this analysis ibrutinib treated patients had increased monocyte frequency, and zanubrutinib treated patients did not. Furthermore zanubrutinib, but not ibrutinib treatment resulted in increased expression of the immunosuppressive ligand PD-L1 on monocytes. Multiple studies have shown that ibrutinib alters the function of monocyte and monocyte derived populations which has largely been attributed to BTK inhibition. However, ibrutinib also inhibits Tec and Bmx, both of which have important roles in myeloid cells and may explain the differences in the reduced effects of the more selective BTK inhibitors.

Interestingly, in contrast to previous findings that ibrutinib depleted MDSC population in a BTK dependent manner in a mouse model of CLL[187], in this study ibrutinib treatment, but not zanubrutinib was associated with a significant increase in the frequency of mMDSC (Figure 4.4). An important consideration in this analysis is that both blood processing[315] and cryopreservation[316] has been shown to decrease the number of MDSCs. As such the enumeration in this analysis may be an underestimate of the true population in patients. However, as all samples were processed and cryopreserved in the same way, the changes overserved between timepoints remains important. A further limitation in the enumeration of MDSCs in this study lies in the method of characterisation. This study used established surface markers to identify the MDSC population[121,317] but this analysis did not confirm the immunosuppressive nature of the cells, and as such the most accurate nomenclature is an MDSC-like population. This study also did not include CD15 staining in the identification of MDSCs and as such does not provide information about granulocytic MDSCs. However, a large proportion of the MDSC-like cells expressed CD123+, which has been previously identified as a distinct subpopulation of MDSC[318].

Venetoclax treated patients also had increased frequency of multiple myeloid populations, including monocytes, mMDSC and mDC. As a Bcl-2 inhibitor, it is unlikely that the changes observed in venetoclax treated cohorts are due to expansion of myeloid

subsets. Rather, the changes are likely due to the relative Bcl-2 inhibitor resistance of myeloid cells as compared to lymphocyte subsets. This is supported by findings in venetoclax treated mice which had significant deceased numbers of lymphocytes and plasmacytoid DC but not conventional DCs [250]. A further study of Bcl-2 mutant mice found that the numbers of monocytes, granulocytes and eosinophils was unaffected indicating a relative lack of Bcl-2 reliance in some myeloid immune populations[249]. While the potential implications of increased myeloid populations is hard to predict, both monocytes and MDSC have been identified as key components of the CLL supportive microenvironment[112,115,319] and greater frequency of multiple myeloid populations have been identified as a poor prognostic markers in CLL[109–111,123]. Higher frequency of CD14+ $HLADR^{low}$ cells have also been identified as a poor prognostic marker in CLL[122,123].

NK cell maturation has been shown to depend on Bcl-2[249] and in this study venetoclax treated patients, but not those treated with either BTK inhibitor had significantly reduced frequency of mature NK cells. This finding suggests that the sensitivity of normal immune populations may depend on situational Bcl-2 dependence, cells may be more susceptible at different stages of maturation or activation. Difference in Bcl-2 dependence may also explain the relative increase in unconventional T cells. This finding aligns with the proposition that it is not outright Bcl-2 expression that determines venetoclax sensitivity but rather the balance of expression of the whole Bcl-2 family. Given the rapid reactivity and acquired self-tolerance of T_{VM} cells[320], coupled with their increased capacity for homeostatic proliferation T_{VM} cells are of particular interest as a potential substrate population in the generation of CAR-T cells. Interestingly, despite the identification of T_{VM} cells as a population that expands in lymphodeplete conditions[180,321], R/R CLL patients who had received prior lymphodepleting therapy had no significant difference in the frequency of T_{VM} cells.

Similarly γδT cells tend to have higher expression of Bcl-2 than αβT cells[322], which may explain why venetoclax treated patients also had an increased frequency of γδT cells (Figure 4.11). However, the changes observed in the memory phenotype, which tended toward decreased naïve and central memory and a significant increase in the effector

memory subsets, is suggestive of population expansion. Furthermore, the increase in γδT cells was mainly due to the Vδ2 subpopulation (Figure 4.12), further supporting that the increased frequency represents an expansion rather than relative resistance to Bcl-2 inhibition. The implications of these findings require further exploration as little is known about the role of γδT cells in CLL immunity. Vδ2 cells have been identified as being capable of efficiently killing follicular lymphoma cells[323]. However, dysfunctional Vδ2 γδT cells have been shown to be a poor prognostic indicator in CLL[324]. Others have suggested that Vδ2 dysfunction may be reversible and this subset may be a good target for immunotherapy in CLL[171]. Although the specific role that γδT cells play in CLL patient immunity is yet to be defined, these findings, in conjunction with the T_{VM} cell findings, further highlight that Bcl-2 inhibition may be having a subtle, yet appreciable effect on the T cell compartment in CLL with potential implications for the use of T cell directed immunotherapies.

Notably, despite the increase in unconventional T cells in venetoclax treated patients there was no change in the frequency of either CD4 or CD8 T cells and thus despite good disease control at 12 months, there was not a restoration of normal T cell ratio. These findings suggest that treatment with targeted therapies does not restore normal T cell homeostasis and that T cell dysfunction must be taken into account when designing immunotherapeutic strategies for these patients. Furthermore, *ex vivo* functional analysis of T cells isolated from patients treated with ibrutinib showed a significant decrease in degranulation and cytokine production. These findings suggest that ibrutinib results in functional impairment of T cells which will be further explored in subsequent chapters. The reduced cytokine production of ibrutinib treated PBMC is also in line with findings of decreased plasma cytokine concentrations in ibrutinib treated patients[309]. Ibrutinib has also been shown to reduce cytokine release syndrome in CART cell treated patients[325] and infusion reactions associated with anti-CD20 mAb treatment[326].

Conversely, this apparent decreased T cell function is in contrast to published data which suggested that T cell cytotoxicity is improved after ibrutinib treatment[234]. It has also been proposed that prior treatment with ibrutinib improves the capacity for CART cell

generation[286]. This discrepancy in *ex vivo* T cell function may be explained by the half-life of ITK. The half-life of ITK is approximately 1 hour in resting CD4 T cells, which was extended to 22 hours when stabilised by covalent binding of an ITK inhibitor[327]. There is no published data on the half-life of the ibrutinib-ITK complex. In these experiments, the functional assays were performed immediately after thawing of PBMCs. Other *ex vivo* functional studies ibrutinib treated patient T cells have measured functional outcomes after multiple day long cultures[222,286].

4.5 Conclusion

This study provides insight into the long-term effects of novel targeted therapies in CLL who were treated for up to 5 years. This analysis demonstrates that the different targeted therapies have distinct effects on the immune system. Both the Bcl-2 inhibitor venetoclax and the BTK inhibitor ibrutinib resulted in changes to the immune profile, increasing the relative frequency of myeloid subsets while the more selective BTK inhibitor zanubrutinib had limited if any effect on the composition of the immune system. These changes to immune populations should be considered when combining these targeted therapies with immune directed therapies.

5 TARGETED THERAPIES ALTER NK AND T CELL FUNCTION IN VITRO

5.1 SUMMARY

Targeted therapies have been developed to inhibit specific molecular interactions that are essential to the cancer cells growth or survival. However, through both on-target and off-target mechanisms these therapies have the potential to affect normal cells. The effect of targeted therapies on immune cells is particularly salient as effective immunity is important for not only protecting patients from infections but in anti-tumour immunity and the potential for combination with immunotherapies. This chapter focuses on the *in vitro* effects of BTK and Bcl-2 inhibitors on T cells and NK cells. Using functional assays to assess the effector functions of these populations this analysis demonstrates that the BTK inhibitor ibrutinib has significant effects on both T cells and NK cells, while the effects of the second generation BTK inhibitors zanubrutinib and acalabrutinib are more restricted. This analysis also shows that the Bcl-2 inhibitor venetoclax does not alter the effector functions of either T cells or NK cells but results in decreased mature activated subsets.

5.2 INTRODUCTION

Ibrutinib is not only an inhibitor of BTK but also multiple other kinases, including all the members of the Tec family. To date, the most studied alternate target of ibrutinib is ITK. ITK inhibition is the suggested mechanism by which ibrutinib affects the function of NK and T cell populations[218,235]. More selective BTK inhibitors, including zanubrutinib and acalabrutinib, were developed to limit ITK inhibition, the proposed advantage being the decreased impact on NK and T cells. Subsequently, the effect of the more selective inhibitors on NK cell degranulation has been investigated *in vitro* with some inconsistent findings. While some studies found that zanubrutinib and acalabrutinib do not inhibit NK cell ADCC[237,328] others have suggested that acalabrutinib has a mild effect on NK cell degranulation in some contexts[329].

Ibrutinib, and to varying degrees the more selective BTK inhibitors, also inhibit other TEC family kinases including TXK and TEC, both of which are also expressed in NK and T cells and have non-redundant signalling roles with ITK. Published data using biochemical kinase inhibition assays have shown that zanubrutinib and acalabrutinib have very different TEC family kinase inhibition profiles. While zanubrutinib has a more than 100-fold higher IC_{50} for ITK than BTK the IC_{50} for TXK and TEC are 2.2 nM and 44 nM respectively. Acalabrutinib is the most selective of the BTK inhibitors in this study, with an IC_{50} for ITK of greater than 1 μM and for TXK and TEC of 368 nM and 126nM respectively[219] (summarised in Table 5.1).

Table 5.1 Reported IC_{50} (nM) for TEC family kinases of various BTK inhibitors#

	IBRUTINIB	ZANUBRUTINIB	ACALABRUTINIB
BTK	1.5+/- 0.2	0.5 +/- 0.0	5.1+/- 1.0
BMX	0.8 +/- 0.1	1.4 +/- 0.4	46 +/- 12
ITK	4.9 +/- 1.2	50 +/- 5	>1000
TEC	10 +/- 12	44 +/- 19	126 +/- 11
TXK	2.0 +/- 0.3	2.2 +/- 0.6	368 +/- 141

adapted from Kaptein et al. 2018

Thus far, much of what is understood about the absence of ITK, TXK and TEC and the consequences for immune function is based on studies using knock-out mice. However, in the context of the genetic loss of Tec kinases, both the development and function of T

cells is affected[36,330,331]. While only limited data is available from humans with primary immunodeficiency resulting from mutations in ITK[332–334], these patients also have defects in T cell development and defective viral immunity. It remains unclear how the effects of ITK deficiency on the development of T cells alter the subsequent function of these immune subsets and therefore, how closely the effect of inhibition of Tec kinases aligns with the functional impact of the permanent absence of the kinases. In this chapter, the effect of the off-target inhibition of the Tec family by various BTK inhibitors on the function of mature human immune cells was investigated. Based on the distinct inhibition profiles of these three drugs, this analysis aimed to understand what, if any impact the more selective inhibitors had on T cell and NK cell function.

Unlike BTK inhibition, Bcl-2 inhibition does not impact signalling pathways but rather modulates cell survival. As such it is not expected that the function of immune cells will be adversely affected by venetoclax. However, while Bcl-2 is ubiquitously expressed and plays a role in the regulation of survival in all immune cells, different immune subsets have been shown to have varying degrees of Bcl-2 expression and Bcl-2 dependence. For example both malignant and normal B cell populations are significantly more susceptible to Bcl-2 inhibition than other immune populations[247]. However, the regulation of Bcl-2 has been shown to play an indispensable role in both T cell and NK cell maturation [241,249,335] and the balance of Bim and Bcl-2 is critical to the maintenance of peripheral T cell memory homeostasis[243]. As such, this analysis investigated the effect of venetoclax on activated T cells and NK cells.

Through increased understanding of how targeted therapies impact the presence and function of cytotoxic immune populations, this analysis will provide insight into how these therapies affect anti-tumour immunity and inform the combination of these therapies with immunotherapy. Finally, given the known immune defects in CLL patients this analysis aimed to understand how BTK and Bcl-2 inhibitors impacted the function of T cells from both age matched healthy donors and CLL patients. This is particularly important as it allows for a better understanding of direct drug effects in addition to the interaction of T cell dysfunction and the effects of targeted therapies.

5.3 RESULTS

5.3.1 DEGRANULATION

It has been previously demonstrated that the NK cell responses to antibody coated cells is impaired by ibrutinib but not more specific BTK inhibitors [235,237]. My first objective was to test if the same defect in degranulation was observed using bead-based stimulation. Purified NK cells from five healthy donors were pre-treated with ibrutinib, zanubrutinib, venetoclax or vehicle control (DMSO) prior to stimulation with CD2/NKp46 NK stimulation beads for four hours. Compared to the vehicle control, both ibrutinib and zanubrutinib treated NK cells exhibited significantly diminished degranulation and IFNγ responses, though the effect of ibrutinib appeared to be greater than that observed with zanubrutinib treatment. Venetoclax did not have a significant impact on NK cell degranulation or intracellular IFN production (Figure 5.1).

A similar assay using CD2/CD3/CD28 T cell stimulation beads allowed for the measurement of CD8 T cell degranulation. PBMC from either healthy donors or CLL patients were pre-treated with ibrutinib, zanubrutinib, acalabrutinib or venetoclax. Ibrutinib treatment resulted in significantly impaired degranulation and IFNγ production on CD8 T cells from both healthy donors (Figure 5.2 a-b) and CLL patients (Figure 5.2 c-d). There was no significant effect of either zanubrutinib or acalabrutinib on the expression of CD107a. However, zanubrutinib, but not acalabrutinib, treated healthy donor CD8 T cells showed significantly diminished IFNγ production (Figure 5.2 b). Venetoclax had no effect on either degranulation or IFNγ production in CD8 T cells.

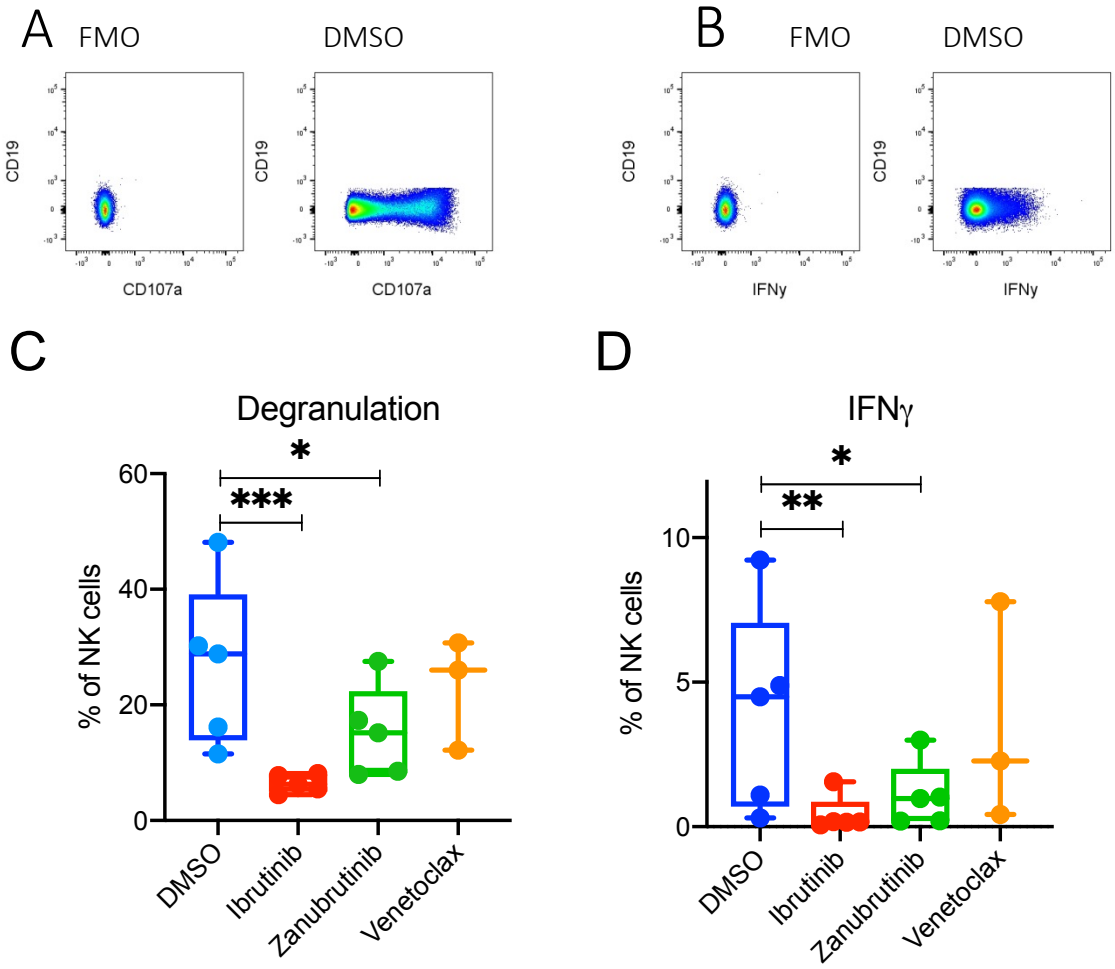

Figure 5.1 Effect of targeted therapies on NK cell degranulation

A) Representative flow cytometry plots of CD107a and B) IFNγ staining in fluorescence-minus-one staining control and vehicle treated NK cells. C-D) NK cells isolated from healthy donor PBMC were treated with 1 μM ibrutinib or 1 μM zanubrutinib or 1 nM venetoclax or DMSO vehicle control for 18 hours prior to stimulation with CD2/NKp46 NK stimulation beads for 4 hours. C) Boxplot summarising the degranulation of NK cells (percent CD107a positive) and D) Percent IFNγ positive NK cells from five healthy donors in two independent experiments. Mixed effects analysis, with Dunnett's multiple comparisons test *p<0.05, **p<0.01 ***p<0.001.

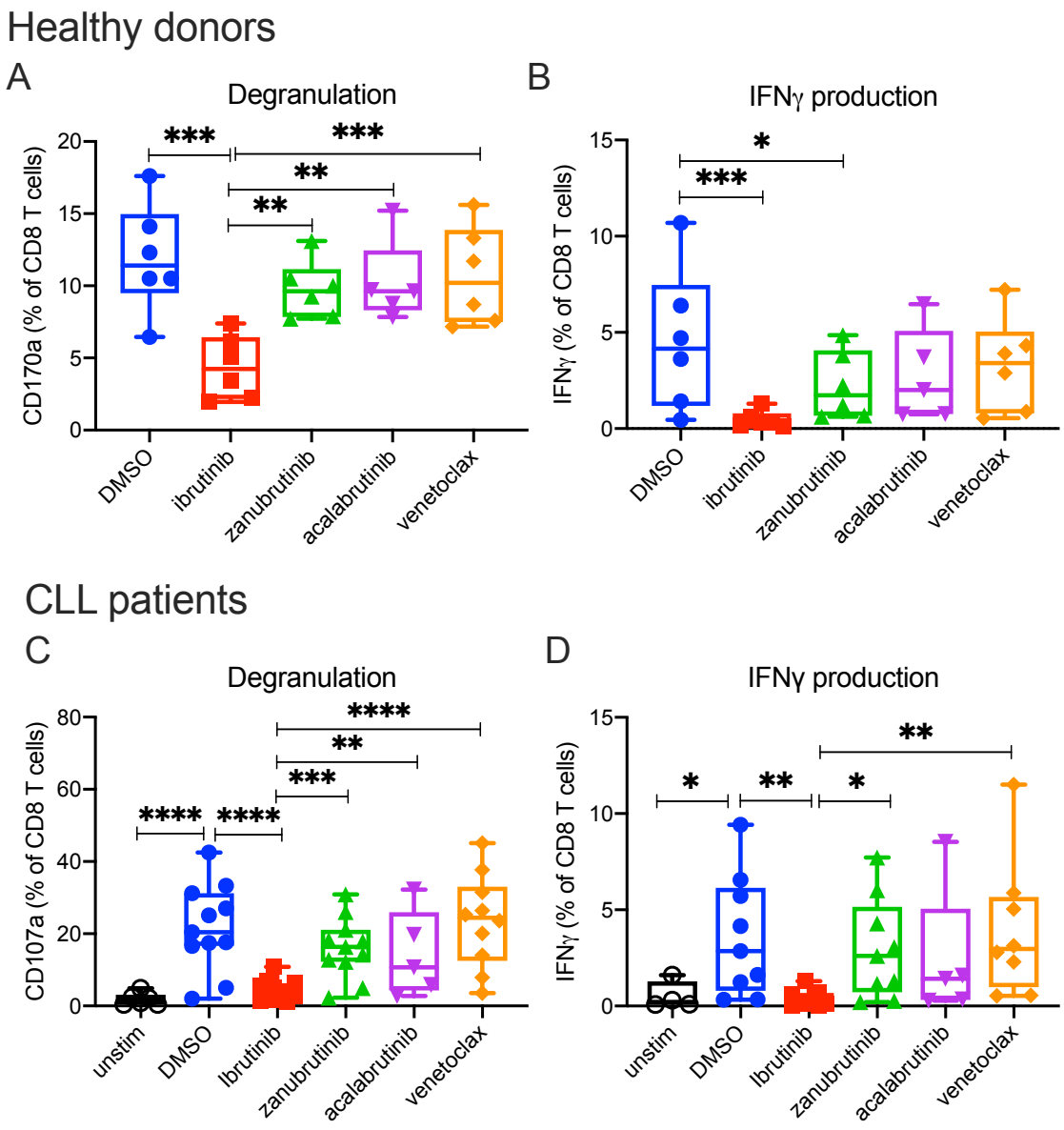

Figure 5.2 Effect of targeted therapies on CD8 T cells from healthy donors and CLL patients

PBMC were treated with 1 μM ibrutinib or 1 μM zanubrutinib or 1 nM venetoclax or DMSO vehicle control for 18 hours prior to stimulation with CD2/CD3/CD28 T cell stimulation beads for 4 hours. Box plots summarising CD8 T cell A) CD107a and B) IFNγ expression in six healthy donors. CLL patient CD8 T cell C) CD107a expression and D) IFNγ expression in eleven CLL patients in two independent experiments. Mixed effects analysis with Tukey-Kramer test for multiple comparisons, *p<0.05 **p<0.01 ***p<0.0001.

NKT cells have been shown to have a greater dependence on ITK than conventional T cells[231]. Therefore, the impact of BTK inhibitors on NKT cell responses was also investigated in *ex vivo* expanded NKT cells from healthy donors. As with CD8 T cells, NKT cells treated with ibrutinib had significantly diminished degranulation and IFNγ production in response to bead stimulation (Figure 5.3 a-b). Interestingly, zanubrutinib also had a significant impact on NKT cell degranulation and IFNγ production in response to bead stimulation. However, this effect was less pronounced than that observed with ibrutinib treatment. Acalabrutinib and venetoclax had no significant impact on NKT cell degranulation.

Due to their restricted TCR, all NKT cells can recognise αGalCer presented in the context of CD1d. Therefore, it is possible for *ex vivo* expanded healthy donor derived NKT cells to recognise allogeneic CLL cells presenting αGalCer. CLL cells from a single donor were stimulated by co-culture with HS-5 bone marrow stromal cells which resulted in increased CLL cell activation and immunogenicity (Appendix A1 and A2). These CLL cells were then co-cultured with pre-treated healthy donor NKT cells. Only CLL cells presenting αGalCer elicited a response from NKT cells and of the inhibitors tested, only ibrutinib significantly reduced the response of NKT cells to antigen recognition (Figure 5.3 c-d).

Finally, to test if ibrutinib also impaired NKT cell killing a cell death assay was performed. In this assay activated CLL cells that had been co-cultured with HS-5 bone marrow stromal cells had significantly improved survival (Figure 5.3 e). Furthermore, the addition of αGalCer to the CLL cells further increased their survival. Somewhat unexpectedly, the viability of CLL cells co-cultured with acalabrutinib and venetoclax treated NKT cells was significantly higher than either vehicle, ibrutinib or zanubrutinib treated NKT cells.

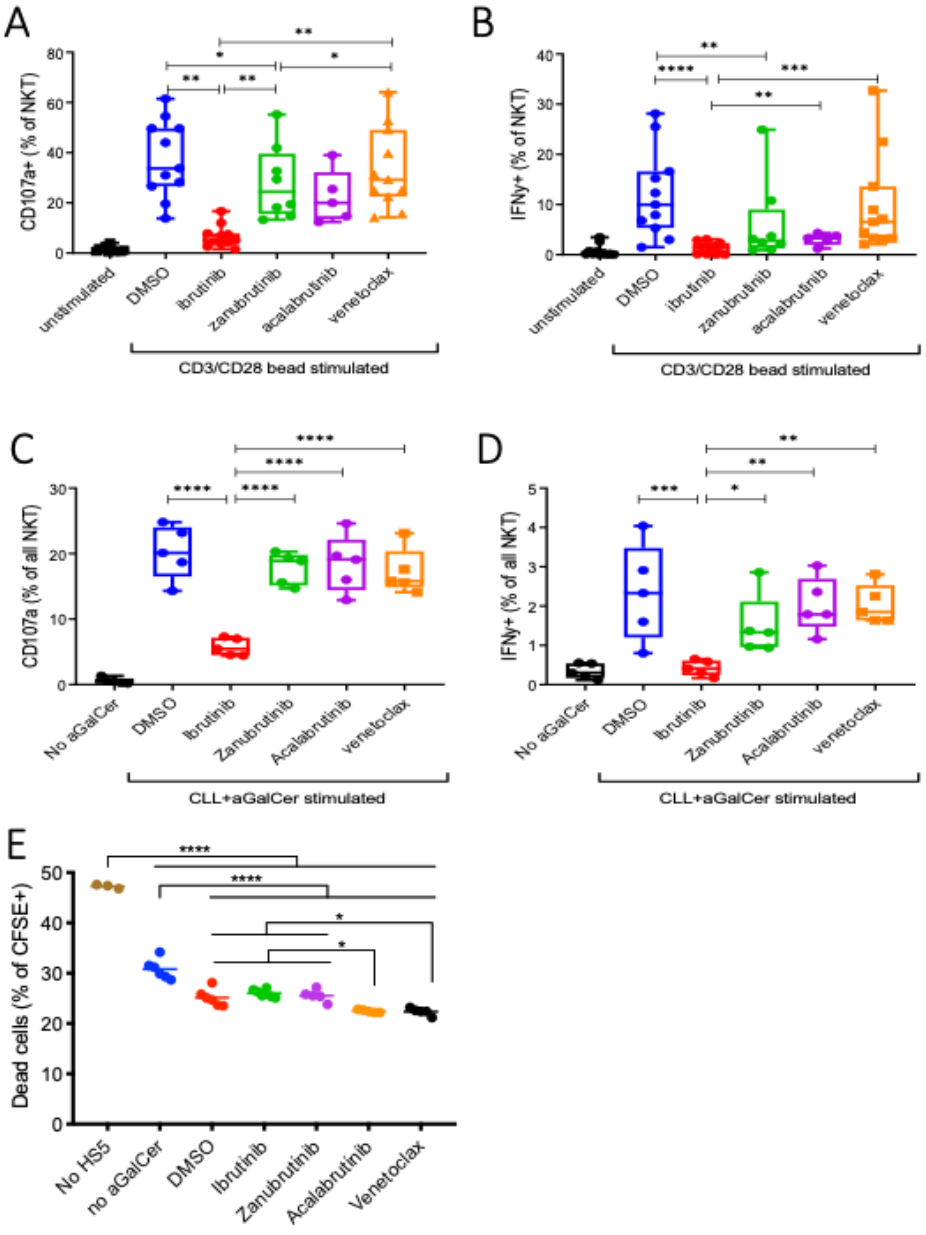

Figure 5.3 Effect of targeted therapies on the cytotoxicity of NKT cells

Ex vivo expanded NKT cells from 11 healthy donors were treated with 1 μM ibrutinib or 1 μM zanubrutinib or 1 nM venetoclax or DMSO vehicle control for 18 hours prior to stimulation. Boxplots summarising A) CD107a expression and B) IFNγ production in NKT cells stimulated for 4 hours with CD2/CD3/CD28 T cell stimulation beads in two independent experiments. Boxplots summarising the frequency of C) CD107a and D) IFNγ expression of NKT cells from five healthy donors stimulated with αGalCer loaded activated CLL cells. E) CFSE stained activated CLL cells presenting αGalCer were co-cultured with drug treated NKT cells. Percent cell death measured using Annexin V/7AAD staining as a percent of total CFSE stained cells. Mixed effects analysis with Tukey-Kramer test for multiple comparisons test *p <0.05 ** p <0.01 ***p <0.001 ****p<0.0001.

5.3.2 *CYTOKINE PRODUCTION*

As discussed in the previous section, NK cells, CD8 T cells and NKT cells treated with ibrutinib and zanubrutinib showed significantly reduced IFNγ production in response to stimulation. To further understand the effect of BTK inhibitors on T cell cytokine production, CD4 T cell production of IFNγ and IL-4 was also investigated. Both ibrutinib and zanubrutinib treated healthy donor CD4 T cells produced significantly more IL-4, while only ibrutinib treatment resulted in significantly decreased IFNγ production (Figure 5.4 c-d). Interestingly, this is not the case in CD4 T cells from CLL patients which exhibited the same decrease in IFNγ production but no change in the IL-4 production (Figure 5.4 e-f).

Intracellular cytokine staining provides information about cytokine production over a short window of activation in which the protein transport inhibitors are present, in these experiments, 4 hours. Measuring cytokine release in the supernatant allowed for the measurement of cytokine production over longer periods. A cytometric bead array was performed on the supernatant of 24-hour cultures of healthy donor or CLL patient PBMC activated with CD2/CD3/28 beads, to measure the T cell associated cytokines IL-2, IL-4, IL-6, IL-10, IL17A, IFNγ and TNFα. Unstimulated CLL and healthy donor PBMC produced undetectable levels of all measured cytokines. After activation with CD2/CD3/CD28 T cell stimulation beads, in healthy donor PBMC cultures treated with ibrutinib there was significantly lower concentrations of all cytokines measured except IL-4 (Figure 5.5), compared with DMSO vehicle controls, a trend also seen in CLL patient PBMC cultures (Figure 5.6). Interestingly, zanubrutinib, acalabrutinib and venetoclax treated healthy donor cultures had significantly increased production of the T_H2 cytokine IL-4 (Figure 5.5 d).

Zanubrutinib treated PBMC produced significantly less TNFα and IL-6 than vehicle treated cells (Figure 5.5 c, f) but had no impact on the secretion of IL-2, IL-17A or IL-10 (Figure 5.5 a, e, g). Acalabrutinib and venetoclax treated cultures had significantly increased IL-17A and IL-10 production than vehicle treated cells (Figure 5.5 e, g). Ibrutinib treatment resulted in significantly reduced IL-2 and IFNγ release in CLL PBMC cultures

(Figure 5.6 a, b). There was no significant effect of any inhibitor on IL-17A or IL-4 production in CLL PBMC cultures (Figure 5.6 d, e). Interestingly venetoclax treated cultures had significantly greater concentrations of TNFα and IL-6 than vehicle treated cultures (Figure 5.6 c, f).

The significant differences in cytokine production by healthy donor and CLL PBMC treated with targeted therapies as compared to vehicle control are summarised in Table 3.2 and 3.4. Notably, while the absolute number of T cells was lower in the CLL PBMC cultures[‡], the supernatant concentration of IL-2 was roughly equal to that in healthy donor PBMC cultures. This is in contrast to the other cytokines measured, all of which had lower concentrations in CLL cultures than in healthy donor cultures, including significantly less IL-6 ($p= 0.0487$), IL-10 ($p = <0.0001$) and TNFα ($p=0.0260$) (Figure 5.7).

[‡] Equivalent numbers of PBMC per mL were aliquoted. Therefore, given that CLL patient PBMC contains a lower percentage of T cells than healthy donors, CLL PBMC cultures contained fewer T cells. Equivalent numbers of stimulation beads were added per number of PBMC.

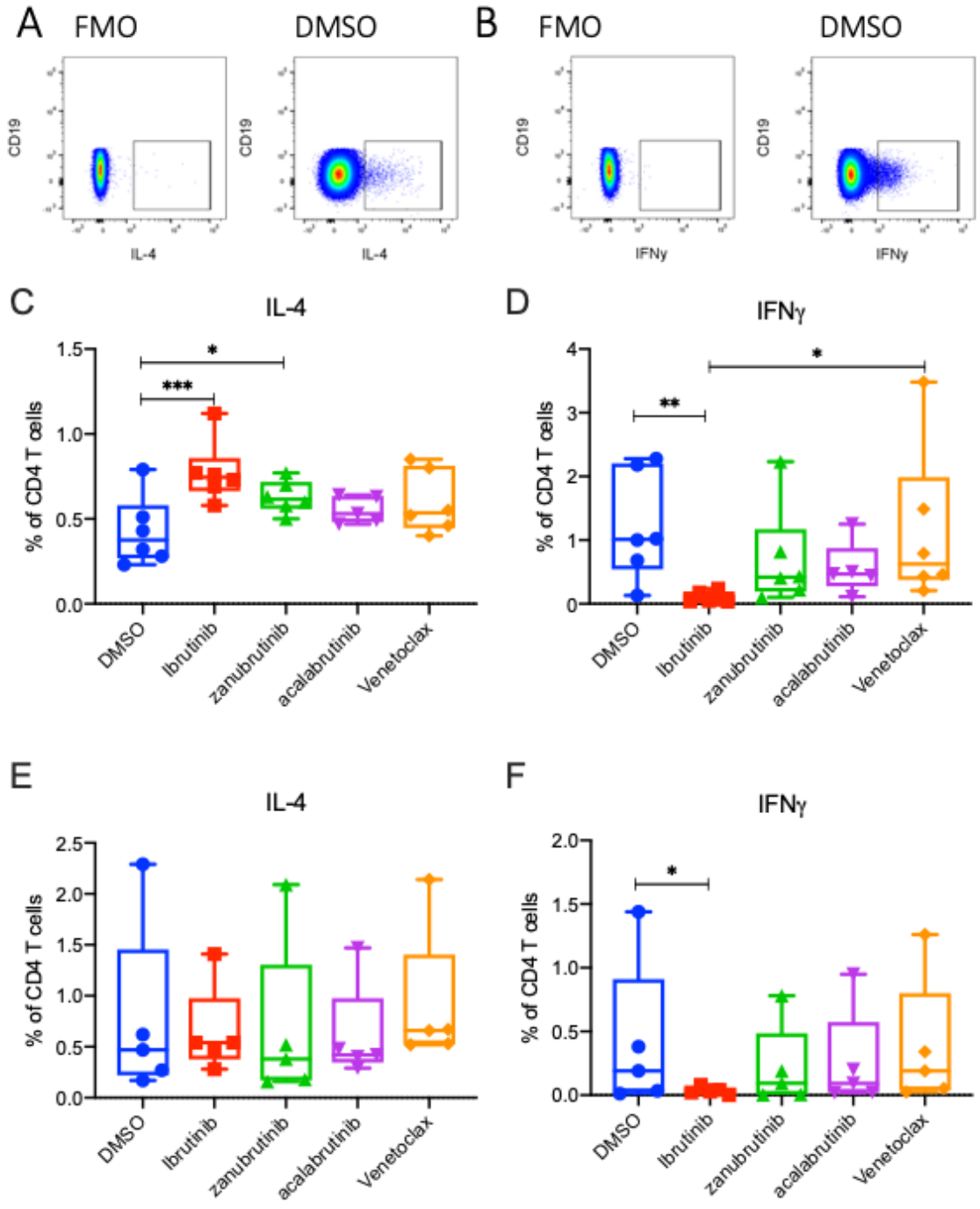

Figure 5.4 CD4 T cell cytokine production

PBMC were treated with 1 μM ibrutinib or 1 μM zanubrutinib or 1 nM venetoclax or DMSO vehicle control for 18 hours prior to stimulation with CD2/CD3/CD28 T cell stimulation beads for 4 hours. Boxplots representing intracellular a) IL-4 and b) IFNγ staining in CD4 T cells from six healthy donors and c-d) five CLL patients. Mixed effects analysis, with Dunnett's test for multiple comparisons *p<0.05, **p<0.01 ***p<0.001.

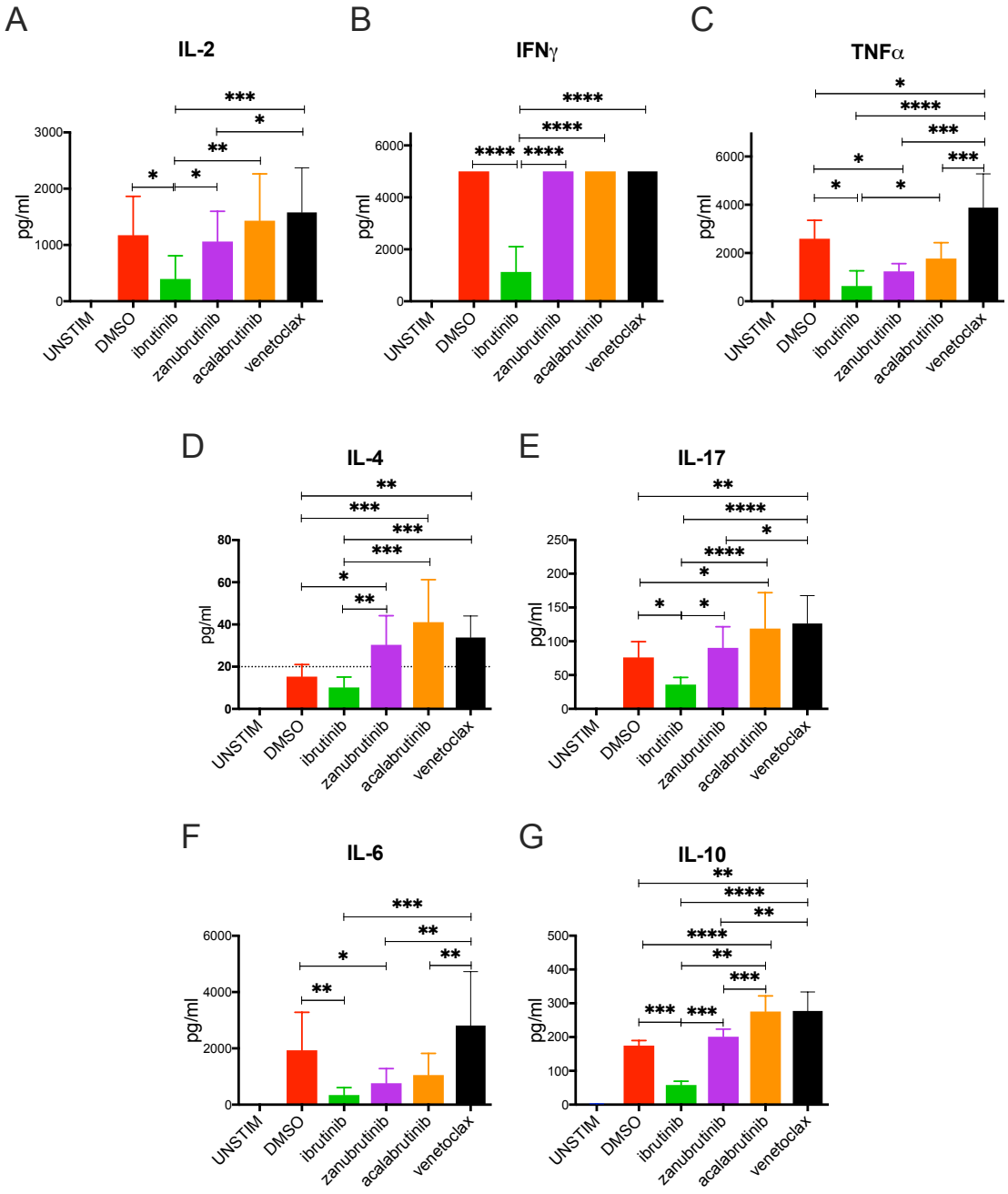

Figure 5.5 Healthy donor PBMC cytokine release

Bar graphs of supernatant cytokine concentrations after 24 hours T cell bead stimulation of whole PBMC from four healthy donors. The sensitivity of the assay was limited to 5000 pg/mL. Bars represent the mean ± SD, RM one-way ANOVA with Fisher's LSD, *p<0.05 ** p<0.01 ***p<0.001 ****p<.0001

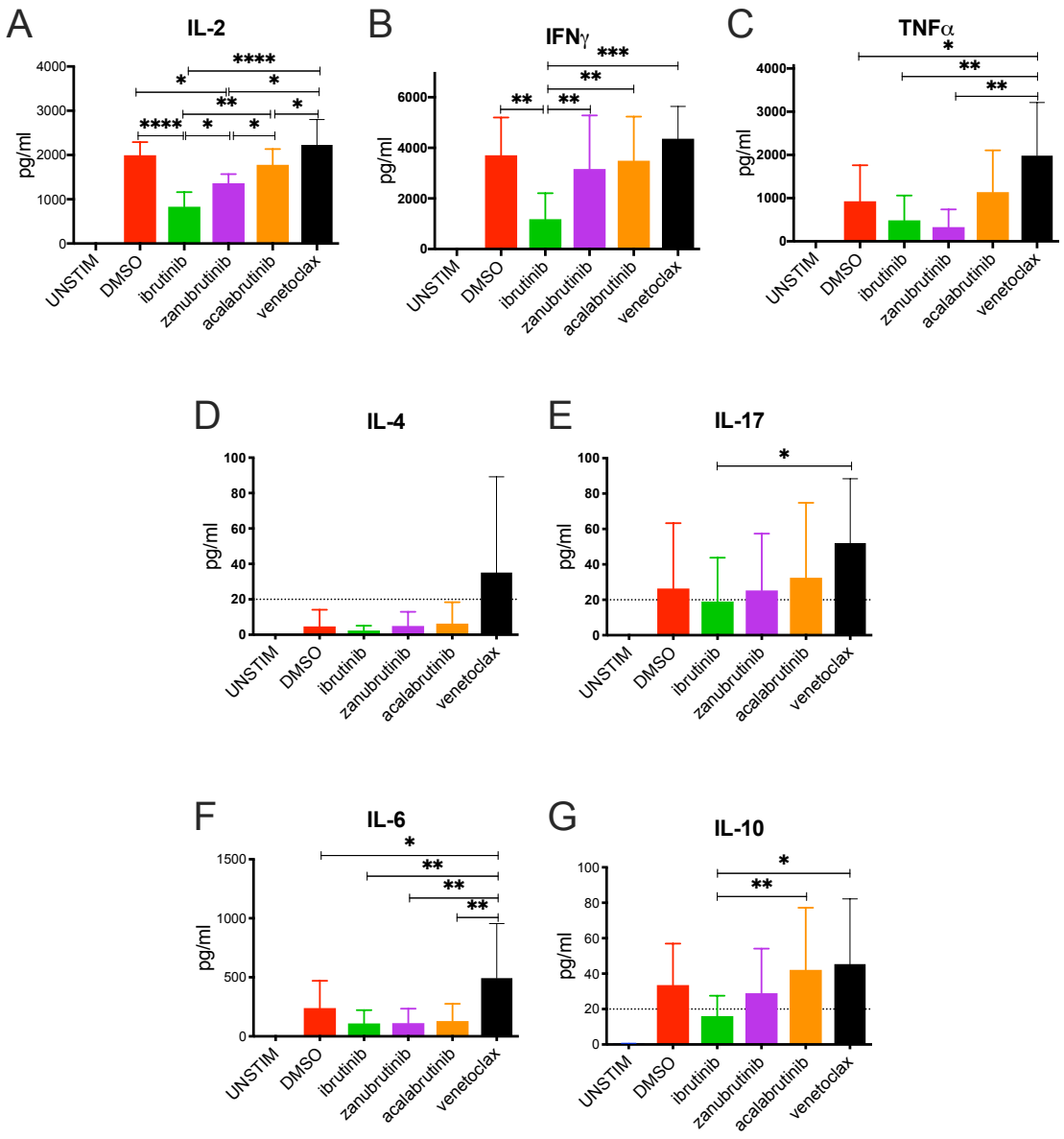

Figure 5.6 CLL patient PBMC cytokine release

Bar graphs of supernatant cytokine concentrations after 24 hours bead stimulation of whole PBMC from four CLL patients. The sensitivity of the assay was limited to 5000 pg/mL. Bars represent the mean and SD RM one-way ANOVA with Fisher's LSD. *p<0.05 ** p<0.01 ***p<0.001 ****p<.0001

Table 5.2 Summary of significant differences in cytokine production between healthy donor PBMC treated with targeted therapies as compared to vehicle

	IBRUTINIB	ZANUBRUTINIB	ACALABRUTINIB	VENETOCLAX
IL-2	↓			
IFNγ	↓			
TNFα	↓	↓		↑
IL-4		↑	↑	↑
IL-17	↓		↑	↑
IL-6	↓	↓		
IL-10	↓		↑	↑

Table 5.3 Summary of significant differences in cytokine production CLL patient PBMC treated with targeted therapy as compared to vehicle treated cultures

	IBRUTINIB	ZANUBRUTINIB	ACALABRUTINIB	VENETOCLAX
IL-2	↓	↓		
IFNγ	↓			
TNFα				↑
IL-4				
IL-17				
IL-6				↑
IL-10				

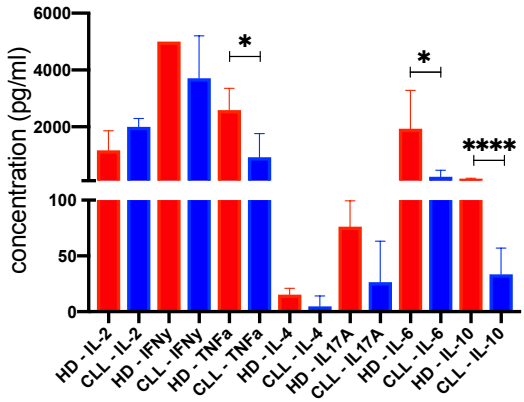

Figure 5.7 Comparison of cytokine production in CLL patient and healthy donor PBMC

Bar graphs of supernatant cytokine concentrations after 24 hours bead stimulation of whole PBMC from 4 healthy donors (red) and 4 CLL patients (blue). Data recorded above detection limit reported as 5000 pg/mL. Bars represent the mean and SD RM one-way ANOVA with Fisher's LSD. *p<0.05 ** p<0.01 ***p<0.001 ****p<.0001.

5.3.3 PROLIFERATION

5.3.3.1 T cell proliferation

The previous cytokine secretion data suggests that T cell activation is severely impaired by ibrutinib treatment. This is most likely due to the inhibition of TCR signalling by ibrutinib binding ITK and it has been reported that T cells with redundant signalling are able to retain their effector function [336]. To further characterise the defect in activation caused by ibrutinib a proliferation assay was performed. Whole PBMC from age matched healthy donors or CLL patients were stimulated with CD2/CD3/CD28 T cell stimulation beads and IL-2 and the resultant proliferation measured using CellTrace violet dilution and analysed using FlowJo proliferation modelling, after 3, 5 and 7 days. Representative histograms of CellTrace violet dilution can be seen in Figure 5.8 a. Proliferation modelling was used to determine the 'percent divided' which represents the proportion of the original population of cells which had undergone at least one division. Ibrutinib significantly reduced the percent divided in both the CD4 and CD8 T cell populations from healthy donors and CLL patients (Figure 5.8 b-e). However, ibrutinib, nor any other inhibitor tested had a significant impact on the 'replication index' which measures the average number of divisions that the responding cells underwent, disregarding the undivided cells (Figure 5.9). Dividing cells in ibrutinib treated cultures proliferated at a similar rate to untreated cells or those treated with other targeted therapies.

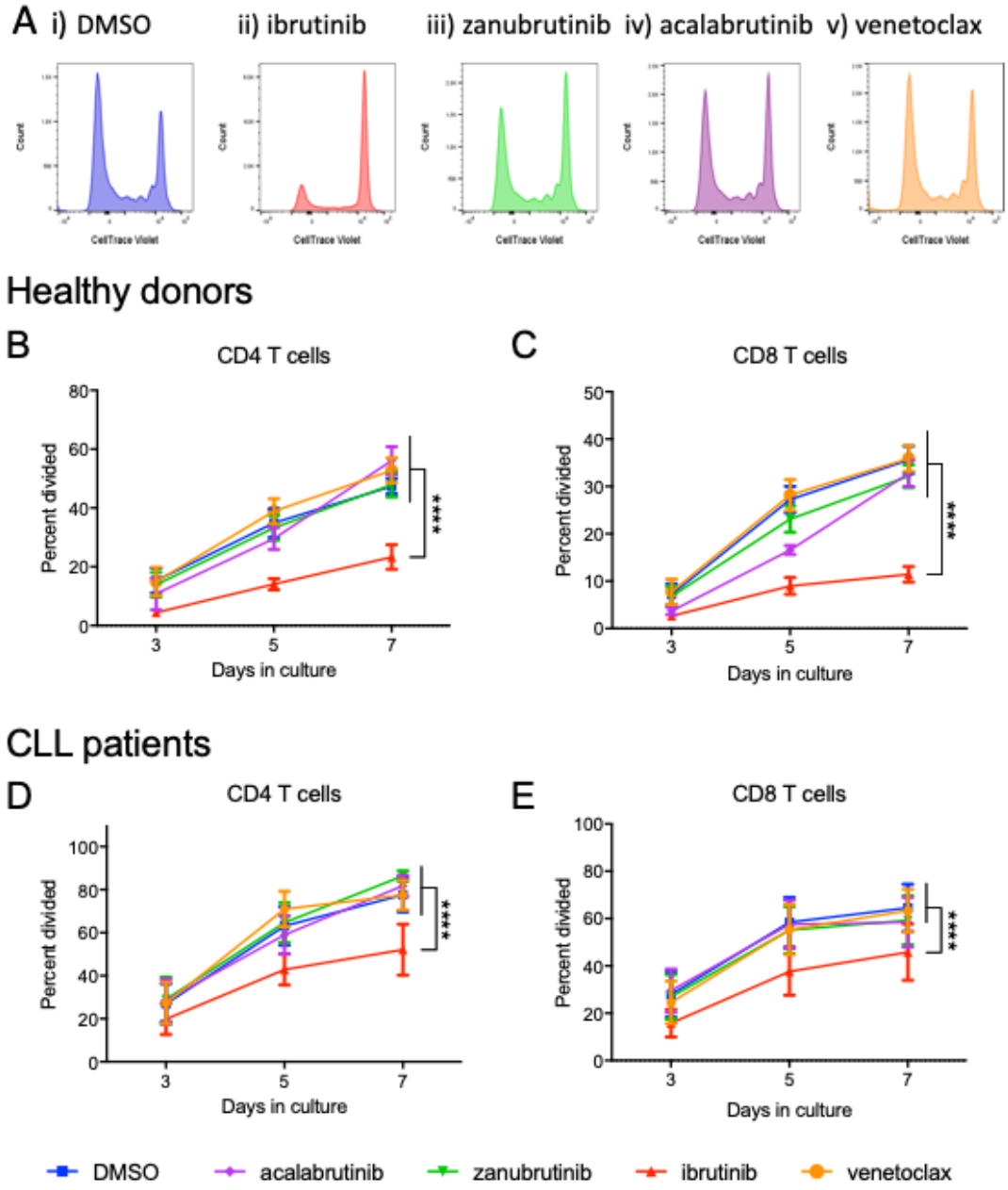

Figure 5.8 CD4 and CD8 T cell proliferation in healthy donor and CLL patient PBMC

A) Representative histograms of CellTrace violet dilution five days after CD2/CD3/CD28 bead and IL-2 stimulation in CD8 T cells. B) Percent divided CD4 T cells and C) Percent divided CD8 T cells from seven healthy donors in two independent experiments. Percent divided in D) CD4 T cells and E) CD8 T cells from eight CLL patients in two independent experiments. Mixed effects analysis with Tukey-Kramer test for multiple comparisons test **** $p < 0.0001$. Lines represent mean ± SEM of the percent divided derived from FlowJo proliferation modelling based on CellTrace violet dilution.

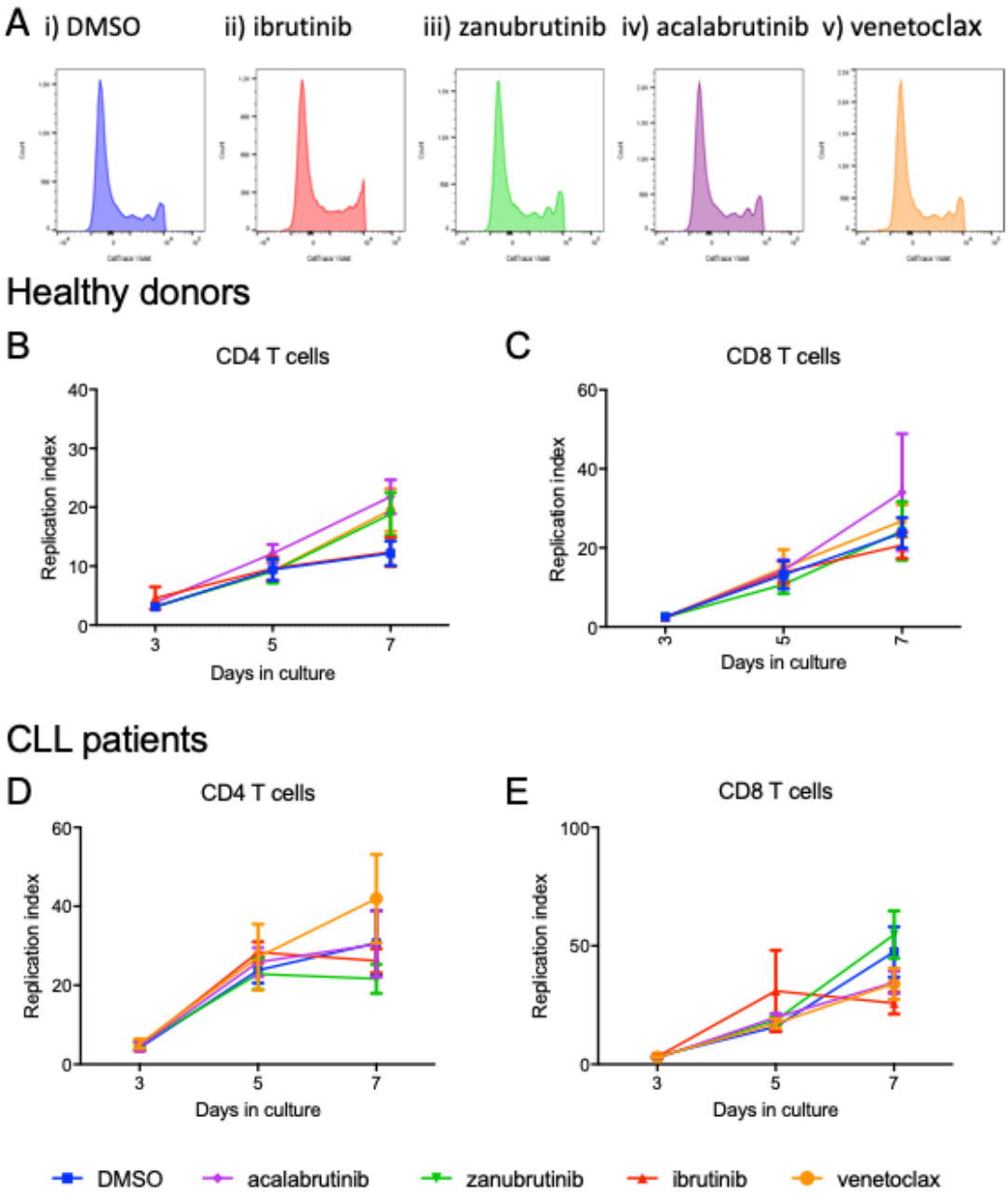

Figure 5.9 Replication index of healthy donor and CLL patient CD4 and CD8 T cells
A) representative histograms of CD8 T cells which have undergone at least one division. Replication index of B) CD4 T cells and C) CD8 T cells after bead stimulation from eleven healthy donors from three independent experiments. Replication index of D) CD4 T cells and E) CD8 T cells from eight CLL patients from two independent experiments. Mixed effects analysis with Tukey-Kramer test for multiple comparisons test. Lines represent mean ± SD of replication index derived using FlowJo proliferation modelling.

Given the delayed proliferation in ibrutinib treated cultures and the potential of Bcl-2 inhibition to have a greater effect on memory T cells, the effect of the targeted therapies on the memory phenotype of proliferating T cells was also measured. Representative plots of CD45RA and CD27 staining are presented in Figure 5.10 a and Figure 5.11 a. After 5 days of stimulation, Ibrutinib treated healthy donor CD4 T cells had significantly fewer central memory, and more effector memory and T_{EMRA} cells than vehicle treated CD4 T cells (Figure 5.10 b-e). The memory phenotype of CLL patient CD4 T cells was not significantly altered by ibrutinib (Figure 5.10 f-i). Similarly, ibrutinib had a greater effect on the memory phenotype of heathy donors than CLL patients CD8 T cells. After 5 days stimulation, ibrutinib treated CD8 T cells from healthy donors had significantly reduced naïve cells and significantly increased T_{EMRA} cells (Figure 5.11 b-e). Venetoclax treated CD8 T cells from both heathy donors and CLL patients had a significantly greater proportion of naïve cells (Figure 5.11 b, f) and there was a trend to decreased central memory and effector memory subsets.

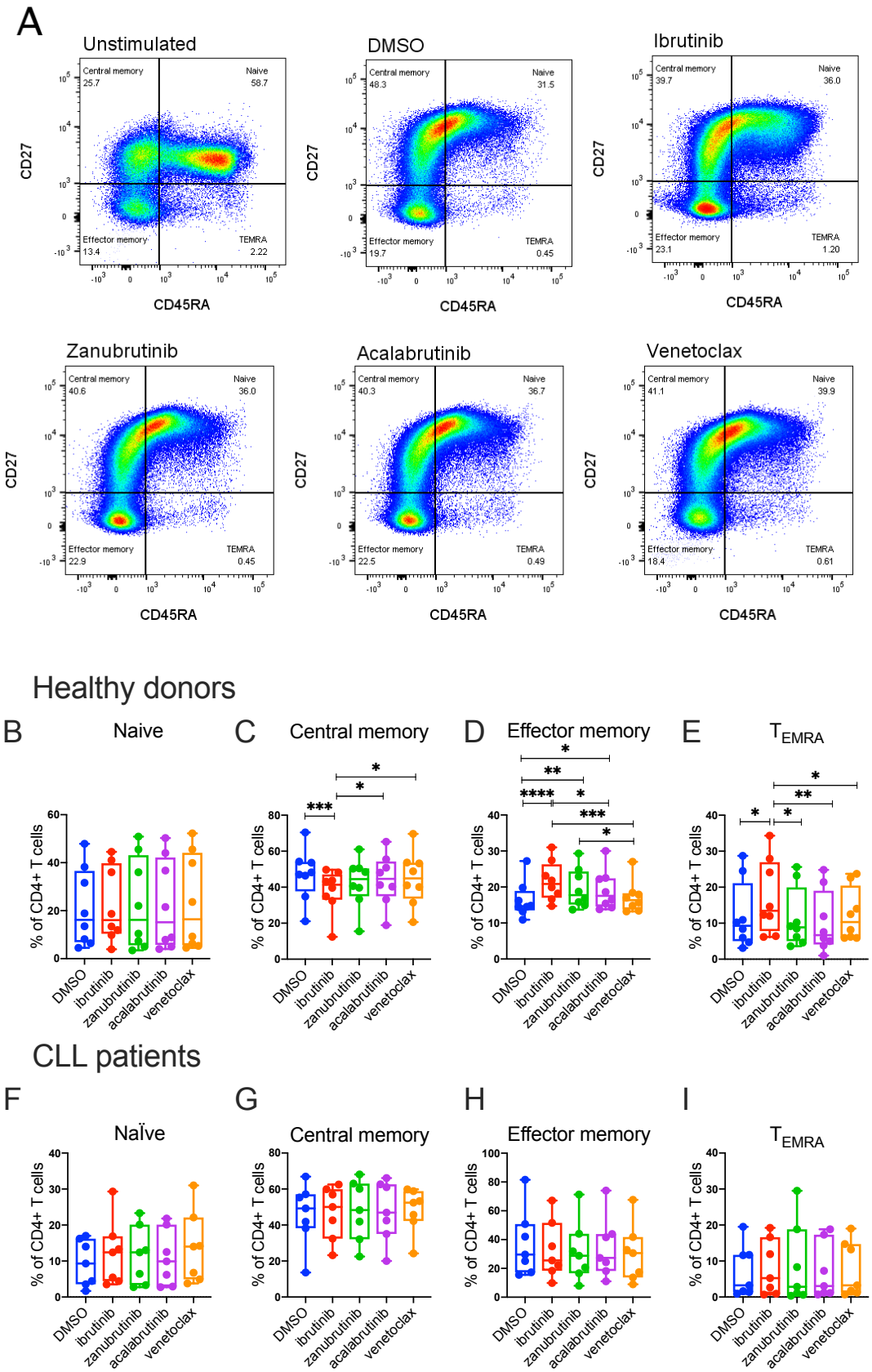
A
Unstimulated
Central memory
25.7
Naive
58.7
Effector memory
13.4
TEMRA
2.22
DMSO
Central memory
48.3
Naive
31.5
Effector memory
19.7
TEMRA
0.45
Ibrutinib
Central memory
39.7
Naive
36.0
Effector memory
23.1
TEMRA
1.20
Zanubrutinib
Central memory
40.6
Naive
36.0
Effector memory
22.9
TEMRA
0.45
Acalabrutinib
Central memory
40.3
Naive
36.7
Effector memory
22.5
TEMRA
0.49
Venetoclax
Central memory
41.1
Naive
39.9
Effector memory
18.4
TEMRA
0.61
CD27
CD45RA
Healthy donors
B
Naive
C
Central memory
D
Effector memory
E
TEMRA
% of CD4+ T cells
DMSO
ibrutinib
zanubrutinib
acalabrutinib
venetoclax
CLL patients
F
Naïve
G
Central memory
H
Effector memory
I
TEMRA

Figure 5.10 Effect of targeted therapies on the memory phenotype of CD4 T cells

PBMC from healthy donors or CLL patients were treated with 1 μM ibrutinib, 1 μM zanubrutinib, 1 μM acalabrutinib or 1 nM venetoclax and stimulated with CD2/CD3/CD28 T cell stimulation beads and IL-2 for 5 days. The proportion of naïve (CD45RA+CD27+) central memory (CD45RA-CD27+) effector memory (CD45RA-CD27-) and T_{EMRA} (CD45RA+CD27-) CD8 T cells was measured as a proportion of total CD4 T cells. A) representative plots of CD45RA and CD27 determination of memory subsets. Memory phenotype of CD4 T cells from a-d) healthy donors and e-f) CLL patients. Mixed effects analysis with Fisher's LSD tests, *p<0.05 ** p<0.01 ***p<0.001 ****p<.0001.

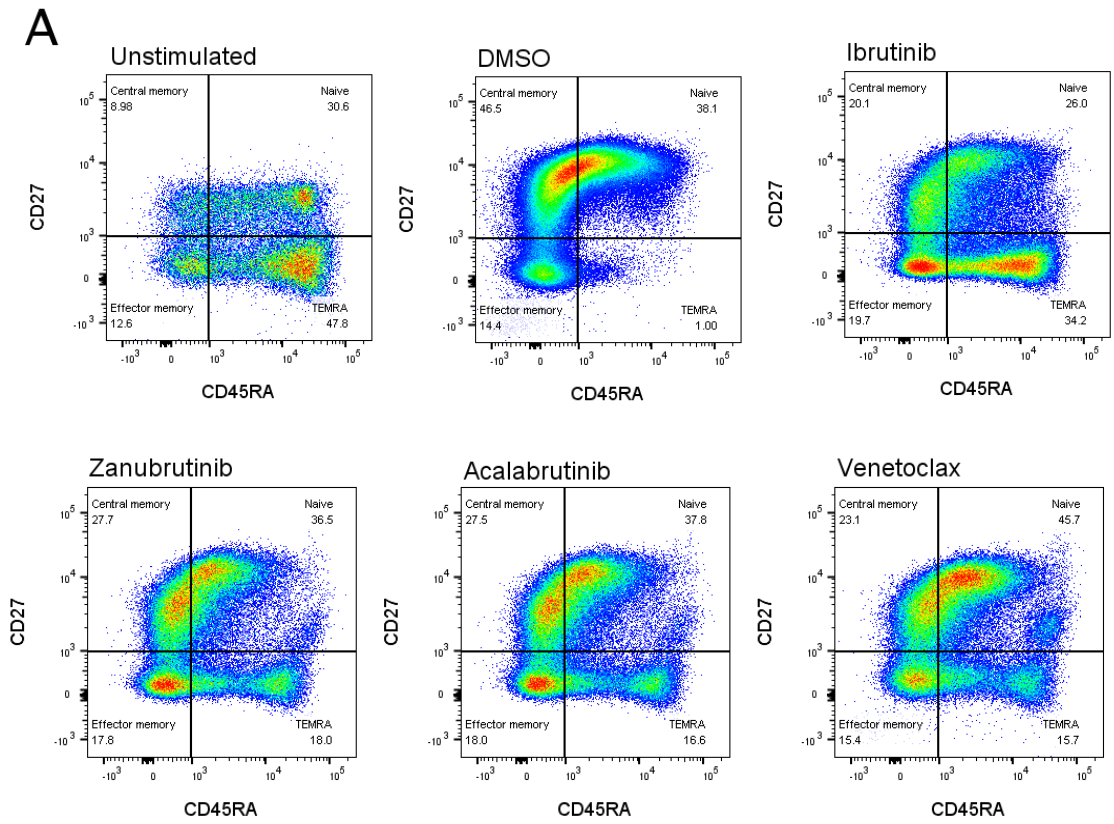

Healthy donors

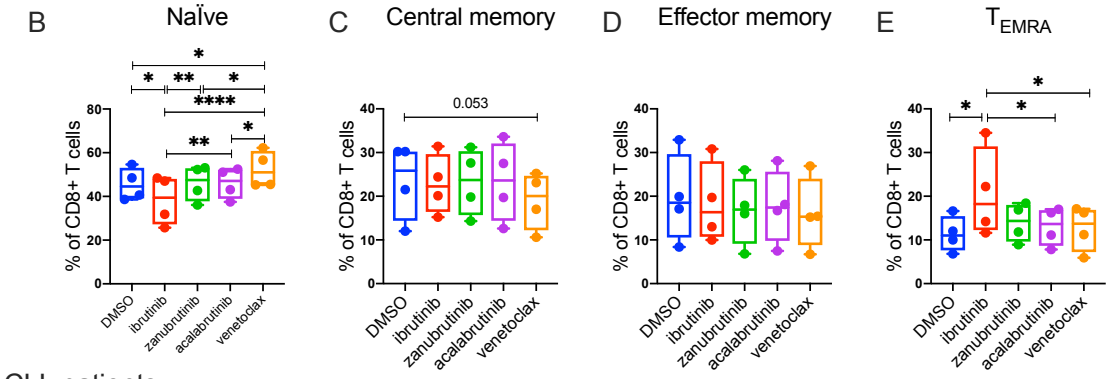

CLL patients

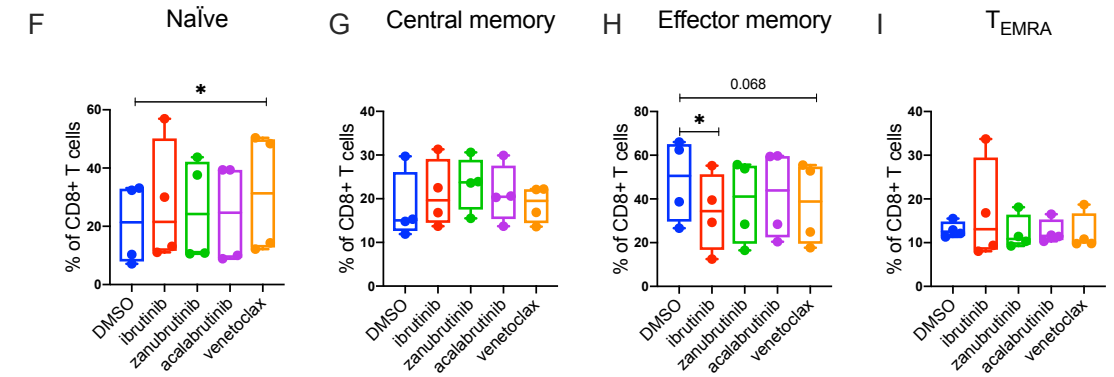

Figure 5.11 Effect of targeted therapies on memory phenotype of CD8 T cells

PBMC from healthy donors or CLL patients were treated with 1 μM ibrutinib, 1 μM zanubrutinib, 1 μM acalabrutinib or 1 nM venetoclax and stimulated with CD2/CD3/CD28 T cell stimulation beads and IL-2 for 5 days. The proportion of naïve (CD45RA+CD27+) central memory (CD45RA-CD27+) effector memory (CD45RA-CD27-) and T_{EMRA} (CD45RA+CD27-) CD8 T cells was measured as a proportion of total CD8 T cells. A) representative plots of CD45RA and CD27 determination of memory subsets. Memory phenotype of CD8 T cells from B-E) healthy donors and F-I) CLL patients. Mixed effects analysis with Fisher's LSD tests, *p<0.05 ** p<0.01 ***p<0.001 ****p<.0001.

CLL patient T cells have profound functional defects and CLL cells have been shown to be both directly and indirectly immunosuppressive. Therefore, the effect of the presence of CLL cells on the proliferation of T cells was investigated. CLL patient PBMC was split and either depleted of CD19+ cells using MACS bead separation or left as whole PBMC. These cultures were then stimulated with CD2/CD3/CD28 T cell stimulation beads and IL-2 for 7 days and proliferation was analysed. When cultured as whole PBMC, a significantly greater proportion of CLL patient T cells proliferated than T cells cultured in CD19+ cell depleted PBMC (Figure 5.12). However, when the CLL cells were depleted, both the percent divided and the proliferation index of CD8 T cells was significantly lower than T cells from heathy donors (Figure 5.12 c-d).

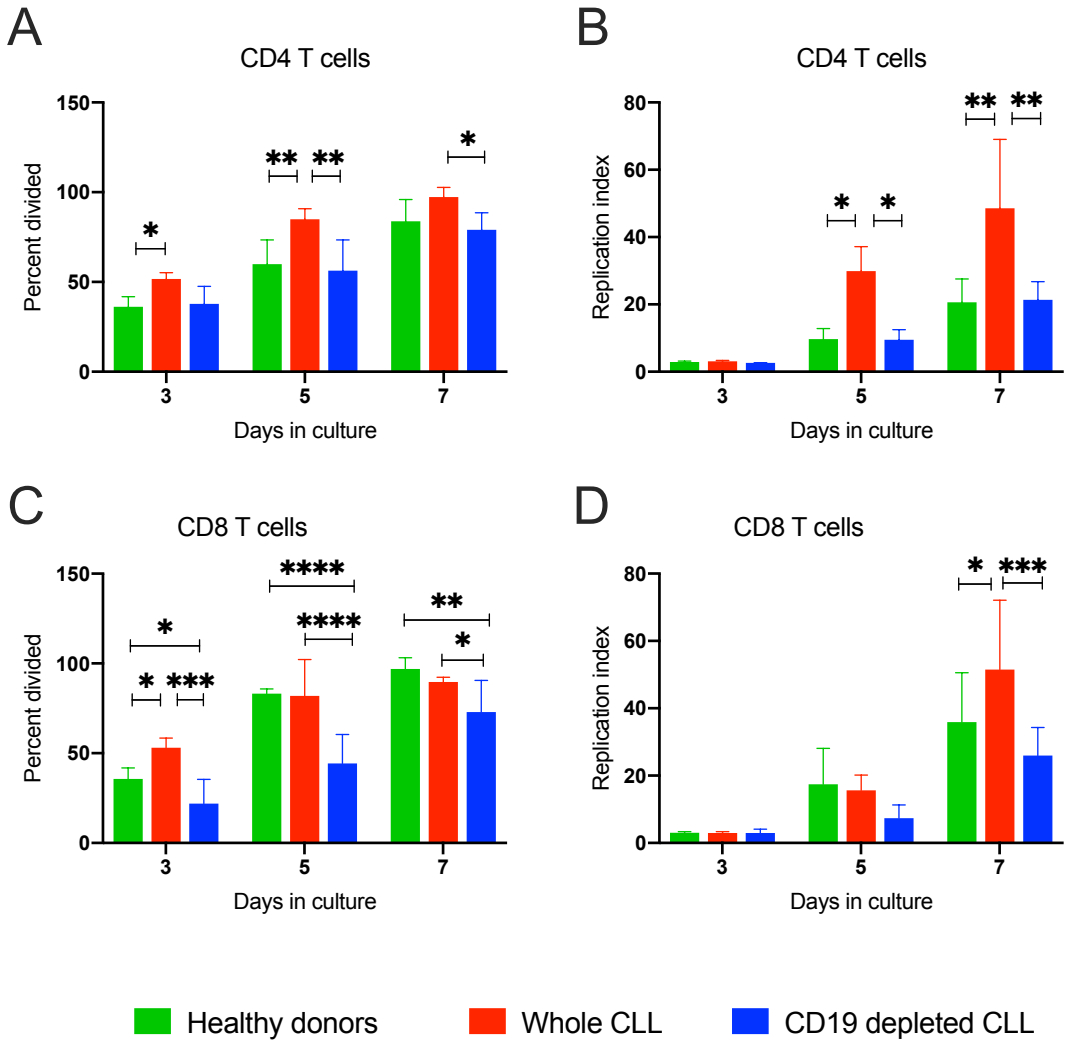

Figure 5.12 Comparison of healthy donor and CLL T cell proliferation

PBMC from 8 CLL patient PBMC and 11 healthy donors were stimulated with CD2/CD3/CD28 T cell stimulation beads and IL-2 for 7 days. Proliferation was assessed using CellTrace violet dilution on days 3,5 and 7. Analysis of proliferation was performed using FlowJo proliferation modelling. A) Percent of CD4 T cells that divided B) CD4 T cells replication index and C) Percent CD8 T cells that divided and D) CD8 T cell replication index. Bars represent mean and standard deviation. Mixed effects with sidak's multiple comparisons *p<0.05, ** p<0.01 ***p<0.001 and **** p<0.0001.

5.3.3.3 Effect of targeted therapies on the expression of inhibitory receptors

Decreased expression of exhaustion markers, in particular PD-1 has been used as a marker of improvement in T cell fitness in patients treated with ibrutinib[222,233]. However, PD-1, TIM-3, and LAG-3 are all upregulated during T cell activation[337]. To address the effect of ibrutinib on the expression of inhibitory receptors, CD4 and CD8 T cells were analysed over seven days of stimulation for their expression of PD-1, TIM-3, and LAG-3. After 3 days stimulation, both ibrutinib and zanubrutinib significantly reduced the expression of PD-1 and TIM-3 in CD8 T cells as compared to either vehicle control or acalabrutinib treated cells, while only ibrutinib treated CD8 T cells had significantly reduced expression of LAG-3 (Figure 5.13 d-f). After 5- and 7-days stimulation there was no significant impact of any of the BTK inhibitors on PD-1 expression (Figure 5.13 g, j). Conversely, ibrutinib treated CD8 T cells maintained significantly lower TIM-3 and LAG-3 expression (Figure 5.13 h-i, k-l).

However, as demonstrated in the previous section, ibrutinib treatment resulted in a significant reduction in activation, and greater numbers of T cells failed to proliferate in response to stimulation. As such proliferation modelling was used to measure exhaustion marker expression in populations that had undergone different numbers of divisions. Using CellTrace violet dilution, T cells from each generation were analysed separately for the expression of inhibitory receptors, allowing for comparison of cells that have undergone the same number of divisions.

This analysis showed that in healthy donor CD8 T cells that had undergone the fewest divisions there was a significantly lower expression of PD-1 and LAG-3 (Figure 5.14 c, e). Alternatively, ibrutinib treated CD8 T cells that had undergone multiple successive divisions had higher expression of PD-1 than cells that had undergone the same number of divisions in the zanubrutinib, acalabrutinib or vehicle treated conditions (Figure 5.14 c). Similarly, ibrutinib and zanubrutinib treated CD8 T cells which had undergone at least five divisions had higher expression of TIM-3 than equivalently proliferated CD8 T cells treated with acalabrutinib or vehicle (Figure 5.14 d).

Conversely, CD8 T cells from CLL patients exhibited a different pattern of exhaustion marker expression. Neither ibrutinib, nor any other BTK inhibitor altered the expression of PD-1 on proliferating CLL patient CD8 T cells (Figure 5.14 f). However, ibrutinib significantly decreased the expression of TIM-3 and LAG-3 in CD8 T cells that had undergone multiple divisions. Zanubrutinib and acalabrutinib also significantly reduced TIM-3 expression with a trend to decreasing LAG-3 expression (Figure 5.14 g-h).

In order to explore the differences in inhibitory receptor expression healthy donor and CLL patient T cells were compared. In both CD4 and CD8 T cells there was a trend to greater expression of PD-1, TIM-3 and LAG-3 on CLL patient CD8 and CD4 T cells as compared to healthy donors (Figure 5.15a-f). When proliferating T cells were examined by gating on individual generations, CLL patient CD8 T cells which had undergone multiple divisions showed a significantly greater expression of PD-1, Tim3 and LAG-3 than healthy donor T cells (Figure 5.15 g-i).

In order to examine if the increased expression of inhibitory receptors was intrinsic to CLL patient T cells or due to the presence of CLL cells in the culture, the expression of PD-1, TIM3 and LAG-3 was examined on T cells stimulated in the presence of CLL cells, or after CD19+ cells were depleted from the PBMC. Depletion of CD19+ cells from CLL PBMC resulted in a trend to decreased expression of PD-1, TIM-3, and LAG-3 after 5 days stimulation on both CD4 and CD8 T cells (Figure 5.16 a-f). Generational gating was used to examine the changes in inhibitory receptor expression in proliferating CD8 T cells. When compared to matched samples cultured in the absence of CD19+ cells, CD8 T cells had lower expression of PD-1 in the earlier generations and higher expression of LAG-3 in later generations (Figure 5.16 g-i).

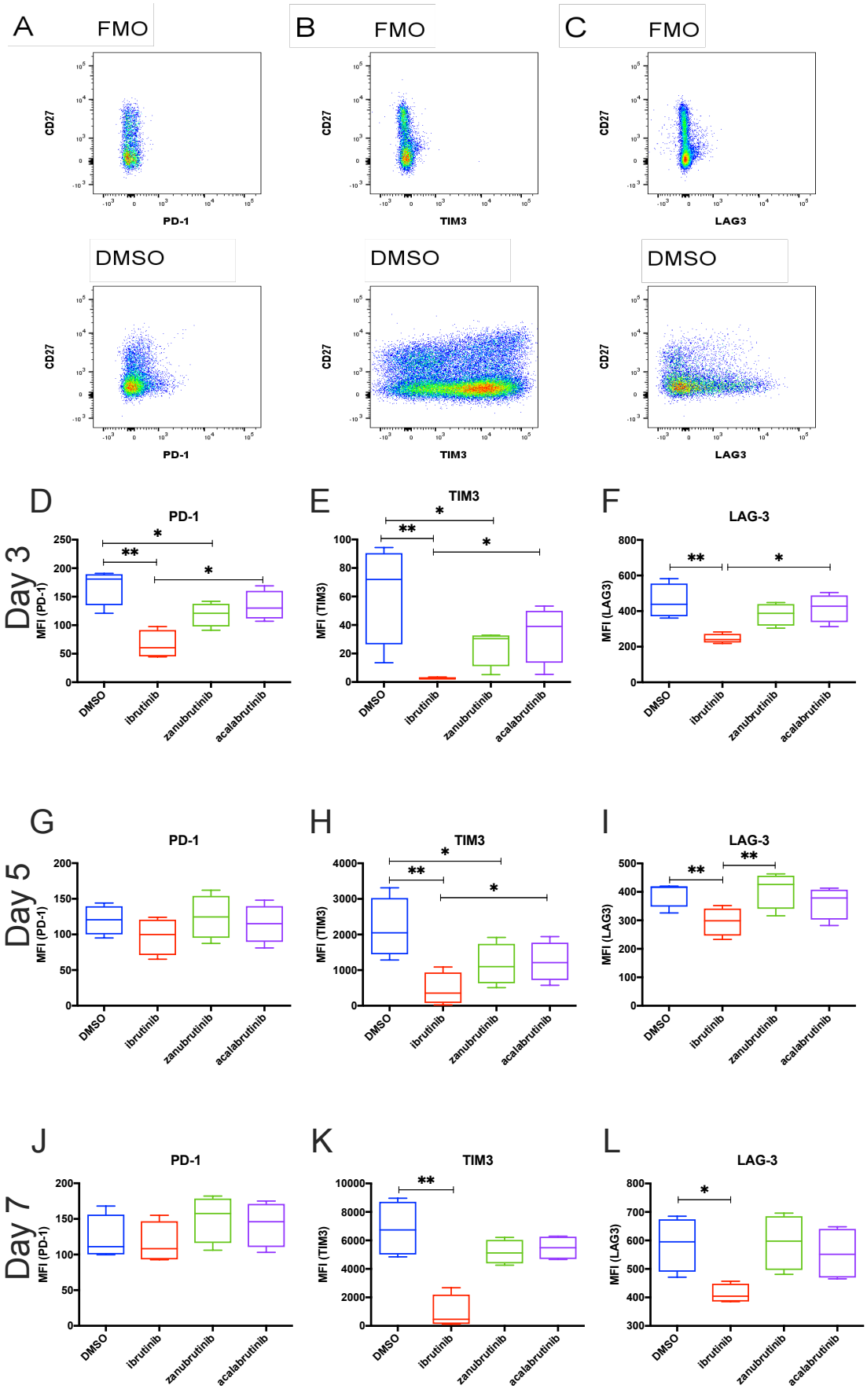
A
FMO
B
FMO
C
FMO
CD27
PD-1
TIM3
LAG3
DMSO
D
PD-1
E
TIM3
F
LAG-3
Day 3
MFI (PD-1)
MFI (TIM3)
MFI (LAG3)
G
PD-1
H
TIM3
I
LAG-3
Day 5
J
PD-1
K
TIM3
L
LAG-3
Day 7
DMSO
ibrutinib
zanubrutinib
acalabrutinib

Figure 5.13 Inhibitory receptor expression on stimulated CD8 T cells

A-C) representative dot-plots of exhaustion marker expression on FMO and DMSO treated controls. Boxplots representing the mean fluorescence intensity (MFI) PD-1, TIM3 and LAG-3 on CD8 T cells from four healthy donor stimulated for D-F) 3 days, G-I) 5 days or J-L) 7 days with CD2/CD3/CD28 T cell stimulation beads and rhIL-2. Friedman ANOVA with Dunn's multiple comparisons tests *p<0.05 ** p<0.01 ***p<0.001 ****p<.0001

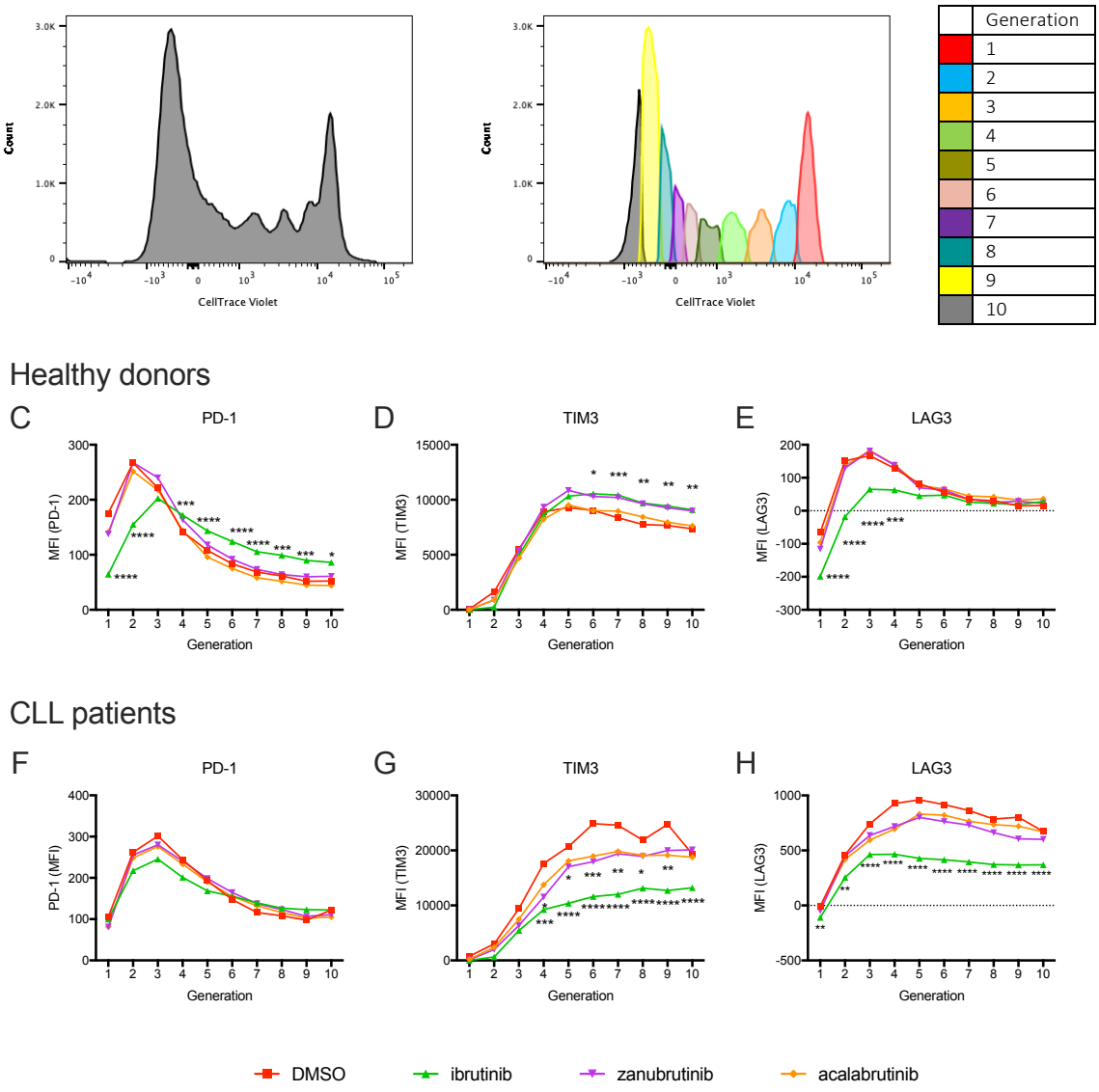

Figure 5.14 Ibrutinib alters the expression of inhibitory receptor expression on individual CD8 T cell generations

PBMC from heathy donors and CLL patients were stained with CTV, treated with 1 μM ibrutinib, zanubrutinib, or acalabrutinib or vehicle control (DMSO). All treatment conditions were then stimulated with CD2/CD3/CD28 beads and rhIL-2 for five days. A) representative histogram of CellTrace violet dilution. B) representative model of gating on individual generations. C-E) expression of PD-1, TIM3 and LAG-3 on CD8 T cells from healthy donors. F-H) expression of PD-1, TIM3 and LAG-3 on CD8 T cells from CLL patients. Lines represent median MFI of 4 donors. Individual t tests *p<0.05 ** p<0.01 ***p<0.001 ****p<.0001.

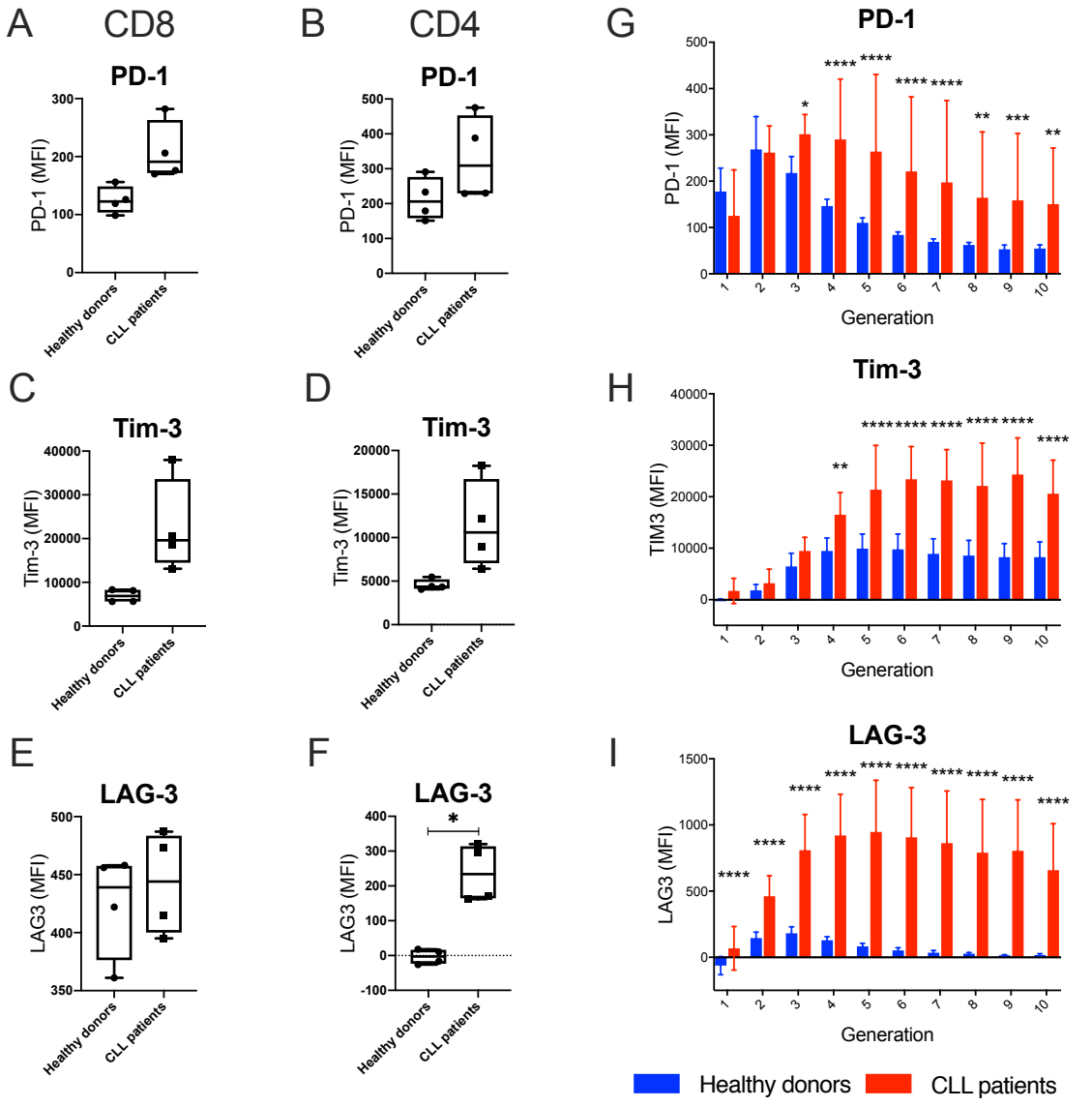

Figure 5.15 Differences in inhibitory receptor on healthy donor and CLL patient PBMC

PBMC from CLL patients or healthy donors were stimulated with CD2/CD3/CD28 beads and IL-2 for 5 days. The expression of PD-1, TIM-3 and LAG3 were assessed by flow cytometry on both the whole CD4 and CD8 T cell populations. Box plots summarising the expression of A) PD-1, C) TIM-3 and E) LAG-3 on all CD8 T cells. Box plots summarising the expression of B) PD-1, D) TIM-3 and F) LAG-3 on total CD4 T cell population. Individual t tests *p<0.05 ** p<0.01 ***p<0.001 ****p<.0001. Each generation of CD8 T cells was gated using CellTrace violet dilution. Expression of G) PD-1, H) TIM-3, and I) LAG-3, Bars represent mean ± SD of 4 donors. One-way ANOVA with Fisher's LSD multiple comparisons *p<0.05 ** p<0.01 ***p<0.001 ****p<.0001.

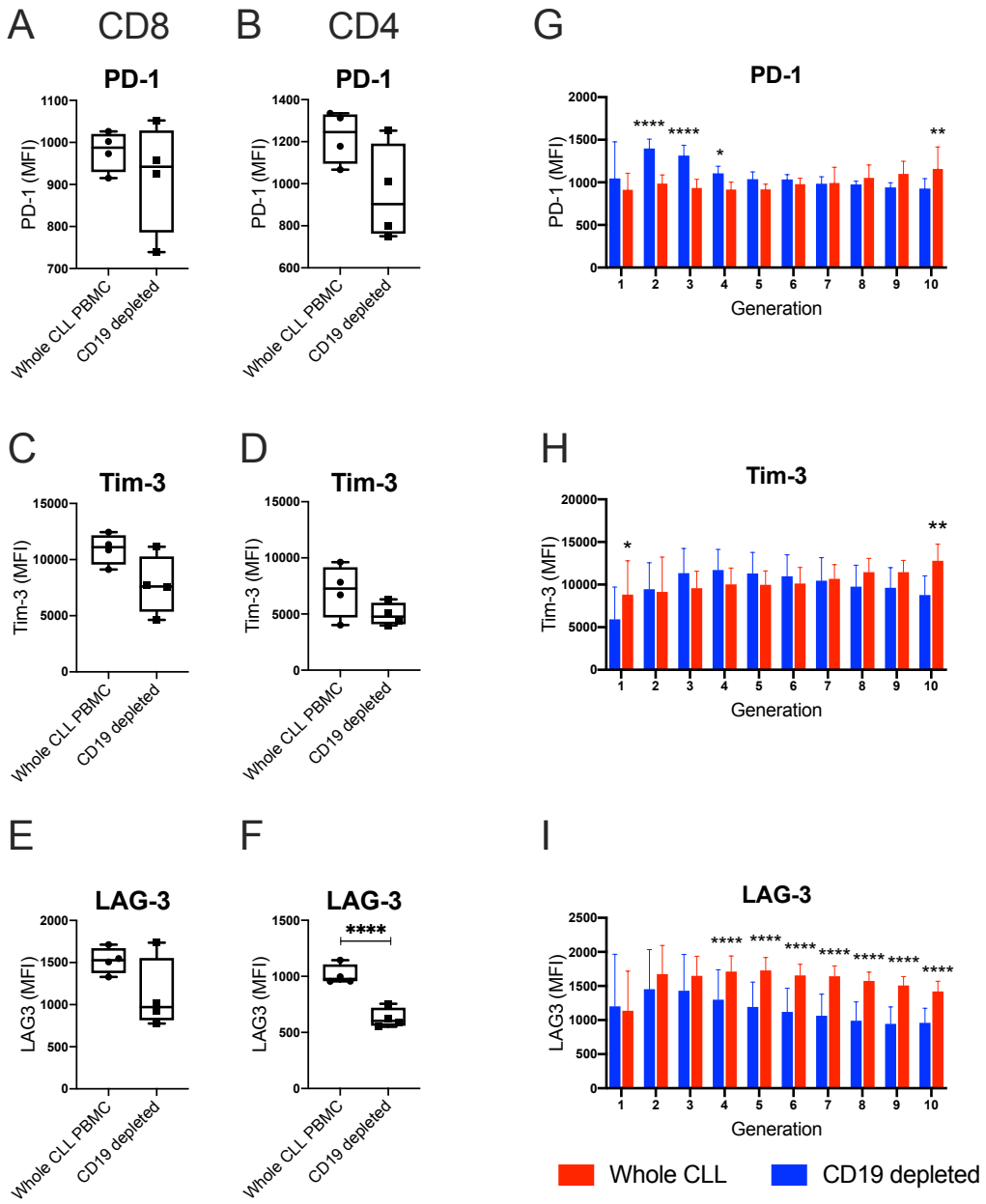

Figure 5.16 Depleting CD19+ cells alters the expression of inhibitory receptor expression

CLL patient PBMC and matched samples depleted of CD19+ cells were stimulated with CD2/CD3/CD28 beads and IL-2 for 5 days. The expression of PD-1, TIM-3 and LAG3 were assessed by flow cytometry on both the whole CD4 and CD8 T cell populations. Box plots summarising the expression of A) PD-1, C) TIM-3 and E) LAG-3 on total CD8 T cell population. Box plots summarising the expression of B) PD-1 D) TIM3 and F) LAG-3 on total CD4 T cell populations. Individual t tests *p<0.05 ** p<0.01 ***p<0.001 ****p<.0001. Individual generations of CD8 T cells was gated using CellTrace violet dilution and FlowJo proliferation modelling. Expression of G) PD-1, H) TIM-3, and I) LAG-3. Bars represent mean ± SD of 4 donors. One-way ANOVA with Fisher's LSD multiple comparisons *p<0.05 ** p<0.01 ***p<0.001 ****p<.0001.

5.3.3.4 NK cell proliferation

Previously published studies on the effect of BTK inhibitors on NK cell function have primarily focused on measures of NK cell cytotoxicity[235,236]. In order to further understand the functional impact of targeted therapies on NK cells this analysis examined the *in vitro* proliferation of NK cells. NK cells were isolated from healthy donor PBMC, treated with either 1 μM ibrutinib, 1 μM zanubrutinib, 1 μM acalabrutinib or 1 nM venetoclax and stimulated using CD2/NKp46 NK stimulation beads and IL-2. Based on CellTrace violet dilution the proliferation of NK cells was measured over 7 days. Ibrutinib treated cultures had significantly reduced NK cell proliferation, both in the percent divided and the replication index, indicating that fewer NK cells were induced to proliferate and the proliferating NK cells underwent fewer divisions than vehicle treated cells (Figure 5.17 a-b). In contrast to the effect on T cell proliferation, both zanubrutinib and acalabrutinib also reduced the proportion of proliferating NK cells, albeit to a lesser degree than ibrutinib. Conversely, in venetoclax treated NK cell cultures after 7 days stimulation there was a greater proportion of divided NK cells and a higher replication index than vehicle treated NK cells.

CD16 and CD57 are markers of greater NK cell differentiation and cytotoxic capacity[338,339]. In order to assess the effect of targeted therapies on this subset the frequency of CD16+CD57+ NK cells were compared over the 7-day stimulation. Ibrutinib treated cultures had a significantly increased proportion of CD16+CD57+ mature NK cells as compared to the vehicle control. Conversely, venetoclax treated cultures had a significantly reduced proportion of the CD16+CD57+ population (Figure 5.17 c)

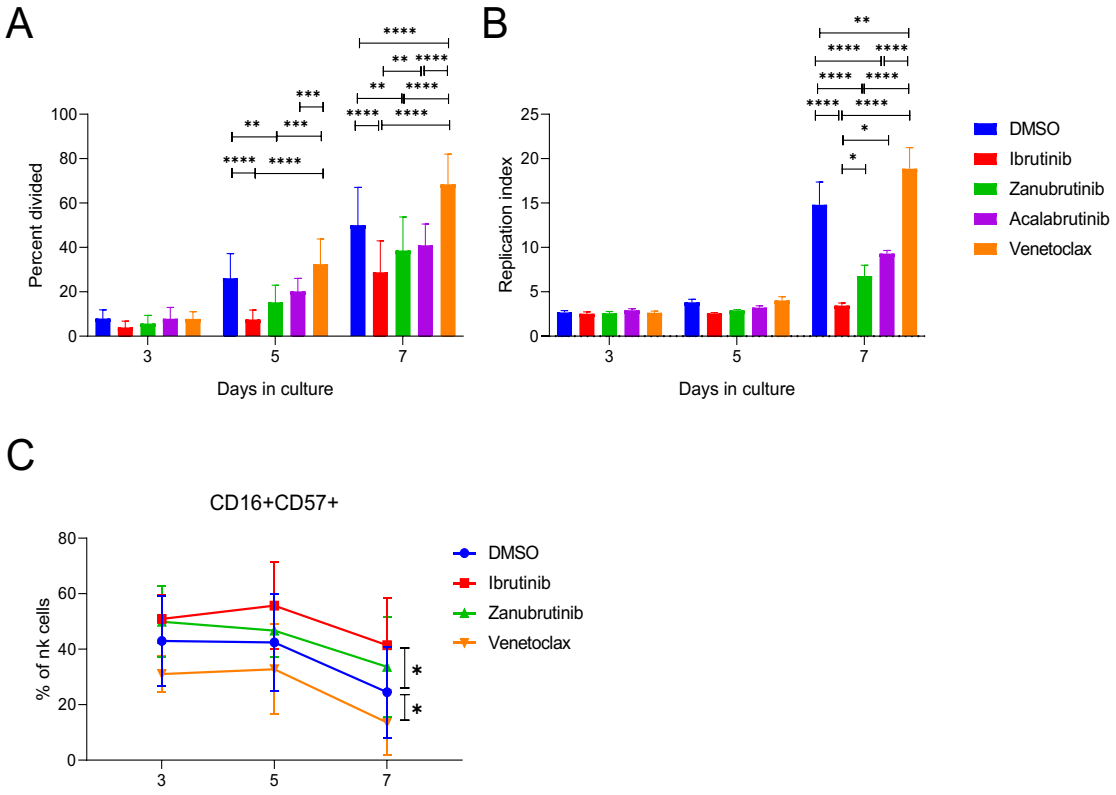

Figure 5.17 NK cell proliferation is altered by targeted therapies

Purified NK cells isolated from healthy donor PBMC were treated with targeted therapies and stimulated with CD2/NKp46 NK stimulation beads and IL-2 for 7 days. Proliferation was measured on day 3, 5 and 7 using CellTrace violet dilution. A) the percent of the original NK population that underwent at least one division. B) the replication index of proliferating NK cells. Bars represent the mean ± SD for 6 healthy donors in two independent experiments, 2-way AONVA with Tukey-Kramer multiple comparisons. C) Percent of NK cells (CD56+ cells) co-expressing CD16 and CD57 in stimulated cultures. Lines represent mean ± SD of 3 healthy donors. 2-way ANOVA with Holm-Sidak's multiple comparisons test. *p<0.05 ** p<0.01 ***p<0.001 ****p<.0001

5.4 DISCUSSION

Both BTK and Bcl-2 inhibitors are highly effective therapies in CLL. This chapter examined the impact of these emergent targeted therapies on the effector function of multiple lymphocyte subsets. The first generation BTK inhibitor ibrutinib, in addition to the two most clinically advanced second generation BTK inhibitors zanubrutinib and acalabrutinib were used in this analysis and compared to the Bcl-2 inhibitor venetoclax. Together these results show that ibrutinib broadly supressed both T cell and NK cell function, impairing the degranulation, cytokine production, and proliferation responses. The more selective BTK inhibitors, zanubrutinib and acalabrutinib, had only limited impacts on T cell function, with more significant effects on NK cells. Venetoclax did not alter the response of T cells to stimulation, however there were measurable effects on the viability of more terminally differentiated NK and T cell populations. Together these findings highlight the impact of BTK inhibitors on the function of immune populations that do not express BTK.

Consistent with other published studies, this study used a 1 μM concentration for all three BTK inhibitors, which also correlates with the reported plasma concentration in patients treated with these drugs. In patients treated with 420 mg/day ibrutinib the mean peak plasma concentration for ibrutinib was approximately 300 nM, however 1 CD4 T cells replication index and M plasma concentrations were also within the range observed [340]. The mean peak plasma concentration of zanubrutinib was also approximately 1 μM at the 320 mg/day dose[§] [341]. The mean peak plasma concentration of acalabrutinib was measured at approximately 1.2 CD4 T cells replication index and M after a single 100 mg dose [61,68].

In an *in vitro* cell death assay the venetoclax concentration leading to 50% dead cells (LC_{50}) for resting CD4 and CD8 T cell populations from healthy donors was 2.5 ±0.6 mM and 1.3 ±0.7 mM respectively, much higher than the 3.0±0.9 nM LC_{50} from healthy donor B cells or CLL cells[247]. In CLL patients receiving a daily 400 mg venetoclax dose, the

[§] More recent trials have used a 160 mg twice daily, pharmacokinetic studies are pending

average pre-dose plasma concentration was between 0.771 and 1.14 μM over two years on drug [342]. However, given our desire to study long term function and not cell death the *in vitro* dose in this analysis was 1 nM.

This study utilised stimulation beads to assess the response of multiple immune subsets. The NK cell degranulation assay indicated that while the effect of ibrutinib was more profound, zanubrutinib had a measurable impact on NK cell degranulation (Figure 5.1). These findings are in contrast to a study which measured NK ADCC using CD107a and IFNγ expression in response to anti-CD20 coated DHL-4 or anti-HER2 coated Her18 cell lines which, using the same drug concentrations (1 μM), found that neither zanubrutinib or acalabrutinib had any significant impact on NK cell responses[237]. This difference in zanubrutinib sensitivity may be due to differences in the dependence of the receptors engaged during the stimulation on the Tec family. While the Tec family is involved in the downstream signalling of F_C receptors[192] as well as NKp46 and CD2[190], the relative dependency on the Tec family members TXK and TEC is unknown.

The differences described above may also be explained by the strength of the stimulus used. This analysis used CD2/NKp46 NK cell stimulation beads which provide a strong stimulus for the NK cell degranulation assay. Previously published data had focused on a more physiological stimulus of the antibody opsonised cells and NK cell activation mediated by CD16 ($F_C\gamma$RIII). The difference between cell-based stimulation and bead stimulation is best demonstrated in this study by the response of NKT cells. In the degranulation assay using CD2/CD3/CD28 T cell stimulation beads, up to 60% of cells degranulated and up to 30% expressed IFNγ (Figure 5.3 a-b). Conversely when using CLL cells presenting an NKT specific antigen, only 15- 25% NKT cells degranulated and less than 5% of cells expressed IFNγ (Figure 5.3 c-d). In the context of cell mediated stimulation the effect of zanubrutinib on NKT cells was not seen and was only statistically significant in the more potent stimulation of the bead-based assay.

Previously it has been suggested that the mechanism by which ibrutinib decreased NK and T cell responses was via inhibition of ITK. This data suggests that zanubrutinib also impacts NK and T cell function, which may be due to the partial inhibition of ITK, as

zanubrutinib has a reported IC_{50} for ITK of 50 nM. However, zanubrutinib can also inhibit TXK, with an IC_{50} of 2.0 nM (Table 5.1). Notably, in CD8 T cells zanubrutinib did not significantly reduced CD107a surface expression, but did significantly reduce IFNγ production (Figure 5.2) in line with the role of TXK in the transcriptional regulation of IFNγ[207,208]. However, the relative contribution of ITK and TXK to NK cell activation is not well understood but it has been suggested that ITK has been shown to have a negative regulatory effect on NKG2D mediated cytotoxicity[192].

Zanubrutinib only significantly diminished the IFNγ production of CD8 T cells from heathy donor cells and did not have a significant effect on CD8 T cells from CLL patents (Figure 5.2 b, d), this being despite similar proportions of the cells expressing IFNγ. Similarly, zanubrutinib had a greater impact on healthy donor PBMC cytokine production. Finally, while zanubrutinib treated healthy donor T cells had increased expression of TIM-3 in proliferated CD8 T cells, CLL patient T cells had decreased expression levels of TIM-3. Why the responses of healthy T cell and CLL patient T cells would be differently affected by zanubrutinib remains unclear. Further investigation into the differences in baseline T cell function may elucidate why healthy T cells are more sensitive to zanubrutinib.

It is also notable that the *ex vivo* functional assays presented in Chapter 4 (Figure 4.16) demonstrated that only ibrutinib treated patients, and not those treated with zanubrutinib had a significant decrease in the CD8 T cell degranulation response. Furthermore, the *ex vivo* effect was less substantial than seen in the *in vitro* data. This may be explained by a lower serum concentration of ibrutinib in these patients resulting in lower ITK occupancy, or because of the time from ibrutinib administration to sample acquisition resulted in ITK turnover, restoring TCR signalling capacity. It remains pertinent that ibrutinib has such a profound effect on both CD4 and CD8 T cells it may have implications for the patient's ability to fight infections as well as implications for combining ibrutinib with T cell directed immunotherapies.

Despite the significant inhibition of NKT cell degranulation by ibrutinib, the NKT cytotoxicity assay did not demonstrate differential CLL cell killing by treated NKT cells. This may be due to the relatively short incubation period of 6 hours being insufficient to

induce significant cellular cytotoxicity. Indeed, the high degree of similarity in CLL cell death between the different NKT cell donors suggests that the main determinant of cell death was not the NKT cells (which also displayed a wide variety of degranulation responses) but rather an intrinsic CLL cell effect which came from a single donor. This is supported by the fact that in the CLL culture conditions, both the presence of HS5 cells and of αGalCer, prior to the addition of NKT cells had the greatest impact on viability (Figure 5.3 e).

The focus of prior studies on the effect of ibrutinib on T cells have focused mainly on the effect on T helper cells. In this analysis, in both CLL patient CD4 T cells and healthy donor CD4 T cell populations only ibrutinib significantly reduced the production of the T_H1 cytokine IFNγ and in healthy donors the expression of the T_H2 cytokine IL-4 was increased with both ibrutinib and zanubrutinib treatment. Conversely, there was no significant effect of any inhibitor on IL-4 expression in CLL patient CD4 T cells. This data is in contrast with suggestions that ITK inhibition by ibrutinib leads to inhibition of T_H2 cells [218]. However, as discussed in Chapter 1, the suggested mechanism of T_H1 skewing relies on the competent redundant signalling of TXK which may not be the case for ibrutinib which has a reported IC_{50} for TXK of 2.0 nM[219]. Instead the increase in IL-4 production aligns with data from $ITK^{-/-}$ $TXK^{-/-}$ dual knockout mice which are equally capable of mounting effective T_H2 repossesses as wild-type counterparts [201]. Interestingly zanubrutinib, which has a similar IC_{50} of TXK as ibrutinib, (2.2 nM), but a lower IC_{50} of ITK (50 nM) [219], also resulted in increased IL-4 expression in stimulated CD4 T cells suggesting that TXK inhibition may be equally important in regulating the T_H1/T_H2 balance. Indeed, regardless of an effect on the production of IL-4, due to the effect on IFNγ there remained a T_H2 skew in ibrutinib treated CD4 T cells from CLL patients.

In addition to intracellular cytokine staining of IL-4 and IFNγ, the supernatant cytokine concentration of PBMC stimulated with CD2/CD3/CD28 T cell stimulation beads was also measured. In the absence of T cell stimulation, there were no detectable levels of any cytokine tested in the supernatant. As such it may be concluded that the cytokines measured are either secreted by activated T cells or that other cytokine producing immune populations, such as monocytes producing IL-6, are doing so in response to

activated T cells. Regardless of the cell of origin, at equivalent concentrations both ibrutinib and zanubrutinib result in significantly reduced IL-6 production by PBMC and trended toward decrease in acalabrutinib treated cultures. This suggests that the decrease in IL-6 may be an on-target effect of ibrutinib, supporting the hypothesis that it is not only T cells producing IL-6 in these cultures. This finding highlights that care must be taken in the interpretation of this cytokine data, as it represents the cumulative result of cytokine production of multiple immune subsets.

Overall, the cytokine data demonstrates that ibrutinib broadly inhibited cytokine release in heathy donor PBMC, excluding IL-4. Unfortunately, the concentration of IFNγ exceeded the detection limit of the assay (5000 pg/ml), while IL-4 was often below the lower limit of the detectable range (20 pg/ml). As such, it can only be concluded that ibrutinib significantly decreased the concentration of IFNγ. Interestingly, the more specific BTK inhibitors increased the expression of some cytokines, including IL-4, IL-17 and IL-10 while decreasing the production of others such as TNFα and IL-6. The mechanism by which this occurs is unclear and analysis of specific immune subsets would be required to determine the relevant subsets in which the expression of these cytokines occurs. Furthermore, venetoclax treatment also resulted in increased release of multiple cytokines compared with either the vehicle control or BTK inhibitors. Mechanistically, as a Bcl-2 inhibitor, venetoclax is unlikely to upregulate cytokine production and is more likely increasing supernatant cytokine levels as a result of increased cell death in the cultures.

Despite some effects on degranulation and cytokine production, neither of the more specific BTKi had any significant impact on the proliferation of T cells, and only ibrutinib significantly delayed T cell proliferation. Somewhat unexpectedly, while ibrutinib inhibited the proportion of T cells that were induced to proliferate, it did not affect their division rate once division occurred, as compared to untreated counterparts. This may be due to intrinsic differences in the TCR signalling strength required to initiate proliferation in some T cell subpopulations. This is supported by the significant increase in terminally

differentiated cells in ibrutinib treated cultures, suggesting greater proliferation of more differentiated cells.

As expected venetoclax had no significant effect on the proliferation of either CD4 or CD8 T cells[343]. However, there was a mild effect on the memory phenotype of resultant CD8 T cell populations. After 5 days of stimulation, venetoclax treated cultures had significantly more naïve CD8 T cells, with a trend to less central and effector memory than vehicle treated cells. This suggests that activated CD8 T cells may have increased sensitivity to Bcl-2 inhibition. This finding is in contrast to previous reports that naïve T cells are highly Bcl-2 dependent and therefore are more susceptible to venetoclax inhibition[248] while activated T cells upregulate Bcl-2[243] suggesting greater resistance to Bcl-2 inhibition. However, there is evidence that CD8+ memory T cells are more sensitive to bcl-2 inhibition by ABT-737, an inhibitor of Bcl-2, Bcl-W and Bcl-X_L[246]. Furthermore, the dynamic regulation of other Bcl-2 family members during T cell responses[344], in particular the downregulation of MCL-1 during the effector to memory switch, may play an important role in determining the sensitivity of T cell memory subsets to venetoclax.

When compared to T cells from healthy donors, CLL patient T cells had a higher rate of proliferation. However, when comparing T cells from matched samples with and without CD19+ cell depletion, there was a significant reduction in the proliferation of both CD4 and CD8 T cells in the CD19 depleted cultures (Figure 5.12). This difference may due to a difference in the bead to T cell ratio in these cultures. As the number of beads added to the cultures was determined by the total number of PBMC, the presence of a large proportion of CLL cells resulted in a larger number of beads per T cell in the CLL PBMC cultures and thus it is possible that this resulted in the increased proliferation of T cells in whole CLL PBMC. An alternative explanation is that the presence of CLL cells stimulates the proliferation of T cells, however in the absence of stimulation beads there was no difference in proliferation between healthy donors and CLL patient T cells. Therefore, the depletion of CLL cells from the CLL PBMC permitted a better direct comparison between the proliferation of healthy donor and CLL donor T cells. Using this comparison, this data suggests that CLL patient CD8 T cells have an intrinsic lower propensity to proliferate than

healthy T cells, reflecting the probable T cell dysfunction induced by, but not dependent on continued contact with CLL cells.

Ibrutinib treated patients have lower expression of inhibitory receptors, usually described as a reflection of reduced T cell exhaustion[222,233]. In this analysis ibrutinib treatment also resulted in decreased expression of PD-1, TIM-3 and LAG-3 on healthy donor CD8 T cells when analysed as a whole population. However, when only considering those T cells that have undergone multiple divisions, ibrutinib treated T cells had higher expression of PD-1 and TIM-3 than T cells which had undergone the same number of divisions in untreated cultures. This finding highlights the complexity of interpreting the upregulation of inhibitory receptors as it relates to activation and exhaustion. The reduction in inhibitory marker expression in the early generations in ibrutinib treated healthy donor T cells is mostly likely due to inhibition of activation due to reduced TCR signalling rather than reduction in T cell exhaustion. With the exception of LAG-3 expression on CD4 T cells, the removal of CD19 cells from CLL PBMC cultures did not significantly alter the expression of inhibitory receptors. This may reflect the pre-existing exhaustion of T cells in CLL patients, which is not reversed when the CLL cells are removed. CLL patient T cells had significantly higher expression of PD-1, TIM-3 and LAG-3 than healthy donors, especially in more proliferated cells, possibly due to the higher proportion of memory T cells which have higher expression of inhibitory receptors[345345].

The changes to the proliferation and exhaustion profile of ibrutinib treated T cells is interesting when considered in the context of using ibrutinib in conjunction with immunotherapies. It was recently reported that T cells from ibrutinib treated patients were better able to respond to CD3/CD19 bi-specific antibodies ex vivo [346346] and prior ibrutinib treatment resulted in better CAR-T cell generation [286].[286]. In this context, the data presented in this chapter suggests that a key role of ibrutinib may be in preserving T cell function which results in improved *ex vivo* activity. Furthermore, the same group found that, in a mantle cell lymphoma mouse model, concurrent ibrutinib and CAR-T cell treatment resulted in greater numbers of CAR-T cells in the peripheral blood and more sustained remissions than CAR-T treatment alone [305],[305] and it was recently reported that in CLL patients, concurrent ibrutinib and CAR-T therapy resulted in deeper responses than

CAR-T therapy alone [285]. Ibrutinib has also been shown to decrease activation induced cell death and activation induced FAS upregulation[222]. Interestingly, the decreased cytotoxicity of CLL patients NK cells was found to be associated with increased NK cell apoptosis[138], suggesting that improved viability of CLL patient effector cells may result in improved killing. Together with the data presented herein, this suggests that ibrutinib improves engraftment and CAR-T cell persistence rather than promoting CAR-T function, though further analysis is required.

This analysis found that NK cell function was more sensitive to BTK inhibitors than T cells. Both ibrutinib and zanubrutinib resulted in reduced NK cell IFNγ production and NK cell proliferation. The decrease in proliferation was also associated with an increase in the proportion of mature NK cells, which is most likely explained by the greater proliferative potential of $CD56^{high}$ NK cells. Strikingly, acalabrutinib, which has an IC_{50} for ITK of greater than 1 μM also resulted in significantly reduced NK cell proliferation. While NK cells have been shown to upregulate BTK on maturation and activation[347347], the degree of NK cell inhibition suggests that the inhibition is not primarily driven by BTK. Each of the BTK inhibitors in this study have an IC_{50} for BTK in the very low nanomolar range (1.5 nM, 0.5 nM and 5.1 nM for ibrutinib zanubrutinib and acalabrutinib respectively) and thus if the effect of these inhibitors was due to BTK inhibition it would be expected that all three would result in similar levels of inhibition. This study found that ibrutinib had the greatest impact on proliferation, followed by zanubrutinib and then acalabrutinib. This pattern better reflects the inhibition of other TEC family members, ITK, TXK, and TEC (Table 3.1), and suggests that inhibition of these kinases is more likely responsible for the observed effect on NK cell proliferation. Elucidating the specific roles that each TEC family member is playing in the function of NK cells requires further investigation using more specific forms of TEC family inhibition than the drugs used in this study.

Venetoclax also had a greater effect on NK cells than T cells. In T cells venetoclax treatment resulted in a modest shift in the memory phenotype but did not impact the overall T cell proliferation. In venetoclax treated NK cell cultures there was a significant loss in mature NK cells from day 3 and maintained over the 7-day stimulation. The loss of

this population, which has lower proliferative potential than CD56^{bright} NK cells, may explain the increased percent divided and the increased proliferation index in venetoclax treated cultures. These findings are also in line with findings that suggest that after treatment with venetoclax and obinutuzumab, NK cell function improved and greater proportions of cells degranulated and produced IFNγ[311]. Venetoclax also had a greater effect on NK cells than T cells. In T cells venetoclax treatment resulted in a modest shift in the memory phenotype but did not impact the overall T cell proliferation. In venetoclax treated NK cell cultures there was a significant loss in mature NK cells from day 3 and maintained over the 7-day stimulation. The loss of this population, which has lower proliferative potential than CD56^{bright} NK cells, may explain the increased percent divided and the increased proliferation index in venetoclax treated cultures. These findings are also in line with findings that suggest that after treatment with venetoclax and obinutuzumab, NK cell function improved and greater proportions of cells degranulated and produced IFNγ[311].

5.5 Conclusion

This study demonstrates that targeted therapies used to treat CLL can have both on target and off target effects on the immune system, outside of their effect on B cells. While venetoclax does not appear to alter the functional capacity of NK and T cells, the effect on mature subsets suggests that the maintenance of terminally differentiated subsets may be affected by venetoclax. Both ibrutinib and the more selective BTK inhibitors have off-target effects on the function of cytotoxic immune populations which may impair the ability of these cells to respond to immuno-stimulatory agents. This data provides valuable insights into how the immune effects of targeted therapies may impact their successful combination with immunotherapies.

6 EFFECT OF IMMUNOTHERAPIES ON *IN VITRO* T CELL FUNCTION

6.1 SUMMARY

The rational combination of immunotherapies requires understanding the mechanisms and immune effects of both the immunotherapy and the therapies with which they are combined. Previously this thesis explored the effects of targeted therapies, in particular BTK inhibitors on the function of T cells. This chapter explores two immunotherapies, lenalidomide and the anti-PD-1 mAb BGB-A317, both of which have been investigated in clinical trials as potential therapies for CLL. Using *in vitro* functional assays, this study explored the effect of immunotherapy alone, or in combination with ibrutinib on the function of T cells. This analysis found that the PD-1 inhibitor alone had no effect on the proliferation or inhibitory marker expression of T cells but augmented the effect of ibrutinib on inhibitory receptor expression. Lenalidomide increased the proliferation of CD8 T cells but decreased the proliferation of CD4 T cells and augmented the expression of inhibitory receptors on activated T cells, both alone and when combined with ibrutinib.

6.2 INTRODUCTION

The most widely used immunotherapy in CLL are anti-CD20 mAbs, in particular rituximab. However, despite the significant efficacy of both ibrutinib and rituximab as monotherapies, large phase 3 clinical studies of combination ibrutinib and rituximab treatment have shown no clinical benefit over single agent ibrutinib in CLL[293,294]. While NK mediated ADCC is not the only mechanism by which anti-CD20 mAbs exert anti-tumour effects, it remains pertinent that ibrutinib inhibits NK cell ADCC, thus potentially limiting the additive effect of rituximab treatment. The results of these trials highlight the importance of understanding the immune mediated mechanisms of both the immunotherapies as well as the targeted therapies with which they are combined.

Both lenalidomide and checkpoint inhibitors are being actively pursued in combination with BTKi and part of the preclinical rationale for these combinations relies on the immunomodulatory effects of ibrutinib, presumably mediated by ITK inhibition. As discussed in Chapter 1, lenalidomide has clinical efficacy in CLL and has been shown to increase T cell proliferation and tumour cell killing as well as reversing the exhaustion profile of T cells. However, lenalidomide is also associated with significant risk of tumour flare syndrome, a potentially life-threatening side effect that is associated with increased CLL cell immunogenicity. Ibrutinib has been shown to dampen CLL cell activation and therefore is an attractive option for combination with therapies associated with cytokine release syndrome and other immune mediated adverse effects such as lenalidomide. As such this study aimed to understand the effect of lenalidomide on T cell proliferation and on the expression of inhibitory receptors, in order to determine if lenalidomide augments the effect of ibrutinib on T cell activation.

Similarly, the rationale for combining ibrutinib with PD-1 inhibition also relies on the inhibition of ITK. The combination of ibrutinib and PD-1 inhibition improved killing in mouse models of lymphoma and solid tumours that did not express BTK, and was dependent on the presence of T cells[300]. These studies suggest that ibrutinib, through regulating T cells results in improved T cell function in the absence of any direct anti-tumour effect. Furthermore, ibrutinib treated patients have been shown to have

decreased expression of inhibitory receptors on T cells. Therefore, this analysis aimed to understand if PD-1 inhibition altered the inhibitory receptor expression in proliferating T cells, and if PD-1 blockade augmented the effect of ibrutinib on T cell exhaustion.

6.2.1 *LENALIDOMIDE ALTERS T CELL PROLIFERATION IN VITRO*

PBMC from healthy donors was treated with either ibrutinib, lenalidomide, or BGB-A317 or the combination of ibrutinib and either lenalidomide or BGB-A371 and stimulated using CD2/CD3/CD28 T cell stimulation beads and IL-2 for 7 days. Drug concentrations and IL-2 were maintained over the duration of the experiment. Proliferation was tracked using CellTrace violet dilution, and assessed by flow cytometry on days 3, 5, and 7.

Lenalidomide treatment significantly reduced the percent of CD4 T cells that underwent at least one division, compared to vehicle treated cells (Figure 6.1 a). Conversely, lenalidomide treated CD8 T cells had a significantly greater proportion of dividing cells by day 7 (Figure 6.1 b). Interestingly both CD4 and CD8 T cells had a significant increase in the replication index, a measure of the propensity of the responding cells to proliferate, excluding the undivided cells (Figure 6.1 c-d). BGB-A317 treatment had no significant impact on either the percent divided or the proliferation index of either CD4 or CD8 T cells (Figure 6.1 a-d).

Given the inhibitory effect of ibrutinib on both CD4 and CD8 T cell proliferation demonstrated in the previous chapter, the effect of the combination of ibrutinib and lenalidomide treatment was also investigated. Ibrutinib had a significantly greater effect on CD4 T cell proliferation than lenalidomide alone ($p<0.01$) and the inhibitory effect of ibrutinib and lenalidomide were additive resulting in significantly less CD4 T cell proliferation in the combination treated cultures than with either drug alone (Figure 6.2 a). In CD8 T cells, ibrutinib alone or in combination with lenalidomide resulted in significantly decreased proliferation and the addition of lenalidomide did not significantly augment the inhibitory effect of ibrutinib (Figure 6.2 b).

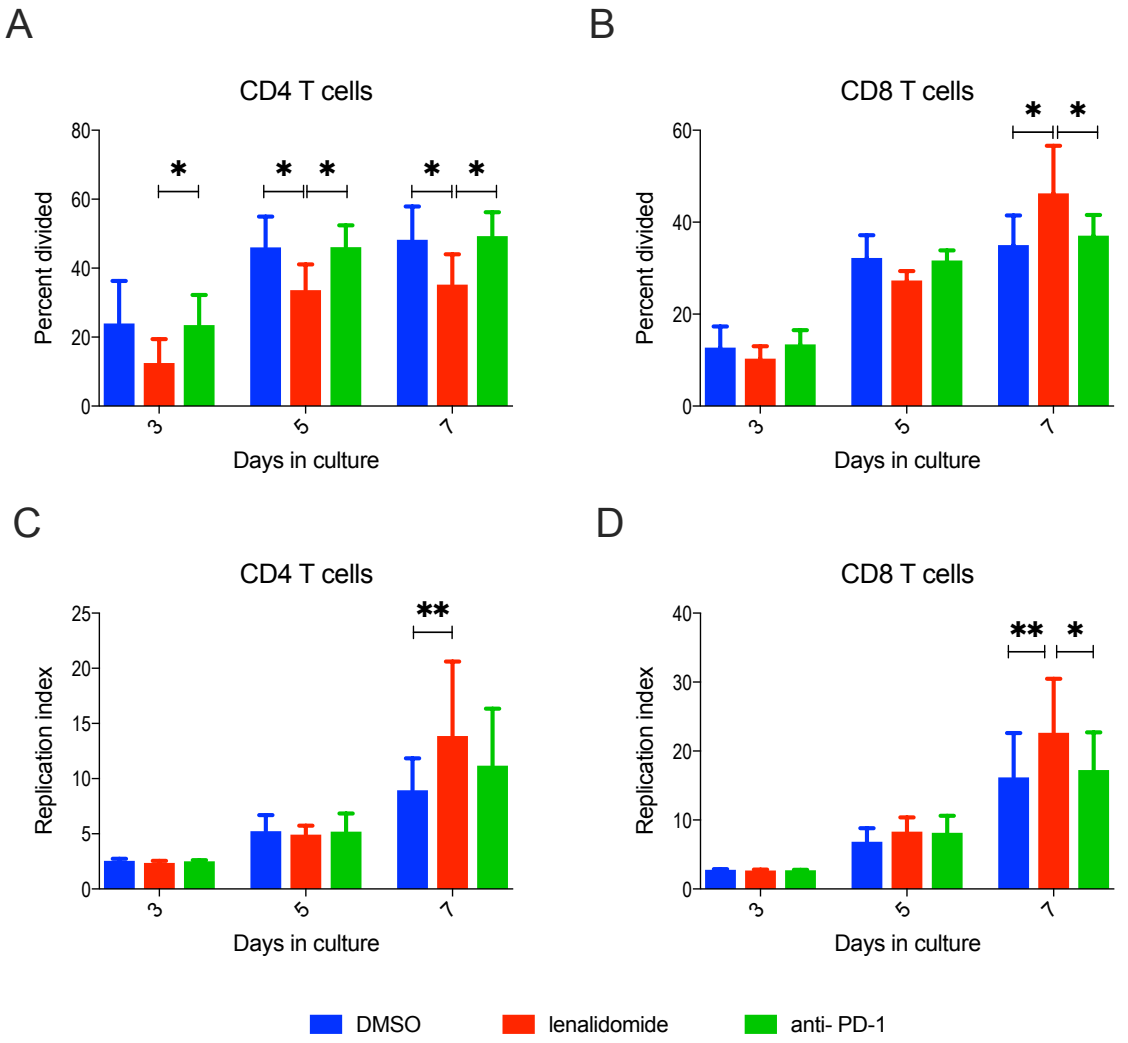

Figure 6.1 Lenalidomide enhances CD8 but not CD4 T cell proliferation

PBMC from 3 healthy donors was stained with CellTrace violet and stimulated for up to 7 days with CD2/CD3/CD28 beads and IL-2, cultures were treated with lenalidomide, anti-PD-1 mAb (BGB-A317) or vehicle on day 0, day 3 and day 5. Proliferation was measured using FlowJo proliferation modelling. Percent divided A) CD4 T cells and B) CD8 T cells. Replication index of C) CD4 T cells and D) CD8 T cells. Bars represent mean ± SD, Tukey's multiple comparisons test, * $p < 0.05$, ** $p < 0.01$, *** $p < 0.001$

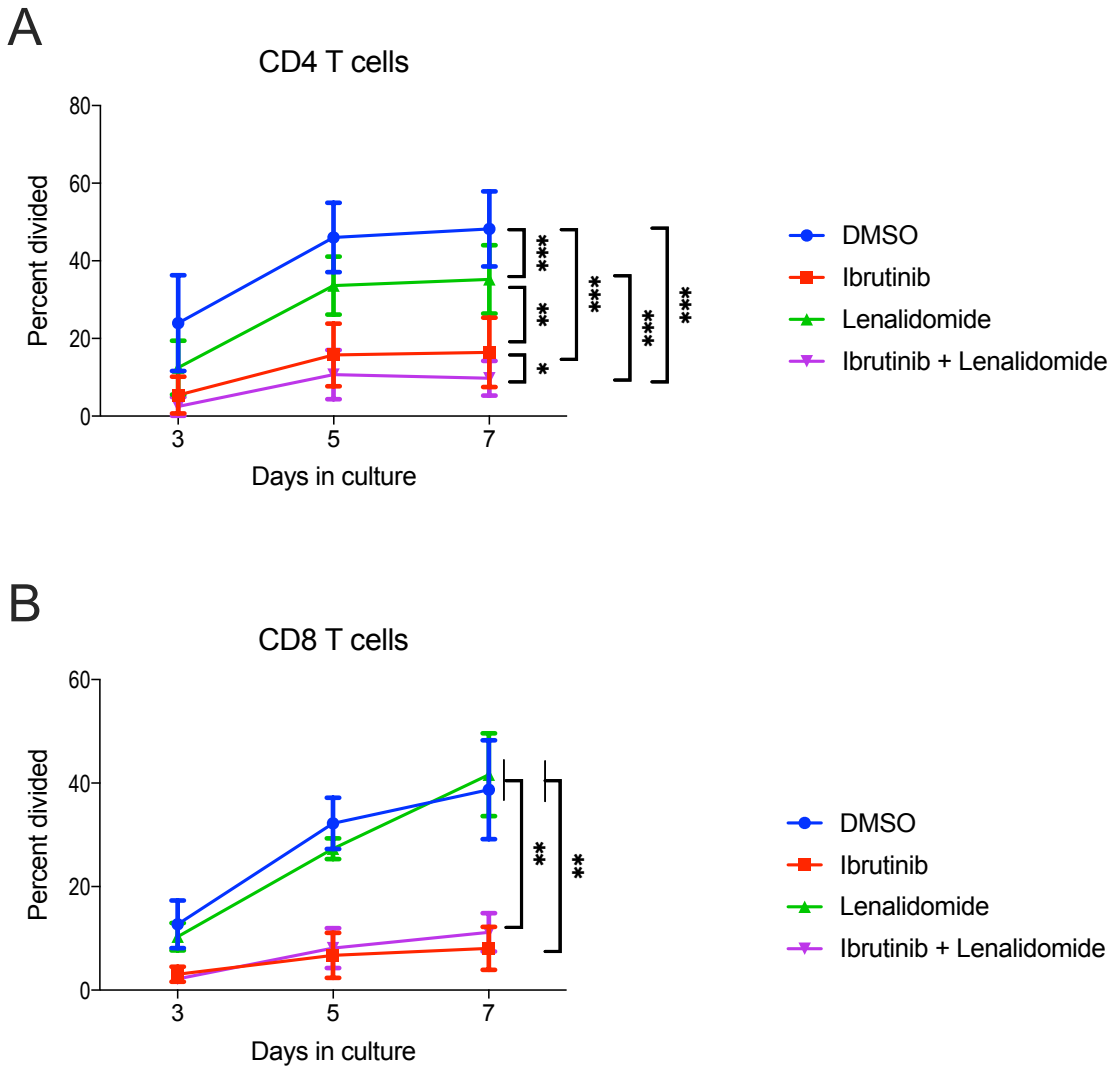

Figure 6.2 Ibrutinib and lenalidomide have an additive effect on CD4 T cell proliferation

PBMC from 3 healthy donors was stained with CellTrace violet and stimulated for up to 7 days with CD2/CD3/CD28 beads and IL-2, cultures were treated with lenalidomide, anti-PD-1 mAb (BGB-A317) or vehicle on day 0, day 3 and day 5. Proliferation of CD4 and CD8 T cells was measured using CellTrace violet dilution and FlowJo proliferation modelling. Percent divided in A) CD4 T cells (2-way ANOVA p=0.013) and B) CD8 T cells (2-way ANOVA p=0.025). Lines represent mean ± SD with Tukey's multiple comparisons test, * p <0.05, ** p <0.01, *** p <0.001.

6.2.2 *Effect of immunotherapies on T cell exhaustion*

Both lenalidomide and PD-1 inhibition have been shown to alter the expression of inhibitory receptors on T cells. Using generational gating based on CellTrace violet dilution the expression of PD-1, TIM-3 and LAG-3 were assessed in each generation of proliferating T cells separately. BGB-A317, by binding to PD-1, prevented most of the binding of the fluorescently labelled anti-PD-1 antibody. As such in BGB-A317 treated cultures there was a significant reduction in the MFI of the PD-1 antibody. This binding was maintained for 48 hours after BGB-A317 was last added to the cultures (Figure 6.3 a-b, 4.4 a-b).

After 5 days stimulation there was no significant change in the expression of either TIM-3 or LAG-3 on BGB-A317 treated CD8 or CD4 T cells, compared to vehicle treated cells (Figure 6.3 c, e) however there was significantly higher expression of TIM-3 on day 7 (Figure 6.3 d). CD8 T cells from lenalidomide treated cultures exhibited no significant change in the expression of PD-1, however these cells expressed significantly higher levels of both TIM-3 and LAG-3 (Figure 6.3). Conversely, lenalidomide treated CD4 T cells had significantly reduced expression of PD-1 (Figure 6.3 a-b) but significantly higher expression of both TIM-3 and LAG-3 on both days 5 and 7 (Figure 6.3 c-f).

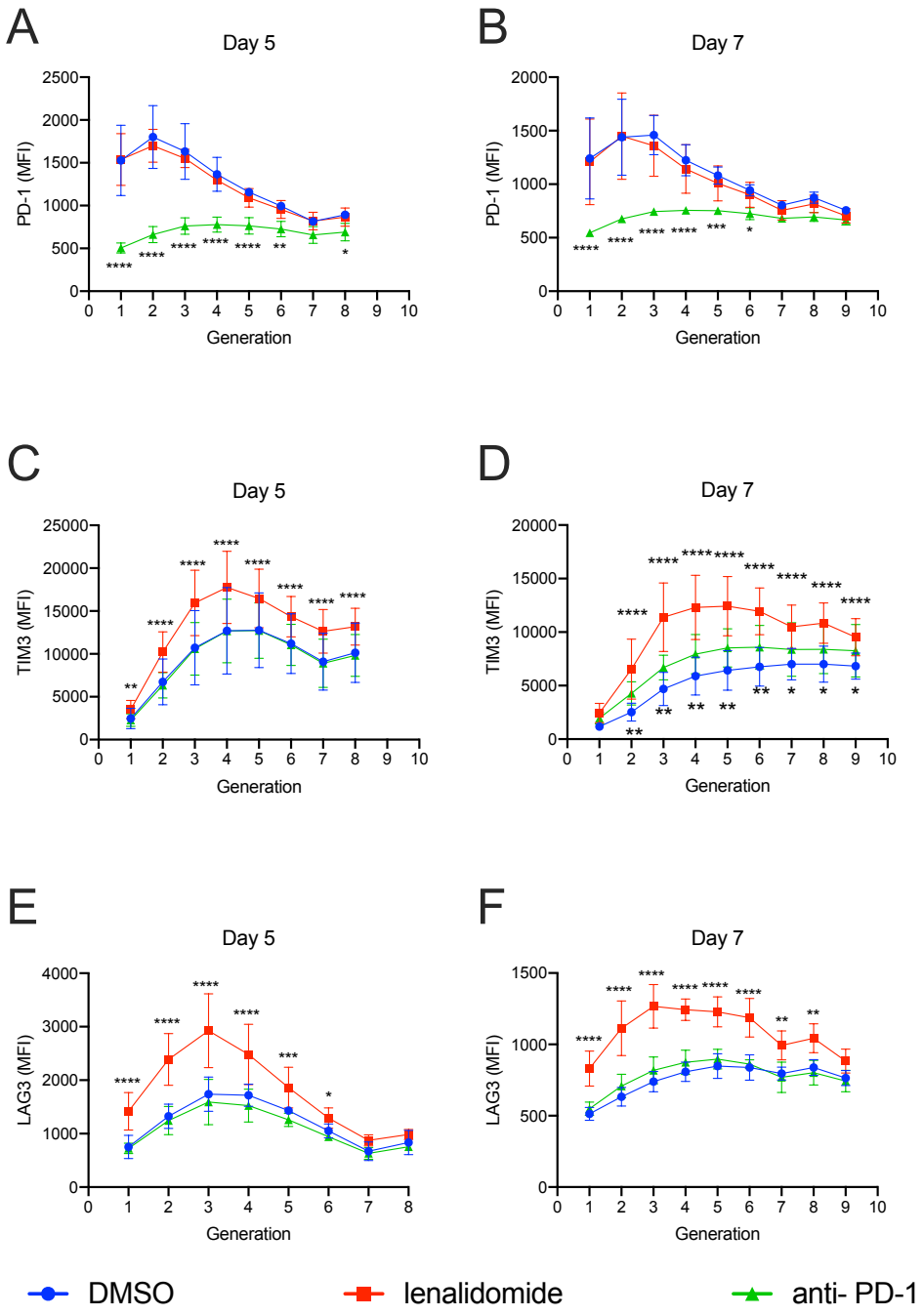

Figure 6.3 Effect of immunotherapies on the expression of co-stimulatory receptor expression in proliferating CD8 T cells

PBMC from healthy donors was treated with vehicle, lenalidomide or anti-PD1 antibody (BGB-A317) and stimulated for up to 7 days with CD2/CD3/CD28 T cell activation beads and IL-2 (20 IU/mL). MFI of A&B) PD-1, C&D) TIM-3 and E&F) LAG-3 in proliferating CD8 T cells using generational gating based on CellTrace violet dilution was assessed on day 5 and 7 of stimulation. Lines represent mean ± SD of 3 donors. 2way RM ANOVA with Tukey's multiple comparisons test, *p<0.05, **p<0.01, ***p<0.001, ****p<0.0001.

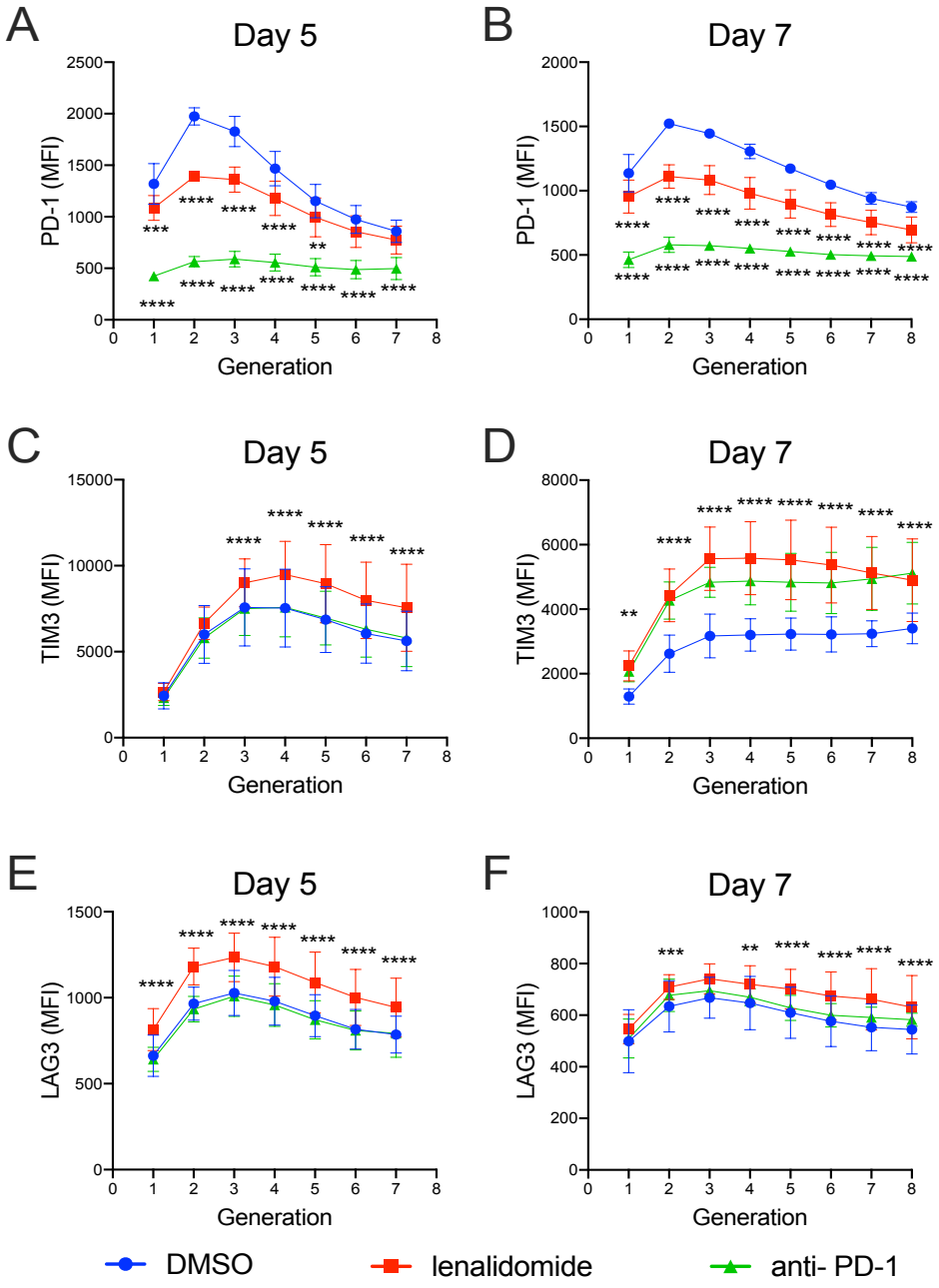

Figure 6.4 Effect of immunotherapies on inhibitory marker expression in proliferating CD4 T cells

PBMC from healthy donors was treated with vehicle, lenalidomide or anti-PD1 antibody (BGB-A317) and stimulated for up to 7 days with CD2/CD3/CD28 T cell activation beads and IL-2 (20 IU/mL). MFI of A-C) PD-1, D-E) TIM-3 and G-H) LAG-3 in proliferating CD4 T cells using generational gating based on CellTrace violet dilution was assessed on day 5 and 7 of stimulation. Lines represent mean ± SD of 3 donors. 2way RM ANOVA with Turkey's multiple comparisons test, *p<0.05, **p<0.01, ***p<0.001, ****p<0.0001.

Ibrutinib, lenalidomide and PD-1 blockade alter the expression of inhibitory receptors in different ways. Therefore, the effects of concurrent treatment with ibrutinib and either lenalidomide or BGB-A317 on the expression of PD-1, TIM-3 and LAG-3 was also investigated. PBMC cultures were treated with a DMSO vehicle control, immunotherapy alone, ibrutinib alone, or the combination of immunotherapy and ibrutinib. After 5 days of stimulation the expression of inhibitory receptors was measured on individual generations using CellTrace violet dilution.

As previously demonstrated, after 5 days of stimulation ibrutinib treatment resulted in a significant decrease in PD-1 on undivided CD8 T cells but an increase in PD-1 expression on proliferating CD8 T cells (Figure 5.14). At this timepoint lenalidomide alone did not significantly alter PD-1 expression as compared to vehicle. However, when combined with ibrutinib, lenalidomide delayed the upregulation of PD-1 leading to consistently lower expression in the combination treated cells than with ibrutinib alone (Figure 6.5 a). This effect cannot be attributed to lenalidomide altering T cell proliferation as there was no significant effect of lenalidomide on the proliferation of CD8 T cells at this timepoint (Figure 6.3 a).

Ibrutinib treated cells also had decreased TIM-3 expression in less proliferated CD8 T cells and increased expression in the more extensively proliferated cells. In contrast, lenalidomide consistently increased TIM-3 expression, though to a lesser degree than ibrutinib in later generations. Conversely lenalidomide treated CD8 T cells had the highest expression of LAG-3, especially in the early generations, while ibrutinib significantly reduced LAG-3 expression. The expression of LAG-3 in cells treated with the combination of lenalidomide and ibrutinib mirrored the expression levels seen with ibrutinib monotherapy (Figure 6.5 c). The effect of combination of ibrutinib and BGB-A317 treatment on CD8 T cells expression of inhibitory receptors was also tested. As observed in anti-PD-1 monotherapy, the presence of the therapeutic antibody in the ibrutinib combination treated cells precluded staining with the fluorescently labelled PD-1 antibody. However, TIM-3 and LAG-3 expression was highest in CD8 T cells that had undergone many divisions, and the expression of TIM3 with combination treatment was significantly higher than with ibrutinib treatment alone (Figure 6.6 b, c).

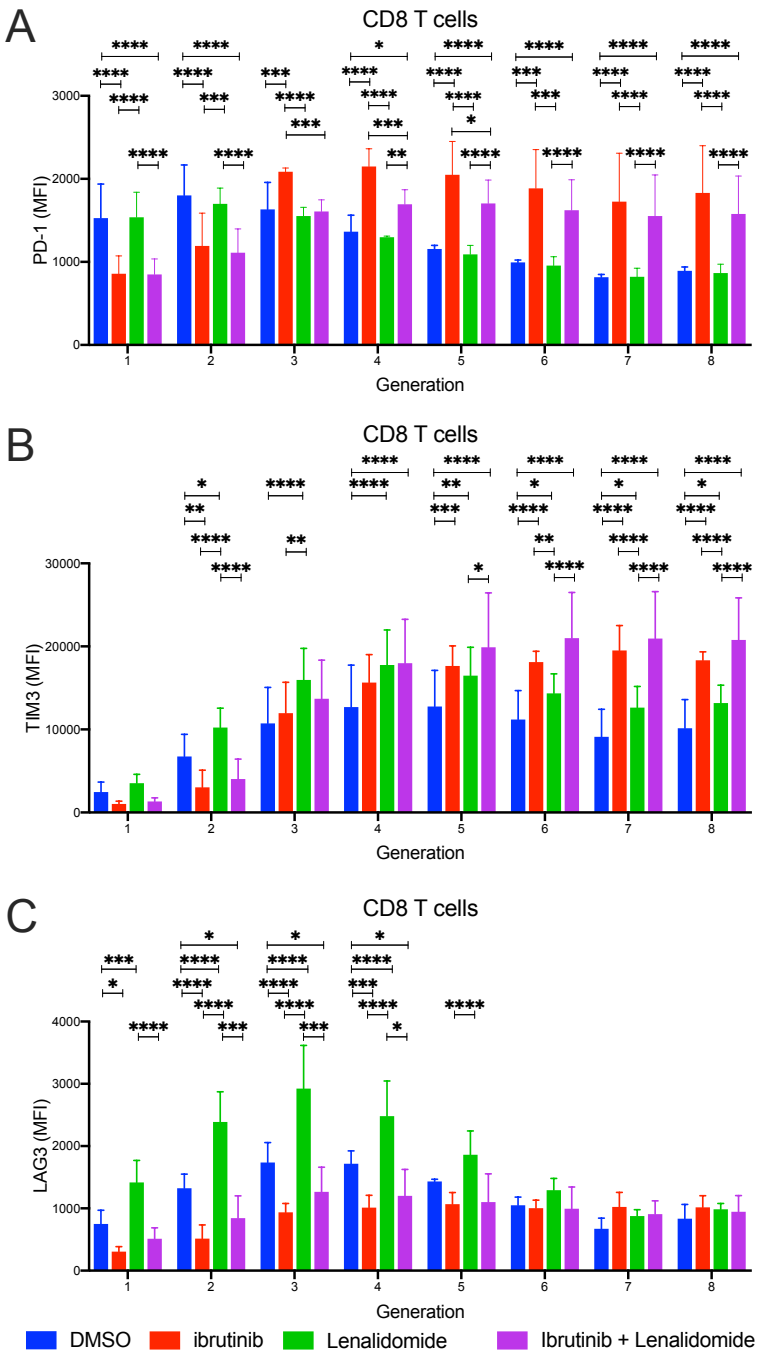

Figure 6.5 Effect of ibrutinib and lenalidomide on the expression of inhibitory receptor expression on proliferating CD8 T cells

Whole PBMC was stained with CellTrace violet and treated with ibrutinib ± lenalidomide or vehicle control. Expression of A) PD-1 B) TIM-3 and C) LAG-3 on individual generations of proliferating CD8 T cells after 5 days stimulation with CD2CD3/CD28 T cell stimulation beads and IL-2. Bars indicate mean + SD in 3 healthy donors. 2way RM ANOVA with Tukey's multiple comparisons test, * p <0.05, ** p <0.01, *** p <0.001, **** p <0.0001.

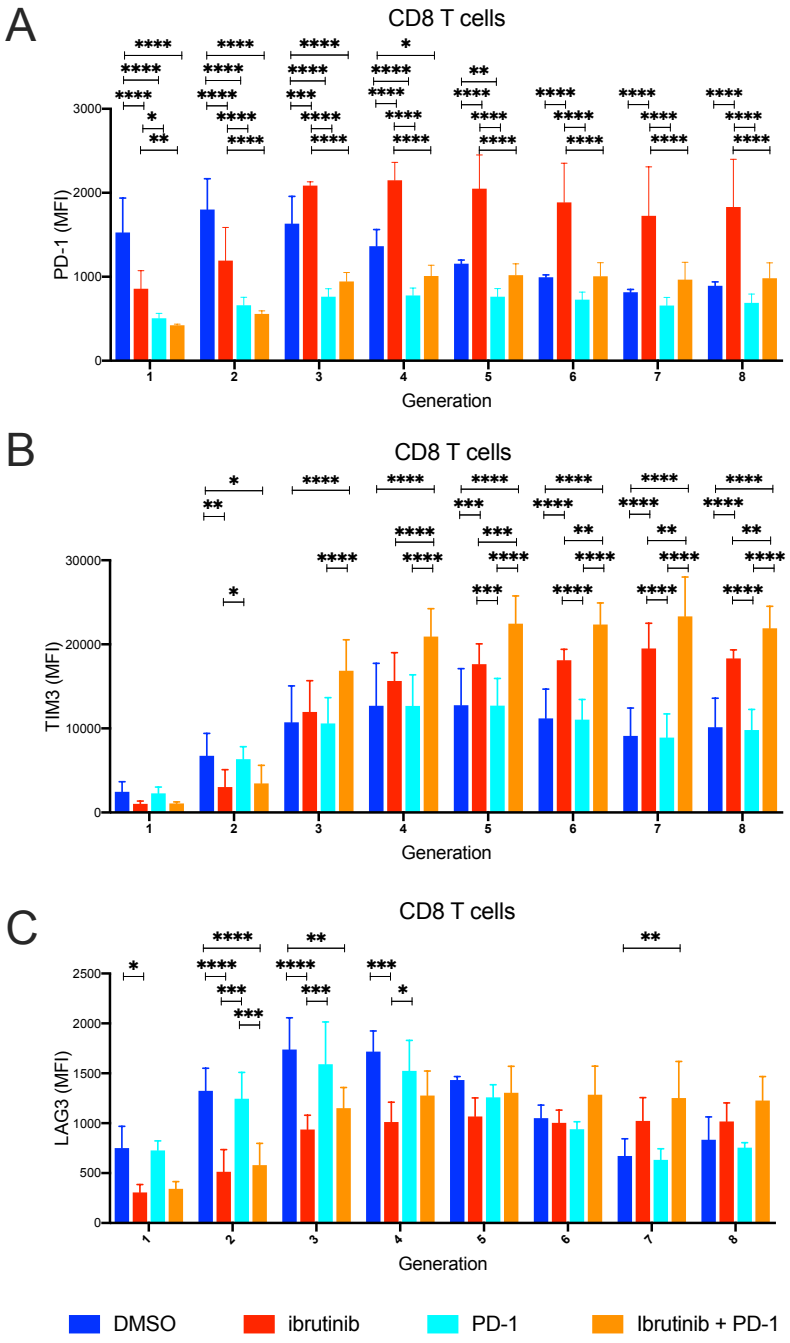

Figure 6.6 Effect of ibrutinib and BGB-A317 on the expression of co-stimulatory receptors in proliferating CD8 T cells

Whole PBMC was stained with CellTrace violet and treated with ibrutinib ± BGB-A317 or vehicle control. The expression of A) PD-1 B) TIM-3 and C) LAG-3 was measured on each generation of proliferating CD8 T cells after 5 days stimulation with CD2/CD3/CD28 T cell stimulation beads and IL-2. Bars indicate mean + SD in 3 healthy donors. 2way RM ANOVA with Tukey's multiple comparisons test, *p<0.05, **p<0.01, ***p<0.001, ****p<0.0001.

Both ibrutinib and lenalidomide inhibited the proliferation of CD4 T cells. However, while ibrutinib only reduced the expression of PD-1 in early generation CD4 T cells, lenalidomide consistently reduced the expression of PD-1 in all generations (Figure 6.4 a–b). As in CD8 T cells, lenalidomide treatment reduced the upregulation of PD-1 on late generation CD4 T cells seen in ibrutinib treated cultures (Figure 6.6 a). Similarly, while ibrutinib reduced the expression of TIM-3 and LAG-3 on undivided CD4 T cells and increased expression on later generations, lenalidomide consistently increased the expression of TIM-3 and LAG-3 in all CD4 T cells (Figure 6.7 b, c).

Again, treatment with BGB-A317 precluded binding of the fluorescently labelled antibody, demonstrating that it effectively blocks PD-1 interactions (Figure 6.8 a). Despite this, CD4 T cells cultured with BGB-A317 had no change in the expression of the other inhibitory receptors TIM-3 or LAG-3, and CD4 T cells treated with both ibrutinib and BGB-A317 had significantly higher expression of TIM-3 and LAG-3 than with either ibrutinib or PD-1 treatment alone (Figure 6.8 b, c).

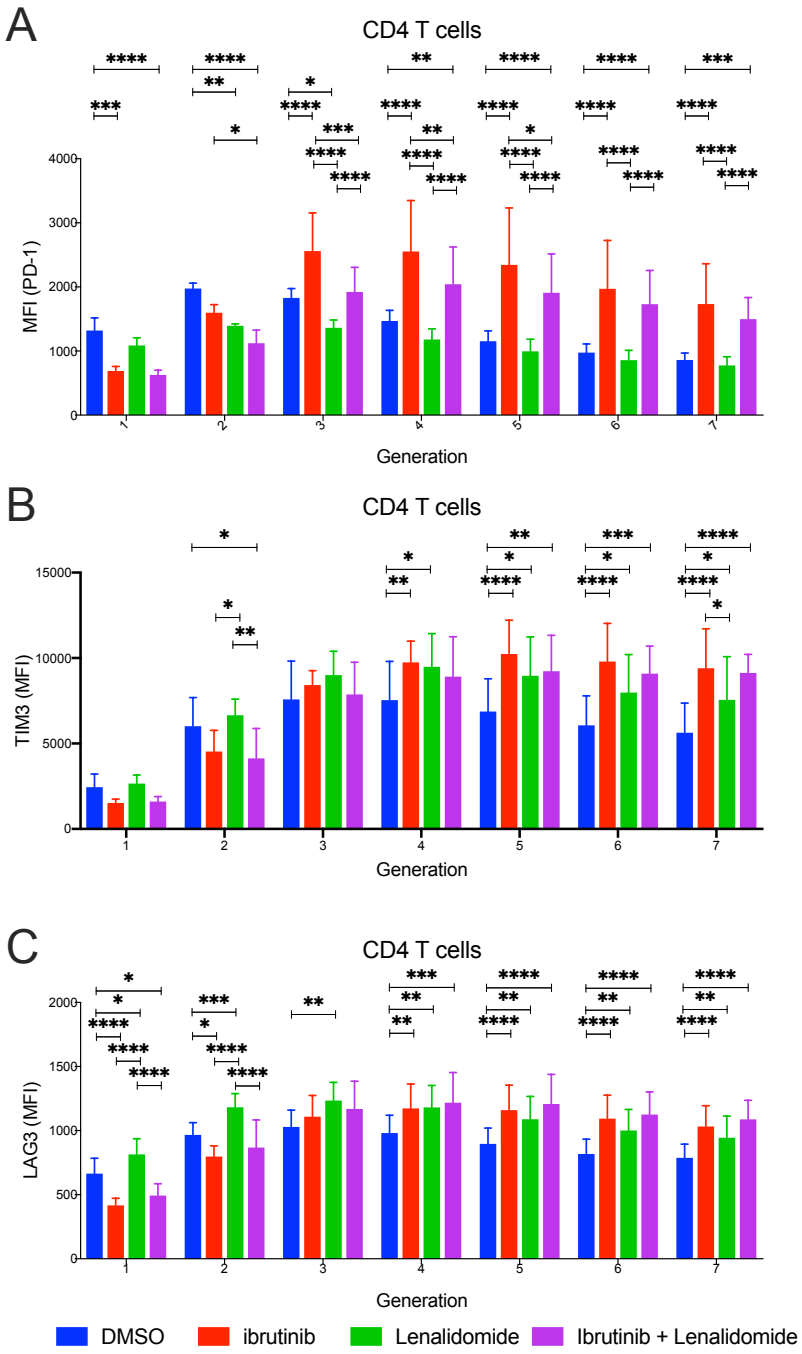

Figure 6.7 Effect of ibrutinib and lenalidomide on inhibitory receptor expression on proliferating CD4 T cells

Whole PBMC from 3 healthy donors was stained with CellTrace violet and treated with ibrutinib ± lenalidomide or vehicle control. The expression of A) PD-1 B) TIM-3 and C) LAG-3 was measured on each generation of proliferating CD4 T cells after 5 days stimulation with CD2/CD3/CD28 T cell stimulation beads and IL-2. Bars indicate mean + SD, 2way RM ANOVA with Tukey's multiple comparisons test, *p<0.05, **p<0.01, ***p<0.001, ****p<0.0001.

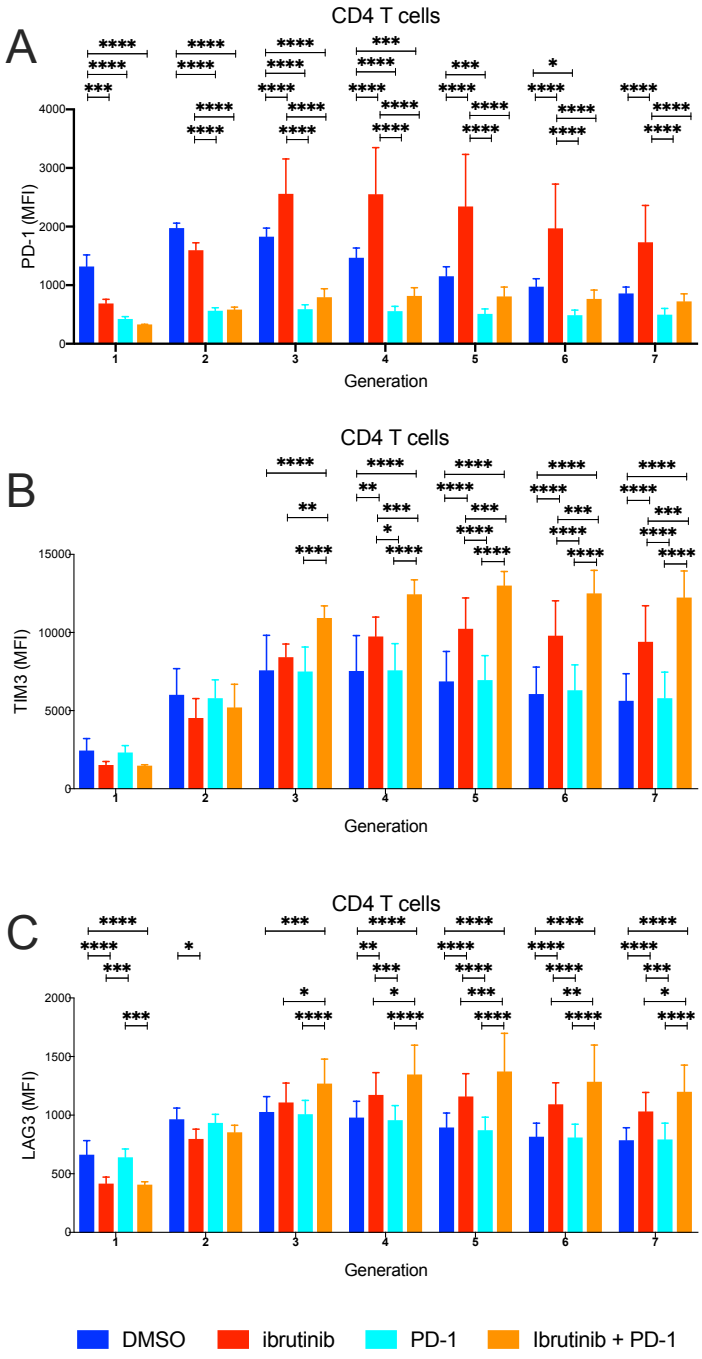

Figure 6.8 Effect of ibrutinib and BGB-A317 on the expression of co-stimulatory receptor expression on proliferating CD4 T cells

Whole PBMC was stained with CellTrace violet and treated with ibrutinib ± (BGB-A317) or vehicle control. The expression of A) PD-1 B) TIM-3 and C) LAG-3 was measured on each generation of proliferating CD8 T cells after 5 days stimulation with CD2/CD3/CD28 T cell stimulation beads and IL-2. Bars indicate mean + SD in 3 healthy donors. 2way RM ANOVA with Tukey's multiple comparisons test, *p<0.05, **p<0.01, ***p<0.001, ****p<0.0001.

6.2.3 *DEGRANULATION*

In contrast to ibrutinib, lenalidomide has been shown to increase NK cell ADCC against anti-CD20 antibody labelled cells[348]. Therefore, the effect of lenalidomide and anti-PD-1 mAb on CD8 T cell degranulation was examined. Neither immunotherapy had a significant effect on the proportion of CD8 T cells which degranulated in response to bead stimulation (Figure 6.9 a) however a greater proportion of the lenalidomide treated CD8 T cells expressed IFNγ (Figure 6.9 b). To test if this pattern was maintained in combination with the targeted therapies, PBMC from a single healthy donor were treated with ibrutinib, zanubrutinib, venetoclax, ibrutinib and venetoclax, or zanubrutinib and venetoclax either with the targeted therapies alone or in combination with lenalidomide and BGB-A317. Ibrutinib containing cultures had a significant decrease in both degranulation and IFNγ production, which was not rescued by the presence of the immunotherapies (Figure 6.9 c-d).

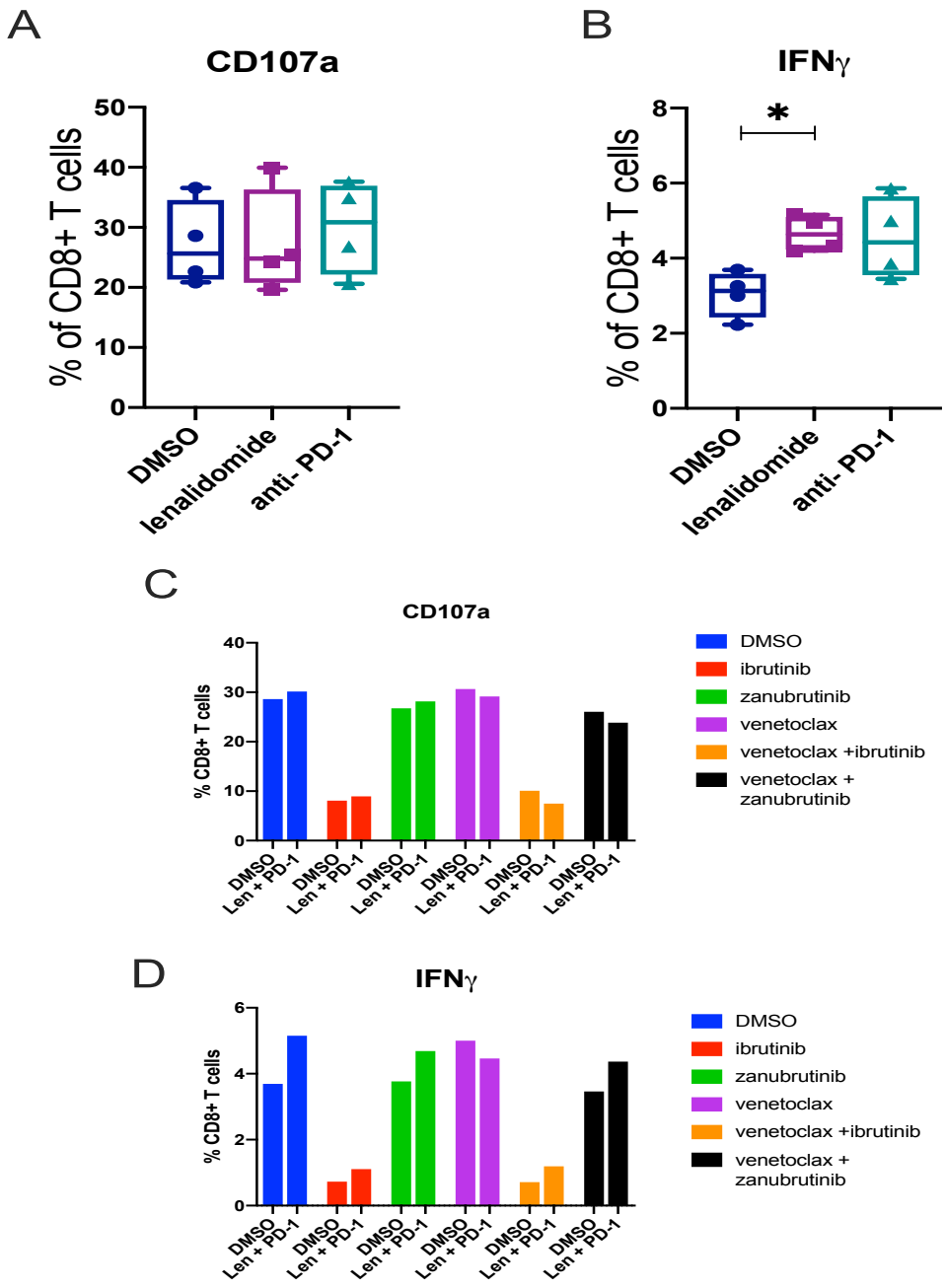

Figure 6.9 Lenalidomide has no effect of CD8 T cell degranulation but increases IFNγ production

PBMC was treated with immunotherapies and/or targeted therapies overnight prior to performing a degranulation assay using CD2/CD3/CD28 T cell stimulation. Summary boxplot of 4 CLL patient's PBMC pre-treated with either lenalidomide or BGB-A317 A) surface CD107a expression and B) IFNγ production in CD8 T cells, paired t tests, * $p<0.05$. PBMC from single CLL donor was treated with lenalidomide and BGB-A317, ibrutinib, zanubrutinib or venetoclax alone or in combination. CD8 T cell C) CD107a and D) IFNγ expression. Bars indicate mean of 2 replicates.

6.3 DISCUSSION

This chapter explored the effect of lenalidomide and BGB-A317 on the proliferation of CD4 and CD8 T cells from healthy donors and the ability of these immunotherapies to modulate the effects of ibrutinib. This data supports the immune activating effects of lenalidomide on CD8 T cells, resulting in greater proliferation and IFNγ production. However, it also suggests that CD4 and CD8 T cells are differentially affected by lenalidomide, reducing CD4 T cell proliferation. Finally, neither lenalidomide or BGB-A317 restored the functional capacity of ibrutinib treated T cells.

Lenalidomide increased *in vitro* CD8 T cell proliferation and IFNγ production, suggesting a potential for increased anti-leukaemia cytotoxicity. However, while both the proportion of CD8 T cells that had undergone at least one division and average number of generations of CD8 T cells increased these two measures of proliferation were incongruent in CD4 T cells. Lenalidomide simultaneously reduced the proportion of proliferating CD4 T cells whilst also increasing the average number of CD4 T cell generations. Thus far, much of the effect on T cell activation has focused on the lenalidomide induced degradation of Ikaros leading to upregulation of IL-2 production[273]. In particular, Ikaros has been shown to regulate CD8 T cell IL-2 responsiveness[349,350]. However lenalidomide is also a potent TNFα inhibitor[351] and lenalidomide decreases TNF-receptor-2 expression on CD4 T cells[352]. TNF-receptor-2 acts as a co-stimulatory receptor, lowering the threshold for TCR mediated activation[353,354] and as such, the contrasting effect of lenalidomide on CD4 and CD8 T cell proliferation may be attributed to distinct effects on cytokine responsiveness which results in different thresholds of activation. However, once the threshold is reached, proliferating CD4 T cells are similarly activated by lenalidomide.

Commensurate with increased activation there was also a significant increase in the expression of co-inhibitory receptors, specifically TIM-3 and LAG-3, on both CD4 and CD8 T cells. Interestingly, despite the proliferation of ibrutinib treated T cells not being altered by the addition of lenalidomide, the addition of lenalidomide dampened PD-1 upregulation in late generation CD8 T cells. Conversely, the upregulation of LAG-3 on

early generation CD8 T cells in lenalidomide treated cultures was perturbed in combination treated cells. Together, this suggests that ibrutinib and lenalidomide influence the expression of inhibitory receptors by distinct mechanisms and may have favourable combinatorial effect on CD8 T cell activation. In CD4 T cells, ibrutinib and lenalidomide had an additive effect on proliferation, while inhibitory marker expression mirrored the pattern observed in cell treated with ibrutinib alone.

This data highlights the fact that the expression of 'exhaustion markers' cannot be uncoupled from T cell activation. The expression of inhibitory receptors is a physiological response that is important for the regulation of T cell activation. Therefore, the expression of co-inhibitory receptors cannot be simply understood as equating to decreased functional capacity. In fact, the lower expression of exhaustion markers in T cells treated with ibrutinib may be evidence of the lack of T cell activity. Furthermore, the increased expression of inhibitory receptors in lenalidomide treated cultures may be evidence of greater activation rather than exhaustion. The uncoupling of inhibitory receptor expression and functional exhaustion is further exemplified by the observation that despite effectively blocking PD-1, BGB-A317 treated cultures did not have increased proliferation and actually resulted in increased expression of TIM-3 and LAG-3 in late generation T cells.

Understanding the immunomodulatory effects of lenalidomide on T cells is complicated by the multitudinous and context dependent effects of treatment. Ikaros degradation and subsequent upregulation of IL-2 undoubtedly contributes to the T cell activation effects of lenalidomide. However it has also been suggested that lenalidomide increases co-stimulation through CD28 phosphorylation[355]. As such, differences in culture systems and stimulants may explain the variation in reported T cell responses to lenalidomide. The data herein was derived in a culture system that contained both strong CD28 co-stimulation and exogenous IL-2. As such this system may not demonstrate the full capacity for lenalidomide to increase T cell proliferation. Furthermore, the effects of lenalidomide presented in this chapter likely substantially different to the *in vivo* effect in which these exogenous factors are not present.

6.4 CONCLUSION

How the data presented in this chapter relates to the *in vivo* efficacy of these immunotherapies in patients, especially in combination with ibrutinib, remains unclear. This *in vitro* system may not be the most effective for showing the effect of anti-PD-1 therapy on reversing T cell exhaustion, however it does suggest that the upregulation of co-inhibitory receptors is not prevented by blocking PD-1 interactions. Interpreting these *in vitro* findings on the effect of lenalidomide is more complex. As previously noted, the clinical efficacy of lenalidomide in CLL may be due to the combination of direct leukaemia cells effects, immune modulation and effects on the microenvironment. While these findings do support the immune activating effect of lenalidomide, further investigation of the effect of *in vivo* lenalidomide and ibrutinib on T cell function is required to better understand if these drugs can be effectively combined.

7 CONCLUSION

The treatment landscape in CLL has dramatically changed over the last 5 years, moving away from chemotherapy-based treatment to an increased reliance on targeted therapies. While FCR remains the standard of care for first-line treatment of fit patients, the incorporation of small molecule inhibitors into routine clinical practice has provided new highly effective options for particularly high risk and relapsed or chemo-immunotherapy refractory patients. This thesis focused on the two most successful targeted therapies in CLL, ibrutinib and venetoclax, each of which have provided significant improvements in survival for R/R CLL patients. The time to progression in ibrutinib responsive patients has been reported as 37.6 months[356] and in an analysis of four clinical trials of R/R CLL patients the time to progression on venetoclax was 36.9 months[357]. However, high risk cohorts, especially those with del17p, remain at a greater risk of relapse on both ibrutinib[358] and venetoclax[87]. Furthermore, targeted therapies usually have continuous dosing schedules which increases the likelihood that patients will acquire resistance exemplified by the BTK^{C481S} and $Bcl\text{-}2^{G101V}$ mutations in ibrutinib and venetoclax treated patients respectively[94,359]. New therapeutic options are still needed for patients who do not respond or become resistant to these combinations of targeted therapies.

Both BTK and Bcl-2 inhibitors are at also the forefront of combination treatment strategies that prove high response rates. Recent trials using combination targeted therapies, such as ibrutinib and venetoclax combination regimens that have impressive response rates of approximately 90%, including more than 50% of patients with undetectable disease after 1 year on treatment[360,361]. However, it is too early to demonstrate the durability of these responses and there remain some patients who do not respond to the combination[362]. As such, the challenge moving forward is to determine optimal treatment combinations that will result in deep and durable responses which are maintained after treatment cessation.

There are many indications that immunotherapy holds promise for CLL. CLL is an immunologically relevant disease demonstrated by the success of alloHSCT and anti-CD20 antibodies which both suggest that CLL cells are susceptible to immune mediated killing. However, the application of immunotherapies in CLL has been far from straight forward. Despite sporadic success, such as promising CAR-T cell clinical trial results, checkpoint blockade and immunomodulatory therapies such as lenalidomide have yet proven to have the efficacy and tolerability that warrant inclusion in routine CLL treatment. The expansion of targeted therapies from the setting of relapsed disease to use as font-line therapy represents a new opportunity for treatment regimens that combine immunotherapy with targeted therapies without the potent

immunosuppressive effects of prior chemotherapy. This study was conceived under the principle that an improved understanding of the immunological impacts of targeted therapies would elucidate how they can be most successfully combined with immunotherapy.

This thesis hypothesised that treatment with targeted therapies would allow for the normalisation of the immune profile of patients. Using both flow cytometry and gene expression profiling a comprehensive analysis of the immune system of treated patients demonstrated that the targeted therapies investigated had limited effects on the immune system and may allow for the normalisation of the immune profile of treated patients (Figure 4.2). However, while they are substantially less immunosuppressive than chemotherapy, targeted therapies are far from immunologically inert. In order to further understand the effect of targeted therapies on T cells and NK cells *in vitro* functional assays were performed. This study demonstrated that ibrutinib, which is the most commonly used BTK inhibitor, is broadly immunosuppressive. Ibrutinib, and to some extent the more selective BTK inhibitor zanubrutinib, perturbs cellular cytotoxicity (Figure 5.2), cytokine production (Figure 5.5) and proliferation (Figure 5.8). These results may help explain the notable risk of significant infections in ibrutinib treated patients[314,363] as well as the lack of efficacy of combination with anti-CD20 antibodies[293,294]. Together these findings suggest that more selective BTK inhibitors such acalabrutinib may be a better option for combination with immunotherapies that aim to enhance T cell and NK cell activation.

This study also explored the link between the effect of ibrutinib on T cell activation and the expression of exhaustion markers. This data suggested that while ibrutinib reduced the expression of exhaustion markers, this was linked to a lack of T cell activation (Figure 5.14) and may not translate to greater functional capacity or greater responsiveness to immunotherapy (Figure 6.2). The optimal strategies for combining targeted therapies and immunotherapies has proven more complex than initially understood. Indeed, ibrutinib in particular should be thought of as an immunomodulatory therapy in its own right. However, this thesis did not find the expected immunomodulatory effect of ibrutinib on CD4 T cells. The inconsistent changes to T_H1 and T_H2 CD4 T cell populations in CLL patients during long term ibrutinib treatment (Figure 4.14) and the increased IL-4 production of ibrutinib treated T cells (Figure 5.4) provides contradictory evidence to the proposed helper T cell skewing of ibrutinib[218]. Indeed, this study highlighted that inhibition of Tec family kinases other than ITK by more selective BTK inhibitors also contributes to significant changes in T cell and NK function (Figure 5.1 and Figure 5.17). Unlike ibrutinib, venetoclax did not alter the function of immune effector cells, rather this study found subtle changes in the abundance of terminally differentiated NK cells (Figure 4.7 and Figure 5.17). The significance of this finding as it relates to the efficacy of anti-CD20

monoclonal antibody therapy require further investigation. This study also found that venetoclax treated patients had a significant increase in the frequency of γδT cells (Figure 4.12) which suggests that this subset in particular may be an attractive target for immunotherapy in combination with venetoclax.

This thesis contributes to our understanding of the immunological effects of prominent targeted therapies used to treat CLL. These findings provide a mechanistic explanation for the failure of some combination targeted therapies and immunotherapy regimens and provides insights into new opportunities for more effective therapy combinations. As the use of the targeted therapies investigated expands from CLL to other malignancies and diseases states, this thesis provides a basis from which to consider the immunological implications and future use in combination with immunotherapy.

APPENDIX

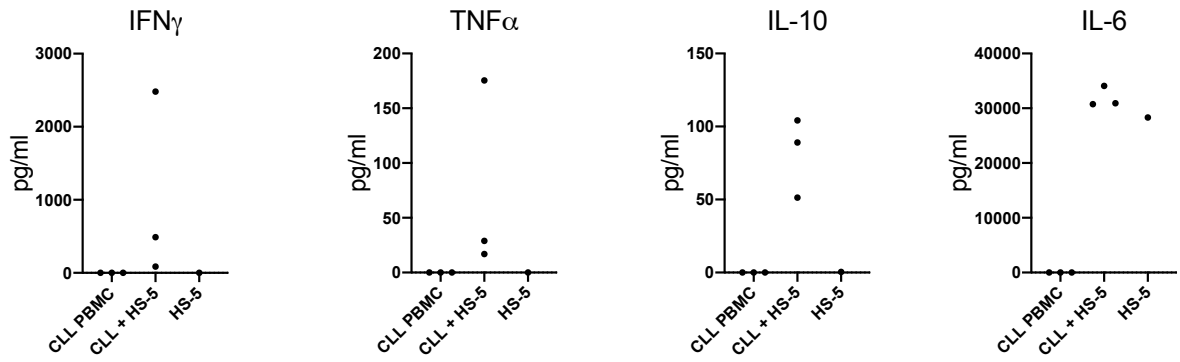

FIGURE A1 EFFECT OF HS-5 CO-CULTURE ON CLL PBMC CYTOKINE PRODUCTION

CLL PBMC and HS5 bone marrow stromal cells were cultured either separately or co-cultures together for 24 hours. Supernatant cytokine concentration was quantified using a CBA. Levels of IL2, IL17A, and IL4 were undetectable in all groups.

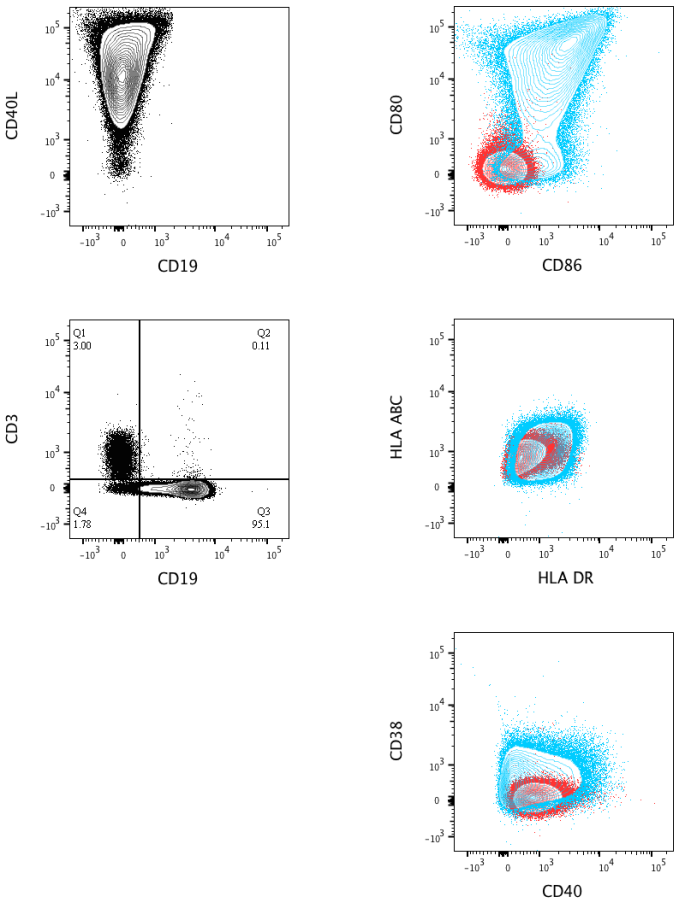

FIGURE A2 EFFECT OF CO-CULTURE ON CLL CELL EXPRESSION OF ACTIVATION MARKERS

CLL cells were in media (red) or co-cultured with HS-5 stromal cells (blue) for 24 hours and then analysed by flow cytometry.

REFERENCES

1. Hallek, M. *et al.* Guidelines for the diagnosis and treatment of chronic lymphocytic leukemia: a report from the International Workshop on Chronic Lymphocytic Leukemia updating the National Cancer Institute-Working Group 1996 guidelines. *Blood* **111**, 5446–56 (2008).

2. Australian Institute of Health and Welfare. *Cancer in Australia: an Overview 2014. Cancer series No 90. Cat. no. CAN 88.* (2014).

3. Australian Institute of Health and Welfare. *Australian Cancer Incidence and Mortality (ACIM) books: Chronic lymphocytic leukaemia.* (2015).

4. Rai, K. R. *et al.* Clinical staging of chronic lymphocytic leukemia. *Blood* **46**, 219–234 (1975).

5. Binet, J. L. *et al.* A new prognostic classification of chronic lymphocytic leukemia derived from a multivariate survival analysis. *Cancer* **48**, 198–206 (1981).

6. Jarošová, M., Plevová, K., Kotašková, J., Doubek, M. & Pospíšilová, Š. The importance of complex karyotype in prognostication and treatment of chronic lymphocytic leukemia (CLL): a comprehensive review of the literature. *Leuk. Lymphoma* 1–8 (2019). doi:10.1080/10428194.2019.1576038

7. Cavallari, M. *et al.* Biological significance and prognostic/predictive impact of complex karyotype in chronic lymphocytic leukemia. *Oncotarget* **9**, 34398–34412 (2018).

8. Rigolin, G. M. *et al.* In CLL, comorbidities and the complex karyotype are associated with an inferior outcome independently of CLL-IPI. *Blood* **129**, 3495–3498 (2017).

9. Baliakas, P. *et al.* Recurrent mutations refine prognosis in chronic lymphocytic leukemia. *Leukemia* **29**, 329–336 (2014).

10. Rossi, D. *et al.* The Prognostic Value of TP53 Mutations in Chronic Lymphocytic Leukemia Is Independent of Del17p13: Implications for Overall Survival and Chemorefractoriness. *Clin. Cancer Res.* **15**, 995–1004 (2009).

11. Parikh, S. A., Strati, P., Tsang, M., West, C. P. & Shanafelt, T. D. Should IGHV status and FISH testing be performed in all CLL patients at diagnosis? A systematic review and meta-analysis. *Blood* **127**, 1752–60 (2016).

12. da Cunha-Bang, C., Christiansen, I. & Utoft Niemann, C. The CLL-IPI applied in a population-based cohort. *Blood* **128**, 2181–2183 (2016).

13. The International CLL-IPI working group. An international prognostic index for patients with chronic lymphocytic leukaemia (CLL-IPI): a meta-analysis of individual patient data. *Lancet Oncol.* **17**, 779–790 (2016).

14. Rossi, D. *et al.* Molecular prediction of durable remission after first-line

fludarabine- cyclophosphamide-rituximab in chronic lymphocytic leukemia. *Blood* **126**, 1921–1925 (2016).

15. Thompson, P. A. *et al.* Fludarabine, cyclophosphamide, and rituximab treatment achieves long-Term disease-free survival in IGHV-mutated chronic lymphocytic leukemia. *Blood* **127**, 303–309 (2016).

16. Brown, J. R., Hallek, M. J. & Pagel, J. M. Chemoimmunotherapy Versus Targeted Treatment in Chronic Lymphocytic Leukemia: When, How Long, How Much, and in Which Combination? *Am. Soc. Clin. Oncol. Educ. Book* **35**, e387-98 (2016).

17. Hallek, M. J. *et al.* Addition of rituximab to fludarabine and cyclophosphamide in patients with chronic lymphocytic leukaemia: A randomised, open-label, phase 3 trial. *Lancet* **376**, 1164–1174 (2010).

18. Gassner, F. J. *et al.* Fludarabine modulates composition and function of the T cell pool in patients with chronic lymphocytic leukaemia. *Cancer Immunol. Immunother.* **60**, 75–85 (2011).

19. Bergmann, L., Fenchel, K., Jahn, B., Mitrou, P. S. & Hoelzer, D. Immunosuppressive effects and clinical response of fludarabine in refractory chronic lymphocytic leukemia. *Ann. Oncol.* **4**, 371–375 (1993).

20. Ysebaert, L. *et al.* Immune recovery after fludarabine-cyclophosphamide-rituximab treatment in B-chronic lymphocytic leukemia: implication for maintenance immunotherapy. *Leukemia* **24**, 1310–1316 (2010).

21. Fischer, K. *et al.* Long-term remissions after FCR chemoimmunotherapy in previously untreated patients with CLL: updated results of the CLL8 trial. *Blood* **127**, 208–215 (2016).

22. Tam, C. S. *et al.* Long-term results of the fludarabine, cyclophosphamide, and rituximab regimen as initial therapy of chronic lymphocytic leukemia. *Blood* **112**, 975–980 (2008).

23. Tam, C. S. *et al.* Long-term results of first salvage treatment in CLL patients treated initially with FCR (fludarabine, cyclophosphamide, rituximab). *Blood* **124**, 3059–3064 (2014).

24. Seifert, M. *et al.* Cellular origin and pathophysiology of chronic lymphocytic leukemia. *J. Exp. Med.* **209**, 2183–98 (2012).

25. Hamblin, T. J., Davis, Z., Gardiner, A., Oscier, D. G. & Stevenson, F. K. Unmutated Ig V(H) genes are associated with a more aggressive form of chronic lymphocytic leukemia. *Blood* **94**, 1848–54 (1999).

26. Damle, R. N. *et al.* Ig V gene mutation status and CD38 expression as novel prognostic indicators in chronic lymphocytic leukemia. *Blood* **94**, 1840–1847 (1999).

27. Chiorazzi, N. & Ferrarini, M. B cell chronic lymphocytic leukemia: lessons learned from studies of the B cell antigen receptor. *Annu. Rev. Immunol.* **21**, 841–94 (2003).

28. Ghia, P., Chiorazzi, N. & Stamatopoulos, K. Microenvironmental influences in chronic lymphocytic leukaemia: The role of antigen stimulation. in *Journal of Internal Medicine* **264**, 549–562 (Blackwell Publishing Ltd, 2008).

29. Fais, F. *et al.* Chronic lymphocytic leukemia B cells express restricted sets of mutated and unmutated antigen receptors. *J. Clin. Invest.* **102**, 1515–1525 (1998).

30. Dühren-von Minden, M. *et al.* Chronic lymphocytic leukaemia is driven by antigen-independent cell-autonomous signalling. *Nature* **489**, 309–312 (2012).

31. Mockridge, C. I. *et al.* Reversible anergy of sIgM-mediated signaling in the two subsets of CLL defined by V H -gene mutational status Reversible anergy of sIgM-mediated signaling in the two subsets of CLL defined by V H -gene mutational status. *Blood* **109**, 4424–4431 (2007).

32. Collins, R. J. *et al.* Spontaneous programmed death (apoptosis) of B-chronic lymphocytic leukaemia cells following their culture in vitro. *Br. J. Haematol.* **71**, 343–350 (1989).

33. Rawlings, D. J. *et al.* Mutation of unique region of Bruton's tyrosine kinase in immunodeficient XID mice. *Science (80-.).* **261**, 358–361 (1993).

34. Pedersen, I. M. *et al.* Protection of CLL B cells by a follicular dendritic cell line is dependent on induction of Mcl-1. *Blood* **100**, 1795–801 (2002).

35. Yang, W.-C., Collette, Y., Nunès, J. A. & Olive, D. Tec kinases: a family with multiple roles in immunity. *Immunity* **12**, 373–382 (2000).

36. Berg, L. J., Finkelstein, L. D., Lucas, J. A. & Schwartzberg, P. L. Tec family kinases in T lymphocyte development and function. *Annu. Rev. Immunol.* **23**, 549–600 (2005).

37. Antony, P. *et al.* B Cell receptor directs the activation of NFAT and NF-kB via distinct molecular mechanisms. *Exp. Cell Res.* **291**, 11–24 (2003).

38. Petro, J. B., Rahman, S. M. J., Ballard, D. W. & Khan, W. N. Bruton's Tyrosine Kinase Is Required for Activation of Iκb Kinase and Nuclear Factor κb in Response to B Cell Receptor Engagement. *J. Exp. Med.* **191**, 1745–1754 (2000).

39. Anderson, J. S., Teutsch, M., Dong, Z. & Wortis, H. H. An essential role for Bruton's tyrosine kinase in the regulation of B-cell apoptosis. *Proc. Natl. Acad. Sci. U. S. A.* **93**, 10966–71 (1996).

40. Lindvall, J. M. *et al.* Bruton's tyrosine kinase: Cell biology, sequence conservation, mutation spectrum, siRNA modifications, and expression profiling. *Immunological*

Reviews **203**, 200–215 (2005).

41. Hendriks, R. W., Yuvaraj, S. & Kil, L. P. Targeting Bruton's tyrosine kinase in B cell malignancies. *Nat. Rev. Cancer* **14**, 219–32 (2014).

42. Mangla, A. *et al.* Pleiotropic consequences of Bruton tyrosine kinase deficiency in myeloid lineages lead to poor inflammatory responses. *Blood* **104**, 1191–1197 (2004).

43. Mirsafian, H. *et al.* Transcriptome profiling of monocytes from XLA patients revealed the innate immune function dysregulation due to the BTK gene expression deficiency. *Sci. Rep.* **7**, 6836 (2017).

44. Horwood, N. J. *et al.* Bruton's tyrosine kinase is required for lipopolysaccharide-induced tumor necrosis factor alpha production. *J. Exp. Med.* **197**, 1603–11 (2003).

45. Futatani, T. *et al.* Deficient expression of Bruton's tyrosine kinase in monocytes from X-linked agammaglobulinemia as evaluated by a flow cytometric analysis and its clinical application to carrier detection. *Blood* **91**, 595–602 (1998).

46. Melcher, M. *et al.* Essential Roles for the Tec Family Kinases Tec and Btk in M-CSF Receptor Signaling Pathways That Regulate Macrophage Survival. *J. Immunol.* **180**, 8048–8056 (2008).

47. Tampella, G. *et al.* The Tec Kinase-Regulated Phosphoproteome Reveals a Mechanism for the Regulation of Inhibitory Signals in Murine Macrophages. *J. Immunol.* **195**, 246–256 (2015).

48. Pan, Z. *et al.* Discovery of Selective Irreversible Inhibitors for Bruton's Tyrosine Kinase. *ChemMedChem* **2**, 58–61 (2007).

49. Honigberg, L. A. *et al.* The Bruton tyrosine kinase inhibitor PCI-32765 blocks B-cell activation and is efficacious in models of autoimmune disease and B-cell malignancy. *Proc. Natl. Acad. Sci. U. S. A.* **107**, 13075–13080 (2010).

50. Herman, S. E. M. *et al.* treatment of chronic lymphocytic leukemia and is effectively targeted by Bruton tyrosine kinase represents a promising therapeutic target for treatment of chronic lymphocytic leukemia and is effectively targeted by PCI-32765. *Blood* **117**, 6287–6296 (2012).

51. Herman, S. E. M. *et al.* Ibrutinib inhibits BCR and NF-kappaB signaling and reduces tumor proliferation in tissue-resident cells of patients with CLL. *Blood* **123**, 3286–3295 (2014).

52. Cheng, S. *et al.* BTK inhibition targets in vivo CLL proliferation through its effects on B-cell receptor signaling activity. *Leukemia* **28**, 649–57 (2014).

53. Advani, R. H. *et al.* Bruton tyrosine kinase inhibitor ibrutinib (PCI-32765) has significant activity in patients with relapsed/refractory B-cell malignancies. *J. Clin.*

Oncol. **31**, 88–94 (2013).

54. Byrd, J. C. *et al.* Targeting BTK with Ibrutinib in Relapsed Chronic Lymphocytic Leukemia. *N. Engl. J. Med.* **369**, 32–42 (2013).

55. Byrd, J. C. *et al.* Three-year follow-up of treatment-naïve and previously treated patients with CLL and SLL receiving single-agent ibrutinib. *Blood* **125**, 2497–2506 (2015).

56. Burger, J. A. *et al.* Ibrutinib as Initial Therapy for Patients with Chronic Lymphocytic Leukemia. *N. Engl. J. Med.* **373**, 2425–2437 (2015).

57. Chen, S.-S. *et al.* BTK inhibition results in impaired CXCR4 chemokine receptor surface expression, signaling and function in chronic lymphocytic leukemia. *Leukemia* **30**, 833–43 (2016).

58. de Rooij, M. F. M. *et al.* The clinically active BTK inhibitor PCI-32765 targets B-cell receptor- and chemokine-controlled adhesion and migration in chronic lymphocytic leukemia. *Blood* **119**, 2590–2594 (2012).

59. Woyach, J. A. *et al.* Prolonged lymphocytosis during ibrutinib therapy is associated with distinct molecular characteristics and does not indicate a suboptimal response to therapy. *Blood* **123**, 1810–1817 (2014).

60. Cheson, B. D. *et al.* Refinement of the Lugano classification response criteria for lymphoma in the era of immunomodulatory therapy. *Blood* **128**, blood-2016-05-718528 (2016).

61. Barf, T. *et al.* Acalabrutinib (ACP-196): A covalent Bruton tyrosine kinase (BTK) inhibitor with a differentiated selectivity and in vivo potency profile. *J. Pharmacol. Exp. Ther.* **383**, 240–252 (2017).

62. Rauf, F. *et al.* Ibrutinib inhibition of ERBB4 reduces cell growth in a WNT5A-dependent manner. *Oncogene* 1–14 (2018). doi:10.1038/s41388-017-0079-x

63. Chen, J., Kinoshita, T., Sukbuntherng, J., Chang, B. Y. & Elias, L. Ibrutinib Inhibits ERBB Receptor Tyrosine Kinases and HER2-Amplified Breast Cancer Cell Growth. *Mol. Cancer Ther.* **15**, 2835–2844 (2016).

64. Kim, E. *et al.* Ibrutinib inhibits pre-BCR+ B-cell acute lymphoblastic leukemia progression by targeting BTK and BLK. *Blood* **129**, 1155–1165 (2017).

65. Levade, M. *et al.* Ibrutinib treatment affects collagen and von Willebrand factor-dependent platelet functions. *Blood* **124**, 3991–3995 (2014).

66. Evans, E. K. *et al. Inhibition of Btk with CC-292 provides early pharmacodynamic assessment of activity in mice and humans. The Journal of pharmacology and experimental therapeutics* **346**, (2013).

67. Brown, J. R. *et al.* Phase I study of single-agent CC-292, a highly selective bruton's

tyrosine kinase inhibitor, in relapsed/refractory chronic lymphocytic leukemia. *Haematologica* **101**, e295–e298 (2016).

68. Byrd, J. C. *et al.* Acalabrutinib (ACP-196) in Relapsed Chronic Lymphocytic Leukemia. *N. Engl. J. Med.* **374**, 323–332 (2016).

69. Tam, C. S. *et al.* Twice Daily Dosing with the Highly Specific BTK Inhibitor, Bgb-3111, Achieves Complete and Continuous BTK Occupancy in Lymph Nodes, and Is Associated with Durable Responses in Patients (pts) with Chronic Lymphocytic Leukemia (CLL)/Small Lymphocytic Lymph…. *Blood* **128**, (2016).

70. Vaux, D., Cory, S. & Adams, J. M. Bcl-2 gene promotes haemopoietic cell survival and cooperates with c-myc to immortalize pre-B cells. *Nature* **335**, 440–442 (1988).

71. Buggins, A. G. S. & Pepper, C. J. The role of Bcl-2 family proteins in chronic lymphocytic leukaemia. *Leuk. Res.* **34**, 837–842 (2010).

72. Czabotar, P. E., Lessene, G., Strasser, A. & Adams, J. M. Control of apoptosis by the BCL-2 protein family: implications for physiology and therapy. *Nat. Rev. Mol. Cell Biol.* **15**, 49–63 (2014).

73. Youle, R. J. & Strasser, A. The BCL-2 protein family: Opposing activities that mediate cell death. *Nature Reviews. Molecular Cell Biology* **9**, 47–59 (2008).

74. Del Gaizo Moore, V. *et al.* Chronic lymphocytic leukemia requires BCL2 to sequester prodeath BIM, explaining sensitivity to BCL2 antagonist ABT-737. *J. Clin. Invest.* **117**, 112–121 (2007).

75. Hanada, M., Delia, D., Aiello, A., Stadtmauer, E. & Reed, J. C. Bcl-2 Gene Hypomethylation and High-Level Expression in B-Cell Chronic Lymphocytic Leukemia. *Blood* **82**, 1820–1828 (1993).

76. Kitada, S. *et al.* Expression of apoptosis-regulating proteins in chronic lymphocytic leukemia: correlations with In vitro and In vivo chemoresponses. *Blood* **91**, 3379–89 (1998).

77. Kienle, D. L. *et al.* Evidence for distinct pathomechanisms in genetic subgroups of chronic lymphocytic leukemia revealed by quantitative expression analysis of cell cycle, activation, and apoptosis-associated genes. *J. Clin. Oncol.* **23**, 3780–3792 (2005).

78. Johnston, J. B. *et al.* Role of myeloid cell factor-1 (Mcl-1) in chronic lymphocytic leukemia. *Leuk. Lymphoma* **45**, 2017–2027 (2004).

79. Robertson, L. E., Plunkett, W., McConnell, K., Keating, M. J. & McDonnell, T. J. Bcl-2 expression in chronic lymphocytic leukemia and its correlation with the induction of apoptosis and clinical outcome. *Leukemia* **10**, 456–9 (1996).

80. Saxena, A. *et al.* Mcl-1 and Bcl-2/Bax Ratio Are Associated with Treatment Response but Not with Rai Stage in B-Cell Chronic Lymphocytic Leukemia. *Am. J. Hematol.* **75**, 22–33 (2004).

81. Chonghaile, T. N. *et al.* Pretreatment Mitochondrial Priming Correlates with Clinical Response to Cytotoxic Chemotherapy. *Science (80-.).* **334**, 1129–1133 (20011).

82. Davids, M. S. *et al.* Decreased mitochondrial apoptotic priming underlies stroma-mediated treatment resistance in chronic lymphocytic leukemia. *Blood* **120**, 3501–3509 (2012).

83. Roberts, A. W. *et al.* Substantial susceptibility of chronic lymphocytic leukemia to BCL2 inhibition: results of a phase I study of navitoclax in patients with relapsed or refractory disease. *J. Clin. Oncol.* **30**, 488–496 (2012).

84. Souers, A. J. *et al.* ABT-199, a potent and selective BCL-2 inhibitor, achieves antitumor activity while sparing platelets. *Nat Med* **19**, 202–208 (2013).

85. Anderson, M. A. *et al.* The BCL2 selective inhibitor venetoclax induces rapid onset apoptosis of CLL cells in patients via a TP53 independent mechanism. *Blood* **127**, 3215–3224 (2016).

86. Roberts, A. W. *et al.* Targeting BCL2 with Venetoclax in Relapsed Chronic Lymphocytic Leukemia. *N. Engl. J. Med.* **374**, 311–322 (2016).

87. Anderson, M. A. *et al.* Clinicopathological features and outcomes of progression of CLL on the BCL2 inhibitor venetoclax. *Blood* **129**, 3362–3370 (2017).

88. Stilgenbauer, S. *et al.* Venetoclax in relapsed or refractory chronic lymphocytic leukaemia with 17p deletion: a multicentre, open-label, phase 2 study. *Lancet Oncol.* **17**, 768–778 (2016).

89. Song, T. *et al.* Bcl-2 phosphorylation confers resistance on chronic lymphocytic leukaemia cells to the BH3 mimetics ABT-737, ABT-263 and ABT-199 by impeding direct binding. *Br. J. Pharmacol.* **173**, 471–83 (2016).

90. Thijssen, R. *et al.* Resistance to ABT-199 induced by microenvironmental signals in chronic lymphocytic leukemia can be counteracted by CD20 antibodies or kinase inhibitors. *Haematologica* **100**, e302-6 (2015).

91. Fresquet, V., Rieger, M., Carolis, C., García-Barchino, M. J. & Martinez-Climent, J. A. Acquired mutations in BCL2 family proteins conferring resistance to the BH3 mimetic ABT-199 in lymphoma. *Blood* **123**, 4111–9 (2014).

92. Thompson, E. R. *et al.* Acquisition of the recurrent Gly101Val mutation in BCL2 confers resistance to venetoclax in patients with progressive chronic lymphocytic leukemia. *Cancer Discov.* **132**, CD-18-1119 (2018).

93. Blombery, P. *et al.* Acquisition of the recurrent Gly101Val mutation in BCL2 confers resistance to venetoclax in patients with progressive chronic lymphocytic leukemia. *Cancer Discov.* **9**, 342–353 (2019).

94. Birkinshaw, R. W. *et al.* Structures of BCL-2 in complex with venetoclax reveal the molecular basis of resistance mutations. *Nat. Commun.* **10**, (2019).

95. Schena, M. *et al.* The role of Bcl-2 in the pathogenesis of B chronic lymphocytic leukemia. *Leuk. Lymphoma* **11**, 173–9 (1993).

96. Rosenwald, A. *et al.* Relation of gene expression phenotype to immunoglobulin mutation genotype in B cell chronic lymphocytic leukemia. *J. Exp. Med.* **194**, 1639–1647 (2001).

97. Messmer, B. T. *et al.* In vivo measurements document the dynamic cellular kinetics of chronic lymphocytic leukemia B cells. *J. Clin. Invest.* **115**, 755–64 (2005).

98. Hamilton, E. *et al.* Mimicking the tumour microenvironment: three different co-culture systems induce a similar phenotype but distinct proliferative signals in primary chronic lymphocytic leukaemia cells. *Br. J. Haematol.* **158**, 589–99 (2012).

99. Purroy, N. *et al.* Co-culture of primary CLL cells with bone marrow mesenchymal cells, CD40 ligand and CpG ODN promotes proliferation of chemoresistant CLL cells phenotypically comparable to those proliferating in vivo. *Oncotarget* **6**, 7632–7643 (2014).

100. Schulz, A. *et al.* Inflammatory cytokines and signaling pathways are associated with survival of primary chronic lymphocytic leukemia cells in vitro: a dominant role of CCL2. *Haematologica* **96**, 408–416 (2011).

101. Trimarco, V. *et al.* Cross-talk between chronic lymphocytic leukemia (CLL) tumor B cells and mesenchymal stromal cells (MSCs): implications for neoplastic cell survival. *Oncotarget* **6**, 42130–42149 (2015).

102. Patel, V., Chen, L. S., Wierda, W. G., Balakrishnan, K. & Gandhi, V. Impact of bone marrow stromal cells on Bcl-2 family members in chronic lymphocytic leukemia. *Leuk. Lymphoma* **55**, 899–910 (2013).

103. Balakrishnan, K. *et al.* Regulation of Mcl-1 Expression in Context to Bone Marrow Stromal Microenvironment in Chronic Lymphocytic Leukemia. *Neoplasia* **16**, 1036–1046 (2014).

104. Herishanu, Y. *et al.* The lymph node microenvironment promotes B-cell receptor signaling, NF- B activation, and tumor proliferation in chronic lymphocytic leukemia. *Blood* **117**, 563–574 (2011).

105. Pascutti, M. F. *et al.* IL-21 and CD40L signals from autologous T cells can induce antigen-independent proliferation of CLL cells. *Blood* **122**, 3010–9 (2013).

106. Heinig, K. *et al.* Access to follicular dendritic cells is a pivotal step in murine chronic lymphocytic leukemia b-cell activation and proliferation. *Cancer Discov.* **4**, 1448–1465 (2014).

107. Ziegler-Heitbrock, L. *et al.* Nomenclature of monocytes and dendritic cells in blood. *Blood* **116**, e74-80 (2010).

108. Herishanu, Y. *et al.* Absolute monocyte count trichotomizes chronic lymphocytic leukemia into high risk patients with immune dysregulation, disease progression and poor survival. *Leuk. Res.* **37**, 1222–1228 (2013).

109. Friedman, D. R. *et al.* Relationship of blood monocytes with chronic lymphocytic leukemia aggressiveness and outcomes: A multi-institutional study. *Am. J. Hematol.* **91**, 687–691 (2016).

110. Mazumdar, R., Evans, P., Culpin, R., Bailey, J. & Allsup, D. The automated monocyte count is independently predictive of overall survival from diagnosis in chronic lymphocytic leukaemia and of survival following first-line chemotherapy. *Leuk. Res.* **37**, 614–618 (2013).

111. Lapuc, I. *et al.* Circulating classical CD14++CD16- monocytes predict shorter time to initial treatment in chronic lymphocytic leukemia patients: Differential effects of immune chemotherapy on monocyte-related membrane and soluble forms of CD163. *Oncol. Rep.* **34**, 1269–1278 (2015).

112. Maffei, R. *et al.* The monocytic population in chronic lymphocytic leukemia shows altered composition and deregulation of genes involved in phagocytosis and inflammation. *Haematologica* **98**, 1115–1123 (2013).

113. Bruns, H. *et al.* CLL-cell-mediated MDSC induction by exosomal miR-155 transfer is disrupted by vitamin D. *Leukemia* **31**, 985–988 (2017).

114. Jitschin, R. *et al.* CLL-cells induce IDOhi CD14+ HLA-DRlo myeloid derived suppressor cells that inhibit T-cell responses and promote TRegs. *Blood* **124**, 750–760 (2014).

115. Galletti, G. *et al.* Targeting Macrophages Sensitizes Chronic Lymphocytic Leukemia to Apoptosis and Inhibits Disease Progression. *Cell Rep.* **14**, 1748–1760 (2016).

116. Hanna, B. S. *et al.* Depletion of CLL-associated patrolling monocytes and macrophages controls disease development and repairs immune dysfunction in vivo. *Leukemia* **30**, 570–9 (2016).

117. Lefebvre, M.-L., Krause, S. W., Salcedo, M. & Nardin, A. Ex Vivo-activated Human Macrophages Kill Chronic Lymphocytic Leukemia Cells in the Presence of Rituximab: Mechanism of Antibody-dependent Cellular Cytotoxicity and Impact of Human Serum. *J. Immunother.* **29**, 388–397 (2006).

118. Buhtoiarov, I. N., Lum, H. D., Berke, G., Sondel, P. M. & Rakhmilevich, A. L.

Synergistic activation of macrophages via CD40 and TLR9 results in T cell independent antitumor effects. *J. Immunol.* **176**, 309–318 (2006).

119. Wu, Q.-L., Buhtoiarov, I. N., Sondel, P. M., Rakhmilevich, A. L. & Ranheim, E. A. Tumoricidal effects of activated macrophages in a mouse model of chronic lymphocytic leukemia. *J. Immunol.* **182**, 6771–6778 (2009).

120. De Veirman, K. *et al.* Myeloid-derived suppressor cells as therapeutic target in hematological malignancies. *Front. Oncol.* **4**, 349 (2014).

121. Bronte, V. *et al.* Recommendations for myeloid-derived suppressor cell nomenclature and characterization standards. *Nat. Commun.* **7**, 12150 (2016).

122. Liu, J., Zhou, Y., Huang, Q. & Qiu, L. CD14(+)HLA-DR(low/-) expression: A novel prognostic factor in chronic lymphocytic leukemia. *Oncol. Lett.* **9**, 1167–1172 (2015).

123. Gustafson, M. Association of an increased frequency of CD14 + HLA-DR lo / neg monocytes with decreased time to progression in chronic lymphocytic leukaemia (CLL). *Br. J. Hematol.* 674–676 (2012).

124. Maecker, H. T., McCoy, J. P. & Nussenblatt, R. Standardizing immunophenotyping for the Human Immunology Project. *Nat. Rev. Immunol.* **12**, 191–200 (2012).

125. Saulep-Easton, D. *et al.* Cytokine-driven loss of plasmacytoid dendritic cell function in chronic lymphocytic leukemia. *Leukemia* **28**, 2005–2015 (2014).

126. Orsini, E., Guarini, A., Chiaretti, S., Mauro, F. R. & Foa, R. The circulating dendritic cell compartment in patients with chronic lymphocytic leukemia is severely defective and unable to stimulate an effective T-cell response. *Cancer Res.* **63**, 4497–506 (2003).

127. Toniolo, P. A. *et al.* Deregulation of SOCS5 suppresses dendritic cell function in chronic lymphocytic leukemia. *Oncotarget* **7**, 46301–46314 (2016).

128. Messmer, D. *et al.* Dendritic cells from chronic lymphocytic leukemia patients are normal regardless of Ig V gene mutation status. *Mol. Med.* **10**, 96–103 (2004).

129. Rezvany, M. R. *et al.* Dendritic cells in patients with non-progressive B-chronic lymphocytic leukaemia have a normal functional capability but abnormal cytokine pattern. *Br. J. Haematol.* **115**, 263–271 (2001).

130. Vuillier, F. *et al.* Functional monocyte-derived dendritic cells can be generated in chronic lymphocytic leukaemia. *Br. J. Haematol.* **115**, 831–844 (2001).

131. Knudsen, J. H., Kjversgaard, E., Jensen, E. W. & Christensen, N. J. Percentage of NK-cells in peripheral blood in resting normal subjects is negatively correlated to plasma adrenaline. *Scand. J. Clin. Lab. Invest.* **54**, 221–225 (1994).

132. Pascal, V. *et al.* Comparative analysis of NK cell subset distribution in normal and

lymphoproliferative disease of granular lymphocyte conditions. *Eur. J. Immunol.* **34**, 2930–2940 (2004).

133. Vivier, E. *et al.* Innate Lymphoid Cells: 10 Years On. *Cell* **174**, 1054–1066 (2018).

134. Caligiuri, M. A. Human natural killer cells. *Blood* **112**, 461–469 (2008).

135. Pahl, J. & Cerwenka, A. Tricking the balance: NK cells in anti-cancer immunity. *Immunobiology* **222**, 11–20 (2017).

136. Watzl, C. & Long, E. O. Signal transduction during activation and inhibition of natural killer cells. *Curr. Protoc. Immunol.* **Chapter 11**, Unit 11.9B (2010).

137. Huergo-Zapico, L. *et al.* Expansion of NK cells and reduction of NKG2D expression in chronic lymphocytic leukemia. Correlation with progressive disease. *PLoS One* **9**, e108326 (2014).

138. MacFarlane, A. W. *et al.* NK cell dysfunction in chronic lymphocytic leukemia is associated with loss of the mature cells expressing inhibitory killer cell Ig-like receptors. *Oncoimmunology* **6**, e1330235 (2017).

139. Palmer, S. *et al.* Prognostic importance of T and NK-cells in a consecutive series of newly diagnosed patients with chronic lymphocytic leukaemia. *Br. J. Haematol.* **141**, 607–614 (2008).

140. Coles, S. J. *et al.* CD200 expression suppresses natural killer cell function and directly inhibits patient anti-tumor response in acute myeloid leukemia. *Leukemia* **25**, 792–799 (2011).

141. Attia, M. A., Nosair, N. A., Gawally, A., Elnagar, G. & Elshafey, E. M. HLA-G expression as a prognostic indicator in B-cell chronic lymphocytic leukemia. *Acta Haematol.* **132**, 53–58 (2014).

142. Maki, G. *et al.* NK resistance of tumor cells from multiple myeloma and chronic lymphocytic leukemia patients: Implication of HLA-G. *Leukemia* **22**, 998–1006 (2008).

143. Hilpert, J. *et al.* Comprehensive analysis of NKG2D ligand expression and release in leukemia: implications for NKG2D-mediated NK cell responses. *J. Immunol.* **189**, 1360–71 (2012).

144. de Weerdt, I. *et al.* Innate lymphoid cells are expanded and functionally altered in chronic lymphocytic leukemia. *Haematologica* **101**, e461–e464 (2016).

145. Ghia, P. *et al.* Chronic lymphocytic leukemia B cells are endowed with the capacity to attract CD4+, CD40L+ T cells by producing CCL22. *Eur. J. Immunol.* **32**, 1403–13 (2002).

146. Christopoulos, P. *et al.* Definition and characterization of the systemic T-cell dysregulation in untreated indolent B-cell lymphoma and very early CLL. *Blood*

117, 3836–3846 (2011).

147. Ramsay, A. G. *et al.* Chronic lymphocytic leukemia T cells show impaired immunological synapse formation that can be reversed with an immunomodulating drug. *J. Clin. Invest.* **118**, 2427–37 (2008).

148. Riches, J. C. *et al.* T cells from CLL patients exhibit features of T-cell exhaustion but retain capacity for cytokine production. *Blood* **121**, 1612–1621 (2013).

149. Nunes, C. *et al.* Expansion of a CD8+PD-1+ replicative senescence phenotype in early stage CLL patients is associated with inverted CD4:CD8 ratios and disease progression. *Clin. Cancer Res.* **18**, 678–687 (2012).

150. Muftuoglu, M. *et al.* Mass Cytometry Reveals Heterogeneity in the Exhaustion Profile of T-Cells in Chronic Lymphocytic Leukemia and the CD4:CD8 Ratio May be a Reliable Predictor of CD8+ T Cell Compartment. *Blood* **128**, (2016).

151. Os, A. *et al.* Chronic lymphocytic leukemia cells are activated and proliferate in response to specific T helper cells. *Cell Rep.* **4**, 566–77 (2013).

152. Patten, P. E. M. *et al.* CD38 expression in chronic lymphocytic leukemia is regulated by the tumor microenvironment. *Blood* **111**, 5173–5181 (2008).

153. Burgler, S. *et al.* Chronic Lymphocytic Leukemia Cells Express CD38 in Response to Th1 Cell-Derived IFNγ by a T-bet-Dependent Mechanism. *J. Immunol.* **194**, 827–835 (2015).

154. Mongini, P. K. A. *et al.* TLR-9 and IL-15 Synergy Promotes the In Vitro Clonal Expansion of Chronic Lymphocytic Leukemia B Cells. *J. Immunol.* **195**, 901–23 (2015).

155. Hock, B. D., Macpherson, S. A., Fernyhough, L. J. & McKenzie, J. L. Chronic lymphocytic leukaemia cells become both activated and immunosuppressive following interaction with CD3 and CD28 stimulated PBMC. *Leuk. Res.* **38**, 1217–1223 (2014).

156. Smallwood, D. T. *et al.* Extracellular vesicles released by CD40/IL-4-stimulated CLL cells confer altered functional properties to CD4+ T cells. *Blood* **128**, 542–52 (2016).

157. Brennan, P. J., Brigl, M. & Brenner, M. B. Invariant natural killer T cells: an innate activation scheme linked to diverse effector functions. *Nat. Rev. Immunol.* **13**, 101–117 (2013).

158. Kawano, T. *et al.* CD1d-Restricted and TCR-Mediated Activation of V14 NKT Cells by Glycosylceramides. *Science (80-.).* **278**, 1626–1629 (1997).

159. Fernandez, C. S., Cameron, G., Godfrey, D. I. & Kent, S. J. Ex-vivo α-Galactosylceramide activation of NKT cells in humans and macaques. *J. Immunol.*

Methods **382**, 150–159 (2012).

160. Gumperz, J. E., Miyake, S., Yamamura, T. & Brenner, M. B. Functionally distinct subsets of CD1d-restricted natural killer T cells revealed by CD1d tetramer staining. *J. Exp. Med.* **195**, 625–36 (2002).

161. Lee, P. T., Benlagha, K., Teyton, L. & Bendelac, A. Distinct functional lineages of human V(alpha)24 natural killer T cells. *J. Exp. Med.* **195**, 637–41 (2002).

162. Montoya, C. J. *et al.* Characterization of human invariant natural killer T subsets in health and disease using a novel invariant natural killer T cell-clonotypic monoclonal antibody, 6B11. *Immunology* **122**, 1–14 (2007).

163. Jing, Y. *et al.* Aging is associated with a rapid decline in frequency, alterations in subset composition, and enhanced Th2 response in CD1d-restricted NKT cells from human peripheral blood. *Exp. Gerontol.* **42**, 719–732 (2007).

164. Faunce, D. E., Palmer, J. L., Paskowicz, K. K., Witte, P. L. & Kovacs, E. J. CD1d-Restricted NKT Cells Contribute to the Age-Associated Decline of T Cell Immunity. *J. Immunol.* **175**, 3102–3109 (2005).

165. Gorini, F. *et al.* Invariant NKT cells contribute to chronic lymphocytic leukemia surveillance and prognosis. *Blood* **129**, blood-2016-11-751065 (2017).

166. Fais, F. *et al.* CD1d is expressed on B-chronic lymphocytic leukemia cells and mediates alpha-galactosylceramide presentation to natural killer T lymphocytes. *Int. J. Cancer* **109**, 402–411 (2004).

167. Jadidi-Niaragh, F. *et al.* Reduced frequency of NKT-like cells in patients with progressive chronic lymphocytic leukemia. *Med. Oncol.* **29**, 3561–3569 (2012).

168. Weinkove, R., Brooks, C. R., Carter, J. M., Hermans, I. F. & Ronchese, F. Functional invariant natural killer T-cell and CD1d axis in chronic lymphocytic leukemia: Implications for immunotherapy. *Haematologica* **98**, 376–384 (2013).

169. Zaborsky, N. *et al.* CD1d expression on chronic lymphocytic leukemia B cells affects disease progression and induces T cell skewing in CD8 positive and CD4CD8 double negative T cells. *Oncotarget* **7**, (2016).

170. Andreu-Ballester, J. C. *et al.* Values for αβ and γδ T-lymphocytes and CD4+, CD8+, and CD56+ subsets in healthy adult subjects: Assessment by age and gender. *Cytom. Part B Clin. Cytom.* **82B**, 238–244 (2012).

171. de Weerdt, I. *et al.* Improving CLL Vγ9Vδ2-T cell fitness for cellular therapy by ex vivo activation and ibrutinib. *Blood* **132**, 2260–2272 (2018).

172. Siegers, G. M. *et al.* Human Vδ1 γδ T cells expanded from peripheral blood exhibit specific cytotoxicity against B-cell chronic lymphocytic leukemia-derived cells. *Cytotherapy* **13**, 753–764 (2011).

173. Almeida, A. R. *et al.* Delta one T cells for immunotherapy of chronic lymphocytic leukemia: Clinical-grade expansion/differentiation and preclinical proof of concept. *Clin. Cancer Res.* **22**, 5795–5804 (2016).

174. Correia, D. V., Lopes, A. & Silva-Santos, B. Tumor cell recognition by γδ T lymphocytes: T-cell receptor vs. NK-cell receptors. *Oncoimmunology* **2**, (2013).

175. Poggi, A. *et al.* Vδ1 T lymphocytes from B-CLL patients recognize ULBP3 expressed on leukemic B cells and up-regulated by trans-retinoic acid. *Cancer Res.* **64**, 9172–9179 (2004).

176. Tokuyama, H. *et al.* Vγ9Vδ2 T cell cytotoxicity against tumor cells is enhanced by monoclonal antibody drugs - Rituximab and trastuzumab. *Int. J. Cancer* **122**, 2526–2534 (2008).

177. Akue, A. D., Lee, J.-Y. & Jameson, S. C. Derivation and Maintenance of Virtual Memory CD8 T Cells. *J. Immunol.* **188**, 2516–2523 (2012).

178. White, J. T. *et al.* Virtual memory T cells develop and mediate bystander protective immunity in an IL-15-dependent manner. *Nat. Commun.* **48**, 829–834 (2016).

179. Jacomet, F. *et al.* Evidence for eomesodermin-expressing innate-like CD8 $^{+}$ KIR/NKG2A $^{+}$ T cells in human adults and cord blood samples. *Eur. J. Immunol.* **45**, 1926–1933 (2015).

180. Cho, B. K., Rao, V. P., Ge, Q., Eisen, H. N. & Chen, J. Homeostasis-stimulated proliferation drives naive T cells to differentiate directly into memory T cells. *J. Exp. Med.* **192**, 549–56 (2000).

181. Sosinowski, T. *et al.* CD8α+ dendritic cell trans presentation of IL-15 to naive CD8+ T cells produces antigen-inexperienced T cells in the periphery with memory phenotype and function. *J. Immunol.* **190**, 1936–47 (2013).

182. Quinn, K. M. *et al.* Age-Related Decline in Primary CD8+T Cell Responses Is Associated with the Development of Senescence in Virtual Memory CD8+T Cells. *Cell Rep.* **23**, 3512–3524 (2018).

183. Ping, L. *et al.* The Bruton’s tyrosine kinase inhibitor ibrutinib exerts immunomodulatory effects through regulation of tumor-infiltrating macrophages. *Oncotarget* **8**, 39218–39229 (2017).

184. Borge, M. *et al.* Ibrutinib impairs the phagocytosis of rituximab-coated leukemic cells from chronic lymphocytic leukemia patients by human macrophages. *Haematologica* **100**, e140-2 (2015).

185. Fiorcari, S. *et al.* Ibrutinib modifies the function of monocyte/macrophage population in chronic lymphocytic leukemia. *Oncotarget* **7**, 65968–65981 (2016).

186. Colado, A. *et al.* Effect of the BTK inhibitor ibrutinib on macrophage- and γδ T cell-

mediated response against Mycobacterium tuberculosis. *Blood Cancer J.* **8**, 100 (2018).

187. Stiff, A. *et al.* Myeloid-derived suppressor cells express Bruton's tyrosine kinase and can be depleted in tumor bearing hosts by ibrutinib treatment. *Cancer Res.* **76**, 2125–36 (2016).

188. Natarajan, G. *et al.* Ibrutinib enhances IL-17 response by modulating the function of bone marrow derived dendritic cells. *Oncoimmunology* **5**, e1057385 (2016).

189. Kawakami, Y. *et al.* Regulation of dendritic cell maturation and function by Bruton's tyrosine kinase via IL-10 and Stat3. *Proc. Natl. Acad. Sci. U. S. A.* **103**, 153–8 (2006).

190. King, P. D. *et al.* CD2 signaling in T cells involves tyrosine phosphorylation and activation of the Tec family kinase, EMT/ITK/TSK. *Int. Immunol.* **8**, 1707–1714 (1996).

191. Takesono, A., Horai, R., Mandai, M., Dombroski, D. & Schwartzberg, P. L. Requirement for Tec Kinases in Chemokine-Induced Migration and Activation of Cdc42 and Rac. *Curr. Biol.* **14**, 917–922 (2004).

192. Khurana, D. *et al.* Differential Regulation of Human NK Cell-Mediated Cytotoxicity by the Tyrosine Kinase Itk. *J. Immunol.* **178**, 3575–3582 (2007).

193. Wilcox, H. M. & Berg, L. J. Itk phosphorylation sites are required for functional activity in primary T cells. *J. Biol. Chem.* **278**, 37112–21 (2003).

194. Heyeck, S. D., Wilcox, H. M., Bunnell, S. C. & Berg, L. J. Lck phosphorylates the activation loop tyrosine of the Itk kinase domain and activates Itk kinase activity. *J. Biol. Chem.* **272**, 25401–8 (1997).

195. Liu, K. Q., Bunnell, S. C., Gurniak, C. B. & Berg, L. J. T cell receptor-initiated calcium release is uncoupled from capacitative calcium entry in Itk-deficient T cells. *J. Exp. Med.* **187**, 1721–7 (1998).

196. Liao, X. C. *et al.* Itk negatively regulates induction of T cell proliferation by CD28 costimulation. *J. Exp. Med.* **186**, 221–8 (1997).

197. Labno, C. M. *et al.* Itk functions to control actin polymerization at the immune synapse through localized activation of Cdc42 and WASP. *Curr. Biol.* **13**, 1619–24 (2003).

198. Schaeffer, E. M. *et al.* Requirement for Tec Kinases Rlk and Itk in T Cell Receptor Signaling and Immunity. *Science (80-.).* **284**, 638–641 (1999).

199. Zhu, J., Yamane, H. & Paul, W. E. Differentiation of effector CD4 T cell populations. *Annu. Rev. Immunol.* **28**, 445–89 (2010).

200. Fowell, D. J. *et al.* Impaired NFATc Translocation and Failure of Th2 Development in Itk-Deficient CD4+ T Cells. *Immunity* **11**, 399–409 (1999).

201. Schaeffer, E. M. *et al.* Mutation of Tec family kinases alters T helper cell differentiation. *Nat. Immunol.* **2**, 1183–1188 (2001).

202. Mueller, C. & August, A. Attenuation of immunological symptoms of allergic asthma in mice lacking the tyrosine kinase ITK. *J. Immunol.* **170**, 5056–63 (2003).

203. Miller, A. T., Wilcox, H. M., Lai, Z. & Berg, L. J. Signaling through Itk Promotes T Helper 2 Differentiation via Negative Regulation of T-bet. *Immunity* **21**, 67–80 (2004).

204. Hu, Q. *et al.* Identification of Rlk, a novel protein tyrosine kinase with predominant expression in the T cell lineage. *J. Biol. Chem.* **270**, 1928–34 (1995).

205. Sahu, N. *et al.* Selective expression rather than specific function of Txk and Itk regulate Th1 and Th2 responses. *J. Immunol.* **181**, 6125–31 (2008).

206. Sommers, C. L. *et al.* A role for the Tec family tyrosine kinase Txk in T cell activation and thymocyte selection. *J. Exp. Med.* **190**, 1427–1438 (1999).

207. Kashiwakura, J. *et al.* Txk, a nonreceptor tyrosine kinase of the Tec family, is expressed in T helper type 1 cells and regulates interferon gamma production in human T lymphocytes. *J. Exp. Med.* **190**, 1147–1154 (1999).

208. Takeba, Y., Nagafuchi, H., Takeno, M., Kashiwakura, J. & Suzuki, N. Txk, a member of a nonreceptor tyrosine kinase of Tec famile, acts as a Th2 cell-specific transcription factor and regualtes IFNγ gene transcription. *J. Immunol.* **168**, 2365–2370 (2002).

209. Au-Yeung, B. B., Katzman, S. D. & Fowell, D. J. Cutting edge: Itk-dependent signals required for CD4+ T cells to exert, but not gain, Th2 effector function. *J. Immunol.* **176**, 3895–9 (2006).

210. Hwang, E. S., Szabo, S. J., Schwartzberg, P. L. & Glimcher, L. H. T helper cell fate specified by kinase-mediated interaction of T-bet with GATA-3. *Science (80-.).* **307**, 430–433 (2005).

211. Gomez-Rodriguez, J. *et al.* Itk-mediated integration of T cell receptor and cytokine signaling regulates the balance between Th17 and regulatory T cells. *J. Exp. Med.* **211**, 529–543 (2014).

212. Mamontov, P. *et al.* A negative role for the interleukin-2-inducible T-cell kinase (ITK) in human Foxp3+ Treg differentiation. *Unpubl. - not peer Rev.* 386508 (2018). doi:10.1101/386508

213. Gomez-Rodriguez, J. *et al.* Differential Expression of Interleukin-17A and -17F Is Coupled to T Cell Receptor Signaling via Inducible T Cell Kinase. *Immunity* **31**, 587–597 (2009).

214. Schwartzberg, P. L., Finkelstein, L. D. & Readinger, J. A. TEC-family kinases:

Regulators of T-helper-cell differentiation. *Nat. Rev. Immunol.* **5**, 284–295 (2005).

215. Ellmeier, W. *et al.* Severe B Cell Deficiency in Mice Lacking the Tec Kinase Family Members Tec and Btk. *J. Exp. Med* **121300**, 1611–1623 (2000).

216. Yang, W.-C., Ching, K. A., Tsoukas, C. D. & Berg, L. J. Tec Kinase Signaling in T cells is regulated by Phosphatidylinositol 3-Kinase and the Tec Pleckstrin Homology Domain. *J. Immunol.* **166**, 387–395 (2001).

217. Tomlinson, M. G. *et al.* Expression and Function of Tec, Itk, and Btk in Lymphocytes: Evidence for a Unique Role for Tec. *Mol. Cell. Biol.* **24**, 2455–2466 (2004).

218. Dubovsky, J. A. *et al.* Ibrutinib is an irreversible molecular inhibitor of ITK driving a Th1-selective pressure in T lymphocytes. *Blood* **122**, 2539–49 (2013).

219. Kaptein, A. Potency and Selectivity of BTK Inhibitors in Clinical Development for B-Cell Malignancies. *Blood* **132**, 1871–1871 (2018).

220. Kumar, A. *et al.* Pilot trial of ibrutinib in patients with relapsed or refractory T-cell lymphoma. *Blood Adv.* **2**, 871–876 (2018).

221. Cubillos-Zapata, C. *et al.* Ibrutinib as an antitumor immunomodulator in patients with refractory chronic lymphocytic leukemia. *Oncoimmunology* **5**, (2016).

222. Long, M. *et al.* Ibrutinib treatment improves T cell number and function in CLL patients. *J. Clin. Invest.* **127**, 3052–3064 (2017).

223. Niemann, C. U. *et al.* Disruption of in vivo chronic lymphocytic leukemia tumor-microenvironment interactions by ibrutinib - Findings from an investigator-initiated phase II study. *Clin. Cancer Res.* **22**, 1078-0432.CCR-15-1965- (2016).

224. Atherly, L. O., Brehm, M. A., Welsh, R. M. & Berg, L. J. Tec Kinases Itk and Rlk Are Required for CD8+ T Cell Responses to Virus Infection Independent of Their Role in CD4+ T Cell Help. *J. Immunol.* **176**, 1571–1581 (2006).

225. Kapnick, S. M., Stinchcombe, J. C., Griffiths, G. M. & Schwartzberg, P. L. Inducible T Cell Kinase Regulates the Acquisition of Cytolytic Capacity and Degranulation in CD8+ CTLs. *J. Immunol.* **198**, 2699–2711 (2017).

226. Hu, J. & August, A. Naive and innate memory phenotype CD4+ T cells have different requirements for active Itk for their development. *J. Immunol.* **180**, 6544–52 (2008).

227. Nayar, R. *et al.* TCR signaling via Tec kinase ITK and interferon regulatory factor 4 (IRF4) regulates CD8+ T-cell differentiation. *Proc. Natl. Acad. Sci.* **109**, E2794–E2802 (2012).

228. Atherly, L. O. *et al.* The Tec Family Tyrosine Kinases Itk and Rlk Regulate the Development of Conventional CD8+ T Cells. *Immunity* **25**, 79–91 (2006).

229. Dubois, S., Waldmann, T. A. & Müller, J. R. ITK and IL-15 support two distinct subsets of CD8+ T cells. *Proc. Natl. Acad. Sci. U. S. A.* **103**, 12075–80 (2006).

230. Yin, C. C. *et al.* The Tec kinase ITK regulates thymic expansion, emigration, and maturation of γδ NKT cells. *J. Immunol.* **190**, 2659–69 (2013).

231. Felices, M. & Berg, L. J. The Tec kinases Itk and Rlk regulate NKT cell maturation, cytokine production, and survival. *J. Immunol.* **180**, 3007–18 (2008).

232. Gadue, P. & Stein, P. L. NK T Cell Precursors Exhibit Differential Cytokine Regulation and Require Itk for Efficient Maturation. *J. Immunol.* **169**, 2397–2406 (2014).

233. Kondo, K. *et al.* Ibrutinib modulates the immunosuppressive CLL microenvironment through STAT3-mediated suppression of regulatory B cell function and inhibition of the PD-1/PD-L1 pathway. *Leukemia* 1–11 (2017). doi:10.1038/leu.2017.304

234. Papazoglou, D. *et al.* Ibrutinib-Based Therapy Improves Anti-Tumor T Cell Killing Function Allowing Effective Pairing with Anti-PD-L1 Immunotherapy Compared to Traditional FCR Chemoimmunotherapy; Implications for Therapy and Correlative Immune Functional Data from the Phase III E1912 Trial. *Blood* **132**, 236–236 (2018).

235. Kohrt, H. E. *et al.* Ibrutinib antagonizes rituximab-dependent NK cell-mediated cytotoxicity. *Blood* **123**, 1957–60 (2014).

236. Da Roit, F. *et al.* Ibrutinib interferes with the cell-mediated anti-tumor activities of therapeutic CD20 antibodies: Implications for combination therapy. *Haematologica* **100**, 77–86 (2015).

237. Rajasekaran, N. *et al.* Three BTK-Specific Inhibitors, in Contrast to Ibrutinib, Do Not Antagonize Rituximab-Dependent NK-Cell Mediated Cytotoxicity. *Blood* **124**, 3118 (2014).

238. Ryan, C. E. *et al.* Ibrutinib efficacy and tolerability in patients with relapsed chronic lymphocytic leukemia following allogeneic HCT. *Blood* **128**, 2899–2908 (2016).

239. Miklos, D. *et al.* Ibrutinib for chronic graft-versus-host disease after failure of prior therapy. *Blood* **130**, blood-2017-07-793786 (2017).

240. Chang, B. Y. *et al.* The Bruton tyrosine kinase inhibitor PCI-32765 ameliorates autoimmune arthritis by inhibition of multiple effector cells. *Arthritis Res. Ther.* **13**, R115 (2011).

241. Veis, D. J., Sentman, C. L., Bach, E. A. & Korsmeyer, S. J. Expression of the Bcl-2 protein in murine and human thymocytes and in peripheral T lymphocytes. *J. Immunol.* **151**, 2546–54 (1993).

242. Gratiot-Deans, J., Ding, L., Turka, L. A. & Nuñez, G. bcl-2 proto-oncogene

expression during human T cell development. Evidence for biphasic regulation. *J. Immunol.* **151**, 83–91 (1993).

243. Wojciechowski, S. *et al.* Bim/Bcl-2 balance is critical for maintaining naive and memory T cell homeostasis. *J. Exp. Med.* **204**, 1665–75 (2007).

244. Duraiswamy, J. *et al.* Phenotype, function, and gene expression profiles of programmed death-1(hi) CD8 T cells in healthy human adults. *J. Immunol.* **186**, 4200–12 (2011).

245. Hildeman, D. A. *et al.* Activated T Cell Death In Vivo Mediated by Proapoptotic Bcl-2 Family Member Bim. *Immunity* **16**, 759–767 (2002).

246. Kurtulus, S. S. *et al.* Bcl-2 Allows Effector and Memory CD8+ T Cells To Tolerate Higher Expression of Bim. *J. Immunol.* **168**, 5729–5737 (2011).

247. Khaw, S. L. *et al.* Both leukaemic and normal peripheral B lymphoid cells are highly sensitive to the selective pharmacological inhibition of prosurvival Bcl-2 with ABT-199. *Leukemia* **28**, 1207–1215 (2014).

248. Carrington, E. M. *et al.* Anti-apoptotic proteins BCL-2, MCL-1 and A1 summate collectively to maintain survival of immune cell populations both in vitro and in vivo. *Cell Death Differ.* **24**, 878–888 (2017).

249. Viant, C. *et al.* Cell cycle progression dictates the requirement for BCL2 in natural killer cell survival. *J. Exp. Med.* 1–20 (2017). doi:10.1084/jem.20160869

250. Carrington, E. M. *et al.* Prosurvival Bcl-2 family members reveal a distinct apoptotic identity between conventional and plasmacytoid dendritic cells. *Proc. Natl. Acad. Sci. U. S. A.* **112**, 4044–4049 (2015).

251. Krämer, I. *et al.* Allogeneic hematopoietic cell transplantation for high-risk CLL: 10-year follow-up of the GCLLSG CLL3X trial. *Blood* **130**, 1477–1480 (2017).

252. Dreger, P. *et al.* Indications for allogeneic stem cell transplantation in chronic lymphocytic leukemia: the EBMT transplant consensus. *Leukemia* **21**, 12–7 (2007).

253. Dall'Ozzo, S. *et al.* Rituximab-dependent cytotoxicity by natural killer cells: Influence of FCGR3A polymorphism on the concentration-effect relationship. *Cancer Res.* **64**, 4664–4669 (2004).

254. Weiner, G. J. Rituximab: mechanism of action. *Semin. Hematol.* **47**, 115–23 (2010).

255. Ramsay, A. G., Clear, A. J., Fatah, R. & Gribben, J. G. Multiple inhibitory ligands induce impaired T-cell immunologic synapse function in chronic lymphocytic leukemia that can be blocked with lenalidomide: establishing a reversible immune evasion mechanism in human cancer. *Blood* **120**, 1412–1421 (2012).

256. Kamata, T. *et al.* Blockade of programmed death-1/programmed death ligand pathway enhances the antitumor immunity of human invariant natural killer T

cells. *Cancer Immunol. Immunother.* **65**, 1477–1489 (2016).

257. McClanahan, F. *et al.* PD-L1 checkpoint blockade prevents immune dysfunction and leukemia development in a mouse model of chronic lymphocytic leukemia. *Blood* **126**, 203–211 (2015).

258. Gassner, F. J. *et al.* Chronic lymphocytic leukaemia induces an exhausted T cell phenotype in the TCL1 transgenic mouse model. *Br. J. Haematol.* **170**, 515–22 (2015).

259. Chanan-Khan, A. *et al.* Clinical efficacy of lenalidomide in patients with relapsed or refractory chronic lymphocytic leukemia: Results of a phase II study. *J. Clin. Oncol.* **24**, 5343–5349 (2006).

260. Andritsos, L. A. *et al.* Higher doses of lenalidomide are associated with unacceptable toxicity including life-threatening tumor flare in patients with chronic lymphocytic leukemia. *J Clin Oncol* **26**, 2519–2525 (2008).

261. Ferrajoli, A. *et al.* Lenalidomide induces complete and partial remissions in patients with relapsed and refractory chronic lymphocytic leukemia. *Blood* **111**, 5291–5297 (2008).

262. Vitale, C. *et al.* Ofatumumab and Lenalidomide for Patients with Relapsed or Refractory Chronic Lymphocytic Leukemia: Correlation Between Responses and Immune Characteristics. *Clin. Cancer Res.* **22**, 2359–67 (2016).

263. Tam, C. S. & Polliack, A. Defining the appropriate starting dose of lenalidomide in chronic lymphocytic leukemia: remember the old fable of the hare and the tortoise. *Leuk. Lymphoma* **57**, 1247–8 (2016).

264. Wobus, M. *et al.* Impact of lenalidomide on the functional properties of human mesenchymal stromal cells. *Exp. Hematol.* **40**, 867–876 (2012).

265. De Luisi, A. *et al.* Lenalidomide restrains motility and overangiogenic potential of bone marrow endothelial cells in patients with active multiple myeloma. *Clin. Cancer Res.* **17**, 1935–1946 (2011).

266. Acebes-Huerta, A. *et al.* Lenalidomide induces immunomodulation in chronic lymphocytic leukemia and enhances antitumor immune responses mediated by NK and CD4 T cells. *Biomed Res. Int.* **2014**, 265840 (2014).

267. Riches, J. C. *et al.* NK Cells From CLL Patients Exhibit Down-Regulation Of Interferon Response Genes That Can Be Reversed With Lenalidomide. *Blood* **122**, 4131 (2013).

268. Gassner, F. J. *et al.* Chemotherapy-induced augmentation of T cells expressing inhibitory receptors is reversed by treatment with lenalidomide in chronic lymphocytic leukemia. *Haematologica* **99**, 67–9 (2014).

269. Chang, D. H. *et al.* Enhancement of ligand-dependent activation of human natural killer T cells by lenalidomide: therapeutic implications. *Blood* **108**, 618–621 (2006).

270. Fiorcari, S. *et al.* Lenalidomide interferes with tumor-promoting properties of nurse-like cells in chronic lymphocytic leukemia. *Haematologica* **100**, 253–62 (2015).

271. Lee, B. N. *et al.* Treatment with lenalidomide modulates T-cell immunophenotype and cytokine production in patients with chronic lymphocytic leukemia. *Cancer* **117**, 3999–4008 (2011).

272. Ito, T. *et al.* Identification of a primary target of thalidomide teratogenicity. *Science (80-.).* **327**, 1345–50 (2010).

273. Gandhi, A. K. *et al.* Immunomodulatory agents lenalidomide and pomalidomide co-stimulate T cells by inducing degradation of T cell repressors Ikaros and Aiolos via modulation of the E3 ubiquitin ligase complex CRL4(CRBN.). *Br. J. Haematol.* **164**, 811–21 (2014).

274. Morgan, B. *et al.* Aiolos, a lymphoid restricted transcription factor that interacts with Ikaros to regulate lymphocyte differentiatisn. *EMBO J.* **16**, 2004–2013 (1997).

275. Fecteau, J.-F. *et al.* Lenalidomide inhibits the proliferation of CLL cells via a cereblon/p21(WAF1/Cip1)-dependent mechanism independent of functional p53. *Blood* **124**, 1637–44 (2014).

276. Chanan-Khan, A. A. *et al.* Biological effects and clinical significance of lenalidomide-induced tumour flare reaction in patients with chronic lymphocytic leukaemia: In vivo evidence of immune activation and antitumour response. *Br. J. Haematol.* **155**, 457–467 (2011).

277. Lapalombella, R. *et al.* Lenalidomide treatment promotes CD154 expression on CLL cells and enhances production of antibodies by normal B cells through a PI3-kinase-dependent pathway. *Blood* **115**, 2619–29 (2010).

278. Winqvist, M. *et al.* Phase I-II study of lenalidomide and alemtuzumab in refractory chronic lymphocytic leukemia (CLL): effects on T cells and immune checkpoints. *Cancer Immunol. Immunother.* **66**, 1–12 (2016).

279. Görgün, G. *et al.* Lenalidomide Enhances Immune Checkpoint Blockade-Induced Immune Response in Multiple Myeloma. *Clin. cancer Res.* (2015). doi:10.1158/1078-0432.CCR-15-0200

280. Kalos, M. *et al.* T Cells with Chimeric Antigen Receptors Have Potent Antitumor Effects and Can Establish Memory in Patients with Advanced Leukemia. *Sci. Transl. Med.* **3**, 95ra73-95ra73 (2011).

281. Turtle, C. J. *et al.* Durable molecular remissions in chronic lymphocytic leukemia treated with CD19-Specific chimeric antigen Receptor-modified T cells after failure

of ibrutinib. *J. Clin. Oncol.* **35**, 3010–3020 (2017).

282. Kochenderfer, J. N. *et al.* Donor-derived CD19-targeted T cells cause regression of malignancy persisting after allogeneic hematopoietic stem cell transplantation. *Blood* **122**, 4129–4139 (2013).

283. van Bruggen, J. A. C. *et al.* Chronic lymphocytic leukemia cells impair mitochondrial fitness in CD8+ T cells and impede CAR T-cell efficacy. *Blood* **134**, 44–58 (2019).

284. Hoffmann, J.-M. *et al.* Differences in Expansion Potential of Naive Chimeric Antigen Receptor T Cells from Healthy Donors and Untreated Chronic Lymphocytic Leukemia Patients. *Front. Immunol.* **8**, 1956 (2018).

285. Gauthier, J. *et al.* Comparison of Efficacy and Toxicity of CD19-Specific Chimeric Antigen Receptor T-Cells Alone or in Combination with Ibrutinib for Relapsed and/or Refractory CLL. *Blood* **132**, 299–299 (2018).

286. Fraietta, J. A. *et al.* Ibrutinib enhances chimeric antigen receptor T-cell engraftment and efficacy in leukemia. *Blood* **127**, 1117–1127 (2016).

287. Oppermann, S. *et al.* High-content screening identifies kinase inhibitors that overcome venetoclax resistance in activated CLL cells. *Blood* **128**, 934–947 (2016).

288. Bojarczuk, K. *et al.* BCR signaling inhibitors differ in their ability to overcome Mcl-1-mediated resistance of CLL B cells to ABT-199. *Blood* **127**, 3192–3201 (2016).

289. Cervantes-Gomez, F. *et al.* Pharmacological and protein profiling suggests venetoclax (ABT-199) as optimal partner with ibrutinib in chronic lymphocytic leukemia. *Clin. Cancer Res.* **21**, 3705–3715 (2015).

290. Deng, J. *et al.* Bruton's tyrosine kinase inhibition increases BCL-2 dependence and enhances sensitivity to venetoclax in chronic lymphocytic leukemia. *Leukemia* **31**, 2075–2084 (2017).

291. Tam, C. S. *et al.* Ibrutinib plus Venetoclax for the Treatment of Mantle-Cell Lymphoma. *N. Engl. J. Med.* **378**, 1211–1223 (2018).

292. Rogers, K. A. *et al.* Phase 1b study of obinutuzumab, ibrutinib, and venetoclax in relapsed and refractory chronic lymphocytic leukemia. *Blood* 1–16 (2018). doi:10.1182/blood-2018-05-853564

293. Burger, J. A. *et al.* Randomized Trial of Ibrutinib Versus Ibrutinib Plus Rituximab (Ib+R) in Patients with Chronic Lymphocytic Leukemia (CLL). *Blood* **130**, (2017).

294. Woyach, J. A. *et al.* Ibrutinib Regimens versus Chemoimmunotherapy in Older Patients with Untreated CLL. *N. Engl. J. Med.* **379**, 2517–2528 (2018).

295. Seymour, J. F. *et al.* Venetoclax–Rituximab in Relapsed or Refractory Chronic Lymphocytic Leukemia. *N. Engl. J. Med.* **378**, 1107–1120 (2018).

296. Fischer, K. *et al.* Venetoclax and obinutuzumab in chronic lymphocytic leukemia. *Blood* **129**, blood-2017-01-761973 (2017).

297. Pollyea, D. A. *et al.* A Dose Escalation Study of Ibrutinib with Lenalidomide for Relapsed and Refractory Chronic Lymphocytic Leukemia/Small Lymphocytic Lymphoma. in *Blood* **124**, (2014).

298. Ujjani, C. *et al.* A phase 1 study of lenalidomide and ibrutinib in combination with rituximab in relapsed and refractory CLL. *Blood Adv.* **2**, 762–768 (2018).

299. Nastoupil, L. J. *et al.* Safety and Efficacy of Ibrutinib in Combination with Rituximab and Lenalidomide in Previously Untreated Subjects with Follicular and Marginal Zone Lymphoma: An Open Label, Phase II Study. *Blood* **132**, 447–447 (2018).

300. Sagiv-Barfi, I. *et al.* Therapeutic antitumor immunity by checkpoint blockade is enhanced by ibrutinib, an inhibitor of both BTK and ITK. *Proc. Natl. Acad. Sci.* **112**, E966–E972 (2015).

301. Younes, A. *et al.* Safety and activity of ibrutinib in combination with nivolumab in patients with relapsed non-Hodgkin lymphoma or chronic lymphocytic leukaemia: a phase 1/2a study. *Lancet Haematol.* **6**, e67–e78 (2019).

302. Ding, W. *et al.* Pembrolizumab in patients with CLL and Richter transformation or with relapsed CLL. *Blood* **129**, 3419–3427 (2017).

303. Jain, N. *et al.* A Phase II Trial of Nivolumab Combined with Ibrutinib for Patients with Richter Transformation. *Blood* **132**, 296–296 (2018).

304. Ding, W. *et al.* PD-1 blockade with pembrolizumab (MK-3475) in relapsed/refractory CLL including Richter Transformation: an early efficacy report from a phase 2 trial (MC1485) [abstract]. *Blood* **126**, Abstract 834 (2015).

305. Ruella, M. *et al.* The addition of the btk inhibitor ibrutinib to anti-cd19 chimeric antigen receptor T Cells (CART19) improves responses against mantle cell lymphoma. *Clin. Cancer Res.* **22**, 2684–2696 (2016).

306. Gill, S. *et al.* CD19 CAR-T cells combined with ibrutinib to induce complete remission in CLL. *J. Clin. Oncol.* **35**, abstract 7509 (2017).

307. Keating, M. J. *et al.* Early results of a chemoimmunotherapy regimen of fludarabine, cyclophosphamide, and rituximab as initial therapy for chronic lymphocytic leukemia. *J. Clin. Oncol.* **23**, 4079–4088 (2005).

308. Kondo, K. *et al.* Ibrutinib Can Modulate the T Cell Response in Chronic Lymphocytic Leukemia By Reducing PD1/PDL1 Interactions. *Blood* **126**, 1737 (2015).

309. Yin, Q. *et al.* Ibrutinib Therapy Increases T Cell Repertoire Diversity in Patients with Chronic Lymphocytic Leukemia. *J. Immunol.* **198**, 1740–1747 (2017).

310. Ren, L. *et al.* Analysis of the effects of the Bruton's tyrosine kinase (Btk) inhibitor

ibrutinib on monocyte Fcγ receptor (FcγR) function. *J. Biol. Chem.* **291**, 3043–3052 (2016).

311. de Weerdt, I. *et al.* First Evidence of Restoration of T and NK Cell Compartment after Venetoclax Treatment. *Blood* **132**, 1860–1860 (2018).

312. Podhorecka, M. *et al.* Changes in T-cell subpopulations and cytokine network during early period of ibrutinib therapy in chronic lymphocytic leukemia patients: the significant decrease in T regulatory cells number. *Oncotarget* **8**, 34661–34669 (2017).

313. Fischer, A. M., Mercer, J. C., Iyer, A., Ragin, M. J. & August, A. Regulation of CXC chemokine receptor 4-mediated migration by the Tec family tyrosine kinase ITK. *J. Biol. Chem.* **279**, 29816–29820 (2004).

314. Williams, A. M. *et al.* Analysis of the risk of infection in patients with chronic lymphocytic leukemia in the era of novel therapies. *Leuk. Lymphoma* **0**, 1–8 (2017).

315. Grützner, E. *et al.* Kinetics of human myeloid-derived suppressor cells after blood draw. *J. Transl. Med.* **14**, 2 (2016).

316. Kotsakis, A. *et al.* Myeloid-derived suppressor cell measurements in fresh and cryopreserved blood samples. *J. Immunol. Methods* **381**, 14–22 (2012).

317. Damuzzo, V. *et al.* Complexity and challenges in defining myeloid-derived suppressor cells. *Cytometry Part B - Clinical Cytometry* **88**, 77–91 (2015).

318. Gustafson, M. P. *et al.* A method for identification and analysis of non-overlapping myeloid immunophenotypes in humans. *PLoS One* **10**, 1–20 (2015).

319. Kocher, T. *et al.* CD4+ T cells, but not non-classical monocytes, are dispensable for the development of chronic lymphocytic leukemia in the TCL1-tg murine model. *Leukemia* **30**, 1–14 (2015).

320. Drobek, A. *et al.* Strong homeostatic TCR signals induce formation of self-tolerant virtual memory CD8 T cells. *EMBO J.* **37**, e98518 (2018).

321. Murali-Krishna, K. & Ahmed, R. Cutting Edge: Naive T Cells Masquerading as Memory Cells. *J. Immunol.* **165**, 1733–1737 (2000).

322. Cipriani, P. *et al.* Resistance to apoptosis in circulating alpha/beta and gamma/delta T lymphocytes from patients with systemic sclerosis. *J Rheumatol* **33**, 2003–2014 (2006).

323. Braza, M. S., Klein, B., Fiol, G. & Rossi, J. F. γδT-cell killing of primary follicular lymphoma cells is dramatically potentiated by GA101, a type II glycoengineered anti-CD20 monoclonal antibody. *Haematologica* **96**, 400–407 (2011).

324. Coscia, M. *et al.* Dysfunctional V 9V 2 T cells are negative prognosticators and markers of dysregulated mevalonate pathway activity in chronic lymphocytic

leukemia cells. *Blood* **120**, 3271–3279 (2012).

325. Ruella, M. *et al.* Kinase Inhibitor Ibrutinib Prevents Cytokine-Release Syndrome after Anti-CD19 Chimeric Antigen Receptor T Cells (CART) for B Cell Neoplasms. *Blood* **128**, (2016).

326. Velez Lujan, J. *et al.* Ibrutinib reduces obinutuzumab infusion related reactions in patients with chronic lymphocytic leukemia and is associated with changes in plasma cytokine levels. *Haematologica* haematol.2018.212597 (2019). doi:10.3324/haematol.2018.212597

327. Zapf, C. W. *et al.* Covalent Inhibitors of Interleukin-2 Inducible T Cell Kinase (Itk) with Nanomolar Potency in a Whole-Blood Assay. *J. Med. Chem.* **55**, 10047–10063 (2012).

328. Hassenrück, F. *et al.* Sensitive Detection of the Natural Killer Cell-Mediated Cytotoxicity of Anti-CD20 Antibodies and Its Impairment by B-Cell Receptor Pathway Inhibitors. *Biomed Res. Int.* **2018**, (2018).

329. Golay, J., Ubiali, G. & Introna, M. The specific Bruton tyrosine kinase inhibitor acalabrutinib (ACP-196) shows favorable in vitro activity against chronic lymphocytic leukemia B cells with CD20 antibodies . *Haematologica* **102**, e400–e403 (2017).

330. Andreotti, A. H., Schwartzberg, P. L., Joseph, R. E. & Berg, L. J. T-cell signaling regulated by the Tec family kinase, Itk. *Cold Spring Harb. Perspect. Biol.* **2**, (2010).

331. Prince, A. L., Yin, C. C., Enos, M. E., Felices, M. & Berg, L. J. The Tec kinases Itk and Rlk regulate conventional versus innate T-cell development. *Immunol. Rev.* **228**, 115–31 (2009).

332. Dvorsky, R. *et al.* Loss-of-function mutations within the IL-2 inducible kinase ITK in patients with EBV-associated lymphoproliferative diseases. *Leukemia* **26**, 963–971 (2012).

333. Linka, R. M. *et al.* IL-2-inducible T-cell kinase deficiency: clinical presentation and therapeutic approach. *Haematologica* **96**, 472–476 (2010).

334. Ghosh, S., Bienemann, K., Boztug, K. & Borkhardt, A. Interleukin-2-inducible T-cell kinase (ITK) deficiency - clinical and molecular aspects. *J. Clin. Immunol.* **34**, 892–9 (2014).

335. Gratiot-Deans, J., Merino, R., Nuñez, G. & Turka, L. A. Bcl-2 expression during T-cell development: early loss and late return occur at specific stages of commitment to differentiation and survival. *Proc. Natl. Acad. Sci. U. S. A.* **91**, 10685–9 (1994).

336. Dubovsky, J. A. *et al.* Ibrutinib treatment ameliorates murine chronic graft-versus-host disease. *J. Clin. Invest.* **124**, 4867–4876 (2014).

337. Crawford, A. & Wherry, E. J. The diversity of costimulatory and inhibitory receptor pathways and the regulation of antiviral T cell responses. *Curr. Opin. Immunol.* **21**, 179–186 (2009).

338. Nielsen, C. M., White, M. J., Goodier, M. R. & Riley, E. M. Functional Significance of CD57 Expression on Human NK Cells and Relevance to Disease. *Front. Immunol.* **4**, 422 (2013).

339. Luetke-Eversloh, M., Killig, M. & Romagnani, C. Signatures of human NK cell development and terminal differentiation. *Front. Immunol.* **4**, 499 (2013).

340. Marostica, E. *et al.* Population pharmacokinetic model of ibrutinib, a Bruton tyrosine kinase inhibitor, in patients with B cell malignancies. *Cancer Chemother. Pharmacol.* **75**, 111–121 (2015).

341. Tam, C. S. *et al.* Improved depth of response with increased follow-up in phase 1 trial of patients with Waldenström macroglobulinemia (WM) treated with oral Bruton tyrosine kinase (BTK) inhibitor zanubrutinib (BGB-3111). in *International Workshop on Waldenström's macroglobulinemia* (2018).

342. Salem, A. H., Dunbar, M. & Agarwal, S. K. Pharmacokinetics of venetoclax in patients with 17p deletion chronic lymphocytic leukemia. *Anticancer. Drugs* 1–4 (2017). doi:10.1097/CAD.0000000000000522

343. Nakayama, K.-I., Negishi, I., Loh, D. Y., Sawa, H. & Kuida, K. Targeted disruption of Bcl-2 alpha beta in mice: occurrence of gray hair, polycystic kidney disease, and lymphocytopenia. *Proc. Natl. Acad. Sci.* **91**, 3700–3704 (2006).

344. Kim, E. H., Neldner, B., Gui, J., Craig, R. W. & Suresh, M. Mcl-1 regulates effector and memory CD8 T-cell differentiation during acute viral infection. *Virology* **490**, 75–82 (2016).

345. Legat, A., Speiser, D. E., Pircher, H., Zehn, D. & Fuertes Marraco, S. A. Inhibitory Receptor Expression Depends More Dominantly on Differentiation and Activation than "Exhaustion" of Human CD8T Cells. *Front. Immunol.* **4**, 455 (2013).

346. Robinson, H. R. *et al.* A CD19/CD3 bispecific antibody for effective immunotherapy of chronic lymphocytic leukemia in the ibrutinib era. *Blood* **132**, 521–532 (2018).

347. Bao, Y. *et al.* Tyrosine kinase Btk is required for NK cell activation. *J. Biol. Chem.* **287**, 23769–23778 (2012).

348. Wu, L. *et al.* Lenalidomide enhances natural killer cell and monocyte-mediated antibody-dependent cellular cytotoxicity of rituximab-treated CD20+ tumor cells. *Clin. Cancer Res.* **14**, 4650–4657 (2008).

349. Clambey, E. T. *et al.* The Ikaros Transcription Factor Regulates Responsiveness to IL-12 and Expression of IL-2 Receptor Alpha in Mature, Activated CD8 T Cells. *PLoS*

One **8**, e57435 (2013).

350. O'Brien, S. *et al.* Ikaros imposes a barrier to CD8+ T cell differentiation by restricting autocrine IL-2 production. *J. Immunol.* **192**, 5118 (2014).

351. Corral, L. G. *et al.* Differential Cytokine Modulation and T Cell Activation by Two Distinct Classes of Thalidomide Analogues That Are Potent Inhibitors of TNF- α. *J. Immunol.* **163**, 380–386 (1999).

352. Govindaraj, C. *et al.* Lenalidomide-based maintenance therapy reduces TNF receptor 2 on CD4 T cells and enhances immune effector function in acute myeloid leukemia patients. *Am. J. Hematol.* **89**, 795–802 (2014).

353. Aspalter, R. M., Eibl, M. M. & Wolf, H. M. Regulation of TCR-mediated T cell activation by TNF-RII. *J. Leukoc. Biol.* **74**, 572–582 (2003).

354. Kim, E. Y. & Teh, H.-S. TNF type 2 receptor (p75) lowers the threshold of T cell activation. *J. Immunol.* **167**, 6812–20 (2001).

355. LeBlanc, R. *et al.* Immunomodulatory drug costimulates T cells via the B7-CD28 pathway. *Blood* **103**, 1787–1790 (2004).

356. Ahn, I. E. *et al.* Depth and durability of response to ibrutinib in CLL: 5-year follow-up of a phase 2 study. *Blood* **131**, 2357–2366 (2018).

357. Roberts, A. W. *et al.* Efficacy of venetoclax in relapsed chronic lymphocytic leukemia is influenced by disease and response variables. *Blood* **134**, blood.2018882555 (2019).

358. Jones, J. *et al.* Evaluation of 230 patients with relapsed/refractory deletion 17p chronic lymphocytic leukaemia treated with ibrutinib from 3 clinical trials. *Br. J. Haematol.* **182**, 504–512 (2018).

359. Woyach, J. A. *et al.* Resistance mechanisms for the Bruton's tyrosine kinase inhibitor ibrutinib. *N. Engl. J. Med.* **370**, 2286–94 (2014).

360. Hillmen, P. *et al.* Ibrutinib Plus Venetoclax in Relapsed/Refractory Chronic Lymphocytic Leukemia: The CLARITY Study. *J. Clin. Oncol.* JCO.19.00894 (2019). doi:10.1200/JCO.19.00894

361. Jain, N. *et al.* Ibrutinib and Venetoclax for First-Line Treatment of CLL. *N. Engl. J. Med.* **380**, 2095–2103 (2019).

362. Agarwal, R. *et al.* Dynamic molecular monitoring reveals that SWI–SNF mutations mediate resistance to ibrutinib plus venetoclax in mantle cell lymphoma. *Nat. Med.* **25**, 119–129 (2019).

363. Ghez, D. *et al.* Early-onset invasive aspergillosis and other fungal infections in patients treated with ibrutinib. *Blood* **131**, 1955–1959 (2018).